

ISCHEMIA OF THE HEART; A STUDY OF SARCOMERE
DYNAMICS AND CELLULAR METABOLISM

myocard ischemie; een studie naar
sarcomeer dynamica en celstofwisseling

PROEFSCHRIFT

ter verkrijging van de graad van doctor
aan de Erasmus Universiteit Rotterdam
op gezag van de rector magnificus
Prof. dr. C.J. Rijnvos
en volgens besluit van het college van dekanen.
De openbare verdediging zal plaatsvinden op
woensdag 31 maart 1993 om 15.45 uur

door

Jeroen Johannes Jacobus Bucx

geboren te Amersfoort

Promotoren: Prof. Dr. J.R.T.C. Roelandt
Prof. Dr. H.E.D.J. ter Keurs

Overige leden: Prof. Dr. M.I.M. Noble
Prof. Dr. P.D. Verdouw

Het verschijnen van dit proefschrift werd mede mogelijk gemaakt door de financiële steun van de Nederlandse Hartstichting en door bijdragen van Astra Pharmaceutica BV, Bayer Nederland BV, Boehringer Ingelheim BV, Bristol-Myers Squibb BV, Ciba Geigy BV, Hoechst Holland NV, Inpharzam Nederland BV, Leo Pharmaceutical Products BV, Lorex Synthélabo BV, en E. Merck Nederland BV.
This project was supported by the Dutch Heart Foundation (1983-1984) and the Alberta Heritage Foundation for Medical Research (1985-1986).

CONTENTS OF THE THESIS

Chapter 1	Introduction and review of the literature	5
Chapter 2	Objectives of the thesis	40
Chapter 3	General methodology	42
Chapter 4	Comparison between the sarcomere length - force relations of intact and skinned trabeculae from rat right ventricle; influence of calcium concentrations on these relations	48
Chapter 5	Effects of acidosis on force - sarcomere length and force - velocity relations of rat cardiac muscle	63
Chapter 6	Sarcolemma, sarcoplasmic reticulum, and sarcomeres as limiting factors in force production in rat heart	71
Chapter 7	High-energy phosphate metabolism in normoxic and ischemic trabeculae and normoxic papillary muscles from rat heart	82
Chapter 8	Hypoxic contracture in rat cardiac trabeculae: analysis of dynamic sarcomere stiffness	101
Chapter 9	Sarcomere dynamics and relaxation characteristics of rat cardiac trabeculae during repeated hypoxia and reoxygenation	119
Chapter 10	General discussion of the study results and their clinical implications	147
Chapter 11	Summary	157
Chapter 12	Samenvatting	159
Curriculum vitae		162

Voor Monique

Voor Sander en Michel

CHAPTER 1 INTRODUCTION AND REVIEW OF THE LITERATURE

Three billion heartbeats propel blood during the average duration of a mans lifetime into the systemic and pulmonary circulation. Doing so, the heart, normally of less than 400 g weight, imparts an energy to the blood, equal to 400,000 ton.meter. This stable and highly efficient process can be jeopardized by even short periods of myocardial ischemia that result from an obstruction of one of the nutrient coronary arteries. Coronary artery stenosis due to atherosclerosis is one of the most common diseases in the Western world, and responsible for approximately 35% of all deaths. Hence, the ischemic process is a phenomenon of major scientific importance and clinical relevance.

This thesis describes a series of studies aimed to elucidate further the mechanisms which allow stable mechanical function of the myocardium and to describe the effects of ischemia or anoxia and reoxygenation on the mechanical properties of cardiac muscle.

At the outset of this review it should be stressed that it is virtually impossible to mimic and study ischemia *in vitro*. This is related to the complexity of the sequence of events, that occur during ischemia. Amongst others, this involves a limitation of the availability of O_2 and other nutrients on the one hand and stagnation of removal of metabolites and CO_2 on the other hand. Therefore in smaller models like papillary muscles, trabeculae and myocytes, experiments are usually focussed on one aspect of ischemia. For this purpose, in some experiments oxydative phosphorylation is inhibited, whereas in others perfusion flow is limited or oxygen delivery restricted. In many models hypoxia is used as an equivalent of ischemia. It should be noted however that under these experimental conditions, accumulation of metabolites and acidosis is either absent or less outspoken than during ischemia. Ultimately the changed contractile behaviour is determined by the intervention that has been chosen. The interpretation of the observed phenomena therefore should be put into perspective of the experimental conditions. The same applies to reperfusion, which is supposed to result in reoxygenation of ischemic myocardium. Temporary occlusion of coronary arteries, however, may be accompanied by damage of endothelium, microvascular plugging with blood elements and capillary compression (Hearse and Bolli, 1992). These changes may prevent reperfusion, and hence reoxygenation, a phenomenon denoted as the 'no reflow' phenomenon (Braunwald and Kloner, 1985; Kloner et al., 1974). Lastly, myocardial damage may result from a reduction in luminal diameter of a major coronary artery, not affecting resting coronary perfusion. Under these conditions the resulting myocardial damage is not accounted for by ischemia but may be mediated by other mechanisms that are as yet unknown (Burkhoff et al., 1991; Capasso et al., 1991).

Coronary arteries supply the heart with oxygen and the substrates fatty acids, glucose and lactate. These substrates are normally oxidized to CO_2 and H_2O which are washed out. The energy that is set free by this process is stored in adenosine triphosphate (ATP) and creatine phosphate (CrP). When cardiac work -- and hence oxygen consumption -- increase, coronary flow increases in proportion as a result of metabolic regulation (Berne & Rubio, 1979) until maximal dilatation of the coronary vascular bed is reached; at that point coronary flow cannot increase to meet a further increase of cardiac work unless perfusion pressure rises. The condition in which cardiac work is not met by an appropriate coronary flow is denoted as ischemia. The ratio between maximal coronary blood flow and coronary flow at rest is referred to as the coronary flow reserve. In the human heart the maximal coronary flow reserve equals four to five (Wilson et al, 1985); in rat heart coronary blood flow ranges from 40 to 80 ml/min/-100 gm wet weight (Gould, 1991). Narrowing of the coronary arteries as a result of atherosclerosis or concomitant vasospasm increase the resistance of the coronary vascular bed and lead to ischemia at a lower level of cardiac work than under normal conditions.

Insufficient oxygenation of the heart frequently more seriously affects the function of the left

ventricle than the right ventricle. One reason for this is that the pressure in the left chamber is much higher than in the right chamber. Initially it was supposed that flow fluctuation was accounted for by left ventricular pressure resulting in compression of the capillaries; however, recently this hypothesis was challenged by the observation that contraction of a vented left ventricle is still associated with pulsatile coronary blood flow (Krams et al, 1990). Flow in the right coronary system on the other hand is steadier and less dependent on the cardiac cycle. As a result the left ventricle is more vulnerable to flow reduction than the right ventricle (Berne and Rubio, 1979). This phenomenon is most prominent in the subendocardial layers of the left ventricle which are subject to the highest compression. Furthermore, since the muscle mass of the left ventricle is simply greater than that of the right ventricle, the number of arteries in the former is greater than in the latter and it is more probable that ischemia manifests itself in the left than in the right ventricular wall.

Patients with coronary artery disease may present with angina pectoris, myocardial infarction or sudden cardiac death. Already in 1772, William Heberden mentioned that the clinical syndrome of angina pectoris, consisting of a dull, compressing sensation in the chest radiating to the arm(s), neck, jaws, shoulder(s) and back, was an expression of a heart disease (Heberden, 1772 ; Willius and Dry, 1948). Although ischemia seems to be an absolute requisite for angina, it was recently shown that only 30% of the ischemic episodes in patients with symptomatic coronary artery disease are accompanied by angina pectoris (Crea et al, 1990; Deanfield et al., 1983; Stern and Tzivoni, 1974).

When the diagnosis of angina pectoris is confirmed, treatment is aimed at reduction of myocardial oxygen consumption and at increasing the oxygen supply by the coronary arteries. Therefore most patients are treated initially with drugs that increase coronary flow (nitroglycerine, Ca^{2+} entry blockers) or reduce heartrate (β -blockers) and afterload (vasodilators). In addition preload may be reduced (diuretics and venodilators) or contractility reduced (β -blockers, Ca^{2+} entry blockers), the latter measures aimed at reducing oxygen consumption of the jeopardized myocardium. When the complaints continue despite pharmacological interventions and changes in lifestyle, treatment by coronary artery bypass grafting (C.A.B.G.) or percutaneous transluminal coronary angioplasty (P.T.C.A.) are considered (Detre et al, 1988; Laird-Meeter et al., 1987).

It is well known that ischemia may cause ventricular or atrial arrhythmias. Ventricular fibrillation causes death of up to 65 % of the population of patients with coronary artery disease (Braunwald, 1992; Eisenberg et al., 1986).

Ischemia also impairs the force generating ability of ischemic segments of the heart which was already shown by Tennant and Wiggers in 1935 (Tennant and Wiggers, 1935). In two thirds of the patients with ischemic heart disease left ventricular wall motion appears abnormal on biplane ventriculography (Helfant, 1977). In many patients regional wall motion becomes abnormal during spontaneous ischemia or during ischemia induced by atrial pacing or exercise (Sharma, 1980). During ischemia the contractility of the left ventricular wall is severely impaired or even completely lost; in some cases however this may still be reversible, even when ischemia lasted more than one hour.

In order to understand the effects of ischemia on the contractile function and notably pressure - volume relationships of the intact heart, it is essential to gain insight in the mechanical behaviour of the muscle fibers that constitute the wall of the heart. The changes in structure and geometry of the beating heart can be modelled, provided that some assumptions and simplifications are made (Ghista et al., 1983). The architecture of the wall of the ventricles is complex; it consists of many layers of fibers with different orientation. Usually it is represented by a simplified model with a limited number of layers (Streeter et al, 1969). Likewise, the change in fiber orientation that results from contraction may be incorporated into the model (Arts et al, 1980). The cavity of the left ventricle is usually represented as a cylinder or a sphere or a combination of these geometrical forms (Arts et al., 1980). Obviously these

simulations attempt to describe the assumed behaviour of the left ventricle as a whole; the effects of changes in filling or output resistance on cardiac performance are usually not modelled.

The description of the contractile properties of the fibers in the wall, in turn, have to be derived from experiments with isolated preparations i.e. papillary muscles or trabeculae. Assuming that the activation pattern i.e. excitation contraction coupling is identical everywhere, the resulting contraction pattern of the muscle fibers in the model have to follow the pattern that can be observed in the intact heart (Durrer et al., 1955).

Alternatively, intact animal hearts have been used to analyse the effect of ischemia on contractility. In this model ischemia can be induced either regionally or globally and the effects of reoxygenation can be studied (Akaishi et al., 1986; Bush et al., 1983; Tamaki et al., 1986).

Both mathematical models and in vivo measurements of the changes in contractility in the intact heart are difficult to interpret mainly because many assumptions have to be made; in addition, the behaviour of the region with impaired contractility cannot be analysed separate from the normal tissue with which it is in series (Akaishi et al. 1986).

Therefore I have chosen to use thin linear muscle preparations in this study of isolated effects of ischemia on contractility and on high-energy phosphate metabolism (ter Keurs et al., 1980 and 1982).

The ultrastructure of mammalian heart

The wall of the heart is composed of myocytes with an average length and diameter of ≈ 100 and $\approx 10 \mu\text{m}$, respectively. The ratio of capillaries to myocytes is approximately 1 (Berne and Rubio, 1979); each myocyte is surrounded by an extracellular space of the order of 0.2 to $1 \mu\text{m}$ or more in width (Berne and Rubio, 1979; Olsson and Bugni, 1986; Sommer and Jennings, 1986). The capillaries, which run longitudinally along the myocytes, are connected by anastomoses, causing complex spatio-temporal variations of capillary flow (Wieringa et al, 1982).

Adjacent myocytes are connected via intercalated discs such that the heart as a whole functions as an electrical syncytium. This implies that all myocytes are activated in a coordinated way. The organelles that are involved in the excitation-contraction coupling of the individual heart cells are the cell membrane (sarcolemma), sarcoplasmic reticulum, and myofilaments. Mitochondria are involved as well though to a smaller extent. Together these structures occupy almost 90% of the cell volume (Page and McCallister, 1973; Page, 1978).

When the myocytes depolarize as a result of the Na^+ current, voltage-sensitive Ca^{2+} channels in the sarcolemma open (Kass, 1989; McNutt, 1975; Opie, 1992; Robertson, 1958). Ca^{2+} ions, which enter the cell during the plateau phase of the action potential, activate the sarcoplasmic reticulum to release calcium ions (Carafoli and Penniston, 1985). The sarcoplasmic reticulum (SR) is a network of intracellular tubules with a diameter of 25 nm surrounding the myofilaments. The longitudinal portion of the SR forms a mesh around the A and I bands; the junctional SR originates from the longitudinal SR and is located in the vicinity of the transverse tubuli of the sarcolemma and contains the Ca^{2+} release channels (Fleischer and Inui, 1989). Particles (8-9 nm in diameter) located on the membrane that envelops the sarcoplasmic reticulum are believed to constitute the Ca^{2+} pumping protein which actively sequesters Ca^{2+} ions (Bers, 1991). The release of Ca^{2+} from the sarcoplasmic reticulum in turn activates the contractile proteins.

Myofibrils are $\approx 1 \mu\text{m}$ in diameter. Light microscopy reveals dark and light regions (cross striation) that are regularly distributed along the fiber. The cross striation is caused by the different refractive indices of the contractile proteins actin and myosin. Each striation constitutes the fundamental contractile unit in the muscle fiber: the sarcomere.

Contractile proteins

The thin actin filaments are approximately 1 μm in length (Hanson & Lowy, 1963; Winegrad and Robinson, 1978). Each actin filament consists of a double-stranded helical polymere of g-actin molecules. These in turn are slightly ovoid proteins with a diameter of approximately 55 Å. Tropomyosin, a 2 α -helical peptide chain, lies in the grooves that run longitudinally between the two strands of actin. The third component of the thin filament is the troponin complex. It is bound to tropomyosin at intervals of 400 Å. The troponin complex itself is composed of 3 separate proteins. Troponin I regulates the interaction between actin and myosin. Cardiac troponin C has two high and one low affinity binding sites for Ca^{2+} (Babu et al., 1988). Troponin T binds the troponin complex to tropomyosin.

Myosin is a complex, symmetric molecule, consisting of a double stranded α -helix of polypeptide heavy chains with a total length of 160 nm. Each polypeptide chain ends in a head that is surrounded by 2 smaller light chains. The light chains facilitate binding and hydrolysis of ATP. The actin binding activity also resides in polypeptide head. The thick filament (approximate length 1.6 μm and thickness 10 nm) consists of 400 myosin molecules. These molecules are arranged longitudinally in pairs around the center of the thick filament. Their tails are embedded in the thick filament over a distance of 130 nm. Successive pairs are rotated relative to each other by 120° with a distance of 43 nm (Zak and Galhotra, 1983).

Although a number of fundamentally different theories has been proposed (i.g. see Pollack, 1983), the classical crossbridge model is still widely accepted as the explanation of muscle contraction (Huxley, 1957; Huxley, 1969). According to the theory, interaction of actin and myosin is initiated upon an increase in cytosolic Ca^{2+} following excitation of the myocytes. The ensuing geometrical modifications of the contractile and regulatory proteins, notably tropomyosin, allow myosin to bind with actin (Huxley et al, 1982). Subsequently, the shape of the myosin head changes, which supposedly generates the force that causes sliding of actin toward the center of the sarcomeres. During this sequence of events, ADP and inorganic phosphate are released from their binding sites on the myosin molecule (Eisenberg and Green, 1980; Huxley and Simmons, 1971). In order to reestablish the initial geometrical conditions, that are essential for repetitive interactions between both myofilaments, the immediate availability of ATP is essential (Eisenberg and Hill, 1985). This applies in particular to actomyosin detachment, releasing the rigor state.

Mitochondria

The energy that is required for the contraction process is generated in the mitochondria, located immediately adjacent to the sarcomeres. The mitochondria occupy approximately 35% of the volume of the myocyte (Page, 1978). Each mitochondrion is surrounded by a thin outer membrane. The inner membrane is folded into numerous transverse cristae, which envelop the matrix. The enzymes that catalyze the tricarboxylic acid cycle are located in the matrix; the enzymes that are involved in electron transport and oxydative phosphorylation are arranged in clusters in the inner membrane (Lehninger, 1970). The size of the mitochondria, their cristae and density of the matrix and presence of granulae, reflect the activity of the organelle (Langer et al., 1982). In presence of oxygen, mitochondria transfer the energy that is released by breakdown of carbohydrates, lipids and lactic acid, into the energy rich phosphate bonds of adenosine triphosphate (ATP). This process is referred to as oxydative phosphorylation. Eighty percent of the produced ATP is utilized for excitation-contraction coupling and actomyosin ATPase activity (Gibbs, 1987). The total amount of CrP and adenine nucleotides in the cell is kept constant as a result of regeneration of ATP by oxydative phosphorylation. This process is regulated by the rate of delivery of ADP and P_i to the mitochondria or by changes in the NADH-NAD redox state

(Balaban et al., 1986; Fossel et al., 1980; Shrago et al. 1976). Recently, evidence has been presented that calcium transport by the mitochondria may be a third regulatory mechanism for energy metabolism (Hansford, 1985).

Sarcolemma

The myocyte is enclosed by the cell membrane, the sarcolemma, which constitutes the boundary between the cellular cytoplasm and the extracellular space. From the sarcolemma, a complex network of repeating tubular invaginations originates, that communicates with the extracellular space. These T-tubules, that are composed of sarcolemmal membrane, surround the contractile proteins in transverse direction in the area of the Z-bands. In turn, they are in close contact to the sarcoplasmic reticulum that is responsible for Ca^{2+} induced Ca^{2+} release in the vicinity of actin and myosin. The T-tubules and sarcoplasmic reticulum constitutes 1 and 0.5 % of the myocardial cell volume, respectively (Page and McCallister, 1973). However, these organelles cover a large surface (30% and 100%, respectively) when compared to the sarcolemmal surface.

The sarcolemma is a trilaminar membrane, consisting of acid mucopolysaccharides, glycolipids and glycoproteins; it is about 70 - 90 Å thick. A number of specific proteins are inserted in the membrane. Some are located at one surface, others, especially those that are thought to be associated with ion transport, span the membrane. These ion channels are suitable to facilitate transport of Na^+ , K^+ , and Ca^{2+} ions; their pore sizes are 3.0-5.0, 2.6-3.0 and 6.8 Å, respectively (Hille, 1970). The density of Na^+ channels is 16 per μm^2 surface area (Cachelin et al., 1983), compared to 1.6 for K^+ channels (Keynes, 1979) and 0.1 for Ca^{2+} channels, respectively (Reuter, 1984). The ionic fluxes through each channel are governed by complex gating mechanisms that regulate opening and closing as well as recovery of the ability to open. Ion channels are preferentially passed by one ion; however, some channels allow more than one type of ion to cross (Hess and Tsien, 1984). In addition, the sarcolemma contains active ion pumps like the sodium pump, a Na^+/K^+ -ATPase molecule, that extrudes Na^+ ions from the cell. The $\text{Na}^+/\text{Ca}^{2+}$ exchanger, Na^+/H^+ exchanger and Ca^{2+} -ATPase are also incorporated in the cell membrane (Opie, 1992; Smith, 1988; Reuter, 1984).

In an attempt to understand the mechanism of ischemic cell damage, we will first focus on the main functions of the myocardium at the level of the cell i.e. energy metabolism, excitation - contraction coupling, Ca^{2+} homeostasis and the contraction - relaxation cycle.

I.A. HIGH-ENERGY PHOSPHATE METABOLISM DURING NORMOXIA

Oxydative phosphorylation

In essence, energy metabolism in the presence of oxygen consists of 3 steps which are illustrated in figure 1. The substrates lactate, glucose and free fatty acids are converted to acetyl CoA which is metabolized to CO_2 and H^+ ions in the tricarboxylic acid cycle. The protons are bound to nicotinamide adenine dinucleotide (NAD) and flavin adenine dinucleotide (FAD). These compounds in turn are transferred to the inner membrane of the mitochondrion and oxydized to H_2O in the respiratory electron transfer chain. The energy set free by this process, is used to convert ADP to ATP by a process referred to as oxydative phosphorylation (Mitchell, 1979). During normoxia more than 90% of ATP is derived from oxydative phosphorylation. The remaining ATP is generated by anaerobic glycolysis and is used

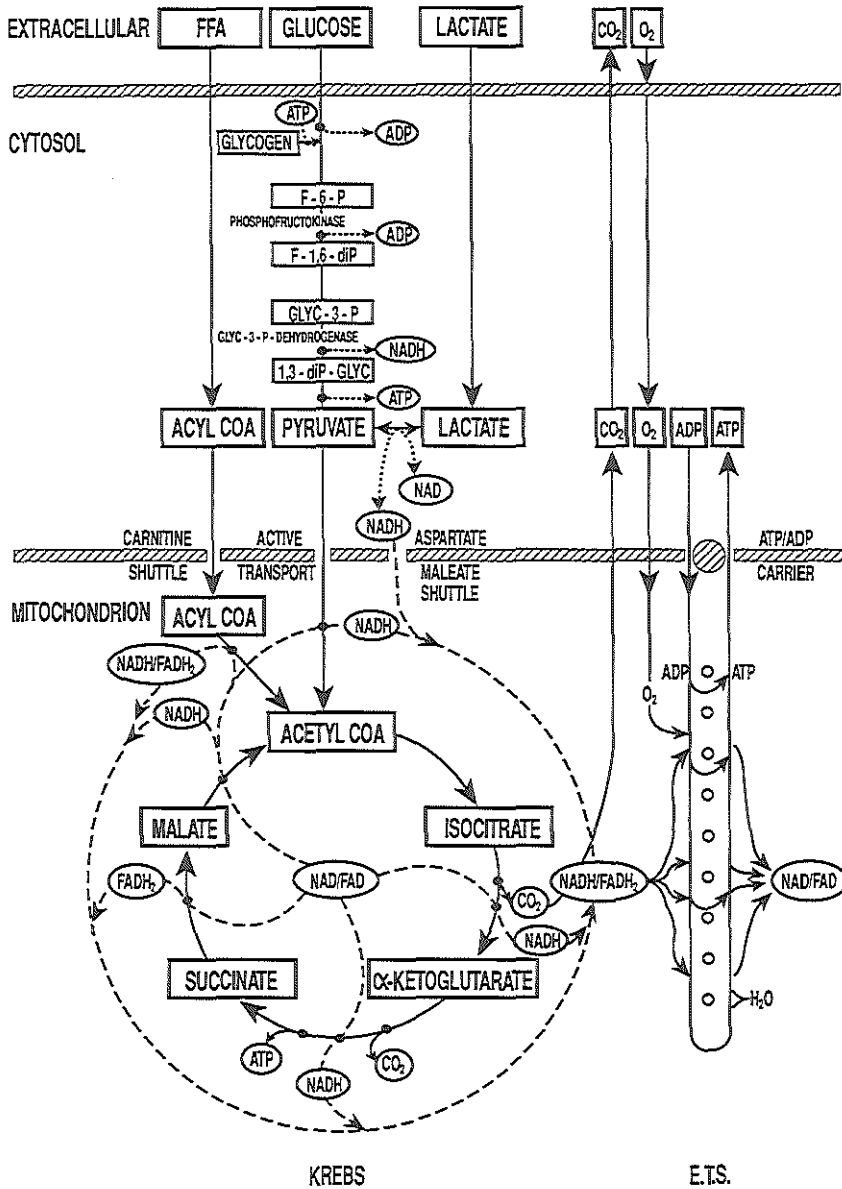


Figure 1: Schematic representation of the energy metabolism of free fatty acids (FFA), glucose and lactate in conjunction with the tricarboxylic acid cycle (Krebs-cycle) and electron transport system (ETS). For further explanation, see text.

mainly for ion pumps and membrane phosphorylation (Kobayashi and Neely, 1979).

In the normoxic heart free fatty acids (FFA) serve as the energy source for 60 - 90% of the ATP that is produced (Neely and Morgan, 1974; van der Vusse et al., 1992). This percentage decreases in presence of carbohydrates such as glucose (see below; Ballard, 1960). Lactate is used preferentially when present at concentrations above 4 mM (Drake-Holland, 1983; Liedtke, 1981). FFA are obtained either from digested triglycerides or from internal adipose tissue stores. Following uptake they are converted at the expense of ATP to acyl-CoA in the presence of Coenzyme A (CoA). Acyl-CoA is either restored via esterification into triglycerides and phospholipids, or further oxidized to H_2O and CO_2 . The latter process involves transfer of acyl-CoA into the matrix of the mitochondria via the carnitine shuttle (Pande, 1975). Subsequently, acyl-CoA is reduced by formation of the 2-carbon fragments compound acetyl-CoA, in a chain of reactions that is referred to as β -oxidation. The cofactors for β -oxidation not only include CoA but also NAD and FAD which are reduced to NADH and $FADH_2$ respectively. Next, acetyl-CoA is further metabolized in the tricarboxylic acid cycle (Krebs cycle) to 2 CO_2 and 8 H^+ . Finally, the so formed protons are oxidized during electron transport and oxydative phosphorylation, ultimately yielding ATP.

The rate of breakdown of acyl-CoA to acetyl-CoA is governed by the turnover of acetyl-CoA in the citric acid cycle. In addition, evidence has been obtained that the conversion rate is impaired by the presence of exogenous fatty acids; under these conditions triglyceride synthesis prevails (Vary et al., 1981).

Oxydation of carbohydrates accounts for the remaining 40% of the activity of the oxydative phosphorylation in the heart; this percentage may reach 100% postprandially (Goodal, 1950; Liedtke, 1981; Randle and Tubbs, 1979). Following transport into the cell, glucose is phosphorylated - initially by hexokinase and then by phosphofructokinase - to fructose-1,6-diphosphate. Further metabolization to pyruvate yields 4 molecules of ATP and 2 molecules of NADH. Alternatively, pyruvate may be formed from lactate, a reaction that is catalyzed by pyruvate dehydrogenase in the presence of NAD. Pyruvate is transferred into the mitochondria (Halstrap and Denton, 1975) and converted to acetyl-CoA by the pyruvate dehydrogenase complex (Lopaschuk et al., 1990). Acetyl-CoA is further processed by the tricarboxylic acid cycle as discussed before.

Regulation of oxydative phosphorylation

The rate of glycolysis is determined by 3 enzymes that are indicated in figure 2. In presence of Ca^{2+} and increased [AMP] and [ADP], activated phosphofructokinase phosphorylates fructose-6-phosphate to fructose-1,6-diphosphate. The subsequent conversion of pyruvate to either lactate (anaerobic glycolysis) or acetyl-CoA (aerobic glycolysis) is determined by the enzyme glyceraldehyde-3-phosphate dehydrogenase. The tricarboxylic acid cycle is the final determinant of the glycolytic rate. Increased concentrations of ATP inhibit the enzymes of the tricarboxylic acid cycle which results in increased concentrations of isocitrate and acetyl-CoA which in turn inhibit the rate of glycolysis. Increased concentrations of ADP and NAD on the other hand tend to accelerate the conversion rate by the Krebs cycle (Neely and Morgan, 1974).

FAD participates both in the tricarboxylic cycle and in β -oxidation of fatty acids. Therefore it probably plays a pivotal role in tuning the speed of both processes. At increased carbohydrate flux, β -oxidation is inhibited due to increased $FADH_2$ concentration. On the one hand, fatty acid metabolism inhibits uptake and phosphorylation of glucose by NADH, that is formed via β -oxidation. In addition, citrate from active glycolysis, inhibits phosphofructokinase and thereby the formation of fructose-1,6-diphosphate. High concentrations of NADH and acetyl-CoA, inhibit the pyruvate dehydrogenase complex and hence impair the glycolytic flux.

The activity of oxydative phosphorylation is determined by the concentration of free ADP and the cytoplasmic phosphorylation potential (Jacobus, 1985; Mela-Riker and Bukoski, 1985). Recently mitochondrial calcium transport has been proposed as an additional regulatory mechanism (Hansford et al., 1989).

ATP is transferred from the mitochondria to the cytosol by the ATP/ADP-carrier adenine nucleotide translocase (Klingenberg et al., 1975). This process either involves simple diffusion or mediation by a creatine-CrP shuttle (Bessman and Geiger, 1981; Meyer et al., 1984). Approximately 80% of the ATP production is consumed by the contractile apparatus in order to complete the contraction - relaxation cycle (Balaban et al, 1986; Matthews et al., 1981; Suga, 1990). This equals 5 - 10 % of the total ATP content of the cell (Jacobus, 1985). The remaining ATP is used for ATP-dependent ion pumps in the sarcolemma and SR, as well as for protein and lipid metabolism (Allen and Orchard, 1987). In earlier studies the free intracellular concentrations of CrP and ATP in the beating heart have been reported to fluctuate by 15 % (Fossel et al., 1980). Recent studies, however, have shown that the fluctuations are probably smaller, suggesting that the production of these compounds is well regulated (Balaban et al., 1986; Heineman and Balaban, 1990). For more detailed discussion see the excellent review by Suga on MVO₂ - PVA relations (Suga, 1990).

The content of adenine nucleotides varies within different cell compartments, which has been referred to as compartmentalization (Gudbjarnson et al., 1970). Recent studies on isolated myocytes have shown that the cytosol adenine nucleotide content was 17 nmol/mg protein, whereas 5 nmol/mg protein was contained in the mitochondria; 1.3 nmol ADP per milligram cell protein was found to be bound to the myofibrils (Geisbuhler et al., 1984).

ADP, resulting from ATP breakdown, is regenerated to ATP by adenylate kinase (Walker and Dow, 1982). This reaction is believed to be the most important mechanism that keeps the cellular content of adenine nucleotides at a constant level. Nevertheless, small amounts of ADP are further metabolized to AMP and adenosine, which may leave the myocyte. Although adenosine is known to be a strong vasodilator, its significance for coronary flow regulation is controversial (Spaan, 1985; Berne and Rubio, 1979; Drury and Szent-Gyorgyi, 1929). Release of adenosine is triggered by ischemia due to the increased [ADP], or by β -adrenergic drugs (Berne et al. 1983; Sparks and Bardenheuer, 1986). It is rapidly metabolized to the purine nucleoside inosine and the oxypurines hypoxanthine and xanthine.

I B HIGH-ENERGY PHOSPHATE METABOLISM DURING ISCHEMIA

During ischemia the supply of oxygen and other nutrients is insufficient. The oxygen concentration in the extracellular volume -- which comprises about 20% of the total tissue volume -- decreases rapidly (Frank & Langer, 1974; Polimeni, 1974) and so does the oxygen concentration in various parts of the myocyte, notably the mitochondria (Jones, 1986). In absence of oxygen, oxydative phosphorylation ceases; NADH and FADH₂ accumulate and ATP production stops (Allen et al., 1985; de Jong, 1988; Esumi et al., 1991; Kloner and Braunwald, 1980; Prinzen, 1982). As a consequence, acetyl-CoA accumulates which in turn inhibits β -oxydation of fatty acids (see figure 1). The concentration of acyl-CoA increases initially in the mitochondria and later in the cytosol. Uptake and breakdown of fatty acids is inhibited by high acyl-CoA. Instead fatty acids are stored as endogenous triglycerides.

The accumulation of acetyl-CoA, NADH and FADH₂ also inhibits pyruvate dehydrogenase which causes preferential conversion of pyruvate to lactate. Formation of lactate provides NAD, required for the preceding reaction steps of the glycolytic pathway. Within one minute following the onset of ischemia anaerobic glycolysis accelerates (Braasch et al., 1968; Opie, 1976; Williamson, 1966). Under ischemic conditions, the maximum rate of glycolysis is determined by glyceraldehyde-3-phosphate dehydrogenase; its activity depends on the availability of NAD. Phosphorylation of glucose is impaired

during hypoxia because phosphofructokinase is inhibited as a result of lack of ATP. As a compensatory mechanism endogenous glycogen stores are mobilized and converted to glucose-1-phosphate. During ischemia, fatty acids no longer contribute to ATP production.

The decreased ATP production in the mitochondria causes a rapid decline of the concentration of CrP followed by a more gradual decrease of the cytosol [ATP]. Anaerobic glycolysis accelerates by a factor of 10 to 20 during ischemia. However, this process generates only 2 molecules of ATP per molecule glucose compared to 36 molecules of ATP by oxidative phosphorylation. The total adenine nucleotide pool decreases since ATP breakdown products are no longer regenerated to ATP. In the pathway of ATP breakdown, as shown in figure 1, ADP increases until the enzymes which catalyze conversion to AMP are activated. When ischemia is prolonged, AMP is further metabolized to hypoxanthine and inosine. The latter accounts for 50% of all nucleosides and oxypurines that are ultimately released in the venous blood (Jennings and Steenbergen, 1985). Ultimately the amount of available ATP is insufficient to maintain basic cell function and structure. Metabolites of ATP and CrP are believed to both inhibit the force generating ability of the myofilaments as well as other energy consuming processes: e.g. ion regulation by the sarcolemma and Ca^{2+} handling by the sarcoplasmic reticulum (Imai et al., 1983; Kentish, 1986; Nakaya et al., 1985; Nosek et al., 1987). When ischemia lasts longer than 15 minutes high-energy phosphate concentrations decrease to very low levels (ATP <35%, total adenine nucleotide pool <45%) (Jennings and Steenbergen, 1985). Glycogen is then depleted by 70% and mitochondria are swollen with amorphous osmiophilic deposits (Gao et al., 1992; Jennings et al., 1978). As soon as ATP production from glucose is reduced to less than 2 mMol/L/minute, contractile activity ceases completely and ischemic contracture develops (Owen et al., 1990).

Ischemia is known to induce deleterious effects on numerous cell organelles and processes. Accumulation of breakdown products from ATP and CrP, has been shown to be able to inhibit the Ca^{2+} -ATPase in the SR and Na^+/K^+ -ATPase in the sarcolemma. Increased concentrations of FFA may damage the cell membrane and trigger arrhythmias (Corr et al., 1984; Katz and Messineo, 1981; Bilsen et al., 1991). Lactate accumulation may induce changes in osmolality in the cell (Tranum-Jensen et al., 1981).

Due to lipolysis and degradation of triglycerides as well as pyruvate production during anaerobic glycolysis, protons are generated, which induce a rapid decline of intracellular pH (Gevers, 1977). This, in turn, inhibits continued glycolysis which initially is accelerated for 3 to 4 minutes.

Mitochondria swell and their matrix becomes less dense and inhomogeneous during ischemia. The observed aggregates in the mitochondrial matrix are caused by denaturated material and by Ca^{2+} deposits; the latter may be prevented by prior administration of ruthenium red (Hagler et al., 1979; Park et al., 1990). Following 45 minutes of ischemia the Ca^{2+} content of the mitochondria is markedly elevated, yet their ability to produce ATP seems only marginally impaired (Nayler, 1980). Even so, reoxygenation following 90 minutes of ischemia is accompanied by Ca^{2+} accumulation in the matrix of the mitochondria and destruction of the cellular ultrastructure (Williams et al., 1982).

Sarcolemma and ischemia

At the moment when damage leads to cell death the sarcolemma shows small breaks on electron micrographs (Jennings and Reimer, 1981). However, the mechanism of cell membrane disruption due to ischemia is unknown. Some authors have proposed that the decreased cytosol ATP and increased $[\text{Ca}^{2+}]_i$ might activate membrane phospholipases that subsequently damage the cell membrane (Gazitt, 1976). Others have suggested that lysosomal phospholipases, fatty acids or free oxygen radicals are involved in cell membrane destruction (Corr et al., 1984; Hess and Manson, 1984; Katz and Messineo, 1981). At any

rate, when the integrity of the cell membrane is lost, ion homeostasis is impossible and $[Ca^{2+}]_i$ increases while enzymes leave the cell. The resulting hypercontraction of the myofilaments may increase membrane damage even further (Reimer et al., 1983; Jennings and Reimer, 1991).

I C HIGH-ENERGY PHOSPHATE METABOLISM DURING REOXYGENATION

Provided that the mitochondria are not damaged irreversibly, oxidative phosphorylation may resume following reoxygenation. Initially ATP levels are decreased and resynthesis is limited because the total purine pool is depleted as a result of loss of purine metabolites from the cell (Harmsen et al., 1985). In addition ATP is used by enzymes activated by increased cytosolic $[Ca^{2+}]_i$ (Katz and Messineo, 1981). Due to reduction of the adenosine nucleotide pool, the conversion of ADP to ATP is restricted, leading to rapid accumulation of CrP to levels that greatly exceed concentrations in normoxic myocardium (Harmsen et al., 1985; Humphrey et al., 1985; Humphrey and Garlick, 1991; Jennings et al., 1991; Swain, 1982).

Gradually the adenine nucleotide pool may be restored by phosphorylation of adenosine or resynthesis from inosine and hypoxanthine in presence of phosphoribosyl pyrophosphate (PRPP), the latter pathway being referred to as 'purine salvage' (Murray, 1971; Pearson and Gordon, 1985). A third pathway is adenine ribophosphorylation, which is more time consuming than the above mentioned pathways (Kaufman et al., 1977). The last and most complex mechanism is de-novo synthesis of AMP from IMP in ten reaction steps directly from amino acid precursors, a process that consumes 4 molecules of ATP (Zimmer et al., 1973). Provided that the decrease during ischemia is limited to 20%, the ATP concentration ultimately returns to control value. The process may be accelerated in presence of adenosine, inosine or creatine phosphate (Down et al., 1983; Harmsen et al., 1984; Hori et al., 1989; Humphrey and Seeley, 1982). Administration of creatine analogues prior to ischemia preserved myocardial adenosine triphosphate during ischemia, delayed the development of acidosis and ischemic contracture and improved recovery of mechanical function on reperfusion by a hitherto unresolved mechanism (Jacobstein et al., 1989). In intact animals several days may be required to restore purine nucleotide pool and contractility, following an ischemic intervention that reduced ATP by 20% (Harmsen, 1984).

II A EXCITATION-CONTRACTION COUPLING DURING NORMOXIA

The cell membrane contains a Na^+/K^+ -ATPase which facilitates transfer of 2 K^+ ions into the cell in exchange for 3 Na^+ ions that are extruded, at the expense of 1 molecule of ATP. As a result, a transmembrane gradient of Na^+ and K^+ ions is created. Consequently the interior of the cell is negatively charged compared to the exterior. This is facilitated since the permeability of the cell membrane for K^+ ions greatly exceeds that for Na^+ and Ca^{2+} ions. Hence, during diastole K^+ ions tend to leave the cell by diffusion according to their concentration gradient as a result of selective permeability of the cell membrane for K^+ ions. This diffusional gradient is exactly balanced by the inward oriented electrical field. The relation between these two opposing gradients is described by the Nernst equation that describes the theoretical membrane potential that may be attained. The actual membrane potential (-85 mV) closely approximates the Nernst potential (-95 mV) due to the high permeability of the cell membrane for K^+ ions. At rest the extracellular concentrations are: $[Na^+]_o = 140$ mM, $[Ca^{2+}]_o = 1.5$ mM and $[K^+]_o = 4$ mM. The intracellular concentrations are $[Na^+]_i = 5$ mM, $[Ca^{2+}]_i = 0.1$ μ M and $[K^+]_i = 150$ mM. Figure 2 shows the timing of activation and deactivation of ion channels during the action potential. Following depolarization, the membrane permeability for Na^+ increases. The resulting inward

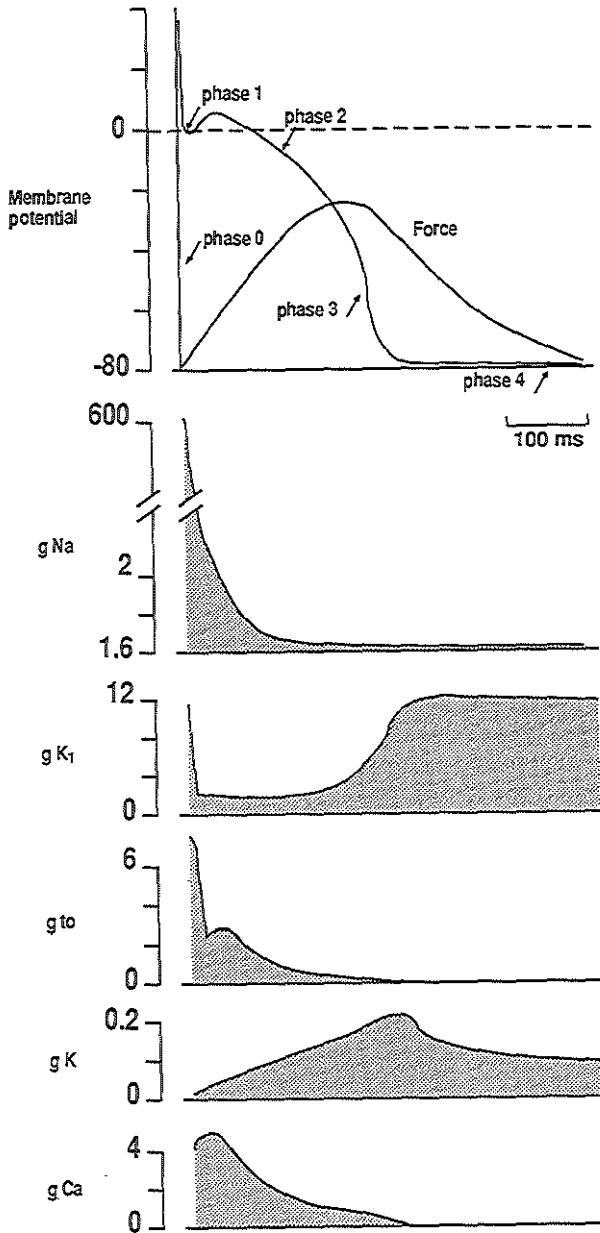


Figure 2: Contribution of ion fluxes to the action potential. g_{Na} : sum of rapid Na^+ conductance and background sodium conductance; g_{K1} : background K conductance; g_{to} : conductance giving rise to the transient outward potassium current; g_{Ca} : slow conductance giving rise to the inward Ca^{2+} current; g_K : conductance associated with the delayed rectifier potassium current. See text for further explanation.

flow of Na^+ ions is responsible for a regenerative inward current through the Na^+ channels (I_{Na}) lasting only a few milliseconds. The Na^+ current causes a rapid increase of the membrane potential toward E_{Na} . At positive membrane potentials K^+ ions no longer leave the cell via the K^+ channels that are linked with the K^+ current I_{K} . Instead, other K^+ channels are activated that generate another K^+ current, I_{K1} (Giles et al., 1986; Irisawa, 1984), and also Ca^{2+} channels open. Activation and deactivation of these channels takes longer than for the Na^+ channels. The inward flow of Ca^{2+} ions (I_{Ca}) balances the outward I_{K1} current, resulting in the plateau phase of the action potential. Ultimately the Ca^{2+} channels close again and the inward flow of Ca^{2+} ceases. The continued outward flow of K^+ via the I_{K1} channels causes rapid repolarization of the cell membrane. The I_{K1} channels deactivate and the I_{K} channels conduct again when the membrane potential returns to -85 mV. During each action potential Na^+ and Ca^{2+} ions enter the cell whereas K^+ leaves. The changes in Na^+ and K^+ concentrations resulting from one action potential are restored by the Na^+/K^+ pump at the expense of 0.3 mM ATP (Schwartz, 1962).

The intracellular Ca^{2+} concentration is in part governed by passive $\text{Na}^+/\text{Ca}^{2+}$ exchange (Chapman et al., 1983). Here again, the driving force is the Na^+ ion gradient across the cell membrane maintained by the Na^+/K^+ pump. $[\text{Ca}^{2+}]_i$ is also regulated by uptake of Ca^{2+} ions in the SR at the expense of ATP. The contribution of the sarcolemmal Ca^{2+} -ATPase is probably of minor importance to sarcolemmal Ca^{2+} transport compared to the mechanisms that have been discussed above (Caroni and Carafoli, 1980).

II B EXCITATION-CONTRACTION COUPLING DURING ISCHEMIA

The decrease of free energy available from ATP during acute hypoxia or ischemia results in inhibition of the Na^+/K^+ ATPase pump which in turn causes an increased in $[\text{K}^+]_o$ and $[\text{Na}^+]_i$ (Fiolet et al., 1984); these factors give rise to cell swelling (Hill and Gettes, 1980; Wilde and Kleber, 1986). Lactate, resulting from anaerobic glycolysis, accumulates and probably also contributes to cell swelling (Tranum-Jensen et al., 1981). $[\text{K}^+]_o$ increases in 10 - 15 min to a level of 10 - 15 mM (Hill and Gettes, 1980). However, $[\text{K}^+]_o$ varies within the ischemic zone, and also between endocardium and epicardium (Kleber, 1984). It has been reported that initially electrical conduction velocity of the action potential accelerates and that the threshold for late diastolic depolarization decreases (Ten Eick et al., 1992; Gambetta and Childers, 1969). At $[\text{K}^+]_o$ exceeding 5 mM however, the number of active Na^+ channels decreases due to depolarization of the cell membrane (Penny and Sheridan, 1983; Weidmann, 1955). Consequently the maximum rate of rise of the action potential, V_{max} declines. Moreover the action potential may become abbreviated. This may be either be accounted for by activation of ATP-sensitive potassium channels or caused by Ca^{2+} channel inactivation by H^+ ions (Jiang et al., 1991; Weiss and Lamp, 1989; Smith et al., 1985). It is probable that the conduction velocity is also decreased due to changes in the Na^+ current and increased resistance of the gap junctions (De Mello, 1982). Local and regional differences in membrane potential may give rise to arrhythmias and ultimately ventricular fibrillation (Koretsune et al., 1989).

Inhibition of the Na^+/K^+ pump probably leads to increased $[\text{Na}^+]_i$, in spite of reduced Na^+ influx during the action potential (Wilde and Kleber, 1986). Increased $[\text{Na}^+]_i$ is likely to diminish Ca^{2+} extrusion by the $\text{Na}^+/\text{Ca}^{2+}$ exchanger, which causes $[\text{Ca}^{2+}]_i$ to increase. Provided that ischemia lasts longer than 15 minutes, $[\text{K}^+]_o$ increases even further, albeit at a slower rate. This is probably due to cell membrane damage and/or activation of K^+ channels by increased $[\text{Ca}^{2+}]_i$ and lowered $[\text{ATP}]_i$ (Isenberg et al., 1983; Noma, 1983). The increased K^+ efflux may also be caused by metabolic anions that are released by anaerobic metabolism (Gaspardone et al., 1986). The abbreviation of the action potential duration contributes to decreased force generation. The negative effect of shortening of the action potential duration on twitch force is more outspoken and faster when glycolysis is inhibited (McDonald et al.,

1986). The effects of ischemia on force development are discussed in more detail in section IV B.

II C EXCITATION-CONTRACTION COUPLING DURING REOXYGENATION

Early after reoxygenation, action potential duration, resting membrane potential, V_{max} , and action potential amplitude normalize (Penny and Sheridan, 1983). However, since the Na^+/K^+ pump is still inhibited and the K^+ permeability of the cell membrane changed, more time is required for normalization of $[\text{K}^+]_o$ (Karli et al., 1979). The rapid yet heterogeneous reversal of elevated $[\text{K}^+]_o$ may serve as a trigger to the development of arrhythmias (Witkowski and Corr, 1984). The observation that reperfusion with elevated K^+ decreases the incidence of arrhythmias compared to reperfusion at normal K^+ seems to be in agreement with this hypothesis (Lubbe et al., 1978). Not the severity but the duration of the preceding ischemia (either by total or partial flow reduction) seems to determine the incidence of reperfusion arrhythmias (Penny and Sheridan, 1983). Furthermore, low flow reperfusion with hypoxic solutions appears to be less arrhythmogenic; the underlying mechanism of this observation is unknown.

Recent evidence suggests that increased $[\text{Ca}^{2+}]_i$ may lead to triggered myocyte contractions and delayed after depolarizations that could elicit triggered arrhythmias (Daniels, 1992). Arrhythmias may also be triggered by amphiphilic compounds. These compounds are formed during reoxygenation - either by free oxygen radicals or by activated phospholipases - and penetrate the plasmalemma and membranes of cell organelles, causing inhibition of Ca^{2+} ATPase and Na^+/K^+ -ATPase (Karli et al., 1979; Katz and Messineo, 1981). Acidosis, due to accumulation of myocardial CO_2 , enhances the arrhythmogenic properties of amphiphilic agents (Gross and Soble, 1982).

Adrenergic stimulation may contribute to the electro-physiological changes and trigger arrhythmias as well (Culling et al., 1984; Sharma and Corr, 1983). However, the exact electrophysiological mechanisms remain to be elucidated (Pogwizd et al., 1986).

III A Ca^{2+} HOMEOSTASIS DURING NORMOXIA

Ca^{2+} ions enter the cell during the slow inward current, I_{ss} , at the plateau phase (phase 2) of the action potential. Although in itself of sufficient amount, it is unable to activate the myofilaments, since it is immediately sequestered by the sarcoplasmic reticulum and bound to calmodulin (Fabiato, 1981; Lewartowski, 1983). Additional release by two cellular mechanisms has been proposed. According to Fabiato, the increase of $[\text{Ca}^{2+}]_i$, particularly at a high rate, triggers release of additional Ca^{2+} ions from release sites in the sarcoplasmic reticulum (Fabiato and Fabiato, 1975; Fabiato, 1985; Fabiato, 1983; Winegrad, 1982). Although the exact working mechanism is still unknown, these investigators have shown that the Ca^{2+} channel in the SR is activated by $[\text{Ca}^{2+}]_i \leq 8 \mu\text{M}$ and inactivated at higher $[\text{Ca}^{2+}]_i$.

Lüllman and Peeters, on the other hand, have proposed that the transverse tubuli, which are extensions of the cell membrane, have high affinity membrane potential-dependent binding sites for Ca^{2+} (Lüllman and Peters, 1977). Following depolarization, these binding sites release Ca^{2+} . The resulting elevation of $[\text{Ca}^{2+}]_i$ would then lead to activation of the myofilaments.

About 60% of the released Ca^{2+} is again sequestered in the SR as a result of the activity of SR Ca^{2+} -ATPase (Ikemoto, 1982). Two Ca^{2+} ions are transported into the SR lumen at the expense of hydrolysis of 1 molecule of MgATP (Kanazama, 1971). Following a delay, the sequestered Ca^{2+} is again available for renewed release, which is supposed to be the basis of the time dependence of recovery of force development (mechanical restitution) (Banijamali et al., 1991; Edman and Johansson, 1976; Schouten, 1985). The pump activity increases following adrenergic stimulation that facilitates phosphorylation of phospholamban by c-AMP (Morad, 1972).

The remaining Ca^{2+} is mainly extruded from the cell by $\text{Na}^+/\text{Ca}^{2+}$ exchange (Chapman, 1979).

The rate and direction of the exchange is determined by: 1) the Na^+ gradient maintained by the Na^+/K^+ ATPase; 2) the Ca^{2+} gradient and; 3) the membrane potential (Mullins, 1979).

In addition, Ca^{2+} -ATPase in the sarcolemma extrudes Ca^{2+} continually from the cell at a low rate (Caroni and Carafoli, 1980). Under normal conditions mitochondria are not involved in Ca^{2+} homeostasis (Langer et al., 1982; Williams, 1983).

The affinity constants for Ca^{2+} (K_m (Ca^{2+})) in vitro of the Ca^{2+} pumps of the sarcolemma, the SR and the mitochondria are 0.3 - 1.0 μM , 1.5 - 1.9 μM and 15 - 100 μM respectively (Caroni and Carafoli, 1980; Crompton et al., 1976; Solaro and Briggs, 1974). Assuming that these data also apply to the living cell, the Ca^{2+} pump in the sarcolemma continually extrudes Ca^{2+} at low $[\text{Ca}^{2+}]_i$, whereas the SR is active at higher concentrations. Although the opposite has been stated, it is still generally assumed that $\text{Na}^+/\text{Ca}^{2+}$ exchange results in net Ca^{2+} efflux during the twitch, in particular during the relaxation phase.

III B Ca^{2+} + HOMEOSTASIS DURING ISCHEMIA

Hypoxia leads to increased $[\text{Na}^+]_i$ by inhibition of the Na^+/K^+ ATPase of the sarcolemma. However, Na^+ ions may also directly enter through the Ca^{2+} channel (Hess and Tsien, 1986). The increased $[\text{Na}^+]_i$, in turn, may reduce $\text{Na}^+/\text{Ca}^{2+}$ mediated Ca^{2+} extrusion and thereby elevate $[\text{Ca}^{2+}]_i$ (Allen and Orchard, 1983; Mandel, 1982; Orchard, 1986; Smith et al., 1985). In addition, palmitoyl carnitine that accumulates due to inhibition of the oxydative phosphorylation during ischemia, is known to enhance Ca^{2+} channel activity (Corr et al., 1984; Spedding and Mir, 1987).

Intracellular $[\text{Ca}^{2+}]_i$ is known to increase gradually during ischemia (Steenbergen et al. 1987; Lee and Allen, 1992). $[\text{Ca}^{2+}]_o$ seems to determine $[\text{Ca}^{2+}]_i$ that is ultimately attained; low $[\text{Ca}^{2+}]_o$ (100 μM) prior to ischemia attenuates the ischemia-induced $[\text{Ca}^{2+}]_i$ rise, delays the onset, and reduces maximal ischemic contracture (Jimenez et al., 1990). During hypoxia $[\text{Ca}^{2+}]_i$ remains elevated since the regulatory function of the SR is lost; its Ca^{2+} ATPase is inoperative as a result of the low energy yield from ATP hydrolysis or due to accumulation of inorganic phosphate or both (Allen et al., 1985; Allen and Orchard, 1983; Fabiato and Fabiato, 1978; Zhu and Nosek, 1991).

Increased $[\text{Ca}^{2+}]_i$ may either directly stimulate Na^+/H^+ exchange or give rise to further elevation of $[\text{H}^+]_i$ via several mechanisms (Villereal, 1981). Ca^{2+} ions either compete with H^+ ions for binding to proteins, or accumulate in mitochondria in exchange for protons (Crompton and Heid, 1978; Vercesi et al., 1978). Alternatively activation of lipases and actomyosin ATP consumption may enhance anaerobic glycolysis, resulting in more cellular acidosis; in addition lipases will damage cell organelles and membranes (Adams, 1979; Imai, 1983).

Increased intracellular proton concentration, in turn, increases Na^+/H^+ exchange which leads to increased $[\text{Na}^+]_i$ (Anderson et al., 1991; Cingolani et al., 1990; Mahnensmith and Aronson, 1985). Unless these mechanisms can be inhibited, a steady increase of the concentrations of Na^+ , Ca^{2+} and H^+ would be expected.

At the onset of hypoxia the Ca^{2+} transient is comparable to normoxia, suggesting that Ca^{2+} homeostasis by the SR is initially intact (Allen and Orchard, 1983). The same applies to the intracellular concentrations of Na^+ , Ca^{2+} and H^+ which initially do not increase dramatically. The observation that $\text{Na}^+/\text{Ca}^{2+}$ exchange is only partially inhibited by acidosis seems in agreement with this assumption; the exchange rate appeared to depend on $[\text{ATP}]_i$ by a hitherto unknown mechanism (Haigney et al., 1992; Philipson et al., 1982; Reinlib et al., 1981). Recent reports of NMR measurements showed that 10 minutes after the onset of total ischemia average Ca^{2+}_i was substantially increased (Marban et al., 1989; Steenbergen et al., 1987; Steenbergen et al., 1990; Carroza et al., 1992).

However, restricted coronary perfusion which does not result in lowered energy phosphate concentrations, has been shown to be accompanied by a marked decline in the amplitude of Ca^{2+}

transients and thereby impaired contractility. Although the underlying mechanism is unresolved, it is conceivable that this mechanism will restrict energy consumption during ischemia (Kaplan et al., 1992; Marban et al., 1988). During ischemia the number of membranous particles of SR, representing the Ca^{2+} ATPase, may be reduced by 50% as shown by electronmicroscopy. Moreover, the SR may swell and ultimately rupture (McCallister, 1978; Tillack, 1974).

III C Ca^{2+} HOMEOSTASIS DURING REOXYGENATION

Following ischemia, intracellular concentrations of Na^+ , Ca^{2+} and H^+ are increased; membrane pumps that are normally involved in Ca^{2+} homeostasis of the cell are inoperative due to low ATP levels. Intracellular acidosis protects the myocardium against a number of unfavourable effects of ischemia; it reduces Ca^{2+} influx into the cells and/or prevents contracture by reversible proton occupation of intracellular Ca^{2+} binding sites (Kitazake et al., 1988). Therefore, as soon as pH_i normalizes early after reperfusion, $\text{Na}^+/\text{Ca}^{2+}$ exchange is no longer inhibited and $[\text{Ca}^{2+}]_i$ increases steadily. This process is enhanced by Na^+ entry that is caused by Na^+/H^+ exchange mediated H^+ extrusion (Mahnensmith and Aronson, 1985). The group of Lakatta and others have shown that the increase of $[\text{Ca}^{2+}]_i$ is accompanied by incremental spontaneous sarcomere shortening and changes in relaxation characteristics. The increase in $[\text{Ca}^{2+}]_i$ following reperfusion appears directly related to $[\text{Na}^+]_i$ prior to reoxygenation, and independent of CrP or ATP (Jeremy et al., 1992; Grinwald, 1982; Lakatta, 1992; Renlund et al., 1984). Complete recovery of Na^+/K^+ pump activity, which enables $[\text{Na}^+]_i$ and thus $[\text{Ca}^{2+}]_i$ to normalize, is an absolute requirement for restoration of cell function (Pike et al., 1990).

Alternatively reperfusion induced Ca^{2+} overload may be explained by direct Ca^{2+} influx and/or disruption of the cell membrane, due to Ca^{2+} activated cytosolic enzymes. Scanning electron micrographs have shown that anoxia gives rise to reversible sarcolemmal protrusions of small 'microblebs' (1 μm in diameter). In addition, subsarcolemmal vesicles have been reported that sometimes communicate with the interstitial space (Piper et al., 1984). Since the number of 'blebs' increases with the duration of anoxia, it has been proposed that they may represent initial local structural weakening of the sarcolemma (Sage and Jennings, 1988). Recently comparable observations have been reported in skeletal muscle. Provided that this hypothesis is correct, it is conceivable that the abnormal sarcolemma of damaged myocytes may be disrupted by contraction of neighbouring cells or development of contracture (Daly et al., 1987; Ganote, 1983). The mechanical hypothesis however is challenged by investigators who were unable to demonstrate considerable release of intracellular enzymes or increased Ca^{2+} uptake, immediately following reoxygenation (Poole-Wilson et al., 1984). Another hypothesis proposes selective damage to the cell membrane, either by phospholipases or by accumulation of acyl esters (Gazitt, 1976; Katz and Messineo, 1981). Subsequent Ca^{2+} overload would result from Ca^{2+} ions that enter the cell directly. The damage could also have been induced by peroxidation of sarcolemmal lipids by free oxygen radicals (Kukreja and Hess, 1992). Free oxygen radicals are formed either from hypoxanthine or because normal scavenger enzymes are disabled. Other possible mechanisms of myocardial cell membrane damage include myocardial cell swelling, the effects of low tissue ATP and NAD on membrane integrity and other hypotheses that have been reviewed extensively elsewhere (Poole-Wilson et al., 1984). Consistent with the central role of $[\text{Ca}^{2+}]_i$ it was shown that postischemic low Ca^{2+} (0.05 mmol/l) perfusion may reduce reperfusion damage, albeit at the expense of enhanced susceptibility of the heart to the calcium paradox (Kirkels et al., 1989).

In conclusion, many of the mechanisms discussed above are involved in the Ca^{2+} fluxes during reoxygenation. However, the precise interaction between the different pathophysiological processes, which predetermine the outcome of reoxygenation, i.e. full recovery or cell death, remains incompletely understood.

IV THE CONTRACTION-RELAXATION CYCLE

IV A FORCE DEVELOPMENT AS A FUNCTION OF TIME, $[Ca^{2+}]$ AND SARCOMERE LENGTH DURING NORMOXIA

Energy consumption by the contracting heart is determined by basal metabolism, ion transport during excitation contraction and ATP hydrolysis by the myofilaments. Recently it has been proposed that total mechanical energy output of the ventricle is represented by the pressure volume area (PVA). The pressure volume area represents the sum of externally performed stroke work and is approximated by $P \cdot (V_{ed} - V_{es})$. The potential energy component is derived from the end systolic pressure volume relationship; it equals to $1/2 P_{es} (V_{ed} - V_{es})$ (Suga, 1990).

The relationship between myocardial oxygen consumption and PVA has been shown to be linear. The slope of the relationship reflects the efficiency of the chemo-mechanical transducer, its intercept is determined by the sum of the energy required for basal metabolism and the excitation contraction coupling. Recent studies indicated that during metabolic inhibition or rigor maximally 50% of the total ATP turnover depends on force (Loiselle, 1987). Another study suggested that only 18 % of total energy expenditure was accounted for by stroke work, 34% by excitation contraction coupling, 39 % by basal metabolism and less than 10 % by generation of the action potential (Gao et al., 1992). The discrepancy between these reports may be explained, at least in part, by differences in external work performed and by differences in endogenous catecholamine release as well as by variations in $[Ca^{2+}]$ and Ca^{2+} cycling. Total external power output is determined on the one hand by the changes in pressure, volume and flow during systole and diastole and on the other hand by aortic pressure and impedance of the vascular bed (Milnor et al., 1966). It is oscillatory since pressure and flow are oscillatory. A stiffer arterial system results in pressure fluctuations that sometimes equal 40% of the total stroke work of the heart (Elzinga, 1983). The contribution of kinetic energy, which is mainly determined by the bloodflow, is only 1% of the total mechanical work (Elzinga, 1983; McDonald, 1974).

The changes in the geometry of a pumping heart indirectly result from changes in length of the sarcomeres. The ability of the heart to generate pressure is not only determined by the sarcomeres but also by their contractile state i.e. contractility. Contractility may be defined as the transient interrelation between force, length, and velocity of shortening that is modulated by shortening and load (Brutsaert, 1987).

Contractility is determined by the level of activation of the contractile proteins. This, in turn, is determined by the amount of Ca^{2+} ions released in the cytosol, the sensitivity of the contractile proteins to Ca^{2+} and the intrinsic ability of the myofilaments to generate force.

The amount of Ca^{2+} ions released in the cytosol has been shown to be determined by the amount and rate of entry of Ca^{2+} ions during the action potential. Thus, shortening of the action potential reduces Ca^{2+} influx and thereby contractility (Antoni et al., 1969), while β catecholamine activation through the c-AMP dependent second messenger increases the Ca^{2+} influx (Reuter, 1974) and enhances contractility. Furthermore, intracellular $[Ca^{2+}]$ may increase as a result of limitation of Ca^{2+} extrusion by inhibition of Na^+/Ca^{2+} exchange; consequently force of contraction will rise (Pitts, 1979; Reuter, 1974).

It has been suggested that the Ca^{2+} sensitivity of the myofilaments decreases upon β adrenergic stimulation due to TnI phosphorylation, which is expected to accelerate the rate of force relaxation. Although force development is expected to decrease as a result, this is apparently offset by the increase of Ca^{2+} influx (see above), such that an increase in force development, concomitant with an increased rate of force relaxation is actually observed. Finally β adrenergic stimulation causes phosphorylation of phospholamban in the SR, which results in an increased rate of Ca^{2+} uptake, mediated by the SR Ca^{2+} ATP-ase. This is expected to increase the amount of Ca^{2+} stored in the SR, as well as increase the rate

of force relaxation. The affinity of the myofilaments may also shift towards higher Ca^{2+} concentrations when $[\text{H}^+]$ or $[\text{Mg}^{2+}]$ increase, particularly in diseased states (Donaldson et al., 1978; Fabiato and Fabiato, 1978). Likewise, increased ADP and P_i concentrations may influence the rate of ATP hydrolysis and hence decrease force development.

The intrinsic ability of the myofilaments to generate force is determined by the myofilament isoenzyme composition. It is generally accepted that changes in the cellular and regional ventricular isomyosin distribution determine work that may be performed (Gorza et al., 1981; Brutsaert, 1987). However, such changes generally occur in the course of days to weeks. Although this has not been confirmed, it has been suggested that the number of contractile elements may change rapidly by activation of fast myosin following β adrenergic stimulation (Winegrad, 1982).

The contractile apparatus is activated following excitation; myosin interacts with actin, resulting in force generation and shortening of the cell by sliding of the filaments along each other. According to the classical crossbridge theory of muscle contraction, this interaction is mediated by crossbridges (Eisenberg and Hill, 1985; Huxley, 1957 and 1969; but see Pollack, 1983). Although other fundamentally different contraction models have been proposed (Noble and Pollack, 1977; Pollack, 1983), this discussion will be confined to Huxley's model which is still widely accepted (). The interaction between actin and myosin begins when Ca^{2+} binds to troponin-C. This causes tropomyosin to shift toward the center of the groove between the actin strands, thereby reversing its inhibitory action. As a result the cross-bridge binding sites are exposed and myosin attaches to actin (Huxley et al, 1982). Then, structural changes of the myosin head are thought to generate the force that causes sliding of actin toward the center of the sarcomeres. Inorganic phosphate is released from myosin during the so-called power stroke of the cross-bridge, followed by ADP release (Eisenberg & Green, 1980; Huxley & Simmons, 1971). Shortening of the myofilaments accelerates the release of ADP and P_i from myosin. Upon rebinding of ATP to myosin, individual crossbridges detach (Eisenberg and Hill, 1985). ATP is hydrolyzed by myosin ATPase and the head returns to its original position. During the next contraction cycle myosin may bind again to actin, leading to repetition of the sequence of events that are described above. Relaxation results when the crossbridges detach from the thin filament and resume their resting position; concomitantly tension decays (Huxley, 1987).

The cycling of crossbridges depends their load, determined by the external load as well as on the number of attached cross bridges which depends on cytosolic $[\text{Ca}^{2+}]$ and $[\text{ATP}]$. The cycling rate is determined by the speed of ATP hydrolysis by myosin ATPase, which depends on the load per bridge. The activity of the Mg-ATPase is also strongly influenced by the concentration of breakdown products in particular P_i , ADP and H^+ (Fabiato and Fabiato, 1978; Kawai and Brandt, 1980; Kentish, 1986).

The minimal operating length of the sarcomeres in heart muscle is $1.6 \mu\text{m}$, equal to the length of the myosin filament. However, shorter sarcomere lengths have been reported in activated skinned preparations (Fabiato and Fabiato, 1976; Huxley and Hanson, 1954; Winegrad and Robinson, 1978). Maximal twitch force is determined by the actomyosin overlap and increases with sarcomere length (Fabiato and Fabiato, 1976; ter Keurs et al., 1980; Patterson et al., 1914). The sarcomere length in resting muscle at slack length is approximately $1.85 \mu\text{m}$. Passive force, i.e. the force that is required to stretch the unstimulated preparation, is negligible at $\text{SL} = 2 \mu\text{m}$ but increases steeply at higher sarcomere lengths. The maximal length of the sarcomeres in heart muscle is $2.4 \mu\text{m}$. The steep increase in passive force above $2.4 \mu\text{m}$ results from stretch of the sarcolemma and intercellular connections and the elastic collagen mesh that envelops the cell, as well as by proteins connecting myosin to the Z-lines (actinin, connectin and others) (Magid et al., 1984; Robinson et al., 1983). It is unlikely that the passive force results from compression of the negatively charged myosin filament lattice, since this force is very small in skeletal muscle at comparable sarcomere lengths (Allen and Kentish, 1985; Elliott et al., 1963).

Under normal conditions the physiological range of sarcomere lengths in the heart is limited to 1.6 - 2.3 μm (ter Keurs, 1983).

The ability of myocytes to generate active force is a function of sarcomere length (Kentish et al., 1986; Pollack and Krueger, 1976; ter Keurs, 1980) and peak twitch force is related to sarcomere length. The relationship between active force and sarcomere length is convex toward the ordinate at $[\text{Ca}^{2+}]_o = 2.5 \text{ mM}$. The relationship is convex toward the abscissa at $[\text{Ca}^{2+}]_o = 0.3 \text{ mM}$ and linear at intermediate $[\text{Ca}^{2+}]_o$. The relationship is similar for hearts of many species like sheep, pig, dog, ferret and rat (ter Keurs et al., 1986). The force - sarcomere length relation at peak twitch force is independent of SL changes during the contraction. However, the duration of a sarcomere isometric twitch varies with the length at which the sarcomeres are clamped (van Heuningen et al., 1982). Even at higher $[\text{Ca}^{2+}]_o$, the force - sarcomere relation does not reach a plateau. In this thesis we will show experiments on fibers following 'skinning' - i.e. chemical disruption of the cell membrane - which allows direct activation of the preparation, that the Ca^{2+} sensitivity of the myofibrils is length dependent (Kentish et al., 1986). Furthermore we will show that the slope of the force - Ca^{2+} concentration relation increased from 2.82 to 4.54 with sarcomere length between 1.75 and 2.15 μm . Since the change in Ca^{2+} sensitivity is seen over the entire range of sarcomere lengths we conclude that this could explain the properties of the contractile machinery, notably the shape of the ascending limb of the force - sarcomere length relation in the intact cardiac muscle (Kentish et al., 1986).

It has been observed that the shortening velocity of heart muscle, which corresponds to the myosin ATP-ase activity (Barany, 1967), is related to force and Ca^{2+} (Katz, 1979). The inverse relationship between force and velocity of shortening in cardiac papillary muscles was first described by Abbott and Mommaerts (Abbott and Mommaerts, 1959). Recent studies with laser diffraction techniques have confirmed that the velocity of sarcomere shortening closely follows this relationship, both during load clamps and muscle releases at constant velocity (Daniels et al., 1984). The velocity of sarcomere shortening deviates from the hyperbolic relationship at high forces (Edman, 1986); as yet this finding is incompletely understood.

Lastly, the velocity of sarcomere shortening (v_o) of intact Rat cardiac trabeculae is maximal beyond 25 ms after the onset of the twitch and at $[\text{Ca}^{2+}]_o$ and SL above 1.2 mM and 1.85 μm respectively. The observation that the velocity of sarcomere shortening reaches a maximum at $[\text{Ca}^{2+}]_o$ where twitch force is approximately 60% of its maximum, may be crucial to the understanding of the underlying mechanisms (ter Keurs, 1983; de Tombe and ter Keurs, 1992).

The contraction begins when Ca^{2+} enters the cell during the slow phase of the action potential; this triggers release of more Ca^{2+} from the SR (see before). The ensuing free calcium transient may be monitored by means of light emitting proteins like aequorin or by changes of fluorescent properties of quin-2 and arsenazo III (Allen and Blinks, 1978; Fabiato, 1980). Following activation, an initial rapid increase of emitted light of aequorin is observed, that is accounted for by an increase of the $[\text{free Ca}^{2+}]_i$. Subsequently the light transient decreases more slowly; the latter transient is determined by the equilibrium between rapid ($< 1 \text{ ms}$) binding and slower dissociation of Ca^{2+} from troponin and extrusion mechanisms like uptake in the SR and $\text{Na}^+/\text{Ca}^{2+}$ exchange (Robertson, Johnson, and Potter, 1981; Pasipoularides et al., 1985). The light transient has almost returned to control values by the time when twitch force is maximal. It should be mentioned that these data refer to uncorrected measurements by aequorin that are known to underestimate the low free $[\text{Ca}^{2+}]_i$.

Active shortening is known to retard the decline of the transient (Housmans, Lee, and Blinks, 1983; Lab, Allen and Orchard, 1984). Simultaneous measurements of force and $[\text{free Ca}^{2+}]_i$ showed that both the amplitude and time course of the decline of the Ca^{2+} transient decreased over the range of muscle lengths at which tension increased (Allen and Blinks, 1978; Allen and Kurihara, 1982).

The relation between force and $[Ca^{2+}]_i$ at constant SL is sigmoidal in cardiac muscle; the relation may be described as a Michaelis-Menten equation (Kentish et al. 1986; Lehninger, 1970). Increased Mg^{2+} , P_i , CrP and H^+ concentrations result in a shift of the relationship toward higher $[Ca^{2+}]_i$ (Donaldson et al., 1978; Fabiato and Fabiato, 1978; Kentish, 1986; Nosek, Fender and Godt, 1987). The affinity of the binding sites is also decreased upon phosphorylation by c-AMP (England, 1983; Weber, 1968). On the other hand, the sensitivity of the myofilaments for Ca^{2+} increases with increasing SL (Endo, 1973; Hibberd and Jewell, 1979; Kentish et al., 1986).

It has been noted that peak twitch force by intact muscles is 70% of the force that may be generated by direct activation following skinning (Fabiato, 1981; Kentish, 1986). This may be accounted for by a limitation of Ca^{2+} release by the SR at increasing $[Ca^{2+}]_i$ in the intact preparation (Fabiato and Fabiato, 1978). In addition, spontaneous Ca^{2+} release by the SR, induced by increasing $[Ca^{2+}]_o$, may give rise to inhomogeneous sarcomere shortening, resulting in decreased twitch force. We will present evidence that maximal twitch force can still be elicited in intact preparations by means of Sr^{2+} containing solutions; the exact mechanism of action however is unknown (Bucx et al., 1986; Moisesescu and Thieleczek, 1979; Schouten et al., 1990).

IV B THE CONTRACTION-RELAXATION CYCLE DURING ISCHEMIA

Several hypotheses have been proposed to explain the rapid decrease of active force development following ischemia (Tennant and Wiggers, 1935).

The initial hypothesis that hypoxia leads to decreased force by changes in the myofilaments and myosin ATPase could not be confirmed (Albert and Gordon, 1962; Barany et al., 1964; Katz and Hecht, 1969; Katz and Maxwell, 1964). However, recently this notion was challenged by the observation that thin filament protein degradation may contribute to changes in cooperativity of Ca^{2+} regulation of the myofibrillar ATPase in rat hearts, following global ischemia and anoxia for one hour (Westfall and Solaro, 1992).

Acidosis is known to inhibit calcium binding to the myofilaments and to impair calcium uptake by the sarcoplasmic reticulum (Fabiato, 1983; Ricciardi et al., 1986; Levitsky and Benevolensky, 1986). Intracellular pH can be measured by means of N.M.R.. However, the spatio-temporal resolution of this technique is insufficient to monitor changes at the subcellular level. Therefore, the location and timing of chemical reactions that give rise to proton accumulation are as yet incompletely understood (Gevers, 1977). Initially hypoxia may even lead to transient alkalosis, as a result of CrP breakdown, which enhances force (Allen et al., 1985; Danforth, 1965). The observation that force is equally depressed by ischemia or hypoxia, in spite of lower intracellular pH in the first condition and less obviously in the second, also argues against intracellular pH as primary cause of contractile failure (Cobbe and Poole-Wilson, 1980).

Ischemia causes ATP depletion which may impair excitation-contraction coupling. Although this seems an appealing concept, ATP content is virtually unchanged at the time when twitch force is already severely depressed. However, this does not discard the possibility that ATP content in subcellular compartments, notably in the vicinity of the sarcolemma or the myofilaments, may be insufficient (Gudbjarnason et al., 1970). However, skinned fiber experiments have shown that maximal force may be attained over a range of $[ATP]$ from 5 to 0.05 mM (Fabiato and Fabiato, 1975). Decreased $[ATP]$ could give rise to direct cell damage and/or activation of K^+ channels (Isenberg et al., 1983; Kubler and Katz, 1977; Noma, 1983). Alternatively, reduced free energy of hydrolysis of ATP has been proposed to explain early ischemic mechanical failure in spite of the presence of substantial amounts of ATP (Fiolet et al., 1984; Gibbs, 1987; Kammermeier et al., 1982). Recently it was shown that inorganic phosphate, resulting from high-energy phosphate hydrolysis, may reduce twitch force instantaneously (Kentish, 1986;

Koretsune and Marban, 1990; Silverman et al., 1991). The diprotonated phosphate, which is formed during acidosis, has a stronger depressant effect than the monoprotonated form in skeletal muscle (Nosek et al., 1987). Initially it was assumed that phosphate would trap cytosolic Ca^{2+} inside organelles as calcium phosphate; however experiments with Ca^{2+} sensitive indicators discarded this possibility (Allen and Orchard, 1983; Kubler and Katz, 1977). The negative inotropic effect of phosphate is probably accounted for by direct inhibition of myosin ATP-ase (Kentish, 1986). However, other metabolites like superoxide anion are also able to depress maximum calcium activated force without alteration of the calcium sensitivity (Macfarlane and Miller, 1992).

Alternative explanations for the acute decrease of twitch force by hypoxia include the negative effect of the diminished action potential duration on Ca^{2+} release by the SR (Downar, Janse, and Durrer, 1977). It is also conceivable that reduced ATP may directly influence Ca^{2+} release sites of the SR since these channels are activated by adenine-nucleotides (ter Keurs et al., 1988; Smith et al., 1985).

A recent hypothesis suggests that the endothelial lining of the coronary vasculature may play a role in the modulation of force development. Indirect evidence suggests that collapse of the intravascular pressure may lead to a reduction in the sarcomere length of the myocardial cells that surround the vessels and a consequent fall in tension development via the Frank-Starling effect (Koretsune et al., 1991). This concept is known in the literature as the 'garden hose' or 'erectile' effect. It has been demonstrated that force generation could increase in response to perfusion pressure in hearts that already had been stretched to their optimal end-diastolic length. This effect was explained by assuming that the vessels act as struts that potentiate the strength of myocardial contraction, independent of sarcomere length (Kitakaze and Marban, 1989).

Observations by Schouten suggested that contractility in postischemic rat hearts was enhanced but pump function as a whole depressed as a result of advanced injury to local contractures and development of general contracture due to Ca^{2+} overload (Schouten et al., 1991). Comparable distinctive contractile, metabolic, and histologic sequelae following transient exposure of Ferret heart to high $[\text{Ca}^{2+}]_i$ without ischemia may indicate that the same underlying mechanism is involved (Kitakaze et al., 1988).

The diastolic properties of cardiac muscle are also modified by ischemia (Lewis et al., 1980). Differences of the effects of ischemia on compliance of heart muscle, observed in experimental models, critically depend on the model of ischemia that is applied i.e. decreased supply versus increased demand by an increase of heart rate (Apstein and Grossman, 1987). In the former, diastolic compliance initially increases, whereas it decreases in the latter. Both the influence of pressure and volume in the coronary vasculature, the mechanical effects of surrounding non-ischemic myocardium and several metabolic factors, notably lower pH and higher phosphate content, may be responsible for the observed differences. Although the pericardium is not actively involved, it may indirectly affect diastolic compliance (Tyberg et al., 1978). In global ischemia the increased compliance is relatively short lived compared to regional ischemia; prolonged ischemia ultimately results in decreased compliance in all models of ischemia (Wyman et al., 1989).

The elevated diastolic force may initially be accounted for by a combination of increased $[\text{Ca}^{2+}]_i$ and lack of ATP in the vicinity of the myofilaments (Holubarsch et al., 1982; Kingsley et al., 1991; Leijendekker et al., 1990; Paulus et al., 1985; Ventura-Clapier and Vassort, 1981). During prolonged ischemia however, decreased [ATP] in the vicinity of the myofilaments may ultimately give rise to rigor bond formation (Allen and Orchard, 1983; Hannon et al., 1992; Holubarsch et al., 1982; Ventura-Clapier and Vassort, 1981). The latter process is reversible until the moment when the ultrastructure of the cell is damaged. The possible mechanisms that contribute to cell destruction and cell death are discussed extensively elsewhere (see Poole-Wilson et al., 1984). Ultimately muscle compliance will decrease due to continuous actomyosin activation and formation of rigor bonds (Apstein and Grossman, 1987; Lowe et

al., 1985). Cell death results when vital cell organelles like SR and mitochondrial and sarcolemmal membranes are destroyed.

IV C THE CONTRACTION-RELAXATION CYCLE DURING REOXYGENATION

It has been observed that recovery of force generation by reperfused myocardium lags behind restoration of ion homeostasis and high-energy phosphate metabolism. This condition is referred to as stunning (Kusuoka and Marban, 1992). Research by the group of Marban and others has indicated that contractile failure in stunned myocardium may be due to a decreased myofilament sensitivity for Ca^{2+} as well as to a decrease in maximal Ca^{2+} activated force whereas activator Ca^{2+} transients exceed normoxic amplitude (Ohgoshi et al., 1991). This implies an increased ATP consumption rate to sequester released Ca^{2+} , resulting in decreased efficiency of energy utilization (Kusuoka et al., 1990). Stunning is accompanied by considerable prolongation of relaxation time and other twitch parameters. This pattern was observed even following ischemia of such short duration (≤ 15 minutes) that histological or histochemical damage is not induced. Repeated, brief episodes of ischemia aggravate the observed changes in contraction (Braunwald and Kloner, 1982; Gefit et al., 1982). Part of these effects may be accounted for by reactive hyperemia which may preclude effective reperfusion (Fox et al., 1985). However, since recovery of contractile function in intact animals may require several weeks, it is possible that factors, like destruction of intracellular matrix by activated endogenous procollagenases, loss of myofibrils or increased spacial separation between the myofilaments, and fibrosis are involved over and above resynthesis of contractile proteins (Charney et al., 1992; Schaper, 1988; Zhao et al., 1991).

One of the underlying mechanisms of these phenomena includes Ca^{2+} overload as a result of inhibition of membrane pumps that are normally involved in Ca^{2+} homeostasis. These include the Ca^{2+} ATPase of the sarcolemma and the SR, as well as the Na^+/K^+ ATPase of the sarcolemma. Increased influx, reduced efflux, changed sequestration in the SR or a combination of these factors may be involved in the observed increase of Ca^{2+} content. Ca^{2+} influx may accelerate as a result of increased alpha-receptor density and membrane damage, secondary to oxygen free radicals or lipid metabolites (Corr et al., 1983; Katz and Messineo, 1981; Nayler et al., 1980; Witkowski and Corr, 1984). Efflux of Ca^{2+} from the cell may be restricted due to decreased $\text{Na}^+/\text{Ca}^{2+}$ exchange - secondary to increased $[\text{Na}^+]_i$ - and limited Ca^{2+} extrusion by the sarcolemmal Ca^{2+} -ATPase. Ca^{2+} uptake by the SR may be limited due to the reduced ATP content of the cell immediately following reoxygenated. We will present evidence in this thesis that twitch duration may be prolonged and relaxation delayed as a result of spontaneous Ca^{2+} release by the SR, triggered by the increase of $[\text{Ca}^{2+}]_i$ (Brutsaert, 1987; Bucx et al., 1987; Nakamura, Wiegner, and Bing, 1986).

The diastolic compliance of the intact heart initially decreases during reperfusion due to increased coronary turgor as a result of coronary hyperemia (Vogel et al., 1985). The improvement or aggravation which follows thereafter is determined by metabolic factors like cellular Ca^{2+} level and ATP content (Apstein and Grossman, 1987). As soon as Ca^{2+} homeostasis is restored and ATP content is normalized, normal diastolic compliance is regained. Provided that cellular ultrastructure is intact, contractile performance may be fully restored. The exact factors that determine irreversibility of ischemic damage however are still unknown.

In summary, in this overview of the currently available data the changes in the main functions of the human myocardium, which may result from ischemia, appear reversible provided ischemia is shortlasting. The time required for energy metabolism, excitation - contraction coupling, Ca^{2+} homeostasis and the contraction - relaxation cycle to recover, depends not only on the first but also on the

duration of the preceding ischemic period. When ischemia exceeds one hour, the changes in the cell function are usually irreversible. Until now, the mechanisms that determine irreversibility are incompletely understood.

REFERENCES

1. Abbott BC, Mommaerts WFHM. A study of inotropic mechanisms in the papillary muscle preparation. *J Gen Physiol* 1959; 42: 533-551
2. Adams RJ, Cohen DW, Gupte S, Johnson JD, Wallick ET, Wang T, Schwartz A. In vitro effects of palmitylcarnitine on cardiac plasma membrane Na,K-ATPase and sarcoplasmic reticulum Ca^{2+} -ATPase and Ca^{2+} transport. *J Biol Chem* 1979; 254: 12404-12410
3. Akaishi M, Weintraub WS, Schneider RM, Klein LW, Agarwal JB, Helfant RH. Analysis of systolic bulging; mechanical characteristics of acutely ischemic myocardium in the conscious dog. *Circ Res* 1986; 58: 209-217
4. Albert NR, Gordon MA. Myofibrillar adenosine triphosphatase activity in congestive heart failure. *Am J Physiol* 1962; 202: 940-946
5. Allen DG, Orchard CH. Myocardial contractile function during ischemia and hypoxia. *Circ Res* 1987; 60: 153-168
6. Allen DG, Morris PG, Orchard CH, Pirolo JS. A nuclear magnetic resonance study of metabolism in the ferret heart during hypoxia and inhibition of glycolysis. *J Physiol* 1985; 361: 185-204
7. Allen DG, Orchard CH. The effect of pH on intracellular calcium transients in mammalian cardiac muscle. *J Physiol* 1983; 335: 555-567
8. Allen DG, Orchard CH. The effect of hypoxia and metabolic inhibition on intracellular calcium in mammalian heart muscle. *J Physiol* 1983; 339: 107-122
9. Allen DG, Kurihara S. The effects of muscle length on intracellular calcium transients in mammalian cardiac muscle. *J Physiol* 1982; 327: 79-94
10. Allen DG, Blinks JR. Calcium transients in aequorin-injected frog cardiac muscle. *Nature [Lond]* 1978; 273: 509-513
11. Allen DG, Kentish J. The cellular basis of the length-tension relation in cardiac muscle. *J Mol Cell Cardiol* 1985; 17: 821-840
12. Allen DG, Morris PG, Orchard CH. A transient alkalosis precedes acidosis during hypoxia in ferret heart. *J Physiol* 1983; 245: 58P
13. Allen DG, Orchard CH. The effect of hypoxia and metabolic inhibition on intracellular calcium in mammalian heart muscle. *J Physiol* 1983; 339: 107-122
14. Anderson SE, Murphy E, Steenbergen C, London RE, Cala PM. Na-H exchange in myocardium: Effects of hypoxia and acidification on Na^+ and Ca^{2+} . *Am J Physiol Cell Physiol* 1990; 259: C940-C948
15. Antoni H, Jacob R, Kaufman R. Mechanische reaktionen des frisch und saugetermyokards bei veränderung aktionspotential-danez durch konstante gleichström impulse. *Pflügers Arch Ges Physiol* 1969; 306: 33-57
16. Apstein CS, Grossman W. Opposite initial effects of supply and demand ischemia on left ventricular diastolic compliance: the ischemia-diastolic paradox. *J Mol Cell Cardiol* 1987; 19: 119-128
17. Aronson PS. Kinetic properties of the plasma membrane Na^+ - H^+ exchanger. *Annu Rev Physiol* 1985; 47: 545-560
18. Arts MGJ. A mathematical model of the dynamics of the left ventricle and the coronary circulation. Thesis. University of Limburg, Maastricht. The Netherlands. 1978.
19. Arts T, Veenstra PC, Reneman RS. Transmural course of stress and sarcomere length in the left ventricle under normal hemodynamic circumstances. In: *Cardiac Dynamics*, edited by J Baan, AC Arntzenius and EL Yellin. Martinus Nijhoff Publishers, The Hague, 1980, pg 115-122
20. Babu A, Sonnenblick E, Gulati J. Molecular basis for the influence of muscle length on myocardial performance. *Science* 1988; 240: 74-76
21. Balaban RS, Kantor HL, Katz LA, Briggs RW. Relation between work and phosphate metabolite in the in vivo paced mammalian heart. *Science* 1986; 232: 1121-1123
22. Ballard FB, Danforth WH, Staegle S, Bing RJ. Myocardial metabolism of fatty acids. *J Clin Invest* 1960; 39: 717-723

23. Banijamali HS, Gao WD, MacIntosh BR, ter Keurs HEDJ. Force-interval relations of twitches and cold contractures in rat cardiac trabeculae. Effect of ryanodine. *Circ Res* 1991; 69: 937-948
24. Barany M. ATPase activity of myosin correlated with speed of muscle shortening. *J Gen Physiol* 1967; 50: 197-216
25. Barany M, Gaetjens E, Barany K, Karp E. Comparative studies of rabbit cardiac and skeletal myosins. *Arch Biochem Biophys* 1964; 106: 280-293
26. Berne RM, Winn HR, Knabb RM, Ely SW, Rubio R. Blood flow regulation by adenosine in heart, brain and skeletal muscle. In: *Regulatory function of adenosine*. Edited by RM Berne, TW Rall, R Rubio. Martinus Nijhoff, The Hague, 1983, pg 293-313
27. Berne RM, Rubio R. Coronary Circulation. In: *Handbook of Physiology; Section 2: Volume 1, The Cardiovascular System*, edited by RM Berne, N Sperelakis, RS Geiger. American Physiological Society, Washington D.C. 1979. pg 873-952
28. Bers DM, Ellis D. Intracellular calcium and sodium activity in sheep heart purkinje fibers. Effect of changes of external sodium and intracellular pH. *Pflügers Arch* 1982; 393: 171-178
29. Bers DM. Excitation-contraction coupling and cardiac contractile force. Kluwer Academic Publishers, Dordrecht, 1991
30. Bessman SP, Geiger PJ. Transport of energy in muscle: the phosphorylcreatine shuttle. *Science* 1981; 211: 448-452
31. Bourdillon PD, Lorell BH, Mirsky I, Paulus WJ, Wynne J, Grossman W. Increased regional myocardial stiffness of the left ventricle during pacing-induced angina in man. *Circulation* 1983; 67: 316-323
32. Braasch W, Gudbjarnason S, Puri PS, Ravens KG, Bing RJ. Early changes in energy metabolism in the myocardium following acute coronary artery occlusion in anesthetized dogs. *Circ Res* 1968; 23: 429-438
33. Braunwald E, Kloner RA. Myocardial reperfusion: a double-edged sword? *J Clin Invest* 1985; 76: 1713-1719
34. Braunwald E. Heart disease. A Textbook of cardiovascular medicine. W.B. Saunders Company. Philadelphia. 1992
35. Braunwald E, Kloner RA. The "stunned" myocardium. *Circulation* 1982; 66: 1146-1149
36. Brutsaert DL. Non-uniformity: a physiologic modulator of contraction and relaxation of the normal heart. *J Am Coll Cardiol* 1987; 9: 341-348
37. Bux JJJ, de Tombe PP, Schouten VJA, and ter Keurs HEDJ. Effect of Sr^{++} on force and sarcomere length in heart muscle of rat. *J Physiol* 1986; 381: 96P
38. Burkhoff D, Weiss RG, Schulman SP, Kalil-Filho R, Wannenburg T, Gerstenblith G. Influence of metabolic substrate on rat heart function and metabolism at different coronary flows. *Am J Physiol Heart Circ Physiol* 1991; 261: H741-H750
39. Bush LR, Buja LM, Samowitz W, Rude RE, Wathen M, Tilton GD, Willerson JT. Recovery of left ventricular segmental function after long-term reperfusion following temporary coronary occlusion in conscious dogs; comparison of 2- and 4-hour occlusions. *Circ Res* 1983; 53: 248-263
40. Cachelin AB, de Peyer JE, Kokubun S, Reuter H. Sodium channels in cultured cardiac cells. *J Physiol* 1983; 340: 389-401
41. Capasso JM, Li P, Anversa P. Nonischemic myocardial damage induced by nonocclusive constriction of coronary artery in rats. *Am J Physiol Heart Circ Physiol* 1991; 260: H651-H661
42. Carafoli E, Penniston JT. The calcium signal. *Sci Am* 1985; 253 (5): 50-58
43. Caroni P, Carafoli E. An ATP-dependent Ca^{2+} -pumping system in dog heart sarcolemma. *Nature* 1980; 283: 765-767
44. Carrozza JP, Bentivegna LA, Williams CP, Kuntz RE, Grossman W, Morgan JP. Decreased myofilament responsiveness in myocardial stunning follows transient calcium overload during ischemia and reperfusion. *Circ Res* 1992; 71: 1334-1340
45. Chapman RA, Coray A, McGuigan JAS. Sodium-calcium exchange in mammalian heart: the maintenance of low intracellular calcium concentration. In: *Cardiac Metabolism* (editors AJ Drake-Holland and MIM Noble), John Wiley and Sons Ltd, Chichester, 1983, page 117-150
46. Chapman RA. Excitation-contraction coupling in cardiac muscle. *Prog Biophys Mol Biol* 1979; 35: 1-52
47. Cingolani HE, Koretsune Y, Marban E. Recovery of contractility and pHi during respiratory acidosis in ferret hearts: role of Na^{+} - H^{+} exchange. *Am J Physiol* 1990; 259(3 Pt 2): H843-848

48. Cobbe SM, Poole-Wilson PA. Tissue acidosis in myocardial hypoxia. *J Mol Cell Cardiol* 1980; 12: 761-770
49. Corr PB, Gross RW, Sobel BE. Amphipathic metabolites and membrane dysfunction in ischemic myocardium. *Circ. Res.* 1984; 55: 135-154
50. Crake T, Poole-Wilson PA. Calcium exchange in rabbit myocardium during and after hypoxia: role of sodium-calcium exchange. *J Mol Cell Cardiol* 1990; 22: 1051-1064
51. Crea F, Pupita G, Galassi AR, Eltamimi H, Kaski JC, Davies G, Maseri A. Role of adenosine in pathogenesis of anginal pain. *Circulation* 1990; 81: 164-172
52. Crompton M, Sigel E, Salzmänn M, Carafoli E. A kinetic study of the energy-linked influx of Ca^{2+} into heart mitochondria. *Eur J Biochem* 1976; 69: 429-434
53. Crompton M, Heid I. The cycling of calcium, sodium and protons across the inner membrane of cardiac mitochondria. *Europ J Biochem* 1978; 91: 599-608
54. Culling W, Penny WJ, Lewis MJ, Middleton K, Sheridan DJ. Effects of myocardial catecholamine depletion on cellular electrophysiology and arrhythmias during ischaemia and reperfusion. *Cardiovasc Res* 1984; 18: 675-682
55. Daly MJ, Elz JS, Nayler WG. Contracture and the calcium paradox in the rat heart. *Circ Res* 1987; 61(4): 560-569
56. Danforth WH. Activation of glycolytic pathway in muscle. In: *Control of energy metabolism* (editors B Chance, RW Eastbrook, JR Williamson), New York, Academic Press, 1965: page 287-297
57. Daniels MCG. Mechanism of triggered arrhythmias in damaged myocardium. Academic Thesis. Utrecht 1991.
58. Daniels MC, ter Keurs HEDJ. Spontaneous contractions in rat cardiac trabeculae. Trigger mechanism and propagation velocity. *J Gen Physiol* 1990; 95(6): 1123-1137
59. Daniels MC, Noble MIM, ter Keurs HEDJ, Wohlfart B. Velocity of sarcomere shortening in rat cardiac muscle: relationship to force, sarcomere length, calcium and time. *J Physiol* 1984; 355: 367-381
60. De Mello WC. Cell-to-cell communications in heart and other tissues. *Prog Biophys Molec Biol* 1982; 39: 147-182
61. Deanfield JE, Maseri A, Selwyn AP, Ribeiro P, Chierchia S, Krikler S, Morgan M. Myocardial ischaemia during daily life in patients with stable angina: its relation to symptoms and heart rate changes. *Lancet* 1983; 2: 753-758
62. Detre K, Holubkov R, Kelsey S et al. Percutaneous transluminal coronary angioplasty in 1985-1986 and 1977-1981; the national heart, lung, and blood institute registry. *N Engl J Med* 1988; 318: 265-270
63. Donaldson SKB, Best PM, Kerrick WGL. Characterization of the effects of Mg^{2+} on Ca^{2+} - and Sr^{2+} -activated tension generation of skinned rat cardiac fibers. *J Gen Physiol* 1978; 71: 645-655
64. Down WH, Chasseand LF, Ballard SA. The effect of intravenously administered phosphocreatine on ATP and phosphocreatine concentrations in the cardiac muscle of the rat. *Drug Res* 1983; 39: 552-554
65. Downar E, Janse JJ, Durrer D. The effect of acute coronary artery occlusion on subepicardial transmembrane potentials in the intact porcine heart. *Circulation* 1977; 56: 217-224
66. Drake-Holland AJ, Elzinga G, Noble MIM, ter Keurs HEDJ, Wempe FN. The effect of palmitate and lactate on mechanical performance and metabolism of cat and rat myocardium. *J. Physiol.* 1983; 339: 1-15
67. Drury AN, Szent-Gyorgyi A. The physiological activity of adenine compounds with especial reference to their action upon the mammalian heart. *J Physiol* 1929; 68: 213-226
68. Durrer D, van der Tweel LH, Berckelouw S, van der Wey AP. Spread of activation in the left ventricular wall of the dog (IV); 2 and 3 dimensional analysis. *Am Heart J* 1955; 50: 860-882
69. Edman KAP. Further characterization of the force-velocity relation in frog skeletal muscle. *J Physiol* 1986; 377: 92P
70. Edman KAP, Johansson M. The contractile state of rabbit papillary muscle in relation to stimulus frequency. *J Physiol* 1976; 254: 565-581
71. Eisenberg E, Green LE. The relation of muscle biochemistry to muscle physiology. *Ann Rev Physiol* 1980; 42: 293-309
72. Eisenberg E, Hill TL. Muscle contraction and free energy transduction in biological systems. *Science* 1985; 227: 999-1006

73. Eisenberg MS, Bergner L, Hallstrom AP, Cummins RO. Sudden cardiac death. *Sci Am* 1986; 254 (5): 25-31
74. Elliott GF, Lowy J, Wothington CR. An X-ray and light-diffraction study of the filament lattice of striated muscle in the living state and in rigor. *J Mol Biol* 1963; 6: 295-305
75. Elzinga G. Cardiac oxygen consumption and the production of heat and work. *In: Cardiac Metabolism* (editors AJ Drake-Holland and MIM Noble), John Wiley and Sons Ltd, Chichester, 1983, page 173-194
76. Endo M. Length dependence of activation of skinned muscle fibers by calcium. *Cold Spring Harbor Symp Quant Biol* 1973; 37: 505-510
77. England PJ. Phosphorylation of cardiac muscle contractile proteins. *In: Cardiac Metabolism* (editors AJ Drake-Holland and MIM Noble), John Wiley and Sons Ltd, Chichester, 1983, page 365-389
78. Fabiato A. Sarcomere length dependence of calcium release from the sarcoplasmic reticulum of skinned cardiac cells demonstrated by differential microspectrophotometry with arsenazo III. *J Gen Physiol* 1980; 76: 15a
79. Esumi K, Nishida M, Shaw D, Smith TW, Marsh JD. NADH measurements in adult rat myocytes during simulated ischemia. *Am J Physiol Heart Circ Physiol* 1991; 260: H1743-H1752
80. Fabiato A, Fabiato F. Myofilament-generated tension oscillations during partial calcium activation and activation dependence of the sarcomere length-tension relation of skinned cardiac cells. *J Gen Physiol* 1978; 72: 667-699
81. Fabiato A. Myoplasmic free calcium concentration reached during the twitch of an intact isolated cardiac cell and during calcium-induced release of calcium from the sarcoplasmic reticulum of a skinned cardiac cell from the adult rat or rabbit ventricle. *J Gen Physiol* 1981; 78: 457-497
82. Fabiato A, Fabiato F. Dependence of calcium release, tension generation and restoring forces on sarcomere length in skinned cardiac cells. *Eur J Cardiol* 1976; 4 (supplement 13): 13-27
83. Fabiato A. Use of aequorin to demonstrate dependence of calcium-induced release of calcium from the sarcoplasmic reticulum of a skinned cardiac cell on active sarcomere length. *Biophys J* 1985; 47: 378a
84. Fabiato A, Fabiato F. Calcium and cardiac excitation-contraction coupling. *Annu Rev Physiol* 1979; 39: 201-220
85. Fabiato A, Fabiato F. Effects of magnesium on contractile activation of skinned cardiac cells. *J Physiol* 1975; 249: 497-517
86. Fabiato A. Calcium-induced release of calcium from the cardiac sarcoplasmic reticulum. *Am J Physiol* 1983; 245: C1-C14
87. Fabiato A. Rapid ionic modifications during the aequorin-detected calcium transient in a skinned canine cardiac purkinje cell. *J Gen Physiol* 1985; 85: 189-246
88. Fabiato A, Fabiato F. Contractions induced by a calcium-triggered release of calcium from the sarcoplasmic reticulum of single skinned cardiac cells. *J Physiol* 1975; 249: 469-495
89. Fabiato A, Fabiato F. Effects of pH on the myofilaments and the sarcoplasmic reticulum of skinned cells from cardiac and skeletal muscles. *J Physiol* 1978; 276: 233-255
90. Fiolet JWT, Baarscheer A, Schumacher CA, Coronel R, ter Wille HF. The change of the free energy of atp hydrolysis during global ischemia and anoxia in the rat heart; its possible role in the regulation of trans-sarcolemmal sodium and potassium gradients. *J Mol Cell Cardiol* 1984; 16: 1023-1036
91. Fleischer S, Inui M. Biochemistry and biophysics of excitation-contraction coupling. *Annu Rev Biophys Biophys Chem* 1989; 18: 333-364
92. Fossel ET, Morgan HE, Ingwall JS. Measurement of changes in high-energy phosphates in the cardiac cycle by using gated ^{31}P nuclear magnetic resonance. *Proc Natl Acad Sci USA* 1980; 77: 3654-3658
93. Fox KAA, Bergmann SR, Sobel BE. Pathophysiology of myocardial reperfusion. *Ann Rev Med* 1985; 36: 125-144
94. Fozzard HA, Makielski JC. The electrophysiology of acute myocardial ischemia. *Ann Rev Med* 1985; 36: 275-284
95. Frank JS, Langer GA. The myocardial interstitium: its structure and its role in ionic exchange. *J Cell Biol* 1974; 60: 586-601
96. Friedrich R, Hierche HJ, Kebbel U, Zylka V, Bissig R. Changes of extracellular Na^+ , K^+ , Ca^{++} and H^+ of the ischemic myocardium in pigs. *Basic Res Cardiol* 1981; 76: 453-456

97. Gambetta M, Childers RW. The initial electrophysiological disturbance in experimental infarction, *Ann Intern Med* 1969; 70: 1076
98. Ganote CE. Contraction band necrosis and irreversible myocardial injury. *J Mol Cell Cardiol* 1983; 15: 67-73
99. Gao WD, Nguyen TTT, ter Keurs HEDJ. The rate of ATP depletion during metabolic inhibition of rat cardiac muscle; contribution of load, excitation contraction coupling and basal metabolism. *Circ Res* 1992 (Submitted).
100. Gaspardone A, Shine KI, Seabroke SR, Poole-Wilson PA. Potassium loss from rabbit myocardium during hypoxia: Evidence for passive efflux linked to anion extrusion. *J Mol Cell Cardiol* 1986; 18: 389-399
101. Gazitt Y, Ohad I, Loyter A. Phosphorylation and dephosphorylation of membrane proteins as a possible mechanism for structural rearrangement of membrane components. *Biochim Biophys Acta* 1976; 436: 1-14
102. Geft IL, Fishbein MC, Ninomiya K, Hashida J, Chaux E, Yano J, Yrit J, Genov T, Shell W, Ganz W. Intermittent brief periods of ischemia have a cumulative effect and may cause myocardial necrosis. *Circulation* 1982; 66: 1150-1153
103. Geisbuhler T, Altschuld RA, Trewyn RW, Ansel AZ, Lamka K, Brierley GP. Adenine nucleotide metabolism and compartmentalization in isolated adult rat heart cells. *Circ Res* 1984; 54: 536-546
104. Gevers W. Generation of protons by metabolic processes in heart cells. *J Mol Cell Cardiol* 1977; 9: 867-874
105. Ghista DN, van Vollenhoven E, Yang W-J, Reul H, Bleifeld W, editors. Cardiovascular Engineering. Part I: Modelling. *Advances in Cardiovascular Physics, Volume 5*. Karger, Basel. 1983, pp 1 - 229
106. Gibbs CL. Cardiac energetics. In: The mechanics of the circulation. HEDJ ter Keurs, JV Tyberg (editors). Martinus Nijhoff Publishers. Dordrecht, 1987. pp 69-86
107. Gibbs C. The cytoplasmic phosphorylation potential: its possible role in the control of myocardial respiration and cardiac contractility. *J Mol Cell Cardiol* 1985; 17: 727-731
108. Giles W, van Ginneken A, Shibata EF. Ionic currents underlying cardiac pacemaker activity: a summary of voltage-clamp data from single cells. In: Cardiac muscle, The regulation of excitation and contraction, 1986, page 1-27
109. Goodale T, Olson RE, Hackel DB. Myocardial glucose, lactate and pyruvate metabolism of normal and failing hearts studied by coronary venous catheterization in man. *Fed Proc* 1950; 9: 49
110. Gordon AM, Godt RE, Donaldson SKB, Harris CE. Tension in skinned frog muscle fibers in solutions of varying ionic strength and neutral salt composition. *J Gen Physiol* 1973; 62: 550-574
111. Gorza L, Pauletto P, Pessina AC, Sartore S, Schiaffino S. Isomyosin distribution in normal and pressure-overloaded rat ventricular myocardium. An immunohistochemical study. *Circ Res* 1981; 49: 1003-1009
112. Gould KL. Chapter 1: Physiology of coronary circulation. In: Coronary artery stenosis. Edited by KL Gould. Elsevier Science Publishing Co. Inc., Amsterdam, 1991, pg 7-15
113. Grinwald PM. Calcium uptake during post-ischemic reperfusion in the isolated rat heart: Influence of extracellular sodium. *J Mol Cell Cardiol* 1982; 14: 359-365
114. Gross RW, Soble BE. The arrhythmogenic amphiphilic lipids and the myocardial cell membrane. *J Mol Cell Cardiol* 1982; 14: 619-626
115. Gudbjarnason S, Mathes P, Raveas KG. Functional compartmentation of ATP and creatine phosphate in heart muscle. *J Mol Cell Cardiol* 1970; 1: 325-339
116. Guyton AC. Textbook of Medical Physiology. Eighth edition, W.B. Saunders Company, Philadelphia, 1991
117. Hagler HK, Sherwin L, Buja LM. Effect of different methods of tissue preparation on mitochondrial inclusions of ischemic and infarcted canine myocardium. Transmission and analytic electron microscopic study. *Lab Invest* 1979; 40: 529-544
118. Haigney MCP, Miyata H, Lakatta EG, Stern MD, Silverman HS. Dependence of hypoxic cellular calcium loading on Na^+ - Ca^{2+} exchange. *Circ Res* 1992; 71: 547-557
119. Halstrap AP, Denton RM. The specificity and metabolic implications of the inhibition of pyruvate transport in isolated mitochondria and intact tissue preparations by α -cyano-4-hydroxycinnamate and related compounds. *Biochem J* 1975; 148: 97-106
120. Hannon JD, Martyn DA, Gordon AM. Effects of cycling and rigor crossbridges on the

- conformation of cardiac troponin C. *Circ Res* 1992; 71: 984-991
121. Hansford RG, Moreno-Sanchez R, Lewartowski B. Activation of pyruvate dehydrogenase complex by Ca^{2+} in intact heart, cardiac myocytes, and cardiac mitochondria. *Ann N Y Acad Sci* 1989; 573: 240-253
 122. Hanson J, Lowy J. The structure of f-actin and of actin filaments isolated from muscle. *J Mol Biol* 1963; 6: 46-60
 123. Harmsen E. Myocardial purine metabolism; aspects of myocardial ATP metabolism and pharmacological intervention. Academic Thesis. Rotterdam. 1984
 124. Harmsen E, de Tombe PP, de Jong JW, Achterberg PW. Enhanced ATP and GTP synthesis from hypoxanthine or inosine after myocardial ischemia. *Am J Physiol* 1985; 246 (Heart Circ Physiol 15): H37-H43
 125. Hearse DJ, Bolli R. Reperfusion induced injury: manifestations, mechanisms, and clinical relevance. *Cardiovasc Res* 1992; 26: 101-108
 126. Hearse DJ, Braimbridge MV, Jyng P. Protection of the ischemic myocardium: cardioplegia. New York: Raven Press, 1981
 127. Heberden W. Some account of a disorder of the breast. *Med Trans Coll Physicians (Lond.)* 1772; 2: 59-67
 128. Heineman FW, Balaban RS. Control of mitochondrial respiration in the heart in vivo. *Ann Rev Physiol* 1990; 52: 523-542
 129. Helfant RH, Bodenheimer MM, Banka VS. Asynergy in coronary heart disease; evolving clinical and pathophysiologic concepts. *Ann Intern Med* 1977; 87: 475-482
 130. Hess ML, Manson NH. Molecular oxygen: friend and foe; the role of the oxygen free radical system in the calcium paradox, the oxygen paradox and ischemia/reperfusion injury. *J Mol Cell Cardiol* 1984; 16: 969-985
 131. Hess P, Tsien RW. Mechanisms of ion permeation through calcium channels. *Nature* 1984; 309: 453-456
 132. Heuningen R van, Rijnsburger WH, ter Keurs HEDJ. Sarcomere length control in striated muscle. *Am J Physiol* 1982; 242 (Heart Circ Physiol 11): H411-H420
 133. Hibberd MG, Jewell BR. Length dependence of the sensitivity of the contractile system to calcium in rat ventricular muscle. *J Physiol* 1979; 290: 30P
 134. Hill JL, Gettes LS. Effect of acute coronary occlusion on local myocardial extracellular K^+ activity in swine. *Circulation* 1980; 61: 768-777
 135. Hille B. Ionic channels in nerve membrane. *Progr Bioph Mol Biol* 1970; 21: 1-32
 136. Holubarsch Ch, Alpert NR, Goulette R, Mulieri LA. Heat production during hypoxic contracture of rat myocardium. *Circ Res* 1982; 51: 777-786
 137. Hori M, Tamai J, Kitakaze M, Iwakura K, Gotoh K, Iwai K, Koretsune Y, Kagiya T, Kitabatake A, Kamada T. Adenosine-induced hyperemia attenuates myocardial ischemia in coronary microembolization in dogs. *Am J Physiol* 1989; 257(1 Pt 2): H244-H251
 138. Housmans PR, Lee NKM, Blinks JR. Active shortening retards the decline of the intracellular calcium transient in mammalian heart muscle. *Science* 1983; 221: 159-161
 139. Hudlicka O. Growth of capillaries in skeletal and cardiac muscle. *Circ Res* 1982; 50: 451-461
 140. Humphrey SM, Secley RN. Improved functional recovery of ischemic myocardium by suppression of adenosine catabolism. *J Thorac Cardiovasc Surg* 1982; 84: 16-22
 141. Humphrey SM, Garlick PB. NMR-visible ATP and P_i in normoxic and reperfused rat hearts: A quantitative study. *Am J Physiol Heart Circ Physiol* 1991; 260: H6-H12
 142. Humphrey SM, Holliss DG, Seelye RN. Myocardial adenine pool depletion and recovery of mechanical function following ischemia. *Am J Physiol* 1985; 248 (Heart Circ Physiol 17): H644-H651
 143. Huxley HE. How do cross-bridges produce the sliding force between actin and myosin filaments in muscle. In: *The mechanics of the circulation*. HEDJ ter Keurs, JV Tyberg (editors). Martinus Nijhoff Publishers. Dordrecht, 1987. pp 1-13
 144. Huxley HE, Hanson J. Changes in the cross-striations of muscle during contraction and stretch and their structural interpretation. *Nature*, 1954; 173: 973-976
 145. Huxley AF. Muscle structure and theories of contraction. *Progr Biophys Chem* 1957; 7: 257-318
 146. Huxley AF, Simmons RM. Proposed mechanism of force generation in striated muscle. *Nature*, 1971; 233: 533-538
 147. Huxley HE, Faruqi AR, Kress M, Bordas J, Koch MHJ. Time-resolved X-ray diffraction studies of

- the myosin layer-line reflections during muscle contraction. *J Mol Biol* 1982; 158: 637-684
148. Huxley HE. The mechanism of muscular contraction. Recent structural studies suggest a revealing model for cross-bridge action at variable filament spacing. *Science*, 1969; 164: 1356-1366
149. Huxley HE. Structural changes in the actin and myosin containing filaments during contraction. *Cold Spring Harbor Symp Quant Biol* 1972; 37: 361-376
150. Ikemoto N. Structure and function of the calcium pump protein of sarcoplasmic reticulum. *Ann Rev Physiol* 1982; 44: 297-317
151. Imai K, Wang T, Millard RW, Ahraf M, Kranias EG, Asano G, Grassi de Gende AO, Nagao T, Solar RJ, Schwartz A. Ischemia-induced changes in canine cardiac sarcoplasmic reticulum. *Cardiovasc Res* 1983; 17: 696-709
152. Irisawa H. Electrophysiology of single cardiac cells. *Jpn J Physiol* 1984; 34: 375-388
153. Isenberg G, Vereecke J, van der Heyden G, Carmeliet E. The shortening of the action potential by DNP in Guinea Pig ventricular myocytes is mediated by an increase of the time-independent K conductance. *Pflügers Arch* 1983; 397: 251-259
154. Jacobstein MD, Gerken TA, Bhat AM, Carlier PG. Myocardial protection during ischemia by prior feeding with the creatine analog: cyclocreatine. *J Am Coll Cardiol* 1989; 14(1): 246-51
155. Jacobus WE. Respiratory control and the integration of heart high-energy phosphate metabolism by mitochondrial creatine kinase. *Ann Rev Physiol* 1985; 47: 707-726
156. Jennings RB, Reimer KA. Lethal myocardial ischemic injury. *Am J Pathol* 1981; 102: 241-255
157. Jennings RB, Hawkins HK, Lowe JE, Hill ML, Klotman S, Reimer KA. Relation between high energy phosphate and lethal injury in myocardial ischemia in the dog. *Am J Pathol* 1978; 92: 187-214
158. Jennings RB, Steenbergen C. Nucleotide metabolism and cellular damage in myocardial ischemia. *Ann Rev Physiol* 1985; 47: 727-749
159. Jennings RB, Reimer KA. The cell biology of acute myocardial ischemia. *Annu Rev Med* 1991; 42: 225-246
160. Jeremy RW, Koretsune Y, Marban E, Becker LC. Relation between glycolysis and calcium homeostasis in postischemic myocardium. *Circ Res* 1992; 70: 1180-1190
161. Jimenez E, del Nido P, Sarin M, Nakamura H, Feinberg H, Levitsky S. Effects of low extracellular calcium on cytosolic calcium and ischemic contracture. *J Surg Res* 1990; 49(3): 252-5
162. Jones DP. Intracellular diffusion gradients of O₂ and ATP. *Am J Physiol* 1986; 250 (Cell Physiol 19): C663-C675
163. Jong JW de. Myocardial Energy Metabolism. Martinus Nijhoff Publishers, Dordrecht. 1988
164. Jong JW de. Biochemistry of acutely ischemic myocardium. In: *The Pathophysiology of Myocardial Perfusion*, edited by W Schaper. Elsevier/North-Holland Biomedical Press 1979
165. Kammermeier H, Schmidt P, Jungling E. Free energy change of ATP hydrolysis: a causal factor of early hypoxic failure of the myocardium? *J Mol Cell Cardiol* 1982; 14: 267-277
166. Kanazawa T, Yamada S, Yamamoto T, Tonomura Y. Reaction mechanism of the Ca²⁺-dependent ATPase of sarcoplasmic reticulum from skeletal muscle. V. Vectorial requirements for calcium and magnesium ions of three partial reactions of ATPase: Formation and decomposition of a phosphorylated intermediate and ATP-formation from ADP and the intermediate. *J Biochem* 1971; 70: 95-123
167. Kaplan P, Hendriks M, Mattheussen M, Mubagwa K, Flameng W. Effect of ischemia and reperfusion on sarcoplasmic reticulum calcium uptake. *Circ Res* 1992; 71: 1123-1130
168. Karli JM, Karikas GA, Hatzipavlou PK, Levis GM, Mouloupoulos. The inhibition of Na⁺ and K⁺ stimulated ATPase activity of rabbit and dog heart sarcolemma by lysophosphatidyl choline. *Life Sci* 1979; 24: 1869-1876
169. Kass RS. Ionic basis of electrical activity in the heart. In: *Physiology and pathophysiology of the heart*. Editor N Sperilakis. Kluwer Academic Publishers. Boston. 1989, pg 81 - 93
170. Katz AM, Messineo FC. Lipid-membrane interactions and the pathogenesis of ischemic damage in the myocardium. *Circ Res* 1981; 48: 1-16
171. Katz AM, Maxwell JB. Actin from heart muscle: sulphhydryl groups. *Circ Res* 1964; 14: 345-350
172. Katz AM, Hecht HH. The early pump failure of ischemic heart. *Am J Med* 1969; 47: 497-502
173. Kaufman LA, Hall NF, DeLuca MA, Ingwall JS, Mayer SE. Metabolism of adenine nucleotides in the cultured fetal mouse heart. *Am J Physiol* 1977; 233: H282-H288
174. Kawai M, Brandt PW. Sinusoidal analysis: a high resolution method for correlating biochemical

- reactions with physiological processes in activated skeletal muscles of rabbit, frog and crayfish. *J Muscle Res Cell Mot* 1980; 1: 279-303
175. Kentish JC. The effects of inorganic phosphate and creatine phosphate on force production in skinned muscles from rat ventricle. *J Physiol* 1986; 370: 585-604
 176. Kentish JC, ter Keurs HEDJ, Ricciardi L, Buxx JJJ, Noble MIM. Comparison between the sarcomere length-force relations in intact and skinned trabeculae from rat right ventricle. Influence of calcium concentrations on these relations. *Circ Res* 1986; 58: 755-768
 177. Keurs HEDJ ter, Mulder BJM, Schouten VJA. Myocardial cell properties and hypertrophy. In: *Cardiac Left Ventricular Hypertrophy*, edited by HEDJ ter Keurs and JJ Schipperheyn. Martinus Nijhoff Publishers. Dordrecht. 1983
 178. Keurs HEDJ ter, Rijnsburger WH, van Heuningen R, Nagelsmit MJ. Tension development and sarcomere length in rat cardiac trabeculae; Evidence of length-dependent activation. *Circ Res* 1980; 46: 703-714
 179. Keurs HEDJ ter, Wohlfart B. Influence of calcium concentration on maximal velocity of sarcomere shortening in rat trabeculae. *J Physiol* 1982;
 180. Keurs HEDJ ter. Calcium and contractility. In: *Cardiac Metabolism* (editors AJ Drake-Holland and MIM Noble), John Wiley and Sons Ltd, Chichester, 1983, page 73-100
 181. Keurs HEDJ ter, Ricciardi L, Buxx JJJ, Grant DA, Lofgren DN. The force-sarcomere length relations in mammalian myocardium. *Eur J Clin Invest* 1986; 16: A4
 182. Keurs HEDJ ter, Buxx JJJ, Harmsen E, de Tombe PP, Leijendekker WJ. Ischemia, high energy phosphate metabolism and sarcomere dynamics in myocardium. In: *Myocardial energy metabolism*, editor JW de Jong, Martinus Nijhoff, 1988, pg 181-194
 183. Keurs HEDJ ter, Rijnsburger WH, van Heuningen R. Restoring forces and relaxation of rat cardiac muscle. *Eur Heart J* 1980; 1 (Supplement A): 67-80
 184. Keynes RD. Ion channels in the nerve-cell membrane. *Scient American* 1979; 240: 98-107
 185. Kingsley PB, Sako EY, Yang MQ, Zimmer SD, Ugurbil K, Foker JE, From AHL. Ischemic contracture begins when anaerobic glycolysis stops: A ^{31}P -NMR study of isolated rat hearts. *Am J Physiol Heart Circ Physiol* 1991; 261: H469-H478
 186. Kirkels JH, Ruigrok TJ, Van Echteld CJ, Meijler FL. Low Ca^{2+} reperfusion and enhanced susceptibility of the postischemic heart to the calcium paradox. *Circ Res* 1989; 64(6): 1158-64
 187. Kitakaze M, Marban E. Cellular mechanism of the modulation of contractile function by coronary perfusion pressure in ferret hearts. *J Physiol (London)* 1989; 414: 455-472
 188. Kitakaze M, Weisman HF, Marban E. Contractile dysfunction and ATP depletion after transient calcium overload in perfused ferret hearts. *Circulation* 1988; 77(3): 685-95
 189. Kitakaze M, Weisfeldt ML, Marban E. Acidosis during early reperfusion prevents myocardial stunning in perfused ferret hearts. *J Clin Invest* 1988; 82(3): 920-7
 190. Kleber AG. Extracellular potassium accumulation in acute myocardial ischemia. *J Mol Cell Cardiol* 1984; 16: 389-394
 191. Klingenberg M, Grebe K, Schever B. The binding of atractylate and carboxy-tractylate to mitochondria. *Europ J Biochem* 1975; 52: 351-363
 192. Kloner RA, Braunwald E. Observations on experimental myocardial ischemia. *Cardiovasc Res* 1980; 14: 371-395
 193. Kloner RA, Ganote CE, Jennings RB. The no reflow phenomenon after temporary occlusion in the dog. *J Clin Invest* 1974; 54: 1496-1508
 194. Kobayashi K, Neely JR. Control of maximum rates of glycolysis in rat cardiac muscle. *Circ Res* 1979; 44: 166-175
 195. Koretsune Y, Corretti MC, Kusuoka H, Marban E. Mechanism of early ischemic contractile failure; inexcitability, metabolite accumulation, or vascular collapse? *Circ Res* 1991; 68: 255-262
 196. Koretsune Y, Marban E. Relative roles of Ca^{2+} -dependent and Ca^{2+} -independent mechanisms in hypoxic contractile dysfunction. *Circulation* 1990; 82: 528-535
 197. Koretsune Y, Marban E. Cell calcium in the pathophysiology of ventricular fibrillation and in the pathogenesis of postarrhythmic contractile dysfunction. *Circulation* 1989; 80(2): 369-79
 198. Koretsune Y, Corretti MC, Kusuoka H, Marban E. Mechanism of early ischemic contractile failure: Inexcitability, metabolite accumulation, or vascular collapse. *Circ Res* 1991; 68: 255-262
 199. Krams R, Sipkema P, Westerhof N. Coronary oscillatory flow amplitude is more affected by perfusion pressure than ventricular pressure. *Am J Physiol* 1990; 258: H1889-98

200. Kubler W, Katz AM. Mechanism of early pump failure of the ischemic heart: possible role of adenosine triphosphate depletion and inorganic phosphate accumulation. *Am J Cardiol* 1977; 40: 467-471
201. Kukreja RC, Hess ML. The oxygen free radical system: from equations through membrane-protein interactions to cardiovascular injury and protection. *Cardiovasc Res* 1992; 26: 641-655
202. Kusuoka H, Marban E. Cellular mechanisms of myocardial stunning. *Annu Rev Physiol* 1992; 54: 243-256
203. Kusuoka H, Koretsune Y, Chacko VP, Weisfeldt ML, Marban E. Excitation-contraction coupling in postischemic myocardium. Does failure of activator Ca^{2+} transients underlie stunning? *Circ Res* 1990; 66(5): 1268-1276
204. Kusuoka H, Weisfeldt ML, Zweier JL, Jacobus WE, Marban E. Mechanism of early contractile failure during hypoxia in intact ferret heart: evidence for modulation of maximal Ca^{2+} -activated force by inorganic phosphate. *Circ Res* 1986; 59: 270-282
205. Lab MJ, Allen DG, Orchard CH. The effects of shortening on myoplasmic calcium concentration and on the action potential in mammalian ventricular muscle. *Circ Res* 1984; 55: 825-829
206. Laird-Meeter K, van Domburg R, Bos E, Hugenholtz PG. Survival at 5 and 10 years after aorto-coronary bypass operations in 1041 consecutive patients. *Eur Heart J* 1987; 8: 449-456
207. Lakatta EG. Functional implications of spontaneous sarcoplasmic reticulum Ca^{2+} release in the heart. *Cardiovasc Res* 1992; 26: 193-214
208. Langer GA, Frank JS, Philipson KD. Ultrastructure and calcium exchange of the sarcolemma, sarcoplasmic reticulum and mitochondria of the myocardium. *Pharmac Ther* 1982; 16: 331-376
209. Langer GA. Sodium-Calcium exchange in the heart. *Ann Rev Physiol* 1982; 44: 435-449
210. Lee JA, Allen DG. Mechanisms of acute ischemic contractile failure of the heart. Role of intracellular calcium. *J Clin Invest* 1991; 88: 361-367
211. Lee JA, Allen DG. EMD 53998 sensitizes the contractile proteins to calcium in intact ferret ventricular muscle. *Circ Res* 1991; 69: 927-936
212. Lee JA, Allen DG. Changes in intracellular free calcium concentration during long exposures to simulated ischemia in isolated mammalian ventricular muscle. *Circ Res* 1992; 71: 58-69
213. Lehninger AL. Biochemistry; the molecular basis of cell structure and function. Worth Publishers Inc. First edition 1970
214. Leijendekker WJ, Gao WD, ter Keurs HEDJ. Unstimulated force during hypoxia of rat cardiac muscle: stiffness and calcium dependence. *Am J Physiol* 1990; 258: H861-H869
215. Leijendekker WJ, Gao WD, ter Keurs HEDJ. The role of calcium in the development of diastolic force during hypoxia in rat myocardium. *Prog Clin Biol Res* 1989; 315: 604-605
216. Levitsky DO, Benevolensky DS. Effects of changing Ca^{2+} -to- H^{+} ratio on Ca^{2+} uptake by cardiac sarcoplasmic reticulum. *Am J Physiol* 1986; 250 (Heart Circ Physiol 19): H360-H365
217. Lewartowski B. Calcium exchange. In: *Cardiac Metabolism* (editors AJ Drake-Holland and MIM Noble), John Wiley and Sons Ltd, Chichester, 1983, page 101-116
218. Lewis MJ, Housmans PR, Clacs VA, Brutsaert DL, Henderson AH. Myocardial stiffness during hypoxia and reoxygenation. *Cardiovasc Res* 1980; 14: 339-344
219. Liedtke AJ. Alterations of carbohydrate and lipid metabolism in the acutely ischemic heart. *Prog Cardiovasc Dis* 1981; 23: 321-336
220. Loiselle DS. Cardiac basal and activation metabolism. *Basic Res Cardiol* 1987; 82(suppl 2): 37-49
221. Lopaschuk GD, Spafford MA, Davies NJ, Wall SR. Glucose and palmitate oxidation in isolated working rat hearts reperfused after a period of transient global ischemia. *Circ Res* 1990; 66: 546-553
222. Lowe JE, Ross G, Adams DH, Jennings RB, Schaper J. The downslope of the rigor curve: appearance of N-lines. *J Moll Cell Cardiol* 1985; 17: 24
223. Lubbe JL, Daries DS, Opie LH. Ventricular arrhythmias associated with coronary artery occlusion and reperfusion in the isolated perfused rat heart: a model for assessment of antifibrillatory action of antiarrhythmic agents. *Cardiovasc Res* 1978; 12: 212-218
224. Lüllman H, Peters T. Plasmalemmal calcium in cardiac excitation - contraction coupling. *Clin Exp Pharmacol Physiol* 1977; 4: 49-57
225. MacFarlane NG, Miller DJ. Depression of peak force without altering calcium sensitivity by the superoxide anion in chemically skinned cardiac muscle of rat. *Circ Res* 1992; 70: 1217-1224
226. Magid A, Ting-Beall HP, Carvell M, Kontis T, Lucaveche C. Connecting filaments, core filaments and side struts: A proposal to add three new load-bearing structures to the sliding filament model.

- In: *Contractile mechanisms in muscle*, edited by GH Pollack and H Sugi, New York, Plenum Press, 1984, pp 307-323
227. Mahnensmith RL, Aronson PS. The plasma membrane sodium-hydrogen exchanger and its role in physiological and pathophysiological processes. *Circ Res* 1985; 56: 773-788
 228. Mandel F, Kranias EG, de Gende AG, Sumida M, and Schwartz A. The effect of pH on the transient-state kinetics of Ca^{2+} - Mg^{2+} -ATPase of cardiac sarcoplasmic reticulum. A comparison with skeletal sarcoplasmic reticulum. *Circ Res* 1982; 50: 310-317
 229. Marban E, Kitakaze M, Koretsune Y, Yue DT, Chacko VP, Pike MM. Quantification of $[\text{Ca}^{2+}]_i$ in perfused hearts. Critical evaluation of the 5F-BAPTA and nuclear magnetic resonance method as applied to the study of ischemia and reperfusion. *Circ Res* 1990; 66(5): 1255-1267
 230. Marban E, Koretsune Y, Corretti M, Chacko VP, Kusuoka H. Calcium and its role in myocardial cell injury during ischemia and reperfusion. *Circulation* 1989; 80(6 Suppl): IV17-IV22
 231. Marban E, Kitakaze M, Chacko VP, Pike MM. Ca^{2+} transients in perfused hearts revealed by gated ^{19}F NMR spectroscopy. *Circ Res* 1988; 63(3): 673-678
 232. Matthews PM, Bland JL, Gadian DG, and Radda GK. The steady-state rate of ATP synthesis in the perfused rat heart measured by ^{31}P NMR saturation transfer. *Biochem. Biophys Res Commun* 1981; 103: 1052-1059
 233. McCallister LP, Daiello DC, and Tyers GFO. Morphometric observations of the effects of normothermic ischemic arrest on dog myocardial ultrastructure. *J Mol Cell Cardiol* 1978; 10: 67-80
 234. McClellan GB, and Winegrad S. The regulation of the calcium sensitivity of the contractile system in mammalian cardiac muscle. *J Gen Physiol* 1978; 72: 737-764
 235. McDonald DA. *Blood flow in arteries*, 2nd edn, Edward Arnold, London, 1974
 236. McDonald TF, Hayashi H, Ponnambalam C, Watanabe T. Electrical activity and tension in guinea pig ventricular muscle during and after metabolic depression. In: *Cardiac function under ischemia and hypoxia*. Edited by K Yamad, AM Katz and J Toyama. Nagoya, Japan, University of Nagoya Press, 1986.
 237. McNutt NS. Ultrastructure of the myocardial sarcolemma. *Circ Res* 1975; 37: 1-13
 238. Mela-Riker LM, and Bukoski RD. Regulation of mitochondrial activity in cardiac cells. *Ann Rev Physiol* 1985; 47: 645-664
 239. Meyer RA, Sweeney HL and Kushmerick MJ. A simple analysis of the "phosphocreatine shuttle". *Am J Physiol* 1984; 246 (Cell Physiol 15): C365-C377
 240. Milnor WR, Bergel DH and Bargainer JD. Hydraulic power association with pulmonary blood flow and its relation to heart rate. *Circ Res* 1966; 19: 467-480
 241. Mitchell P. Keilin's respiratory chain concept and its chemiosmotic consequences. *Science*, 1979; 206: 1148-1159
 242. Moisesescu DG, Thieleczek R. Sarcomere length effects on the Sr^{2+} - and Ca^{2+} - activation curves in skinned frog muscle fibres. *Biochim Biophys Acta* 1979; 546: 64-76
 243. Momomura S, Ingwall JS, Parker JA, Sahagian P, Ferguson JJ, and Grossman W. The relationship of high energy phosphates, tissue pH, and regional blood flow to diastolic distensibility in the ischemic dog myocardium. *Circ Res* 1985; 57: 822-835
 244. Morad M, Rolett EL. Relaxing effects of catecholamines on mammalian heart. *J Physiol* 1972; 224: 537-558
 245. Mullins LJ. The generation of electric currents in cardiac fibers by Na/Ca exchange. *Am J Physiol* 1979; 236(3): C103-C110
 246. Murray AW. The biological significance of purine salvage. *Ann Rev Biochem* 1971; 40: 811-826
 247. Nakamura Y, Wiegner AW, Bing OHL. Measurement of relaxation in isolated rat ventricular myocardium during hypoxia and reoxygenation. *Cardiovas Res* 1986; 20: 690-697
 248. Nakaya H, Kimura S, Kanno M. Intracellular K^{+} and Na^{+} activities under hypoxia, acidosis, and no glucose in dog hearts. *Am J Physiol* 1985; 249 (Heart Circ Physiol 18): H1078-H1085
 249. Nayler WG, Ferrari R, Williams A. Protective effect of pretreatment with verapamil, nifedipine and propranolol on mitochondrial function in the ischemic and perfused myocardium. *Am J Cardiol* 1980; 46: 242-248
 250. Neely JR, Feuvray D. Metabolic products and myocardial ischemia. *Am J Pathol* 1981; 102: 282-291
 251. Neely JR, Morgan HE. Relationship between carbohydrate and lipid metabolism and the energy balance of heart muscle. *Ann. Rev. Physiol.* 1974; 36: 413-459
 252. Noble MIM, Pollack GH. Molecular mechanisms of contraction. *Circ Res* 1977; 40: 333-342

253. Noma, A. ATP-regulated K⁺ channels in cardiac muscle. *Nature* 1983; 305: 147-148
254. Nosek TM, Fender KY, and Godt RE. It is diprotonated inorganic phosphate that depresses force in skinned skeletal muscle fibers. *Science* 1987; 236: 191-193
255. Ohba M. A role of ionic strength on the inotropic effects of osmolarity change in frog atrium. *J Physiol* 1984; 34: 1105-1115
256. Ohgoshi Y, Goto Y, Futaki S, Yaku H, Kawaguchi O, Suga H. Increased oxygen cost of contractility in stunned myocardium of dog. *Circ Res* 1991; 69: 975-988
257. Olsson RA, Bugni WJ. Coronary circulation. In: *The Heart and Cardiovascular System*. Edited by HA Fozzard et al. Raven Press, New York, 1986. pg 987-1037.
258. Opie LH. Effects of regional ischemia on metabolism of glucose and fatty acids; Relative rates of aerobic and anaerobic energy production during myocardial infarction and comparison with effects of anoxia. *Circ Res* 1976; 38 (supplement 1): I52-I68
259. Opie L. Chapter 4: Channels, Pumps and Exchangers. In: *The heart; physiology and metabolism*. Raven Press. New York. 1992; pg 67 - 101
260. Owen P, Dennis S, Opie LH. Glucose flux rate regulates onset of ischemic contracture in globally underperfused rat hearts. *Circ Res* 1990; 66(2): 344-54
261. Page E. Quantitative ultrastructural analysis in cardiac membrane physiology. *Am J Physiol* 1978; 235: C147-C158
262. Page E, and McCallister LP. Quantitative electron microscopic description of heart muscle cells. Application to normal, hypertrophied and thyroxin-stimulated hearts. *Am J Cardiol* 1973; 31: 172-181
263. Pande SV. A mitochondrial carnitine : acylcarnitine translocase system. *Proc Natl Acad Sci USA* 1975; 72: 883-887.
264. Park Y, Bowles DK, Kehr JP. Protection against hypoxic injury in isolated-perfused rat heart by ruthenium red. *J Pharmacol Exp Ther* 1990; 253(2): 628-35
265. Pasipoularides A, Palacios I, Frist W, Rosenthal S, Newell JB, Powell WJ. Contribution of activation-inactivation dynamics to the impairment of relaxation in hypoxic cat papillary muscle. *Am J Physiol* 1985; 248 (Regulatory Integrative Comp Physiol 17): R54-R62
266. Patterson WW, Piper H, Starling EH. The regulation of the heart beat. *J Physiol* 1914; 48: 465-513
267. Paulus WJ, Grossman W, Serizawa T, Bourdillon PD, Pasipoularides A, Mirsky I. Different effects of two types of ischemia on myocardial systolic and diastolic function. *Am J Physiol* 1985; 248 (Heart Circ Physiol 17): H719-H728
268. Paulus WJ, Serizawa T, Grossman W. Altered left ventricular diastolic properties during pacing-induced ischemia in dogs with coronary stenoses; potentiation by caffeine. *Circ Res* 1982; 50: 218-227
269. Pearson JD, Gordon JL. Nucleotide metabolism by endothelium. *Annu Rev Physiol* 1985; 47: 617-627
270. Penny WJ, Sheridan DJ. Arrhythmias and cellular electrophysiological changes during myocardial "ischaemia" and reperfusion. *Cardiovasc Res* 1983; 17: 363-372
271. Philipson KD, Bersohn MM, Nishimoto AY. Effects of pH on Na⁺-Ca²⁺ exchange in canine cardiac sarcolemmal vesicles. *Circ Res* 1982; 50: 287-293
272. Pitts BJR. Stoichiometry of sodium-calcium exchange in cardiac sarcolemmal vesicles. Coupling to the sodium pump. *J Biol Chem* 1979; 254: 6232-6235
273. Pike MM, Kitakaze M, Marban E. ²³Na-NMR measurements of intracellular sodium in intact perfused ferret hearts during ischemia and reperfusion. *Am J Physiol Heart Circ Physiol* 1990; 259: H1767-H1773
274. Pogwizd SM, Onufer JR, Kramer JB, Sobel BE, Corr PB. Induction of delayed afterdepolarizations and triggered activity in canine purkinje fibers by lysophosphoglycerides. *Circ Res* 1986; 59: 416-426.
275. Polimeni PI. Extracellular space and ionic distribution in rat ventricle. *Am J Physiol* 1974; 227: 676-683
276. Pollack GH. The cross-bridge theory. *Physiol Rev* 1983; 63: 1049-1113
277. Pollack GH, Krueger JW. Sarcomere dynamics in intact cardiac muscle. *Eur J Cardiol* 1976; 4 (Supplement): 53-65
278. Poole-Wilson PA, Harding DP, Bourdillon PDV, Tones MA. Calcium out of control. *J Mol Cell Cardiol* 1984; 16: 175-187
279. Prinzen WF. Gradients in myocardial blood flow, metabolism and mechanics across the ischemic

- left ventricular wall. Acad. Thesis, University of Limburg, Maastricht, 1982
280. Randle PJ, Tubbs PK. Carbohydrate and fatty acid metabolism. In: Handbook of Physiology, Section 2: Volume 1, The Cardiovascular System, edited by RM Berne, N Sperelakis, SR Geiger. American Physiological Society, Washington D.C. 1979, pp 805-844
281. Reimer KA, Murry CE, Jennings RB. Cardiac adaptation to ischemia: Ischemic preconditioning increases myocardial tolerance to subsequent ischemic episodes. *Circulation* 1990; 82: 2266-2268
282. Reimer KA, Jennings RB, Tatum AH. Pathobiology of acute myocardial ischemia: metabolic, functional and ultrastructural studies. *Am. J. Cardiol.* 1983; 52: 72A-81A
283. Reinlib L, Caroni P, Carafoli E. Studies on heart sarcolemma: vesicles of opposite orientation and the effect of ATP on the $\text{Na}^+/\text{Ca}^{2+}$ exchange. *FEBS Lett* 1981; 126: 74-76
284. Renlund DG, Gerstenblith G, Lakatta EG, Jacobus WE, Kallman CH, Weisfeldt ML. Reduction of post-ischemic myocardial injury without altering the ischemic insult. *J Mol Cell Cardiol* 1984; 16: 795-801
285. Reuter H. Exchange of calcium ions in the mammalian myocardium. Mechanisms and physiological significance. *Circ Res* 1974; 34: 599-605
286. Reuter H. Ion channels in cardiac cell membranes. *Ann Rev Physiol* 1984; 46: 473-484
287. Ricciardi L, Buxx JJJ, ter Keurs HEDJ. Effects of acidosis on force-sarcomere length and force-velocity relations of rat cardiac muscle. *Cardiovasc Res* 1986; 20: 117-123
288. Robertson SP, Johnson JD, Potter JD. The time course of calcium exchange with calmodulin, troponin, parvalbumin and myosin in response to transient increases in calcium. *Biophys J* 1981; 34: 559-569
289. Robertson JD. The cell membrane concept. *J Physiol* 1958; 140: 58P-59P
290. Robinson TF, Cohen-Gould L, Factor SM. Skeletal framework of mammalian heart muscle. Arrangement of inter- and pericellular connective tissue structures. *Lab Invest* 1983; 49: 482-498
291. Sage MD, Jennings RB. Cytoskeletal injury and subsarcolemmal bleb formation in dog heart during in vitro total ischemia. *Am J Pathol* 1988; 133(2): 327-337
292. Schaper J. Effects of multiple ischaemic events on human myocardium - an ultrastructural study. *Eur Heart J* 1988; 9 (suppl A): 141-149
293. Schouten VJA, Buxx JJJ, de Tombe PP, ter Keurs HEDJ. Sarcolemma, sarcoplasmic reticulum, and sarcomeres as limiting factors in force production in rat heart. *Circ Res* 1990; 67: 913-922
294. Schouten VJA, Los GJ, Kuypers PD, Brinkman CJ, Huysmans HA. Paradox of enhanced contractility in postischemic rat hearts with depressed function. *Am J Physiol* 1991; 260: H89 - H99
295. Schouten VJA. Excitation-contraction coupling in heart muscle. Academic Thesis. Leiden. 1985.
296. Schouten VJA, Los GJ, Kuypers PDL, Brinkman CJ, Huysmans HA. Paradox of enhanced contractility in postischemic rat hearts with depressed function. *Am J Physiol Heart Circ Physiol* 1991; 260: H89-H99
297. Schwartz A. A sodium and potassium stimulated adenosine triphosphatase from cardiac tissues. I. Preparation and properties. *Biochem Biophys Res Commun* 1962; 9: 301-312
298. Sharma AD, Corr PB. Adrenergic factors in arrhythmogenesis in the ischemic and reperfused myocardium. *Eur Heart J* 1983; 4 (Supplement D): 79-90
299. Shrago E, Shug AL, Sul H, Bittar N, Folts JD. Control of energy production in myocardial ischemia. *Circ Res* 1976; Suppl I, 38: 75-79
300. Silverman HS, Ninomiya M, Blank PS, Hano O, Miyata H, Spurgeon HA, Lakatta EG, Stern MD. A cellular mechanism for impaired posthypoxic relaxation in isolated cardiac myocytes: Altered myofilament relaxation kinetics at reoxygenation. *Circ Res* 1991; 69: 196-208
301. Smith TW. Digitalis. Mechanisms of action and clinical use. *N Engl J Med* 1988; 318: 358-365
302. Smith JS, Coronado R, Meissner G. Sarcoplasmic reticulum contains adenine nucleotide-activated calcium channels. *Nature* 1985; 316: 446-449
303. Solaro RJ, Briggs FN. Estimating the functional capabilities of sarcoplasmic reticulum in cardiac muscle. Calcium binding. *Circ Res* 1974; 34: 531-540
304. Sommer JR, Jennings RB. Ultrastructure of cardiac muscle. In: The Heart and Cardiovascular System. Edited by HA Fozzard et al. Raven Press, New York, 1986. pg 61-100.
305. Spaan JA. Coronary diastolic pressure-flow relation and zero pressure explained on the basis of intramyocardial compliance. *Circ Res* 1985; 56: 293-309
306. Sparks HV, Bardenheuer H. Regulation of adenosine formation by the heart. *Circ Res* 1986; 58: 193-201

307. Spedding M, Mir AK. Direct activation of Ca^{2+} channels by palmitoyl carnitine, a putative endogenous ligand. *Br J Pharmacol* 1987; 93: 457-468
308. Steenbergen C, Murphy E, Watts JA. Correlation between cytosolic free calcium, contracture, ATP, and irreversible ischemic injury in perfused rat heart. *Circ Res* 1990; 66: 135-146
309. Steenbergen C, Murphy E, Levy L, London RE. Elevation in cytosolic free calcium concentration early in myocardial ischemia in perfused rat heart. *Circ Res* 1987; 60: 700-707
310. Stern S, Tzivoni D. Early detection of silent ischaemic heart disease by 24-hour electrocardiographic monitoring of active subjects. *Br Heart J* 1974; 36: 481-486
311. Streeter DD, Spotnitz HM, Patle, Ross J, Sonnenblick EH. Fiber orientation in the canine left ventricle during diastole and systole. *Circ Res* 1969; 24: 339-347
312. Suga H. Ventricular energetics. *Phys Rev* 1990; 70: 247-277
313. Sutko J. The calcium pump of cardiac sarcoplasmic reticulum functional alterations at different levels of thyroid state in rabbits. *J Physiol* 1973; 228: 563-582
314. Swain JL, Sabina RL, McHale PA, Greenfield JC, Holmes EW. Prolonged myocardial nucleotide depletion after brief ischemia in the open-chest dog. *Am J Physiol* 1982; 242 (Heart Circ Physiol 11): H818 - H826
315. Tamaki N, Yasuda T, Leinbach RC, Gold HK, McKusick KA, Strauss HW. Spontaneous changes in regional wall motion abnormalities in acute myocardial infarction. *Am J Cardiol* 1986; 58: 406-410
316. Ten Eick RE, Whalley DW, Rasmussen HH. Connections: Heart disease, cellular electrophysiology, and ion channels. *FASEB J* 1992; 6: 2568-2580
317. Tennant R, Wiggers CS. The effect of coronary occlusion on myocardial contraction. *Am J Physiol* 1935; 112: 351-361
318. Tillack TW. The ultrastructure of developing sarcoplasmic reticulum. *J Biol Chem* 1974; 249: 624-633
319. Tombe PP de, ter Keurs HEDJ. Force and velocity of sarcomere shortening in trabeculae from rat heart. Effects of temperature. *Circ Res* 1990; 66: 1239-1254
320. Tombe PP de, ter Keurs HEDJ. An internal viscous element limits unloaded velocity of sarcomere shortening in rat myocardium. *J Physiol* 1992; 454: 619-642
321. Trantum-Jensen J, Janse MJ, Fiolet JWT, Krieger WJG, D'Almoncourt CN, Durrer D. Tissue osmolality, cell swelling, and reperfusion in acute regional myocardial ischemia in the isolated porcine heart. *Circ Res* 1981; 49: 364-381
322. Tyberg JV, Misbach GA, Glantz AS, Moores WY, Parmley WW. A mechanism for shifts in the diastolic, left ventricular pressure-volume curve: the role of the pericardium. *Eur J Cardiol* 1978; 7 (supplement 1): 163-175
323. Van der Vusse GJ, Glatz JFC, Stam HCG, Reneman RS. Fatty acid homeostasis in the normoxic and ischemic heart. *Physiol Rev* 1992; 72: 881-940
324. Vary TC, Reibel DK, Neely JR. Control of energy metabolism of heart muscle. *Ann Rev Physiol* 1981; 43: 419-430
325. Ventura-Clapier R, Vassort G. Rigor tension during metabolic and ionic rises in resting tension in rat heart. *J Mol Cell Cardiol* 1981; 13: 551-561
326. Vercesi A, Reynafarje B, Lehninger AL. Stoichiometry of H^+ ejection and Ca^{2+} uptake coupled to electron transport in rat heart mitochondria. *J Biol Chem* 1978; 253: 6379-6385
327. Villereal ML. Sodium fluxes in human fibroblasts: Effect of serum, Ca^{2+} , and amiloride. *J Cell Physiol* 1981; 107: 359-369
328. Vogel WM, Briggs LL, Apstein CS. Separation of inherent diastolic myocardial fiber tension and coronary vascular erectile contributions to wall stiffness of rabbit hearts damaged by ischemia, hypoxia, calcium paradox and reperfusion. *J Mol Cell Cardiol* 1985; 17: 57-70
329. Walker EJ, Dow JW. Localisation and properties of two isoenzymes of cardiac adenylate kinase. *Biochem J* 1982; 203: 361-369
330. Weber A. The mechanism of the action of caffeine on sarcoplasmic reticulum. *J Gen Physiol* 1968; 52: 760-772
331. Weidmann S. The effect of cardiac membrane potential on the rapid availability of sodium-carrying system. *J Physiol* 1955; 127: 213-224
332. Weiss J, Shine KI. Extracellular potassium accumulation during myocardial ischemia: implications for arrhythmogenesis. *J Mol Cell Cardiol* 1981; 13: 699-704
333. Weiss J, Lamp ST. Cardiac ATP-sensitive K^+ channels: Evidence for preferential regulation by

- glycolysis. *J Gen Physiol* 1989; 94: 911-936
334. Westfall MV, Solaro RJ. Alterations in myofibrillar function and protein profiles after complete global ischemia in rat hearts. *Circ Res* 1992; 70: 302-313
335. Wieringa PA, Spaan JAE, Stassen HG, Laird JD. Heterogeneous flow distribution in a three dimensional network simulation of the myocardial microcirculation. *Microcirculation* 1982; 2: 195-216
336. Wilde AAM, Kleber AG. The combined effects of hypoxia, high K^+ , and acidosis on the intracellular sodium activity and resting potential in guinea pig papillary muscle. *Circ Res* 1986; 58: 249-256
337. Williams A. Mitochondria. In: *Cardiac Metabolism* (editors AJ Drake-Holland and MIM Noble), John Wiley and Sons Ltd, Chichester, 1983, page 151-171
338. Williams AJ. Factors influencing cardiac mitochondrial calcium transport. *J Mol Cell Cardiol* 1981; 13 (supplement 1): 98
339. Williamson JR. Glycolytic control mechanisms. II Kinetics of intermediate changes during the aerobic-anoxic transition in perfused rat heart. *J Biol Chem* 1966; 241: 5026-5036
340. Willis FA, Dry TJ. A history of the heart and the circulation, W.B. Saunders Co, Philadelphia, 1948.
341. Wilson RF, Laughlin DE, Ackell PH, Chilian WM, Holida MD, Hartley CJ, Armstrong ML, Marcus ML, White CW. Transluminal, subselective measurement of coronary artery blood flow velocity and vasodilator reserve in man. *Circulation* 1985; 72: 82-92
342. Winegrad S. Mechanism of contraction in cardiac muscle. *Int Rev Physiol* 1982; 26: 87-117
343. Winegrad S, Robinson TF. Force generation among cells in the relaxed heart. *Eur J Cardiol* 1978; 7 (supplement): 63-70
344. Winegrad S. Calcium release from cardiac sarcoplasmic reticulum. *Ann Rev Physiol* 1982; 44: 451-462
345. Witkowski FX, Corr PB. Mechanisms responsible for arrhythmias associated with reperfusion of ischemic myocardium. *Ann New York Acad Sciences* 1984; 427: 187-198
346. World Health Organization Annual Statistics Report 1985, Geneva, pp 466-487
347. Wyman RM, Farhi ER, Bing OH, Johnson RG, Weintraub RM, Grossman W. Comparative effects of hypoxia and ischemia in the isolated, blood-perfused dog heart: evaluation of left ventricular diastolic chamber distensibility and wall thickness. *Circ Res* 1989; 64(1): 121-128
348. Zak R, Galhotra SS. Contractile and regulatory proteins. In: *Cardiac Metabolism* (eds AJ Drake-Holland and MIM Noble), John Wiley and Sons Ltd, Chichester, 1983, page 339-364
349. Zhao M, Sonnenblick EH, Zhang H, Eng C. Increase in myofilament separation in the "stunned" myocardium. *J Mol Cell Cardiol* 1992; 24: 269-276
350. Zhu Y, Nosek TM. Intracellular milieu changes associated with hypoxia impair sarcoplasmic reticulum Ca^{2+} transport in cardiac muscle. *Am J Physiol Heart Circ Physiol* 1991; 261: H620-H626
351. Zimmer H-G, Trendelenburg C, Kammermeier H, Gerlach E. De novo synthesis of myocardial adenine nucleotides in the rat. Acceleration during recovery from oxygen deficiency. *Circ Res* 1973; 32: 635-642

CHAPTER 2 OBJECTIVES OF THE THESIS

Since 1628, when Harvey was the first to recognize that interruption of coronary flow results in an immediate decrease of force development, researchers were intrigued by the possible explanations of this phenomenon (Harvey, 1628). In the previous chapter I reviewed the possible hypotheses to explain the rapid decay of force development that results from hypoxia.

On the basis of the available experimental and clinical evidence the most likely explanations include: a) impairment of the excitation-contraction coupling process, at least partially explained by abbreviation of the duration of the action potential by ischemia activated ATP-sensitive potassium channels (Weiss and Lamp, 1989), b) impairment of force development as a result of accumulation of metabolites from high-energy phosphates, notably protons and inorganic phosphate (Kentish, 1986), c) decreased free energy change of ATP hydrolysis at normal or slightly decreased high-energy phosphate content (Kammermeier et al., 1982; Fiolet, 1984 but see Hoerter et al., 1988), and d) interaction between myocytes and the coronary vasculature (Koretsune, 1991).

The primary goal of the studies that are included in this thesis was to improve our insights in sarcomere mechanics. For this purpose not only normoxic but also hypoxic preparations were studied, both intact and following skinning. In addition we attempted to define the relationship between sarcomere mechanics and biochemistry, notably the content of energy-rich phosphate compounds.

The following hypotheses were tested:

1. The properties of the cardiac myofibrils, including the length dependence of calcium sensitivity, largely account for the shape of the ascending limb of the force - sarcomere length relation, both in intact and skinned cardiac muscle (Chapter 4).
2. Acidosis causes a shift of the force - pCa^{2+} curve to the right at all sarcomere lengths as a result of competition between H^+ and Ca^{2+} ions for binding to the myofilaments (Chapter 5).
3. Strontium is able to induce maximal force development by direct activation of the contractile apparatus and stimulation of calcium release by the sarcoplasmic reticulum (Chapter 6).
4. During hypoxic perfusion followed by flow standstill, rat cardiac muscle develops rigor in spite of the fact that concentrations of high-energy phosphates are only slightly diminished (Chapter 7).
5. The increased diastolic force that is observed during hypoxia of rat heart can nearly completely be explained on the basis of formation of rigor bonds (Chapter 8).
6. Impaired relaxation during repeated hypoxia is accounted for by calcium overload without evidence for rigor bond formation or a shift of the diastolic force - SL relation (Chapter 9).

These hypotheses will be addressed in more detail in the chapters that are mentioned in parentheses.

REFERENCES

1. Fiolet JWT, Baarscheer A, Schumacher CA, Coronel R, ter Wille HF. The change of the free energy of ATP hydrolysis during global ischemia and anoxia in the rat heart; its possible role in the regulation of trans-sarcolemmal sodium and potassium gradients. *J Mol Cell Cardiol* 1984; 16: 1023-1036
2. Harvey W. *Exercitatio anatomica de Motu Cordis et Sanguinis in Animalibus*. London, 1628. Trans Willis R. Barnes, Surrey, England, 1847
3. Hoerter JA, Lauer C, Vassort G, Gueron M. Sustained function of normoxic hearts depleted in ATP and phosphocreatine; a ³¹P-NMR study. *Am J Physiol* 1988; 255: C192-201
4. Kammermeier H, Schmidt P, Jungling E. Free energy change of ATP hydrolysis: a causal factor of early hypoxic failure of the myocardium? *J Mol Cell Cardiol* 1982; 14: 267-277
5. Kentish JC. The effects of inorganic phosphate and creatine phosphate on force production in skinned muscles from rat ventricle. *J Physiol* 1986; 370: 585-604
6. Koretsune Y, Corretti MC, Kusuoka H, Marban E. Mechanism of early ischemic contractile failure; inexcitability, metabolite accumulation, or vascular collapse? *Circ Res* 1991; 68: 255-262
7. Weiss J, Lamp ST. Cardiac ATP-sensitive K⁺ channels: Evidence for preferential regulation by glycolysis. *J Gen Physiol* 1989; 94: 911-936

CHAPTER 3 GENERAL METHODOLOGY

This chapter gives an overview of the methods that have been used for the studies that are included in this thesis. Specific methodological considerations will be mentioned in the individual chapters.

Muscle preparation

The studies that are included in this thesis were performed on trabeculae from the right ventricle of Rats. Sprague-Dawley or Norwegian Brown rats, weighting 200 - 300 gr, 2-4 months of age and of either sex, were anaesthetized with ethylether. Subsequently the thorax was opened with sturdy scissors and the heart rapidly excised and transferred to a dissection disk. Following removal, the heart was within 30 seconds retrogradely perfused according to the Langendorff technique with a modified Krebs - Henseleit solution with a high (15 mM) potassium concentration in order to stop spontaneous beating. Prior to dissection, the heart was immobilized by means of needles, that were pierced into the silicone bottom of the dissection disc. The heart was opened by means of a pair of scissors, cutting the free wall of the right ventricle from the pulmonary outflow tract along the interventricular septum toward the apex. Right atrial tissue was removed along the atrioventricular ring and the heart was remounted with the right ventricle opened to improve visibility. Subsequently the heart was carefully inspected under a binocular microscope (Nikon SMZ-1, magnification 7 - 30 x). Free running tabeculae were dissected that were connected at one site to the tricuspid valve and on the other side to the free wall of the right ventricle. Only muscles that were ribbon shaped, unbranched and uniform in thickness and width were selected for dissection. Suitable muscles were carefully dissected by cutting through the atrioventricular ring and trimming a piece of the valve on one site and retaining a cube of the right ventricle at the basis on the other side. The average length of the preparations that were used for the experiments was 3 ± 1.1 mm, width 0.4 ± 0.3 mm and thickness 0.1 ± 0.05 mm (mean \pm S.D., $n=49$); the average success rate of obtaining a suitable preparation from one animal was 30%.

Following dissection, the muscles were transferred to the bath (width 3 mm, height 4 mm, length 30 mm, content 360 μ L) that was milled from plastic with a microscope cover slide as bottom. The bath was mounted on the inverted microscope that formed the central part of the experimental setup. It was perfused with medium at a flow of 2 - 6 ml/min; turbulence of flow around the preparation was prevented. The temperature of the perfusion medium was adjusted (± 0.1 °C) prior to entering the bath, using a heat exchanger that was connected to a thermostated water bath (Model F3, Haake, FRG).

The valvular end of the preparation was attached to a stainless steel hook mounted on a carbon fiber arm (Fokker Aviation Industries, The Netherlands) connected to the axis of a motor that was controlled by a dual servo amplifier. The muscular end of the preparation was positioned in a plastic cradle that was covered with silicone cement following mounting; the cradle was glued onto the tip of the silicon force transducer with a minimum of epoxy resin in order not to cover the resistors on the silicon beam.

Displacement during muscle contraction, either in horizontal (translation) or vertical direction, was avoided by repositioning or remounting; in case these artefacts could not be avoided, the muscle was discarded. Since the cover and bottom of the bath consisted of thin glass plates, the incident laser beam illuminated the muscle directly and the generated first order band could be project freely onto the photodiode array (see below).

After mounting, the preparation was stimulated at 1 Hz during 1 hour at 25° C, perfused by

medium at $[Ca^{2+}]_i$ 1.5 mmol/L, after stretching to a sarcomere length of 2.1 μ m. At this sarcomere length passive force development is negligible. During the equilibration period, both sarcomere length at rest and during the twitch decreased, due to relaxation of the passive elastic elements in the muscle. The muscle was discarded if steady state twitch force decreased by more than 30 % during the equilibration period.

Experimental setup

During the experiments the preparations were observed with an inverted microscope (Zeiss, 14612) and T.V. camera (Panasonic TV camera, model WV-1500) and video monitor (Panasonic video monitor, model TR-930 UC) (see figure 1).

Sarcomere length in the preparation was measured by a laser diffraction technique, as has been reported previously (Heuningen, 1980; Iwazumi and Pollack, 1979; Krueger and Pollack, 1975). In short, an incident laser beam (15 mWatt He-Ne laser, Spectra-Physics 105-1, Mt. View, Ca) with a diameter that was reduced to 400 μ m by means of a convergent lens, focal length 50 cm, was projected on the muscle. Since heart muscle has regular cross striations, it will serve as an optical grating and diffract incident monochromatic laser light into one zero order and multiple, spatially symmetrical higher order bands. The angle between the zero order band and the first order band is proportional to the grating constant (i.e. sarcomere length) and the wave length of the incident laser beam (632.8 nm). Consequently sarcomere length can be inferred from the angle under which the first order band deviates from the zero order band. For this purpose one of the generated first order diffraction bands was projected via a mirror on a 512 element photodiode array (Reticon RL 512, Sunnyvale, CA) that was scanned twice per millisecond. An analog electronic circuitry calculated median sarcomere length from the light intensity distribution in a selected observation window of the array, following correction for the zero order intensity distribution and scatter. This was accomplished by comparing the integral of the intensity distribution within the observation window to the integral of the preceding photodiode scan. Resultantly, as soon as the current integral exceeded 50 % of the previous scan, a sample and hold circuitry recorded the position of the median of the intensity distribution of the first order. The output of the sample and hold circuit was converted to a voltage, proportional to median sarcomere length. The integral of the intensity distribution in the window was kept constant by automatic adjustment of the gain of the system. Prior to the experiments, the circuitry was calibrated by means of gratings that were placed at the level of the muscle. The calibration error was smaller than 1%. The resolution of the measurement in cardiac trabeculae was limited by noise to 5 nm optimally and 20 nm nominally.

The muscles were stimulated by means of platinum electrodes that were positioned on either sides of the chamber, parallel to the muscle. Rectangular stimuli were delivered by an isolated pulse generator (Model DS2, Digitimer, UK). The pulse duration was 2 ms; stimulus strength was adjusted to 50% above the threshold stimulus.

Force was measured with a silicium strain gauge covered with silicon adhesive (AME AE 801, Mikro-Elektronikk, Horton, Norway). The sensitivity of the transducer was 3 mV/mN; resonance frequency 3 KHz; drift less than 0.1 mN/hour, the gain was constant in the range from 15 to 35 ° C. In some experiments performed work was expressed as a force-frequency product as follows. Following the change in stimulus rate after the first hour, force attained a stable level within 5 minutes. Then, force was expressed as a percentage of control force at 1 Hz and multiplied by the frequency of stimulation to obtain the force-frequency product.

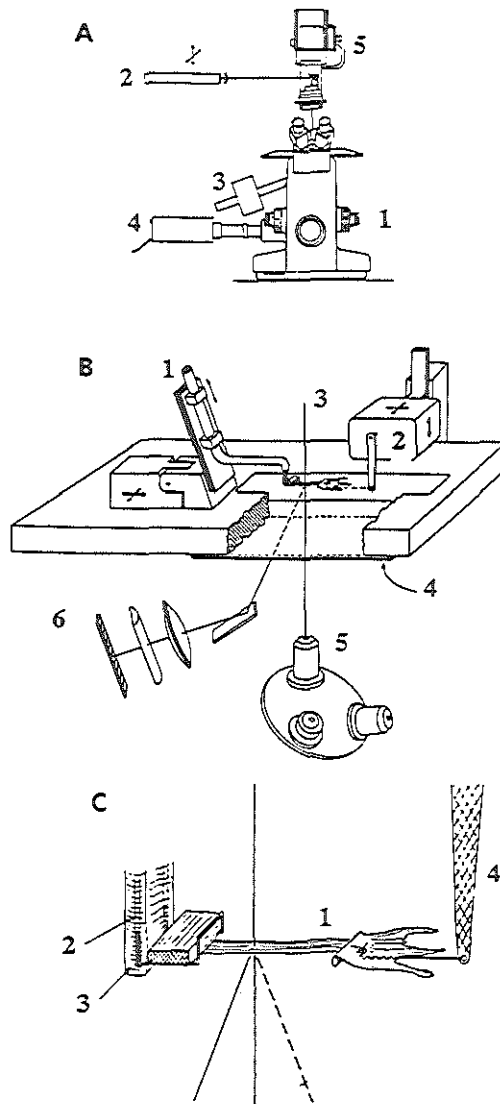


Figure 1: Experimental setup to measure sarcomere length in rat cardiac trabeculae.

A. The experimental chamber is positioned on the stage of an inverted microscope: (1) microscope; (2) He-Ne laser; (3) photodiode array; (4) TV camera; (5) microscope light source.

B. Exploded view of the experimental chamber: (1) force transducer; (2) servo controlled motor (3) He-Ne laser beam; (4) coverslip used as bottom; (5) microscope objective; (6) photodiode array

C. Detail of the trabecula (1) positioned between the force transducer (2), which is insulated with silicon rubber (3), and the servomotor (4). The incident laser beam is diffracted into two symmetrical first order bands; the muscle is mounted perpendicular to the incident laser beam (Modified from de Tombe and ter Keurs, *Circ Res* 1990; 66: 1239-1254).

The valvular end of the preparation was attached to a stainless steel hook (diameter 100 μm) connected on a carbon fiber motor arm (Fokker Aviation Industries, The Netherlands) mounted on the axis of a motor that was controlled by a dual servo amplifier (Model 300S Dual Mode Servo, Cambridge Technology, Cambridge, Massachusetts, U.S.A.) (10). The step response time of the motor arm was 1.5 msec (ter Keurs et al., 1980a; Kentish et al., 1986). During the experiment, muscle length could be changed by adjusting the setpoint of the servo motor. In addition, the setup allowed to construct a complex stretch and release ramp function of the motor axis setpoint, synchronized with the stimulus pulse, and applied to the muscle preparation.

Force, muscle length, sarcomere length as well as temperature and stimulus trigger were recorded on an instrumentation recorder (Gould Instrumentation Recorder 6500) and 8 channel paper pen recorder (Gould 2800S). Selected force and sarcomere length signals were digitized (DT2801, Data Translation, Inc., Marlborough, Mass., U.S.A.) and stored on a Winchester hard disc of a personal computer (IBM PC/AT) for further analysis of twitch characteristics (sampling rate 900 Hz/channel).

Force - Sarcomere length measurement

Following dissection the muscles were mounted in the experimental setup and stimulated at 1 Hz at a $[\text{Ca}^{2+}] = 1.5 \text{ mM}$. The developed stress was calculated from peak twitch force at a sarcomere length of 2.0 μm , and the cross-sectional area of the muscle; the average stress was $71 \pm 30 \text{ mN/mm}^2$.

After one hour of stabilization of the muscles, the relation between force and sarcomere length was determined as follows. First, muscle length was adjusted to a resting sarcomere length of 2.1 - 2.15 μm . Then, muscle length was changed to the test length and kept constant during the subsequent four beats. Force and sarcomere length were measured immediately before and at peak twitch force of the last test beat. Active force was calculated as peak twitch force minus resting force at the sarcomere length that was attained during the twitch; this assumes that the parallel elastic elements are in, or in parallel with the sarcomeres (ter Keurs et al., 1980a). Between each series of test beats, sarcomere length was maintained at 2.1 μm for 6 - 10 beats. The procedure was repeated for a range of sarcomere lengths at calcium concentrations, that were varied between 0.3 mM and 5.1 mM in steps of 0.3 mM.

Maximum twitch force (F_{max}) was assessed by extrasystolic potentiation at $[\text{Ca}^{2+}]_0$ exceeding 0.6 mM; the protocol consisted of administering a series of 3, 5, 7, 10, 15 or 20 stimuli at intervals of 250 or 300 msec. By means of this procedure twitch force could be potentiated to a maximum (F_{max}) that was recorded following the last potentiating beat; this phenomenon was assumed to be related to saturation of the myofilaments (Schouten et al., 1990). An increase of the number of extrasystoles above the optimum resulted in decreased peak force, that was associated with aftercontractions (Schouten et al., 1990).

Force - Sarcomere length shortening velocity measurement

The velocity of sarcomere shortening was measured by inducing isovelocity releases of muscle length. During the initial 80 msec of the twitch sarcomere length was kept constant at 2.1 μm by stretching the muscle from the valvular end. As soon as isometric twitch force exceeded 70% of its maximum, the muscle was rapidly released ($< 1 \text{ msec}$) to a new load level. By applying muscle length release ramps, with predetermined speed and amplitude, twitch force was subsequently maintained at this level. During the first 10 - 50 msec the velocity of sarcomere shortening was calculated by linear regression from the digitized sarcomere length signal (van Heuningen, 1982; de Tombe, 1989).

Transfer function analysis

In a series of experiments changes in sarcomere dynamics were evaluated by transfer function analysis according to the following protocol. Sine waves from a function generator (Hewlett Packard 3310A) at frequencies of 0.1, 0.2, 0.4, 0.8, 1.6, 3.2, 6.4, 12.5, 25, 50, 100, 200 and 400 Hz, were applied to induce muscle length changes smaller than or equal to 1% of the muscle length at SL 2.1 μm . Force, muscle length and sarcomere length tracings were recorded with an instrumentation record (Gould 6500) for further analysis. The dynamic stiffness was expressed as ratio of the force fluctuation that resulted from the muscle length perturbation, and twitch force that was attained without the perturbation; the ratio was corrected for the real sarcomere length perturbation and changes in steady state twitch force during the experiment. The phase shift (in degrees) between the sarcomere length and force tracings was calculated with a digital oscilloscope (Data Precision 2200) from averaged signals. Stiffness and phase shift, plotted as a function of the frequency of the sinusoidal length changes, also denoted as the transfer function, were analyzed.

Likewise, white noise was applied to establish the transfer function of normoxic and hypoxic muscles. White noise was obtained from a white noise generator (Hewlett-Packard, 8057A Precision Noise Generator). Force, muscle length and sarcomere signals were continually filtered with low-pass, fourth order Butterworth filters with a cut-off frequency of 500 Hz and 40 Hz, respectively. During the first 1.4 seconds the signals from the filters at high cut-off frequency were digitized by A/D converters (Data Transduction DT2801 board; sampling rate 2.86 KHz). During the next 4.1 seconds the signals from the filters at low cut-off frequency were digitized at a sampling rate of 1 KHz and stored. For each measurement this protocol was repeated twice. The data were stored on hard disk of an IBM PC-AT (IBM, Boca Raton, Florida 33432) and transferred to a Vax-750 VMS 4.4 (DEC, Maynard, Massachusetts). The magnitude (logarithm of stiffness, ratio of $F(t)/S_{L(t)}$ in dB) and phase (in radians) of the individual records was calculated by Fast Fourier Transformation. The transfer function was calculated by subtracting the sarcomere length spectra from the force spectra, obtained at the same frequency, followed by averaging of the three calculated spectra. To obtain the transfer function spectrum the average spectrum at frequencies beyond 40 Hz was combined with the spectrum at low frequency up to and including a frequency of 40 Hz.

Curve fitting and statistical analysis

A modified Hill's hyperbola of the form $(v + a) * P = (P - P_0) * b$ was fitted on the obtained force - velocity data by means of a least square iterative procedure.

The same applied to the relation between normalized twitch force at constant active sarcomere length and variations in pH of the perfusate. For this purpose, the Michaelis Menten equation: $K_m^n / (K_m^n + pH^n)$ was fitted to the data.

Perfusion solutions

The composition of the modified Krebs - Henseleit solution was (in mM): Na^+ 150, K^+ 5, Cl^- 127.5, Mg^{2+} 1.2, H_2PO_4^- 2, SO_4^{2-} 1.2, HCO_3^- 27, glucose 10.1, Ca^{2+} 1.5. Fifteen mM of KCl was added to stop spontaneous beating.

During the experiments at normoxia, the superfusate was in equilibrium with a gas mixture of 95% O_2 and 5 % CO_2 (pH 7.4, pO_2 500 - 600 mm Hg). During hypoxia, the preparations were superfused with glucose-free medium that was in equilibrium with 95% N_2 and 5% CO_2 (pH 7.4, pO_2 6 - 9 mm Hg).

During the acidosis experiments, the medium was in equilibrium with a gas mixture of 80% O₂ and 20% CO₂, which induced a pH of 6.68 ± 0.02 , as measured with a pH meter (pHm 26, electrode GK 2321c, Radiometer, Copenhagen). In addition, the composition of the gas mixture was varied in order to vary the pH over a range between 6.2 and 8.0.

Determination of high pressure liquid chromatography (H.P.L.C.)

The muscle preparation was quickly (2-4 seconds) frozen following removal of the remnants of the right ventricular free wall and the tricuspid valve. Until further analysis the sample was stored in liquid nitrogen. The frozen specimen was added to 500 μ l of frozen 0.4 M perchloric acid in a precooled (liquid nitrogen) Teflon cup of a Mikro-dismembrator (Braun, Melsungen, BFR). A precooled Teflon marble was added and the acid mixture was shaken at 50 Hz for 60 seconds. Next the frozen homogenate was transferred to a centrifuge tube, that had been weighed before to allow exact determination of the weight of the sample. After thawing and centrifugation (Eppendorf 54148 microcentrifuge, 12,000 rpm, 2 min, 5 °C), the supernatant fluid was neutralized (final pH 5 - 7, 0° C) with a mixture of 2 M KOH and 1 M K₂CO₃. KClO₄ was removed by centrifugation for 30 seconds at 12,000 rpm. The supernatant was kept on ice until analysis (within 1 hour) of high-energy phosphates content. Adenine nucleotide and PCr concentrations were expressed in mmol/l of muscle volume and μ mol/g protein (see below).

ATP, ADP, AMP and PCr were determined in the supernatant by HPLC with slight modifications of the method described by Harmsen. Samples (200 μ l) were injected onto a 30 cm Partisil-10-SAX ion-exchange column (Whatman, Maidstone, UK). The sample was eluted (flow: 2 ml/min) during 30 minutes with an incremental ionic strength buffer gradient from 100% 16 mM H₃PO₄ (pH adjusted to 2.85 with NH₄OH, Buffer A) to 100% 750 mM NH₄H₂PO₄ (pH 4.6, Buffer B) (Waters Model 660 Solvent Programmer, Waters Associates, Milford MA). After this gradient the column was equilibrated (5 min) with 100% buffer B followed by a return gradient to 100 % buffer A (in 10 min), again followed by equilibration with 100% buffer A (15 min). Peaks were determined by UV light absorption (254 nm for ATP, ADP, AMP and 214 nm for PCr (440 and 441 UV Monitors, Waters Associates, Milford MA). Concentrations were calculated from peak heights that were compared with measurements from standard solutions. These solutions (high-energy phosphates plus BSA) were processed as muscles and recoveries were found to be ATP: $92 \pm 1\%$, ADP: $91 \pm 1\%$ and PCr: $92 \pm 5\%$ ($n = 21-26$; mean \pm SD). The minimal detectable amounts of high-energy phosphates were (in pmoles): ATP 20, ADP 15, PCr 20 and AMP 15. AMP was not detected in normoxic trabeculae.

Protein determination

The protein pellet, which remained after as much acid supernatant of the centrifuged mixture as possible had been removed, was dissolved in 1 ml 0.3 M KOH solution (20 °C, 60 min). After centrifugation, 100 μ l of the supernatant fluid was used for protein determination (Biorad Protein Assay; Biorad, Munich, GFR). Bovine serum albumin (BSA, 100 μ l; 5 μ g) was treated like samples in order to determine protein recovery in the procedure. The procedure allowed detection of at least 2 μ g protein per muscle sample. The volume of all preparations that were available for biochemical analysis, was calculated from their dimensions and ranged from 20 to 18000 nl (median 240 nl; $n = 55$). The amount of protein in the preparations varied between 2.6 and 2062.9 μ g (median 32.7; $n = 52$). The relation between protein content and volume of all trabeculae and papillary muscles, where both parameters were available, was $P = 0.05 * V + 26.3$ ($r = 0.938$) where P represents protein in μ g and V = volume in nl. The protein - volume relation of the trabeculae was $P = 0.11 * V + 14.1$ ($r = 0.72$). The difference of the regression coefficients of both relationships was not significant.

CHAPTER 4

COMPARISON BETWEEN THE SARCOMERE LENGTH-FORCE RELATIONS OF INTACT AND SKINNED TRABECULAE FROM RAT RIGHT VENTRICLE; INFLUENCE OF CALCIUM CONCENTRATIONS ON THESE RELATIONS

Jonathan C Kentish, Henk EDJ ter Keurs, Lucio Ricciardi, Jeroen JJ Buxx, and Mark IM Noble

Published in Circulation Research 1986; 58: 755-768

Comparison between the Sarcomere Length-Force Relations of Intact and Skinned Trabeculae from Rat Right Ventricle

Influence of Calcium Concentrations on These Relations

Jonathan C. Kentish, Henk E.D.J. ter Keurs, Lucio Ricciardi, Jeroen J.J. Bucx, and Mark I.M. Noble

From the Department of Experimental Cardiology, University Hospital Leiden, Leiden, The Netherlands; the Department of Physiology, University College London, London WC1E 6BT, U.K.; the Institute of Human Physiology, University of Pavia, 27100 Pavia, Italy; and the King Edward VII Hospital, Midhurst, West Sussex, England

SUMMARY. To investigate the extent to which the properties of the cardiac myofibrils contribute to the length-force relation of cardiac muscle, we determined the sarcomere length-force relations for rat ventricular trabeculae both before and after the muscles were skinned with the detergent Triton X-100. Sarcomere length was measured continuously by laser diffraction. In the unskinned trabeculae stimulated at 0.2 Hz, the relation between active force and sarcomere length at an extracellular calcium concentration of 1.5 mM was curved away from the sarcomere length axis, with zero force at sarcomere length of 1.5–1.6 μm . At 0.3 mM calcium, the sarcomere length-force relation was curved toward the sarcomere length axis. Chemical skinning of the muscle with 1% Triton X-100 in a "relaxing solution" caused an increase in intensity and decrease in dispersion of the first order diffraction beam, indicating an increased uniformity of sarcomere length in the relaxed muscle. During calcium-regulated contractures in the skinned muscles, the central sarcomeres shortened by up to 20%. As the calcium concentration was increased over the range 1–50 μM , the relation between steady calcium-regulated force and sarcomere length shifted to higher force values and changed in shape in a manner similar to that observed for changes in extracellular calcium concentration before skinning. The sarcomere length-force relations for the intact muscles at an extracellular calcium concentration of 1.5 mM were similar to the curves at calcium concentration of 8.9 μM in the skinned preparations, whereas the curves at an extracellular calcium concentration of 0.3 mM in intact muscles fell between the relations at calcium concentrations of 2.7 and 4.3 μM in the skinned preparations. A factor contributing to the shape of the curves in the skinned muscle at submaximal calcium concentrations was that the calcium sensitivity of force production increased with increasing sarcomere length. The calcium concentration required for 50% activation decreased from $7.71 \pm 0.52 \mu\text{M}$ to $3.77 \pm 0.33 \mu\text{M}$ for an increase of sarcomere length from 1.75 to 2.15 μm . The slope of the force-calcium concentration relation increased from 2.82 to 4.54 with sarcomere length between 1.75 and 2.15 μm . This change in calcium sensitivity was seen over the entire range of sarcomere lengths corresponding to the ascending limb of the cardiac length-force relation. It is concluded that the properties of the cardiac contractile machinery (including the length-dependence of calcium sensitivity) can account for much of the shape of the ascending limb in intact cardiac muscle. (*Circ Res* 58: 755–768, 1986)

THE basic mechanism that underlies the length-force relation in the myocardium has been the subject of considerable discussion (for reviews, see Jewell, 1977; ter Keurs, 1983; Allen and Kentish, 1985a). It is generally agreed that the steepness of the relation in intact cardiac muscle must be due to an increase in the Ca^{++} activation of the cardiac myofibrils as muscle length, and therefore sarcomere length (SL), is increased. There are two ways by which this could occur. The first is that more Ca^{++} may be released to the myofibrils at longer sarcomere lengths. There is some evidence that, at least in

skinned ventricular cells, the Ca^{++} -induced release of Ca^{++} from sarcoplasmic reticulum (Fabiato, 1983) may increase with sarcomere length (Fabiato and Fabiato, 1975; Fabiato, 1980). However, a length-dependence of Ca^{++} release in intact muscle may not be important in the short term, because immediately after a step increase in muscle length, the active force development of papillary muscles increases markedly, whereas the $[\text{Ca}^{++}]$ transient (the brief rise in the cytosolic $[\text{Ca}^{++}]$) measured with aequorin decreased in rat and cat myocardium (Allen and Smith, 1985). The simplest interpretation is that

the supply of Ca^{++} to the myofibrils is not changed immediately, and thus cannot account for the immediate change in developed force.

The second possible mechanism for length-dependent activation in intact cardiac muscles is that the sensitivity of the myofibrils to Ca^{++} may increase as muscle length increases. Such a length dependence of myofibrillar Ca^{++} sensitivity has been observed in studies with skinned fibers (muscle fibers with a disrupted sarcolemma), although in most of these studies only the sarcomere length range above 2.2 μm was investigated (see Allen and Kentish, 1985a; Stephenson and Wendt, 1984). The physiological range of sarcomere lengths during contraction in intact cardiac muscle under normal conditions is probably 1.6–2.3 μm (Page, 1974; Sonnenblick and Skelton, 1974; ter Keurs, 1983). Length-dependent variation of the sensitivity of the contractile system to Ca^{++} ions has been observed in mechanically skinned cardiac cell fragments over a range of sarcomere lengths between 1.8 and 2.3 μm (Fabiato, 1980). Subsequently, a quantitative study by Hibberd and Jewell (1982) has shown that Ca^{++} sensitivity of skinned cardiac trabeculae depends on resting sarcomere length between 1.9 and 2.5 μm . To what extent the length-dependence of myofibrillar Ca^{++} sensitivity observed by Hibberd and Jewell (1982) accounts for the length dependence of activation in intact cardiac muscle is not clear, for two reasons: (1) Hibberd and Jewell (1982) did not measure the sarcomere length during contraction of the skinned muscles, and so it is not known whether the length dependence of myofibrillar Ca^{++} sensitivity occurs over the entire range of active sarcomere lengths found in intact cardiac muscle; neither is the effect of shortening of the central sarcomeres that occurs in cardiac muscle (Julian and Sollins, 1975; Krueger and Pollack, 1975; ter Keurs et al., 1980) known. (2) Although comprehensive force-sarcomere length relations for the ascending limb have been determined in maximally activated skinned single cells (Fabiato and Fabiato, 1975, 1976) and in intact trabeculae (ter Keurs et al., 1980; Gordon and Pollack, 1980), the relations are not strictly comparable because of the different degrees of Ca^{++} activation in the two preparations and because of their different structural characteristics.

In the present experiments, we determined the force-sarcomere length relations in trabeculae at various concentrations of Ca^{++} before and after these muscles were skinned with a detergent. A preliminary account of these experiments has been published (Kentish et al., 1983).

Methods

Apparatus

Sarcomere length in the central part of the muscles was measured by laser diffraction, as described previously (ter Keurs et al., 1980). In short, the intensity distribution of

the first order diffraction pattern was monitored by a photodiode array (Reticon 256 EC), which was scanned electronically every 0.5 msec. The median SL was computed electronically after a correction had been made for the contribution of light scattered from zero order. SL could usually be measured to a resolution of 0.02 μm . Muscle length was measured and controlled with a servo motor (Cambridge Technology 300 Dual Mode Servo) with a capacitive length transducer (overall compliance of motor + arm = 0.6 $\mu\text{m}/\text{mN}$). The force transducer was a semiconductor strain gauge (AE801, AME) with a short carbon fiber extension arm (sensitivity = 1.5 mV/mN, compliance = 1 $\mu\text{m}/\text{mN}$, natural frequency = 2.9 kHz). Muscle force, muscle length, and median SL were displayed on an oscilloscope with hard-copy unit (Tektronix 5103, 613, 4631) and were recorded on a Gould chart recorder. In addition, the intensity distribution of the corrected first order diffraction pattern was monitored on an oscilloscope. A position-sensitive photodiode (UDT 45C4) was also used in some experiments to measure the intensity of the first order diffraction band.

The rest of the apparatus was as described by ter Keurs et al. (1980), except that the volume of the flow-through muscle bath was decreased from 2 ml to 250 μl with Lucite inserts in order to accelerate solution changes.

Experimental Protocols

All experiments were performed at room temperature (22°C–24°C). In the first part of each experiment, the relationship between force and SL was determined in the unskinned trabeculae by a procedure similar to that described by ter Keurs et al. (1980). Briefly, unbranched trabeculae were dissected from the right ventricles of 12-week-old Wistar rats and were mounted in the muscle bath. A hook on the force transducer was passed through the tricuspid valve close to the muscle; the other end of the muscle was held by an oval ring of stainless steel wire attached to the motor. A piece of ventricular wall remaining at this end of the muscle prevented the end of the muscle from slipping through the ring. The dimensions of the muscle used were measured when muscle length had been set to a resting SL of 2.1 μm . These dimensions were (in mm): length, 3.29 ± 0.10 ; width, 0.277 ± 0.036 ; thickness, 0.096 ± 0.009 (mean \pm SE, $n = 12$). The muscles were superfused at 3 ml/min with an oxygenated saline (ter Keurs et al., 1980) containing 0.3 or 1.5 mM Ca^{++} , and were stimulated at 0.2 Hz via platinum field electrodes. Muscles were discarded if they did not contract uniformly or if there was twisting of the diffraction pattern. After a 30-minute period for stabilization of the muscles, the force-SL relations were determined as follows. First, the muscle length was set to give a resting SL of 2.10–2.15 μm . Muscle length was then altered for four beats. The resting force and resting SL were measured just before the fourth beat, and the total force and active SL were measured at peak force during the fourth beat (Fig. 1A). Active force in the muscle was calculated as the total force at the SL at the peak of contraction minus the resting force at the same SL; this assumes that the parallel elastic elements are in, or in parallel with, the sarcomere alone (cf. ter Keurs et al., 1980; and see Results). The muscle was maintained at the control SL of 2.1 μm for 6–10 beats between each series of 4 test beats. The process was repeated for a range of test stretches or releases at two Ca^{++} concentrations: 0.3 mM and 1.5 mM.

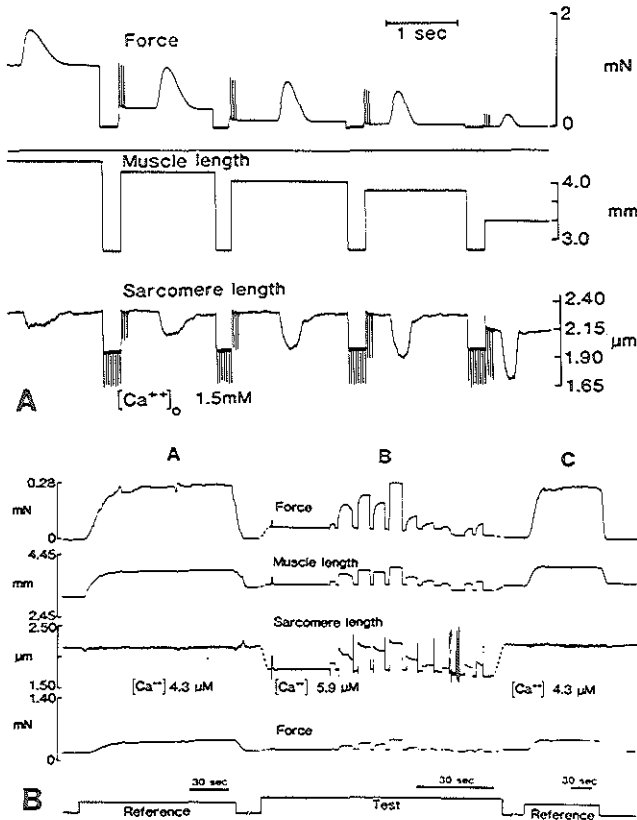


FIGURE 1. Protocols to establish force-sarcomere length relation in intact and skinned muscles. Panel A: experimental protocol used to establish the force-sarcomere length relations in the unskinned trabecula. In the example shown, the bathing $[Ca^{2+}]$ was 1.5 mM. The muscle was stimulated at 0.2 Hz and stretched to different lengths for four beats. Note the different chart speeds. Considerable sarcomere shortening was seen during contraction. Panel B: the protocol for the determination of the force-sarcomere length relations in the skinned muscle. The muscle was activated for 2 or 3 minutes by a known concentration of Ca^{2+} in the test solution (5.9 μM in this case), and in the final minute, the muscle was stretched transiently to different lengths (panel B). The steady force and sarcomere length reached after each stretch were measured. To correct for any deterioration in the contractile performance of the muscles during this protocol, the muscle was bathed in a "reference" solution of 4.3 μM Ca^{2+} before and after the test solution (panels A and C). The sarcomere length was held constant during these reference contractions. Note that the development of force in the test solution caused the sarcomere length (measured in the central part of the muscle) to be 0.4 μm less than in the muscle when relaxed at the same muscle length. Force was recorded at two sensitivities and measured from the bottom trace when saturation (fifth test in Panel B) occurred at the top trace.

The muscle then was skinned by 30-minutes of superfusion with "relaxing solution" (see below for details of solutions) to which had been added 1% Triton X-100 [procedure modified slightly from that of Kentish (1984)]. This "skinning solution" and all subsequent solutions were pumped through the bath at 1 ml/min. If the SL altered during the skinning period, it was reset to 2.1 μm. The skinned muscle then was bathed in solutions containing 1 nM to 200 μM free $[Ca^{2+}]$. The method used to establish the relationships between force and SL at a given Ca^{2+} concentration is illustrated in Figure 1B. First, a "reference" contracture was produced by changing from the relaxing solution (free $[Ca^{2+}] < 0.3$ μM) to an "activating solution" containing 4.3 μM free $[Ca^{2+}]$ (Fig. 1B, panel A). To accelerate the attainment of a steady force in this and other contractures, the 10 mM ethyleneglycol-bis(β-aminoethyl ether)-N,N,N',N'-tetraacetic acid (EGTA) remaining in the muscle from the relaxing solution was washed out with a "pre-activating solution" of low [EGTA] (Ashley and Moisesescu, 1974; Moisesescu, 1976; see below). During the reference contracture, we maintained the SL at 2.1 μm by stretching the muscle. The muscle then was relaxed for 2 minutes and was activated with an activating solution of

the desired $[Ca^{2+}]$ (up to 200 μM) for 2 or 3 minutes. In the last minute, by which time force and SL were steady (Fig. 1B panel B; see also Fig. 3), the muscle was given transient stretches or releases, each lasting for about 5 seconds. Force and SL were measured when they had reached new steady values during each stretch or release. As with the unskinned muscle, the active force was taken as the total force at a given SL minus passive force in the relaxed muscle at the same SL. After the series of length changes shown in Figure 1B, the muscle was returned to relaxing solution for 2 minutes. The reference contracture then was repeated (Fig. 1B, panel C). The forces in the first and second reference contractures were used to correct for the small but progressive loss of contractile force in the skinned preparations (14.3% ± 8.2% per hour, mean ± SE from six muscles). It was assumed that the maximum contractile performance of the muscle declined linearly with time between the reference contractures. Accordingly, a linear interpolation was used in which each value of force measured during the determination of the force-SL relation was multiplied by the appropriate factor to correct for the decline. Preparations in which force declined 50% (or more) during the first three control

contractures, and preparations in which the diffraction pattern disappeared during contractures were rejected.

The protocol shown in Figure 1B was repeated for a range of Ca^{++} concentrations from 1 mM to 200 μM . In some experiments, pairs of Ca^{++} concentrations were tested consecutively, with no relaxation of the muscle in between.

We point out that the activating solutions used to produce the reference contractures did not maximally activate the myofibrils. It is usual to employ activating solutions of optimal $[\text{Ca}^{++}]$ for the correction procedure, but these were not used in the present experiments because contractures at the optimal $[\text{Ca}^{++}]$ often resulted in irreversible degradation of the diffraction pattern (see Results). Theoretically, the use of suboptimal $[\text{Ca}^{++}]$ has the disadvantage that the force in the reference contractures would be altered if there were a permanent change in the Ca^{++} -sensitivity of the muscle during the experiment. However, it has previously been shown that the deterioration of force occurs without any significant change in Ca^{++} sensitivity (Moisescu, 1976; Kentish, 1982).

The major technical problem in these experiments was that the diffraction pattern deteriorated irreversibly if the muscle was activated at high Ca^{++} concentrations and at long sarcomere lengths. Several changes in experimental protocol were tried in an attempt to reduce this deterioration. Previously reported methods for improving the retention of the pattern by slow activation with Ca^{++} (Iwazumi and Pollack, 1981) or by stretches and releases of the muscle (Brenner, 1983) proved to be of little value for the skinned cardiac muscle. To investigate whether the loss of the diffraction pattern resulted from a limitation in the supply of high-energy substrate to the myofibrils (cf. Brenner, 1983), in one experiment we doubled the $[\text{Mg-ATP}]$ from 5 mM to 10 mM and the $[\text{CP}]$ from 15 mM to 30 mM and added 0.1 mM adenosine diphosphate (ADP). The $[\text{Mg}^{++}]$ was maintained at 3.0 mM by raising the $[\text{MgCl}_2]$, and the ionic strength was kept at 0.2 M by lowering the [potassium propionate]. However, this change of solution composition affected neither the force-SL relationships (results not shown) nor the deterioration of the diffraction pattern.

Solutions

All solutions for the skinned muscles contained 100 mM potassium propionate, 20 mM BES buffer (see below), 5 mM $\text{K}_2\text{Na}_2\text{ATP}$, 8.17–9.00 mM MgCl_2 (adjusted to give a calculated $[\text{Mg}^{++}]$ of 3.0 mM), 10 mM Na_2HCP , 1 mM dithiothreitol, and 25 $\mu\text{g}/\text{ml}$ creatine kinase. In addition, relaxing solution contained 10 mM K_2EGTA and 0 or 2.5 mM added Ca^{++} , pre-activating solutions contained 9.85 mM K_2 -2,6-diaminohexane- N,N,N',N' -tetraacetic acid (HDTA) and 0.15 mM K_2EGTA , and activating solutions contained 10 mM K_2EGTA and 4–10 mM Ca^{++} (to give a calculated free Ca^{++} concentration of 0.3–50 μM). The $[\text{K}_2\text{EGTA}]$ was calculated by taking into account the impurity of EGTA [measured purity = 96.2% (see Kentish, 1984)]. The pH was adjusted to 7.00 with KOH. The activating solutions of Ca^{++} concentrations up to 50 μM were made as described by Ashley & Moisescu (1977). An activating solution of 280 μM free Ca^{++} was used in two experiments. The free concentrations of the ions were calculated by an iterative computer program. Details of this calculation, of the measurement of the EGTA purity and the contaminant calcium, and of the calibration of the

pH electrodes are given elsewhere (Kentish, 1984). The calculated ionic strength was 0.20 M.

In the first few experiments, relaxing solution contained 10 mM EGTA and no added Ca^{++} . However, the calculated $[\text{Ca}^{++}]$ of this solution (1 mM) was much less than that which exists in cardiac cytosol during diastole [probably about 0.1 μM Ca^{++} (Fabiato, 1983)]. To produce a more physiological resting $[\text{Ca}^{++}]$, in most experiments we used a relaxing solution of 0.16 μM free Ca^{++} ([total calcium] = 2.5 mM) to achieve relaxation of the muscle. As a check that this $[\text{Ca}^{++}]$ was below the threshold for activation of the muscle at any SL studied, the force in this solution was compared with that in the solution of $[\text{Ca}^{++}] = 1$ mM. The solution with 0.16 μM free Ca^{++} did not produce any activation of the muscle. Even at the longest SL studied (2.3 μm), at which the Ca^{++} sensitivity would be expected to be greatest (see Results), the forces developed in the two solutions were identical. A similar test proved that the preactivating solution (calculated $[\text{Ca}^{++}] = 0.1 \mu\text{M}$) did not activate the muscle.

Chemicals

All chemicals were supplied by BDH or Merck, except for the following: (*N,N*-bis[2-hydroxyethyl]-2-aminoethane sulfonic acid; 2-[bis(2-hydroxyethyl)amino] ethane sulfonic acid (BES), $\text{Na}_2\text{H}_2\text{ATP}$, Na_2HCP , H_2EGTA , dithiothreitol, creatine kinase (Sigma); H_2HDTA (Fluorochem).

Results

Force-SL Relations in the Unskinned Muscles

The results from the unskinned muscles are shown in Figures 1A and 6. Figure 1A illustrates the protocol used to determine the relations between force and SL. The mean results from six muscles are shown in Figure 6A. The force-SL relations are shown both for the resting muscles and for the active muscles at the peak of contraction. These relations were determined at two concentrations of extracellular Ca^{++} : 1.5 mM (the standard concentration in these experiments) and 0.3 mM. The mean resting force, which was the same for both Ca^{++} concentrations, was zero at a SL of 1.9–2.0 μm and increased rapidly as the SL was raised above this sarcomere length (Fig. 4 and Fig. 6A). Above a SL of about 2.2 μm , further stretch of the muscle produced little increase in the length of the sarcomeres in the center of the resting muscle. This behavior indicates that the elastic elements in parallel with the sarcomeres were extremely stiff (viz. ter Keurs et al., 1980).

As in the resting muscle, in the actively contracting muscle, sarcomere lengths above about 2.3 μm were never seen, even if the muscle was highly stretched. Active force development was zero below a SL of 1.5–1.6 μm . Because the force (F)-sarcomere length (SL) relations were frequently nonlinear, the data were fitted to $F = a(\text{SL} - \text{SL}_0)^c$ by nonlinear least squares analysis (see Fig. 5 and Table 1). The average force-sarcomere length data (Fig. 6) were fitted to the same relation, in which the average c of Table 1 was substituted.

TABLE 1
Force-Sarcomere Length Relation

[Ca ²⁺]	SL ₀ (μm)	c	P
1.5 mM*	1.58 ± 0.06	0.52 ± 0.17	<0.01
0.3 mM*	1.60 ± 0.07	1.44 ± 0.44	0.1
1.9 μM†	1.84 ± 0.18	2.31 ± 0.55	<0.005
2.7 μM†	1.78 ± 0.09	2.37 ± 0.38	<0.02
4.3 μM†	1.68 ± 0.12	1.55 ± 0.42	<0.1
8.9 μM†	1.62 ± 0.07	0.69 ± 0.12	<0.1
50 μM†	1.14 ± 0.17	0.93 ± 0.13	NS

Data (mean ± SD) were from six intact* and subsequently skinned† trabeculae. Force-sarcomere length relations were fitted through the data according to $F = a(SL - SL_0)^c$, where SL_0 is the intercept with the abscissa, $c > 1$ indicates curvature toward the abscissa, and $c < 1$ indicates curvature toward the ordinate. Departure from linearity (P of $c = 1$) was tested by analysis of variance (Snedecor and Cochran, 1973).

The average values of c and the intercept with the abscissa (SL_0) are given in Table 1. The relationship between force and SL was significantly curved away from the SL axis at 1.5 mM [Ca²⁺] ($c = 0.52 \pm 0.17$) (cf. Table 1; Fig. 6A). At all sarcomere lengths, active force was greater at 1.5 mM [Ca²⁺] than at 0.3 mM [Ca²⁺]. Figure 5 shows the two experiments in which the decrease of F at any SL with a decrease of [Ca²⁺] to 0.3 mM was the largest (Fig. 5A) and the smallest

(Fig. 5C). The F -SL relation in a 0.3 mM [Ca²⁺] was curved toward the abscissa (cf. Table 1; Fig. 6A) ($c = 1.44 \pm 0.44$). Departure from linearity (seen in five muscles) reached significance for two of the six muscles.

Changes in the Laser Diffraction Pattern during the Skinning Procedure

Figure 2 shows the force, SL, and first order intensity and distribution during the 30-minute perfusion of the muscle with skinning solution. Active force development ceased completely within a few seconds when the skinning solution was applied to the muscle (Fig. 2A). During the first few minutes of the skinning procedure, passive force often fell slightly and then remained constant. In some muscles, the median value of SL changed by up to 0.1 μm during the skinning procedure; if this occurred, the SL was reset to 2.1 μm at the end of the skinning period. The peak intensity of the first order light consistently increased, but in a complex fashion. Initially there was a rapid increase in intensity in the first minute or so after skinning was started. Over the next few minutes, the intensity decreased again, occasionally to its value in the resting un-

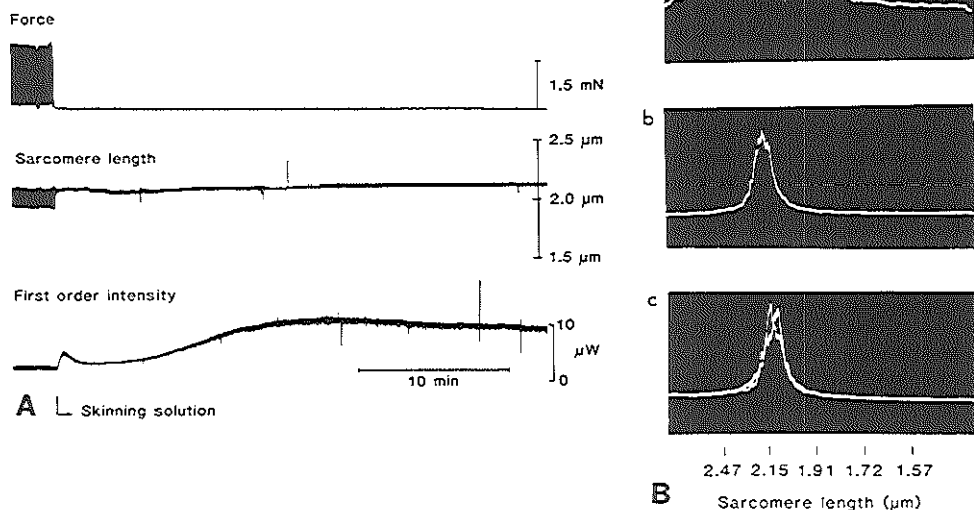


FIGURE 2. Panel A: Chart records of force, median sarcomere length, and first order light intensity in a trabecula immediately before and during the skinning procedure. Sarcomere length was measured with a photodiode array and intensity was measured with a position-sensitive photodiode. Panel B: the intensity distribution of light falling on the photodiode array (a) just before skinning, (b) 15 minutes after the start of skinning, and (c) before and during a test contraction at constant sarcomere length at [Ca²⁺] = 4.3 μM. These records are superpositions of oscilloscope traces. Light intensity distribution was displayed on the oscilloscope after subtraction of light scattered from zero order and with automatic gain control for intensity so that the changes in peak intensity were eliminated.

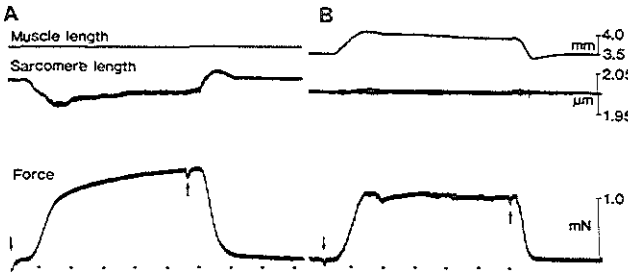


FIGURE 3. Comparison between contractures in the skinned muscle at constant muscle length (panel A) and constant sarcomere length (panel B). The chart records show successive contractures at $4.3 \mu\text{M}$ free Ca^{++} in the same muscle. At constant muscle length, the central sarcomeres shortened by up to $0.06 \mu\text{m}$. Subsequent stretch and the slow rise of force was caused by late contraction of the remnant of the free wall of the right ventricle. To prevent sarcomere length changes (panel B), it was necessary to stretch the muscle by 0.5 mm , followed by a slow release.

skinned muscle. The decrease was associated with the development of an opaque appearance of the muscle. This was followed by a slower but sustained increase in the intensity, the final value of which was usually two or three times that in the unskinned muscle. This second increase in intensity was associated with a visible increase in the transparency of the muscle. The dispersion of the first order intensity pattern was decreased considerably by the skinning procedure (Fig. 2B), and most of this reduction appeared to occur in the first few minutes of skinning, i.e., it was associated with the first increase in peak intensity. The dispersion then remained constant for the remainder of the skinning period.

Muscle width (measured to the nearest $4 \mu\text{m}$ by a graticule in the inverted microscope) did not vary during the skinning procedure.

Force Development in the Skinned Muscles

Figure 3A shows the force development of a skinned trabecula superfused with an activating solution of $[\text{Ca}^{++}] = 4.3 \mu\text{M}$ and held at a constant muscle length; for comparison Figure 3B shows the force development in the same muscle, but with SL held constant by stretching the muscle. At constant muscle length, force rose slowly to reach a plateau in about 60 seconds. The development of force was accompanied by substantial change of SL. Initially, the SL in the central region of the muscle fell from

the resting SL of 2.10 to $2.04 \mu\text{m}$, but then slowly increased again. This slow increase accompanied the slow phase of force development. It seems likely that this was due to the central region of the muscle being stretched by the contraction of the ends. If the SL was held constant at $2.04 \mu\text{m}$ (the smallest value reached during the contracture at constant muscle length) force rose more rapidly to reach a plateau in 10 seconds. The level of force reached was the same as that in the previous contracture (Fig. 3A) at the point when the SL was $2.04 \mu\text{m}$. In the examples of Figure 3 the $[\text{Ca}^{++}]$ was $4.3 \mu\text{M}$; at higher concentrations of Ca^{++} , the internal shortening during isometric muscle contraction was even more pronounced, and varied between 7% and 20% at $[\text{Ca}^{++}]$ of $8.9 \mu\text{M}$ in these experiments. This illustrates why it was necessary to measure the SL during contraction rather than just the SL in the resting muscle. In many preparations at a $[\text{Ca}^{++}]$ just above the threshold for activation, the muscle exhibited internal shortening rather than perceptible force development. For technical reasons, we chose to control muscle length and measure SL rather than try to maintain SL by stretching the muscle.

Force-SL Relations in the Skinned Muscle

The steady force and SL measured from recordings at various Ca^{++} concentrations (Fig. 1) were used to plot a family of force-SL relations at Ca^{++}

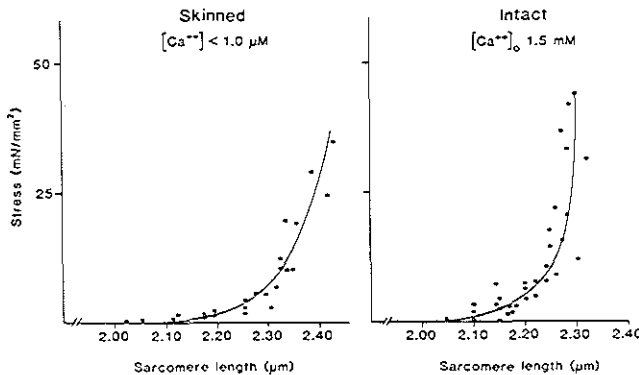


FIGURE 4. Passive force of four trabeculae before (intact) and after skinning (skinned $[\text{Ca}^{++}] < 0.7 \mu\text{M}$). Note the decrease of passive force at sarcomere lengths above $2.2 \mu\text{m}$. No difference was found for the intact trabeculae in passive force at $[\text{Ca}^{++}]_0 = 0.3 \text{ mM}$ and $[\text{Ca}^{++}]_0 = 1.5 \text{ mM}$.

concentrations from 1 nM to 50 μ M. The relations between SL and passive force at Ca^{++} concentrations below 0.7 μ M are shown in Figure 5: Ca^{++} concentrations from 1 nM to 0.7 μ M were insufficient to produce any Ca^{++} activation of the skinned muscle. As the SL was increased above 2.0 μ m, the passive force increased from zero, but this increase was less steep than in the same muscles before they had been skinned (Fig. 4). In addition, the muscle shown in Figure 4 could be stretched to a SL of 2.4 μ m, although this had not been possible in the unskinned muscle.

At Ca^{++} concentrations above 0.7 μ M active force was developed (Figs. 5 and 6). The absolute force at SL = 2.00 μ m in the skinned preparations at 8.9 μ M was $14.4\% \pm 6.9\%$ (sd) higher than in the intact trabeculae (Fig. 6) at the same SL and $[\text{Ca}^{++}]$ of 1.5 mM. No oscillations of force (Fabiato, 1978) or sar-

comere length were observed in these muscles (Fig. 3).

One of the advantages of the protocol in the present experiments is that we were able to compare the force-SL relations in the same muscle before and after it had been skinned. Thus, such variables as the external geometry of the preparation and the number of myofibrils were constant throughout. Moreover, the diffraction patterns at $[\text{Ca}^{++}]$ below 10 μ M remained crisp during contraction (see Fig. 2C). It is clear from Figures 5 and 6 that the shape of the force-SL relation depended largely on the $[\text{Ca}^{++}]$. A direct comparison between the two types of preparation revealed that the curves for 8.9 μ M $[\text{Ca}^{++}]$ were similar in shape to, although slightly steeper than, those for the unskinned muscle at extracellular Ca^{++} concentrations of 1.5 mM (cf. Figs. 5 and 6). The force-SL relations at an extracellular

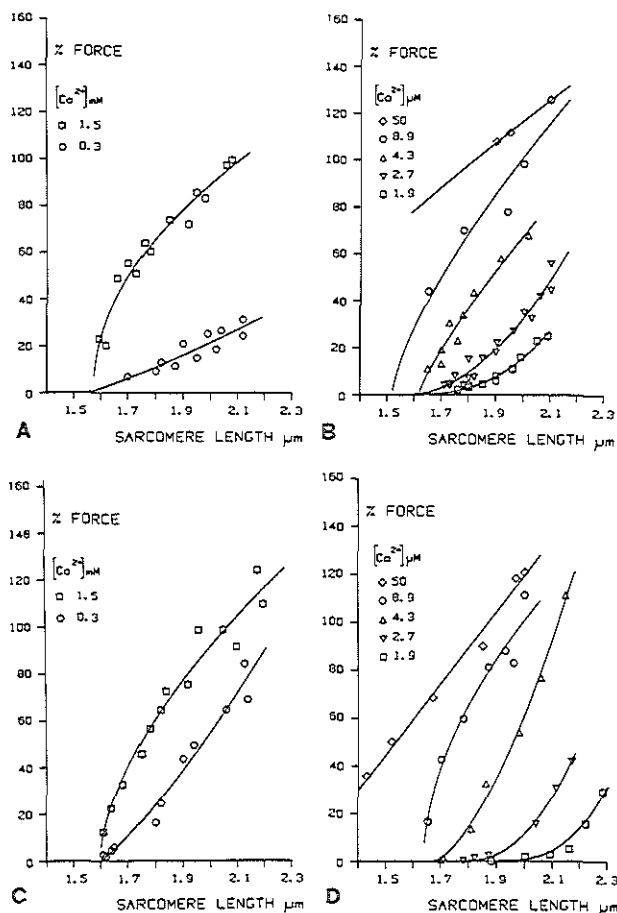


FIGURE 5. Force-sarcomere length relations of two trabeculae before and after skinning. Panels A and C show active force taken as total force at the peak of contraction minus the resting force borne at the sarcomere length measured at peak contraction. The concentration of Ca^{++} was 1.5 mM (squares) or 0.3 mM (circles). Panels B and D show the force-sarcomere length relations of the same trabeculae after skinning in $[\text{Ca}^{++}]$ 1.9 μ M (squares), 2.7 μ M (triangles pointing down), 4.3 μ M (triangles pointing up), 8.9 μ M (circles), and 50 μ M (diamonds). Force was measured as in the intact muscles. The scales of the graphs are identical for each muscle before and after skinning. For further explanation, see text.

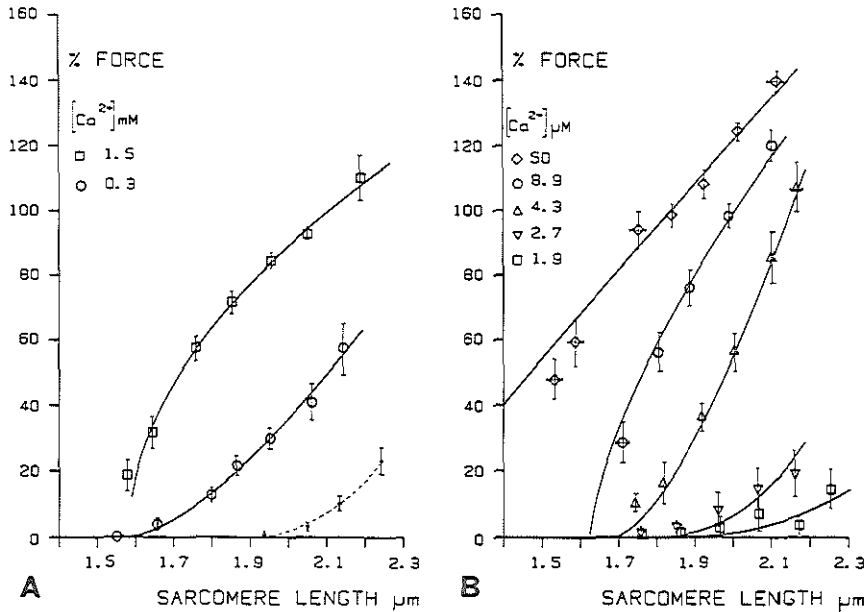


FIGURE 6. Mean force-sarcomere length relations of six trabeculae prior to and after skinning. Sarcomere length was averaged in bins of 0.1 μm . The points show the mean \pm SEM; if 1 SEM was larger than the symbols. Panel A: mean active force (open symbols) and passive force (filled symbols) in the intact trabeculae. The concentration of extracellular calcium was 1.5 mM (squares) and 0.3 mM (circles). Panel B: mean active force in the trabeculae after skinning at five Ca^{++} concentrations (1.9 μM , squares; 2.7 μM , triangles pointing down; 4.3 μM , triangles pointing up; 8.9 μM , circles) between the threshold and the saturating concentration. Note the similarity of the force-sarcomere length relation of the intact trabeculae at an extracellular Ca^{++} concentration of 1.5 mM (panel A) and after skinning at a $[\text{Ca}^{++}]$ of 8.9 μM , whereas the force-sarcomere length relation before skinning at 0.3 mM in panel A falls between those of 4.3 and 2.7 μM in the skinned muscle.

$[\text{Ca}^{++}]$ of 0.3 mM fell between the force-SL relations at free Ca^{++} concentrations of 2.7 μM and 4.3 μM after skinning (Figs. 5 and 6). Figure 5, B and D, shows the range of variation of force of the force-SL relations with variation of free $[\text{Ca}^{++}]$ that we found in the same muscles after skinning. At a free Ca^{++} concentration of 8.9 μM , the force-SL relationship tended to be curved toward the ordinate (Table 1; Figs. 5 and 6), whereas, at low free Ca^{++} concentrations, the force-SL relationship was curved toward the abscissa (cf. the increase of c in Table 1).

At maximally activating Ca^{++} concentrations (50 μM and above), the relation was approximately straight and appeared to differ fundamentally from the relationships for the intact muscle and for the skinned muscle at lower Ca^{++} concentrations, in that a considerable amount of force was generated at $\text{SL} = 1.6 \mu\text{m}$. Note that, in Figures 5D and 6, there are fewer data points at high Ca^{++} concentrations and high sarcomere lengths. This was the case because, under these conditions, the sarcomere diffraction pattern frequently disappeared or became too broad to allow an adequate measurement of the median sarcomere length. More seriously, these conditions

also produced an irreversible deterioration of the diffraction pattern: although the pattern became sharper again as the muscle was made to relax, the pattern in subsequent contractures, even at suboptimal $[\text{Ca}^{++}]$, was compromised. In many muscles, this irreversible degradation of the diffraction pattern occurred even at low sarcomere lengths if the

TABLE 2
Modified Hill Equation: Averaged Data from the Six Individual Experiments

Sarcomere length (μm)	F_{MAX} (mN/mm ²)	n	$[\text{Ca}^{++}]_{50}$ (μM)	n
2.15	86.3 ± 3.4	4.54 ± 0.74	3.77 ± 0.32	5
2.05	75.0 ± 3.8	4.50 ± 0.60	4.36 ± 0.35	6
1.95	69.2 ± 4.2	3.91 ± 0.48	5.38 ± 0.43	6
1.85	63.2 ± 4.3	3.85 ± 0.44	6.76 ± 0.62	6
1.75	55.1 ± 3.6	2.82 ± 0.23	7.71 ± 0.52	3
1.65	46.2	4.35	9.53	2

Average F_{MAX} , n , and $[\text{Ca}^{++}]_{50}$ (\pm SEM) calculated from six individual experiments by nonlinear multiple regression of the modified Hill equation through the $F - [\text{Ca}^{++}]$ data at different sarcomere lengths. n is the number of sigmoid relationships used for calculation of F_{MAX} , n , and $[\text{Ca}^{++}]_{50}$.

[Ca²⁺] was near saturation. Several changes in experimental procedure were tried to attempt to reduce the deterioration in the diffraction pattern, but with little success. Only two factors seemed to influence the loss of the diffraction pattern. First, there was considerable variability between muscles in the quality and durability of the diffraction pattern: only four of the muscles studied exhibited patterns that unequivocally gave a median SL at the optimal Ca²⁺ concentrations of 50 μ M. Thus, we could determine the force-SL relationship at optimal [Ca²⁺] only for relatively few muscles. Second, if the SL was raised above about 2.0 μ m at the optimal [Ca²⁺], a usable diffraction pattern was lost in most muscles. For this reason, we did not routinely subject the muscles to a high Ca²⁺ concentration and long SL simultaneously, and we determined the force-SL relation at maximally activating Ca²⁺ concentrations only at the end of the experiment.

Relation between Force and [Ca²⁺] at Different Sarcomere Lengths

The force-sarcomere length relations at different free Ca²⁺ concentrations calculated (see ter Keurs, 1983) for the average of six muscles (Fig. 6) and for the individual muscles (Fig. 5) were used to derive the force-[Ca²⁺] relationships at different sarcomere lengths shown in Figure 7 and summarized in Table 2. Because force was not measured at predetermined values of SL, we used the curves, rather than the data points, to estimate the active force development at selected sarcomere lengths. The derived [Ca²⁺]-activation curves were approximately sigmoidal on a semilogarithmic scale (Fig. 7A). These curves showed that increases in SL shifted the [Ca²⁺]-activation curves to the left, i.e., to lower Ca²⁺ concentrations. This increase in Ca²⁺ sensitivity with SL appeared to be present at all sarcomere lengths in the range 1.7–2.3 μ m. To obtain an objective

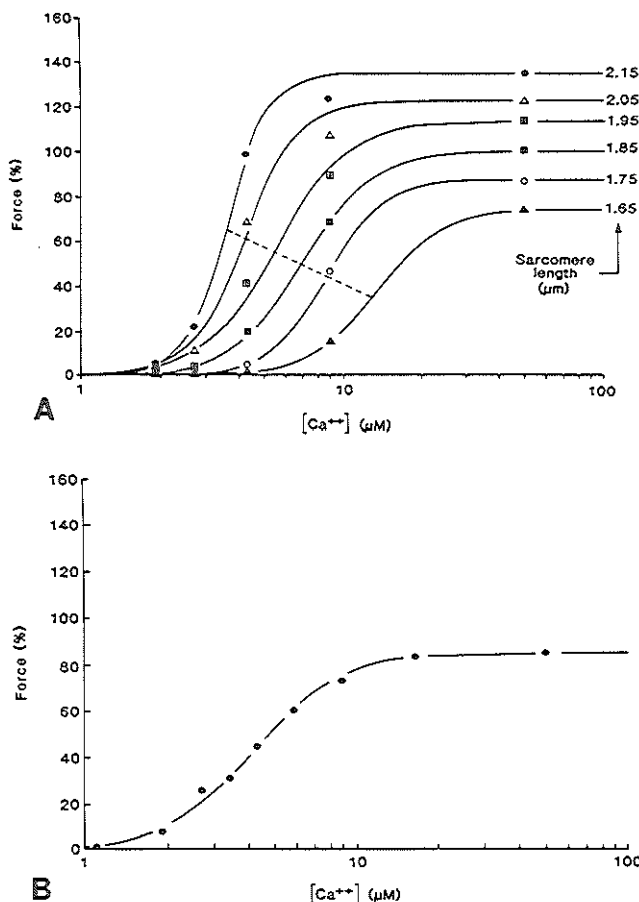


FIGURE 7. Force-[Ca²⁺] relations at selected sarcomere lengths (panel A) and constant muscle length (resting sarcomere length 2.10 μ m; panel B). Panel A: force-[Ca²⁺] relations at selected sarcomere lengths (shown in μ m next to the appropriate curves). These relations were obtained by replotting the curves of Figure 6B. The solid lines show sigmoidal curves drawn according to the modified Hill equation (see text). $n(\pm$ SEM) increased, in the averaged F-[Ca²⁺] relations, from 3.28 ± 0.29 at SL = 1.65 μ m to 5.37 ± 0.82 μ m at SL = 2.15 μ m. [Ca²⁺]₅₀ decreased from 13.4 ± 0.54 μ M at SL = 1.65 μ m to 3.59 ± 0.14 μ M at SL = 2.15 μ m. The decrease of [Ca²⁺]₅₀ is indicated by the dashed line (see also Table 1). Panel B: the force-[Ca²⁺] relation at constant muscle length without correction for internal shortening was less steep ($n = 2.7$), while [Ca²⁺]₅₀ was 3.29 μ M.

estimate of the $[Ca^{++}]$ required for 50% activation at each sarcomere length, we fitted the curves by non-linear least squares analysis (Snedecor and Cochran, 1973) to the modified Hill equation:

$$F = F_{MAX} \frac{[Ca^{++}]^n}{K^* + [Ca^{++}]^n} \times 100\%$$

where: F = developed force, n = the Hill coefficient, (cf. Table 2), K^* = a compound affinity constant, and F_{MAX} = maximal F at that sarcomere length.

The $[Ca^{++}]$ for 50% activation $[Ca^{++}]_{50}$ was then given by

$$[Ca^{++}]_{50} = -(\log_{10} K^*) / n.$$

The $[Ca^{++}]$ for 50% activation decreased from 9.53 μM to 3.77 ± 0.32 (mean of individual experiments \pm SEM) in proportion to an increase in sarcomere length between 1.65 and 2.15 μm . The Hill coefficient increased (Table 2) slightly from 2.82 ± 0.23 to 4.54 ± 0.74 (mean of six individual experiments \pm SEM) but significantly ($P \leq 0.02$ when tested by linear regression) with increasing sarcomere length between 1.75 and 2.15 μm . n is the number of sigmoid relationships used for calculation of F_{MAX} and n and $[Ca^{++}]_{50}$.

Force- $[Ca^{++}]$ relations were also studied in two muscles at constant muscle length (resting SL was 2.15 μm) (see Fig. 7B). They were less steep ($n = 2.64$ and 2.70) than those at constant sarcomere length; $[Ca^{++}]_{50}$ was 5.9 and 3.3 μM , respectively.

Discussion

Intact Muscles

The active force-SL relations in the intact muscle in 1.5 mm $[Ca^{++}]$ were very similar to those previously found with the same type of preparation (Gordon and Pollack, 1980; ter Keurs et al., 1980; ter Keurs, 1983). It is pointed out that the experimental protocol used to determine the force-SL relation did not allow any time for the slow changes in activation that occur with a time course of minutes following a length change (Parmley and Chuck, 1973; Lakatta and Jewell, 1977). Thus, the force-SL relation was an "instantaneous" rather than a steady state relation (viz. Lakatta and Jewell, 1977). Because the contractions were at constant muscle length (ML) rather than constant sarcomere length, there was considerable internal shortening during muscle contraction. Theoretically, this could have produced "shortening deactivation," but it has been shown by previous studies that the force-SL relation obtained from contractions at constant ML is the same as in those at constant SL (Pollack and Krueger, 1976; ter Keurs et al., 1980).

The influence of extracellular $[Ca^{++}]$ on the shape of the force-SL relation has been reported in detail elsewhere (ter Keurs, 1983). The change in shape reproduces the effect of extracellular $[Ca^{++}]$ on the force-length relation of papillary muscles (Allen et

al., 1974) and the effect of post-extrasystolic potentiation on the force-SL relation of rat trabeculae (ter Keurs et al., 1980).

Skinning Procedure

Apart from the rapid loss of muscle excitability, the most striking changes during the skinning procedure were those relating to the intensity and dispersion of the first order diffraction pattern. It is not unlikely that the initial increase in intensity and decrease in dispersion were due to a true increase in the homogeneity of sarcomere length. Possibly, this rapid increase in SL homogeneity upon skinning resulted from spontaneous, uncoordinated contractions of individual sarcomeres in the intact muscle during diastole. Under conditions of a raised resting intracellular $[Ca^{++}]$, cardiac muscle preparations often show spontaneous contractile activity, which is visible as uncoordinated contractions in individual cells or strings of cells and which can be recorded as fluctuations in the intensity of scattered light (Stern et al., 1983) and as oscillations of cytosolic $[Ca^{++}]$ (Orchard et al., 1983). Although visible spontaneous activity died away completely during the stabilization period at the start of each experiment, it is possible that there were still random sarcomere movements that were too small and uncoordinated to be manifested as force development or as intensity fluctuations, but which nevertheless produced uncoordinated shortening of individual sarcomeres and thereby increased the dispersion of sarcomere length.

The second, slow increase in first order intensity occurred simultaneously with a further decrease of the width of the first order of the diffraction pattern, and probably was due to the dissolution of mitochondria and sarcoplasmic reticulum and to the loss of cytosolic proteins, such as myoglobin (Kentish, 1982). In the intact cells, all these structures would tend to absorb or scatter laser light. The transient decrease in intensity that preceded the second slow increase was associated with a visible turbidity (as seen through the binocular microscope), and therefore may have been due to the disruption of membranous organelles, which later dissolved.

Skinned Muscles

Passive Properties

A comparison of the force-SL relations for the resting muscle before and after skinning (Figs. 4 and 6) showed that the skinned muscle was more compliant, in that resting force increased less steeply as SL was increased above 2.0 μm . It is possible that the greater resting force in the intact muscles was due to the presence of some residual activation by Ca^{++} (see above), although various lines of evidence argue against this possibility: (1) there were no light intensity fluctuations in the intact muscles by the time the force-SL relationship was determined, (2) the extracellular $[Ca^{++}]$ did not affect the resting

force in the intact muscles (Fig. 4) and (3) resting force first was seen at the same SL (1.9–2.0 μm) in both preparations. It seems more likely that the greater stiffness of the intact muscle compared with the skinned muscle was due to the contribution of a parallel elastic element, which was altered by the skinning procedure. The sarcolemma could have provided this parallel element, either directly because the membrane itself bore some resting force at SL > 2.0 μm (although this is unlikely, as the sarcolemma is compliant) or indirectly because the membrane conferred constant-volume behavior upon the cells of the intact muscle. Constant-volume behavior causes the negatively charged myofilaments to be forced closer together at longer sarcomere lengths, and mutual repulsion between the filaments conceivably could produce a force that opposes lengthening of sarcomeres above 2.0 μm , although this force is not manifest in skeletal muscle. This force would not be seen in skinned cells, which lack constant-volume behavior (e.g., Matsubara and Elliott, 1972). Another possibility is that an elastic stroma of nonmyofibrillar filaments, which may bear much of the passive force (Wingrad and Robinson, 1978; Price and Sanger, 1983; Magid et al., 1984), suffered a change in its physicochemical properties during the skinning procedure. This could have occurred either as a result of the dissolution of organelles that were enveloped in the stroma or as a result of a direct effect of the skinning solution on the stroma.

Active Properties

After the muscles had been skinned, it was initially much easier to measure the SL because of the increase in intensity and decrease in dispersion of the first order diffraction pattern compared with those in the unskinned muscle. However, this benefit was gradually offset by the major problem with the skinned muscles: the first order diffraction pattern deteriorated in successive Ca^{++} -regulated contractions, especially if the muscle was subjected to a high $[\text{Ca}^{++}]$ at a long SL. A similar loss of the striation pattern has previously been observed in many other skinned preparations at high Ca^{++} concentration (e.g., Endo, 1973; Fabiato and Fabiato, 1978) and is in marked contrast to the situation in the intact cardiac muscle, in which the diffraction pattern during the twitch remained clear and reproducible over several hours of continual activity. Although the diffraction pattern in the resting skinned muscle was distinct throughout the experiment, the resting pattern could not be used as an index of the active SL because, in these preparations, the SL sometimes decreased considerably during activation by Ca^{++} (e.g., Fig. 3).

It is not clear why the sarcomere striation pattern deteriorates in the skinned muscle. One possibility is that the force-generating capabilities of individual sarcomeres or half-sarcomeres decrease non-uniformly during the course of an experiment. Thus,

during activation of the muscle, when each sarcomere in a series must bear the same force, the sarcomeres will be at different degrees of overlap, with the sarcomeres of poorer contractile performance at longer sarcomere lengths (i.e., higher up the ascending limb) than those of better contractile performance. Another possible explanation is that the arrays of thick and thin filaments lose their regular structure during contraction of the skinned muscle: Iwazumi (personal communication, 1983) has observed "smearing" of the A- and I-bands in single cardiac myofibrils during activation at near-maximal Ca^{++} concentrations, although he studied only the SL range above 2.2 μm . However, neither explanation provides a reason for the loss of striations in skinned muscle but not in intact muscle. One likely cause of this difference is the Ca^{++} concentration, because maximally activating Ca^{++} concentrations, as used in the present study, probably are never attained in intact cardiac cells (Fabiato, 1983). Other possibilities are that the sarcomere disruption is caused by the prolonged nature of the Ca^{++} -regulated contractions in the skinned muscle, by a loss of some vital proteins as a result of skinning, or as a result of prolonged exposure to low calcium concentrations between contractions or by the loss of the constant-volume behavior.

To our knowledge, the present study is the first in which the force-SL relations were determined in the same cardiac muscle before and after skinning. Factors such as the geometry of the preparation, the number of myofibrils, and the amount of connective tissue were therefore the same in the two types of preparation. This is a prerequisite if meaningful comparisons are to be made between the force-SL relations of intact and skinned muscles.

For the following discussion, it is important to bear in mind that, in the skinned muscles, the concentration of the activating Ca^{++} (in the bathing solution) was constant during the determination of the force-SL relationship. Thus, any observed length dependence in the contractile characteristics of the muscle must have been due to the properties of the sarcomeres plus connective tissue. In the unskinned muscle, a length dependence of the Ca^{++} supply could have been an additional factor.

The force-SL relationships for the intact muscle and for the skinned muscle seemed to have the same basic shape (Figs. 5 and 6). The only major difference was that, whereas in the intact muscles force development was zero at a SL of 1.6 μm and below, in the skinned muscle a considerable force could be produced at these sarcomere lengths if the $[\text{Ca}^{++}]$ was raised to 50 μM (Figs. 5 and 6). A considerable force has also been observed in maximally activated fragments of single skinned cells from rat ventricle at sarcomere lengths as low as 1.2 μm (Fabiato and Fabiato, 1975). The force-SL relation at maximal activation was however steeper for the trabeculae than for fragments of skinned single cells: extrapo-

lation of the data in Figure 6 indicates that zero force would have occurred at a sarcomere length of about 1.2 μm , whereas, force in fragments in single cells at this SL was 60% of maximum (Fabiato and Fabiato, 1975). This difference was not due to incomplete activation of the myofibrils at the lowest sarcomere lengths in our experiments, because the force was not increased if the $[\text{Ca}^{++}]$ was raised further to 280 μM (results not shown). The apparent discrepancy probably represents a true difference between the two types of preparation: trabeculae, unlike single cells, contain intercellular connections (Winegrad and Robinson, 1978) and extracellular connective tissue (Kentish, 1982) that could produce forces that oppose shortening at the shorter sarcomere lengths. These forces would act to decrease the force measured at the shorter sarcomere lengths and would thus make the force-SL relation steeper. Alternatively, the myofilament lattice spacing of the mechanically skinned cell fragments may have been greater than that of trabeculae described here. This would lead to steeper force-SL relations in the present study (see below).

One of the main findings in the present study is the similarity of the force-SL relations in the skinned muscle compared to those of the intact muscle if the $[\text{Ca}^{++}]$ was below maximally activating levels. For example, the force-sarcomere length relation of the intact trabeculae at an extracellular Ca^{++} concentration of 1.5 mM was quite similar (cf. Table 1 and Fig. 6) to the relation after skinning at a Ca^{++} concentration of 8.9 μM . The mean force-sarcomere length relationship at an extracellular Ca^{++} concentration of 0.3 mM tended to be convex toward the abscissa (Table 1; Fig. 6) and fell between the relations at $[\text{Ca}^{++}] = 2.7$ and 4.3 μM in the skinned muscle, which were also convex toward the abscissa. The force-sarcomere length relationships of individual muscles at an extracellular Ca^{++} concentration = 0.3 mM varied between relationships similar to those at $[\text{Ca}^{++}] = 2.7$ μM (Fig. 5A) or at $[\text{Ca}^{++}] = 4.3$ μM (Fig. 5C) after skinning.

At first sight, this comparison suggests that the shape of the instantaneous force-SL relationship in the intact muscle can be accounted for by the properties of the myofibrils (plus a contribution from extracellular tissue; see above). However, underlying this conclusion is the assumption that the properties of the myofibrils in the skinned muscle accurately reflect the properties of the myofibrils in the intact muscle. For this assumption to be justified, two conditions must have been met: the chemical environment of the myofibrils in the two preparations should have been similar, and the properties of the myofibrils should not have been altered by the skinning procedure. We chose the ionic conditions of the solutions so that they resembled those in intact cardiac cells (e.g., pH \sim 7.0, Poole-Wilson, 1978; $[\text{Mg}^{++}] \sim$ 3.0 mM, Hess et al., 1982; see Kentish, 1982, for further details). The cytosolic $[\text{Ca}^{++}]$ attained during the twitch of cardiac muscle of

course varies with the inotropic status of the muscle, but evidence from aequorin-injected cardiac muscle suggests that under the conditions of our study the peak cytosolic $[\text{Ca}^{++}]$ is likely to have been about 5–10 μM at 1.5 mM extracellular $[\text{Ca}^{++}]$ (Allen and Kurihara, 1980; Fabiato, 1981). In any case, the $[\text{Ca}^{++}]$ range we studied must have encompassed that found in the intact muscle under almost all conditions. However, it should be noted that the solutions used for the skinned muscles were of necessity only simple models of the cytosol, because they lacked the soluble proteins and metabolic intermediates present in normal cytosol. The influences these substances might have on the force-SL relation are unknown.

It is conceivable that the second condition—that skinning did not alter myofibrillar properties—was not met, because, at least in skeletal fibers, skinning causes the myofibrils to swell and lose constant-volume behavior (Matsubara and Elliott, 1972; Godt and Maughan, 1977). Although the detergent-skinned trabeculae did not swell visibly during skinning, it is likely that swelling of the myofibrils occurred, but that it was compensated by some dissolution of intracellular organelles (Kentish, 1982), which account for more than 40% of cell volume in intact cells. The spacing between the myofilaments in skinned muscle can be reduced by adding to the solutions large polymers such as polyvinylpyrrolidone (PVP) that are excluded from the myofilament lattice (Godt and Maughan, 1977). However, Fabiato and Fabiato (1976) found that PVP increased the slope of the force-SL relationship in skinned cardiac cells at optimal $[\text{Ca}^{++}]$. This indicates that any increase in myofilament spacing during skinning in the present experiments would have tended to make the force-SL relationships less steep than they were in the intact muscle. It is also possible that sarcomeres in the skinned muscle may have been in a damaged state (see above). If there had been nonhomogeneity of SL in the skinned muscle, this too would have tended to flatten the force-SL curve. Thus, in both cases, our results for skinned cardiac muscle may have underestimated rather than overestimated the steepness of the force-SL relationship for the myofibrils (plus extracellular tissue) per se in the intact muscle.

With these considerations in mind, we conclude that much, if not all, of the instantaneous force-SL relationship in the intact trabeculae can be explained by the inherent properties of the myofibrils (plus a possible contribution from the mechanical properties of the extracellular tissue). However, this does not exclude the possibility that part of the instantaneous force-SL relationship results from a length-dependence in the supply of Ca^{++} to the myofibrils (Fabiato and Fabiato, 1975), although a major contribution from this factor seems unlikely, because the amplitude of the $[\text{Ca}^{++}]$ transient in intact cells injected with aequorin is not altered in the right direction to account for the alteration of developed

force in the first few beats after a change in muscle length (Allen and Kurihara, 1982; Allen and Smith, 1985). On the other hand, a change in the Ca^{++} supply to the myofibrils is probably responsible for the slow changes in active force development seen in the few minutes after the length change (Allen and Kurihara, 1982).

The steepness of the force-SL relationships in the skinned muscle at suboptimal $[\text{Ca}^{++}]$ was partly a consequence of the fact that Ca^{++} sensitivity of the myofibrils increased with SL (Fig. 7). A similar length dependence of Ca^{++} sensitivity has been observed in many studies on the descending limb of the force-SL relation in skinned fibers (for references, see Allen and Kentish, 1985a; Stephenson and Wendt, 1984). It also confirms the results of Fabiato (1980) in mechanically skinned cell fragments and of Hibberd and Jewell (1982), who found that the Ca^{++} sensitivity of detergent-skinned trabeculae increased as the SL in the relaxed muscle was increased from 1.9–2.0 μm to 2.3–2.5 μm . However the length dependence of Ca^{++} sensitivity in our experiments was almost twice as large as in the study by Hibberd and Jewell (1982). The reason for this discrepancy is not clear. The only major difference between the solutions used in the two studies was that we used a $[\text{Mg}^{++}]$ of 3 mM (viz., Hess et al., 1982) whereas Hibberd and Jewell used 1 mM. It is possible that the discrepancy could merely be due to the fact that Hibberd and Jewell (1982) measured the SL only in the relaxed muscle, whereas we were able to measure the SL throughout Ca^{++} activation of the muscle; internal shortening during contraction can cause the active SL to be considerably less than the resting SL (Fig. 3). The results of the present study show for the first time that the length dependence of myofibrillar Ca^{++} sensitivity occurs over the entire range of active sarcomere lengths (1.6–2.3 μm) that corresponds to the ascending limb of the length-tension relationship in cardiac muscle (Page, 1974; Sonnenblick and Skelton, 1974; ter Keurs, 1983). Thus, it is likely that this phenomenon contributes to the Frank-Starling relation under all physiological conditions.

Our experiments provide no clue as to the mechanism of the length dependence of Ca^{++} sensitivity. One plausible mechanism is that the affinity of troponin for Ca^{++} increases with SL. Recent experiments using skinned muscles loaded with photoproteins (Allen and Kentish, 1985b; Stephenson and Wendt, 1984) have provided evidence in favor of this hypothesis.

All the force- $[\text{Ca}^{++}]$ relations at known sarcomere lengths (Fig. 7A) were considerably steeper than has previously been found for detergent-skinned cardiac muscle during contractions at constant muscle length (e.g., Hibberd and Jewell, 1982; Kentish, 1984). The Hill coefficient n of around 4 was almost twice as great as n at constant muscle length in our study ($n = 2.7$ and 2.6 ; cf. Fig. 7B) and in other studies (mean $n = 2.48$ – 2.94 ; Hibberd and Jewell,

1982, and $n = 2.14$; Kentish, 1984). A decreased slope of the force- $[\text{Ca}^{++}]$ relationship for muscle isometric contractions compared with SL isometric contractions could arise from a combination of the influence of SL on Ca^{++} sensitivity and the internal shortening that occurs in the cardiac trabeculae (Kentish, 1984): as the muscle is activated with progressively greater concentrations of Ca^{++} , more force is generated and more internal shortening occurs; the SL in the central part of the muscle decreases progressively and the appropriate force- $[\text{Ca}^{++}]$ relationship for the sarcomeres shifts to the right (as in Fig. 7A). The overall force- $[\text{Ca}^{++}]$ relationship for isometric muscle contractions is therefore flatter than it would have been if the SL had been held constant.

The observed n of about 4.5 at a sarcomere length of 2.15 μm is also twice the n derived from studies on mechanically skinned cell fragments (Fabiato and Fabiato, 1978; Fabiato, 1981) at the same sarcomere length. This discrepancy remains unexplained, but may be related to the absence of force and sarcomere length oscillations in these skinned muscles (see Figs. 1 and 3) at suboptimal calcium concentrations, whereas such force oscillations usually occur in cell fragments during partial activation by calcium ions (Fabiato, 1978).

The force- $[\text{Ca}^{++}]$ relation at known sarcomere lengths is too steep to be explained by positive cooperativity between the three Ca^{++} -binding sites on cardiac troponin, especially since there is evidence that only one of these sites is directly involved in Ca^{++} regulation of contraction (Holroyde et al., 1980). If, indeed, Ca^{++} sensitivity depends upon the number of crossbridges (see above), the steepness of the relationship can be explained by an increase in the number of crossbridges as the $[\text{Ca}^{++}]$ is raised (cf. Brandt et al., 1980). However there are several other explanations, such as interactions between adjacent tropomyosin molecules, that could explain positive cooperativity (see also Hibberd and Jewell, 1982). The observed tendency of the Hill coefficient n to increase with sarcomere length would be consistent with a model (Brandt et al., 1980) in which an increase of the sarcomere length increases the number of possible crossbridges and by virtue of a cooperative process both increases n and decreases $[\text{Ca}^{++}]_{50}$.

We would like to thank Barbara Mulder, Peter de Tombe, and Hans Klein for technical assistance; also Lenore Doell for her secretarial assistance.

Supported by Grants 74022 and 77086 from the Netherlands Heart Foundation.

Dr. Kentish is affiliated with the University College London, Drs. ter Keurs and Bucx with the University of Calgary, Dr. Ricciardi with the University of Pavia, and Dr. Noble with the King Edward VII Hospital.

Address for reprints: Henk E.D.J. ter Keurs, Department of Medicine and Medical Physiology, Foothills Hospital, University of Calgary, 3330 Hospital Drive N.W., Calgary, Alberta, Canada T2N1N9.

Received June 19, 1985; accepted for publication February 14, 1986.

References

- Allen DG, Kentish JC (1985a) The cellular basis of the length-tension relation in cardiac muscle. *J Mol Cell Cardiol* 17: 821-840
- Allen DG, Kentish JC (1985b) The effects of length changes on the myoplasmic calcium concentration in skinned ferret ventricular muscle. *J Physiol (Lond)* 366: 67P
- Allen DG, Kurihara S (1982) The effects of muscle length on intracellular calcium transients in mammalian cardiac muscle. *J Physiol (Lond)* 327: 79-94
- Allen DG, Jewell BR, Murray JW (1974) The contribution of activation processes to the length-tension relation of cardiac muscle. *Nature* 248: 606-607
- Allen DG, Smith GL (1985) The first calcium transient following shortening in isolated ferret ventricular muscle. *J Physiol (Lond)* 366: 82P
- Ashley CC, Moisescu DG (1974) Tension changes in isolated bundles of frog and barnacle myofibrils in response to sudden changes in the external free calcium concentration. *J Physiol (Lond)* 239: 112P-114P
- Ashley CC, Moisescu DG (1977) Effect of changing the composition of the bathing solutions upon the isometric tension-pCa relationship in bundles of crustacean myofibrils. *J Physiol (Lond)* 270: 627-652
- Brandt PW, Cox RN, Kawai M (1980) Can the binding of Ca^{2+} to two regulatory sites on troponin C determine the steep pCa-tension relationship of skeletal muscle? *Proc Natl Acad Sci USA* 77: 4717-4720
- Brenner B (1983) Technique for stabilizing the striation pattern in maximally calcium-activated skinned rabbit psoas fibers. *Biophys J* 41: 99-102
- Fabiato A (1980) Sarcomere length dependence of calcium release from the sarcoplasmic reticulum of skinned cardiac cells demonstrated by differential microspectrophotometry with Arsenazo III (abstr). *J Gen Physiol* 76: 15a
- Fabiato A (1981) Myoplasmic free calcium concentration reached during the twitch of an intact isolated cardiac cell and during calcium-induced release of calcium from the sarcoplasmic reticulum of a skinned cardiac cell from the adult rat or rabbit ventricle. *J Gen Physiol* 78: 457-497
- Fabiato A (1983) Brief review: Calcium-induced release of calcium from the cardiac sarcoplasmic reticulum. *Am J Physiol* 245: C1-C14
- Fabiato A, Fabiato F (1975) Dependence of the contractile activation of skinned cardiac cells on the sarcomere length. *Nature* 256: 54-56
- Fabiato A, Fabiato F (1976) Dependence of calcium release, tension generation and restoring forces on sarcomere length in skinned cardiac cells. *Eur J Cardiol* 4 (Suppl): 13-27
- Fabiato A, Fabiato F (1978) Myofilament-generated tension oscillations during partial calcium activation and activation dependence of the sarcomere length-tension relation of skinned cardiac cells. *J Gen Physiol* 72: 667-699
- Godt RE, Maughan DW (1977) Swelling of skinned muscle fibers of the frog. Experimental observations. *Biophys J* 19: 103-116
- Gordon AM, Pollack GH (1980) Effects of calcium on the sarcomere length-tension relation in rat cardiac muscle. Implications for the Frank-Starling mechanism. *Circ Res* 47: 610-619
- Hess P, Metzger P, Weingart R (1982) Free magnesium in sheep, ferret and frog striated muscle at rest measured with ion-selective micro-electrodes. *J Physiol (Lond)* 333: 173-188
- Hibberd MG, Jewell BR (1982) Calcium- and length-dependent force production in rat ventricular muscle. *J Physiol (Lond)* 329: 527-540
- Holroyde MJ, Robertson SP, Johnson JD, Solaro RJ, Potter JD (1980) The calcium and magnesium binding sites on cardiac troponin and their role in the regulation of myofibrillar adenosine triphosphatase. *J Biol Chem* 255: 11688-11693
- Iwazumi T, Pollack GH (1981) The effect of sarcomere non-uniformity on the sarcomere length-tension relationship of skinned fibers. *J Cell Physiol* 106: 321-337
- Jewell BR (1977) A reexamination of the influence of muscle length on myocardial performance. *Circ Res* 40: 221-230
- Julian FJ, Sollins MR (1975) Sarcomere length-tension relations in living rat papillary muscle. *Circ Res* 37: 299-308
- Kentish JC (1982) The influence of monovalent cations on myofibrillar function. Ph.D. Thesis, University of London
- Kentish JC (1984) The inhibitory effects of monovalent ions on force development in detergent-skinned ventricular muscle from guinea-pig. *J Physiol (Lond)* 352: 353-374
- Kentish JC, ter Keurs HEDJ, Noble MIM, Ricciardi L, Schouten VJA (1983) The relationships between force, $[Ca^{2+}]$ and sarcomere length in skinned trabeculae from rat ventricle (abstr). *J Physiol (Lond)* 345: 24P
- Krueger JW, Pollack GH (1975) Myocardial sarcomere dynamics during isometric contraction. *J Physiol (Lond)* 251: 627-643
- Lakatta EG, Jewell BR (1977) Length-dependent activation. Its effect on the length-tension relation in cat ventricular muscle. *Circ Res* 40: 251-257
- Magid A, Ting-Beall HP, Carvell M, Kontis T, Lucaveche C (1984) Connecting filaments, core filaments and side struts: A proposal to add three load-bearing structures to the sliding filament model. In *Contractile Mechanisms in Muscle*, edited by GH Pollack, H Sugi. New York, Plenum Press, pp 307-323
- Matsubara I, Elliott GF (1972) X-ray diffraction studies on skinned single fibres of frog skeletal muscle. *J Mol Biol* 72: 657-669
- Moisescu DG (1976) Kinetics of reaction in calcium-activated skinned muscle fibres. *Nature* 262: 610-613
- Orchard C, Eisner DA, Allen DG (1983) Oscillations of intracellular Ca^{2+} in mammalian cardiac muscle. *Nature* 304: 735-738
- Page SG (1974) Measurements of structural parameters in cardiac muscle. The physiological basis of Starling's law of the heart. *Ciba Found Symp* 24: 13-25
- Parnley WW, Chuck L (1973) Length-dependent changes in myocardial contractile state. *Am J Physiol* 224: 1195-1199
- Pollack GH, Krueger JW (1976) Sarcomere dynamics in intact cardiac muscle. *Eur J Cardiol* 4 (Suppl): 53-65
- Poole-Wilson PA (1978) Measurement of myocardial intracellular pH in pathological states. *J Mol Cell Cardiol* 10: 511-526
- Price MG, Sanger JW (1983) Intermediate filaments in striated muscle: A review of structural studies in embryonic and adult skeletal and cardiac muscle. In *Cell and Muscle Motility*, vol 3, edited by RM Dowben, JW Shay. New York, Plenum, pp 1-40
- Snedecor GW, Cochran WG (1973) *Statistical Methods*. Ames, Iowa, Iowa State University Press
- Sonnenblick EH, Skelton CL (1974) Reconsideration of the ultrastructural basis of cardiac length-tension relations. *Circ Res* 35: 517-526
- Stephenson DG, Wendt IT (1984) Length dependence of changes in sarcoplasmic calcium concentration and myofibrillar calcium sensitivity in striated muscle fibres. *J Muscle Res Cell Motil* 5: 243-272
- Stern MD, Kort AA, Bhatnagar GM, Lakatta EG (1983) Scattered-light intensity fluctuations in diastolic rat cardiac muscle caused by spontaneous Ca^{2+} -dependent cellular mechanical oscillations. *J Gen Physiol* 82: 119-153
- ter Keurs HEDJ (1983) Calcium and Contractility. In *Cardiac Metabolism*, edited by AJ Drake-Holland, MIM Noble. New York, J. Wiley & Sons, pp 73-99
- ter Keurs HEDJ, Rijnsburger WH, van Heurigen R, Nagelsmit MJ (1980) Tension development and sarcomere length in rat cardiac trabeculae. Evidence of length-dependent activation. *Circ Res* 46: 703-714
- Winegrad S, Robinson TF (1978) Force generation among cells in the relaxed heart. *Eur J Cardiol* 7 (Suppl): 63-70

INDEX TERMS: Cardiac muscle • Sarcomere length • Ca^{2+}

CHAPTER 5

EFFECTS OF ACIDOSIS ON FORCE-SARCOMERE LENGTH AND FORCE-VELOCITY RELATIONS OF RAT CARDIAC MUSCLE

Lucio Ricciardi, Jeroen JJ Buxx, Henk EDJ ter Keurs

Published in Cardiovascular Research 1986; 20: 117-123

Effects of acidosis on force-sarcomere length and force-velocity relations of rat cardiac muscle

LUCIO RICCIARDI, JEROEN J J BUCX,* HENK E D J TER KEURS*

From the Department of Experimental Cardiology, State University of Leiden, The Netherlands

SUMMARY The effect of hypercapnic acidosis was compared with that of lowering extracellular calcium concentration ($[Ca^{++}]_o$) in rat cardiac trabeculae. The relations between force and sarcomere length and between force and velocity were studied. Sarcomere length was measured by means of laser diffraction techniques and sarcomere shortening velocity by means of isovelocity releases. The curve representing the relation between force and sarcomere length shifted from convex towards the ordinate (pH 7.35) to convex towards the abscissa (pH 6.68) as after $[Ca^{++}]_o$ had been reduced from 1.5 to 0.3 mmol·litre⁻¹. Increasing $[Ca^{++}]_o$ at low pH from 1.5 to 4.0 mmol·litre⁻¹ allowed the shape of the relation to be restored, but force values failed to return to control values. The relation between force and pH over the range 6.22-7.94 was also tested. During steady low pH maximum unloaded sarcomere shortening velocity was not significantly different from control values whereas it was decreased at low $[Ca^{++}]_o$. Under both conditions maximum isometric tension (P_o) was reduced. The results are consistent with the hypothesis that H^+ ions cause a shift of the force-p Ca curve to the right at all sarcomere lengths, as a result of competition between Ca^{++} and H^+ ions for binding to the myofilaments.

Acidosis is one of the most immediate consequences of myocardial ischaemia^{1,2} and, since the early studies of Klug and Gaskell, has been shown to impair contractility.³⁻⁶ Recently, several hypotheses have been proposed in order to define the role of H^+ ions in altering contractility. In vitro experiments showed that H^+ ions may modify Ca^{++} binding to the sarcoplasmic reticulum,^{7,8} to the sarcolemmal membrane,^{9,10} and to the contractile proteins.^{11,12} Moreover, it is known that H^+ ions can induce changes in intracellular ionic content of cardiac muscle¹³ and in the slow inward calcium current.¹⁴

The rapid loss of pump function of the heart, due to acidosis, can be evaluated by studying the relation between force and sarcomere length and between force and velocity. Our research was therefore focussed on these relations, which were studied in isolated rat cardiac trabeculae. The measurements were

performed at pH 7.35, at extracellular Ca^{++} concentration ($[Ca^{++}]_o$) 1.5 (control), 0.8, and 0.3 mmol·litre⁻¹, and at pH 6.68, induced by hypercapnia, at $[Ca^{++}]_o$ of 1.5, 2.5, and 4.0 mmol·litre⁻¹.

When the two effects were compared care was taken to differentiate between an acute and a steady phase of hypercapnic acidosis. This provided further information about force recovery, sarcomere shortening velocity, and its dependence on acidosis.

Materials and methods

Twelve week old Wistar rats (200-300 g body weight) were anaesthetised with ether. The heart was quickly removed and transferred to a saline filled dissection chamber. The aorta was cannulated and perfused with oxygenated high potassium Krebs-Henseleit solution in order to prevent spontaneous beating. Trabeculae of the right ventricle were dissected and transported to the experimental chamber.

A piece of tricuspid valve and a small cube of right ventricular free wall were left attached to the trabeculae for mounting purposes. The trabeculae were ribbon shaped, and their mean dimensions were: length 2.5 mm; width 0.2 mm; thickness 0.1 mm. They were stimulated by two platinum wire electrodes embedded in the chamber wall.

Address for correspondence and reprint requests: Dr Lucio Ricciardi, Istituto di Fisiologia umana, Università di Pavia, via Forlanini 6, 27100 Pavia, Italy.

*Present address: Department of Physiology, University of Calgary, Health Sciences Centre, 3330 Hospital Drive, N.W., Calgary, AB T2N 4N1, Canada.

Key words: rat cardiac trabeculae; sarcomere length; acidosis; Ca^{++} ions.

The perfusion fluid contained (in mmol·litre⁻¹): Na⁺ 141.0, K⁺ 5.0, Cl⁻ 127.5, Mg⁺⁺ 1.2, H₂PO₄⁻ 2.0, SO₄⁻ 1.2, HCO₃⁻ 27, glucose 10.1, Ca⁺⁺ 0.3 to 4.0. For the solutions, deionised millipore filtered water and salts of analytical degree were used. Since respiratory acidosis causes a rapid change in intracellular pH^{6, 13-17} solutions in equilibrium either with 95% O₂ and 5% CO₂ or with 80% O₂ and 20% CO₂ were used for determining force-sarcomere length and force-velocity relations. The mean(SD) pH in the first solution was 7.35(0.02) and in the second 6.68(0.02), as measured with a pH meter (pHm 26, electrode GK 2321c, Radiometer, Copenhagen). Further variations in the gas mixture allowed the pH to be changed over a wider range. Temperature was measured with a thermistor. The perfusion fluid was fed through a heat exchanger connected to a cryostat (Cotara WK 4 DS), resulting in a temperature in the muscle chamber of 23.8(0.3)°C, with a flow rate of 1.6 ml·min⁻¹.

Force was measured with a strain gauge (AME AE 801) connected to the valve side of the preparation. The ventricular side was attached, via a special holder, to a motor arm (General Scanning Inc, Z 1144) controlled by a dual servo amplifier.¹⁸ Length and position of the preparation were determined with a potentiometer and bridge amplifier (Gould Brush 2200) attached to the microscope stage, which was parallel to the muscle axis. Both muscle length and position as well as force were recorded on a chart recorder (Gould Brush 2800) and storage oscilloscope with hard copy unit (Tektronix 613 and 4631). Sarcomere length was measured by laser diffraction techniques as reported elsewhere.^{18, 19} At any sarcomere length peak force was measured in the test beat after four twitches at reference length. To measure sarcomere shortening velocity we induced isovelocity releases as previously described.¹⁹⁻²¹ When the muscle was released to zero force maximum unloaded sarcomere shortening velocity (v_0) could be measured.

By means of a least square statistical approach a rectangular hyperbola, according to Hill's equation $(P+a)v=b(P_0-P)$, was fitted on the obtained data.²²

EXPERIMENTAL PROTOCOL

After being mounted, the trabeculae were allowed to contract at 0.4 Hz at a $[Ca^{++}]_o$ of 1.5 mmol·litre⁻¹ (pH 7.35). Force-sarcomere length and force-velocity relations were measured at this stage after stabilisation. The $[Ca^{++}]_o$ of the perfusing medium was then changed to 0.8 and 0.3 mmol·litre⁻¹, and the same measurements were repeated in both cases when minimal twitch force was achieved. $[Ca^{++}]_o$ was then returned to the control value. Subsequently, acidosis was induced by using a perfusate in equilibrium with 80% O₂, 20% CO₂ (pH 6.68, PCO₂ 20 kPa). Force-sarcomere length and v_0 were measured when twitch force had reached its minimum level, and force-sarcomere length and force-velocity relations were also measured 20 minutes later when force had partially recovered. On reperfusion with control solution ($[Ca^{++}]_o$ 1.5 mmol·litre⁻¹, pH 7.35) developed tension returned to control values and the two relations were determined at that moment. Finally, after a change again to low pH, $[Ca^{++}]_o$ was increased to 2.5 and 4.0 mmol·litre⁻¹, and the force-sarcomere length relation was then measured.

To analyse the dependence of force on pH two experiments were performed in which the pH varied between 6.22 and 7.94. Peak forces were measured at SL=2.00 μ m and normalised by taking their values at the highest pH as 100%.

Results

Figure 1 shows the time course of force and sarcomere shortening when the extracellular pH value was changed. Force decreased to 16% of the control value within about 1 min after a change to acidotic perfusate and returned to about 25% during the next 20 minutes. The return of pH to 7.35 was followed by a transient

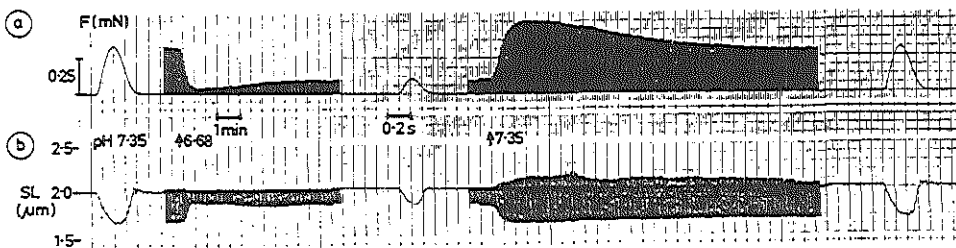


FIG 1 Time course of (a) force and (b) sarcomere length showing how contractile performance is affected by changes in pH.

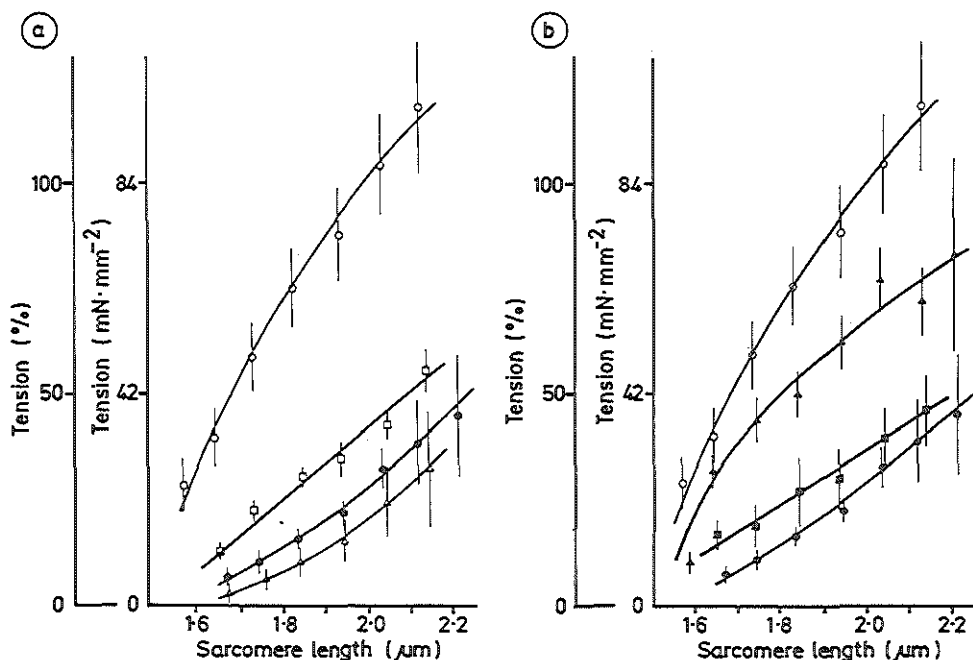


FIG. 2. Relation of force to sarcomere length (a) \bigcirc $[Ca^{++}]_o$ 1.5 mmol·litre⁻¹; pH 7.35 (n=16); \square $[Ca^{++}]_o$ 0.8 mmol·litre⁻¹; pH 7.35 (n=3); \triangle $[Ca^{++}]_o$ 0.3 mmol·litre⁻¹; pH 7.35 (n=7); \bullet $[Ca^{++}]_o$ 1.5 mmol·litre⁻¹; pH 6.68 (n=11); (b) \bigcirc $[Ca^{++}]_o$ 1.5 mmol·litre⁻¹; pH 7.35 (n=16); \bullet $[Ca^{++}]_o$ 1.5 mmol·litre⁻¹; pH 6.68 (n=11); \blacksquare $[Ca^{++}]_o$ 2.5 mmol·litre⁻¹; pH 6.68 (n=4); \blacktriangle $[Ca^{++}]_o$ 4.0 mmol·litre⁻¹; pH 6.68 (n=6). All values are mean (SEM). The SEM for sarcomere lengths is masked by the symbols. See text for further details.

overshoot, and force control values were completely restored within 10 min. The apparent increase in diastolic sarcomere length during the overshoot was caused by a local stretch at the end of the relaxation phase. This was due to a non-uniform pattern of relaxation along the preparation. The degree of local stretch varied among the muscles and, as shown in fig 1, was often force dependent. Actual resting length is marked by the darker line in the low speed record.

Figure 2 shows force-sarcomere length relations under control and different testing conditions. Figure 2a compares the effect of reducing $[Ca^{++}]_o$ from 1.5 to 0.3 mmol·litre⁻¹ (pH 7.35) with that of lowering pH from 7.35 to 6.68 ($[Ca^{++}]_o$ 1.5 mmol·litre⁻¹). An intermediate $[Ca^{++}]_o$ of 0.8 mmol·litre⁻¹ (pH 7.35) is also shown. Figure 2b shows the effect of increasing $[Ca^{++}]_o$ from 1.5 to 2.5 and to 4.0 mmol·litre⁻¹ during acidosis.

Peak twitch force was normalised by expressing the tension developed at SL 2.00 μm, pH 7.35, and

$[Ca^{++}]_o$ 1.5 mmol·litre⁻¹ as 100%. Lowering $[Ca^{++}]_o$ (fig 2a) decreased force development in a length dependent manner, shifting the relation from convex towards the ordinate at $[Ca^{++}]_o$ 1.5 mmol·litre⁻¹ (n=16) to convex towards the abscissa at $[Ca^{++}]_o$ 0.3 mmol·litre⁻¹ (n=7), whereas intermediate concentrations, as the one shown (0.8 mmol·litre⁻¹, n=3), had a linear trend. At low pH ($[Ca^{++}]_o$ 1.5 mmol·litre⁻¹, n=11) the curve was convex towards the abscissa and not significantly different from that measured at $[Ca^{++}]_o$ 0.3 mmol·litre⁻¹.

The effect on the force-sarcomere length relation secondary to an increase in $[Ca^{++}]_o$ at low pH is shown in fig 2b. The curves shifted from convex towards the abscissa to linear and to convex towards the ordinate at $[Ca^{++}]_o$ 1.5 (n=11), 2.5 (n=4), and 4.0 (n=6) mmol·litre⁻¹. Nevertheless, increasing $[Ca^{++}]_o$ to 4.0 mmol·litre⁻¹ and further (data not shown) failed to recover full control tension, whereas spontaneous sarcomere motion was observed

microscopically at this high $[Ca^{++}]_o$. Figure 3 shows the dependence of force development on extracellular pH after prolonged acidosis (two experiments). Force production of the individual muscles at the highest pH

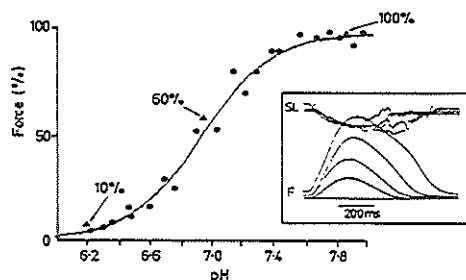


FIG 3 Normalised force (%) as a function of pH (two experiments). $[Ca^{++}]_o$ 1.5 mmol·litre⁻¹. Least square fitting according to the equation $Km^n/(Km^n + pH^n)$ where $n=2.02(0.12)$ and $Km=6.91(0.016)$ (mean(SD)). Inset: peak force at sarcomere length (SL) = 2.00 μ m in four twitches; from the top - pH 7.35, 6.95, 6.83, 6.65. The triangles were calculated from data of Fabiato^{8, 36, 37} on the basis of the assumption that the corresponding intracellular pH ranges from 6.60 (at pH = 6.20) to 7.40 (at pH = 8.00).³²⁻³⁵ For further information see text.

was assumed to be 100%. Lowering pH over a range from 7.94 to 6.22 decreased force to follow a sigmoidal curve, which could be described by the equation: $Km^n/(Km^n + pH^n)$. By means of a least square fitting method n and Km were calculated and appeared to be respectively (SD): 2.02(0.12) and 6.91(0.1). The inset shows peak force at SL 2.00 μ m in four twitches at different pH. The relation between force and velocity obtained under control conditions, low $[Ca^{++}]_o$ and low pH, are shown in fig 4. Hill's hyperbola fitted the data well, as summarised in the table.

Figure 4a shows force-velocity relations obtained at both $[Ca^{++}]_o$ 1.5 and 0.3 mmol·litre⁻¹. Maximum developed tension (P_o) at lower $[Ca^{++}]_o$ had decreased to 16% of control, while v_o decreased from 12 μ m·s⁻¹ ($n=10$) to 9 μ m·s⁻¹ ($n=3$). Figure 4b shows the same relation measured under control conditions compared with that measured after 20 min of hypercapnic acidosis. After a transient undershoot, where both maximum developed tension and maximum sarcomere shortening velocity were comparable to those measured at low $[Ca^{++}]_o$ (see table), force was 25% of control whereas v_o increased to 12 μ m·s⁻¹ ($n=7$), as found before acidosis. On reperfusion with standard solution force-velocity curves did not differ from control data.

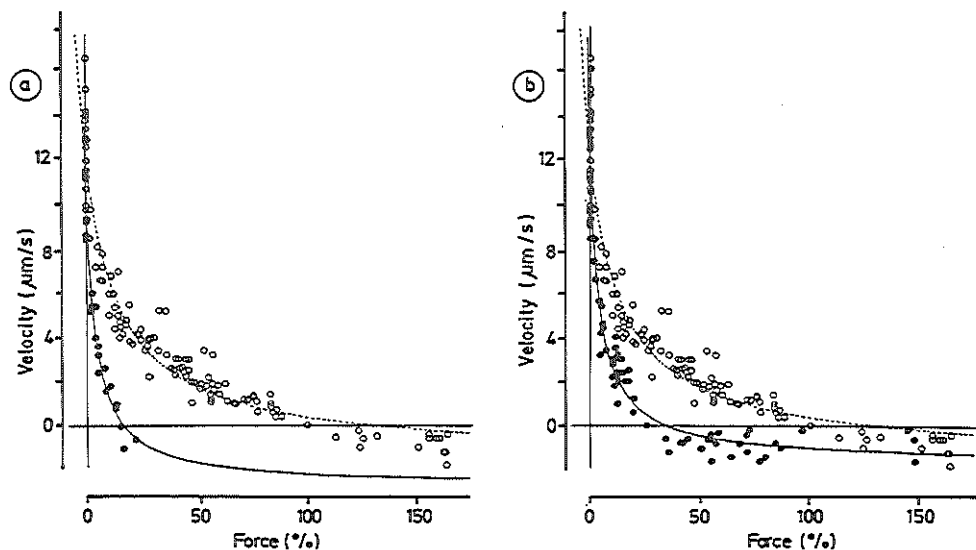


FIG 4 Relation of force to velocity. (a) $\circ [Ca^{++}]_o$ 1.5 mmol·litre⁻¹; pH 7.35 ($n=10$); $\bullet [Ca^{++}]_o$ 0.3 mmol·litre⁻¹; pH 7.35 ($n=3$); (b) $\circ [Ca^{++}]_o$ 1.5 mmol·litre⁻¹; pH 7.35 ($n=10$); $\bullet [Ca^{++}]_o$ 1.5 mmol·litre⁻¹; pH 6.68 ($n=7$). Tension developed at SL 2.00 μ m, pH 7.35, $[Ca^{++}]_o$ 1.5 mmol·litre⁻¹ has been expressed as 100%.

TABLE Relation between force and velocity. Values are mean (SEM); measured values (m) and Hill's fitting (c) are given

P_{m}^{m} (mN·mm ⁻²)	% P_{m}^{m}	v_{m}^{m} (μm·s ⁻¹)	P_{m}^{c} (mN·mm ⁻²)	% P_{m}^{c}	v_{m}^{c} (μm·s ⁻¹)	b (μm·s ⁻¹)	a (mN·mm ⁻²)	r
81.23(10.07)	100.0(12.4)	12.25(0.62)	{Ca ⁺⁺ } _o (1.5 mmol·litre ⁻¹), pH 7.35, n=10					
			107.14(4.54)	131.8(5.6)	11.96(0.05)	1.38(0.09)	12.38(0.37)	0.97
12.47(2.45)	15.4(3.0)	9.57(0.81)	{Ca ⁺⁺ } _o (0.3 mmol·litre ⁻¹), pH 7.35, n=3					
			13.53(1.40)	16.6(1.7)	9.90(0.26)	2.72(0.58)	3.72(0.54)	0.96
13.70(3.97)	16.9(4.9)	9.19(0.60)	{Ca ⁺⁺ } _o (1.5 mmol·litre ⁻¹), pH 6.68 (acute), n=6					
			{Ca ⁺⁺ } _o (1.5 mmol·litre ⁻¹), pH 6.68 (steady), n=7					
20.70(6.98)	25.5(8.6)	12.64(1.34)	27.98(1.23)	34.4(1.5)	11.50(0.16)	1.62(0.11)	3.94(1.19)	0.97

P_{m}^{m} =maximum developed tension; v_{m}^{m} =maximum sarcomere shortening velocity; r =correlation coefficient. P_{m}^{m} under control conditions has been expressed as 100%. All the measured (% P_{m}^{m}) and calculated (% P_{m}^{c}) values are referred to that percentage.

Discussion

Our results are consistent with the hypothesis that the negative inotropic effect of low pH is due to a competition of H⁺ and Ca⁺⁺ ions for binding to the troponin.^{8 11 23-25} The observation that, during respiratory acidosis, force decreases acutely to a minimum and subsequently stabilises at a slightly higher level (fig 1) can be explained on the basis of the work of Allen *et al.*²⁶

These authors found that in cat papillary muscle alkalosis induced a transient increase in developed tension, followed by a slow decline to a new steady state greater than control. Since in our experiments the time course of tension during acidosis showed a symmetrical pattern, it seems reasonable to infer that in the early phase of acidosis force decays, owing to an increase in intracellular H⁺ concentration, whereas intracellular Ca⁺⁺ concentration ([Ca⁺⁺]_i) remains constant; the subsequent increase of force might be due to an increase in [Ca⁺⁺]_i. The long time constant of this increase suggests that pump activities of sarcolemma¹⁰ or sarcoplasmic reticulum^{8 27} are affected by the variation in pH. Na⁺ ions are likely to be involved in these mechanisms^{10 28} since Na⁺/H⁺ exchange may be partially responsible for recovery from acidosis.^{29 30} Moreover, a partial recovery of intracellular pH has been shown and can be accounted for by several exchange and neutralising mechanisms, as recently reviewed by Thomas.³¹ The observed intracellular pH variation in rat cardiac muscle (pH_i) during variation of extracellular pH (pH_o) as a result of varied PCO₂³² is consistent with the action of control systems for pH_i.^{31 33} Saborowski *et al.*³² reported that pH_i varies by 0.45 pH units with pH_o from 6.6 (at pH_o=6.2) to 7.4 (at pH_o=8.0) under conditions that are comparable to those in our experiments. pH_i would be 7.10-7.15 at pH_o=7.40, as has also been reported by other authors.³³⁻³⁵ Our results (fig 3) show that

twitch force (F) at constant sarcomere length varies with pH_o as $F=K^2/K^2 + \text{pH}_o^2$ with $K = 6.91$. Secondly, our results show that a change in pH_o from 7.4 to 6.7 results in a change in the force-sarcomere length relation that is quantitatively similar to a decrease in [Ca⁺⁺]_o from 1.5 to 0.3 mmol·litre⁻¹. The depression of the twitch force by the fall in pH can only partly be restored by increasing [Ca⁺⁺]_o. If we assumed that Saborowski's data are correct, the above effects of extracellular pH changes seem to be quantitatively consistent with the observations made by Fabiato on the effect of pH on calcium loading by the sarcoplasmic reticulum of mechanically skinned cardiac muscle cells of rat and on the effect of pH on the force that is developed by the myofibrils on activation by calcium ions.⁸

Fabiato showed in these studies that, at constant pH (7.0) of the myofilaments, the force transient after caffeine induced calcium release by the sarcoplasmic reticulum increases with the pH at which calcium loading took place⁸ (tables 2 and 3⁸). The myoplasmic [free Ca⁺⁺] that is reached during the above transients can be inferred from the developed force.³⁶ The pCa calculated from the transient appears to be proportional to the pH at which loading took place — that is, pCa decreased by 0.16 units per unit increase of pH³⁶ (table 2, fig 1b³⁶) over a pH range between 6.20 and 7.40. This effect would be enlarged by the shift of the F-pCa curves of the filaments by about 0.6 pCa/pH units towards higher [free Ca⁺⁺].

We calculated the twitch force as a function of pH from the above data. Peak twitch force in our preparations was assumed to be 70% of maximal force of the myofilaments at pCa of 5.4³⁶ (pH_i=7.10³⁶). The effect of changes in pH were deduced from the shift of the F-pCa curves with pH_i.^{8 32} In order to do so it was assumed that the control F-pCa curve in this study was shifted by 0.4 pCa units to lower [free Ca⁺⁺] as a result of the high [free Mg⁺⁺] and lower

pH (=7.00) compared with Fabiato's study in 1981.^{36, 37}

The effect of pH on the release of calcium was assumed to be identical to that reported by Fabiato⁸ and independent of the [free Mg^{++}]. Although the latter assumption has yet to be verified, the relation between calculated and measured twitch force clearly varies identically with pH (see fig 3).

The assumption that the pH determines the position of the F-pCa curves of the filaments and affects calcium release by the sarcoplasmic reticulum is therefore sufficient to explain the steady state force-pH relation. The effect of lowered pH_i (pH<6.6) in depressing force at supraoptimal [free Ca^{++}]^{8, 24} and depressing myofibrillar ATPase activity³⁸ does not need to be invoked, since the lowest intracellular pH in this study was probably 6.6.³² Our results show that the effect of lowering pH on the force-sarcomere length relation (fig 2a) is quantitatively similar to that of lowering $[Ca^{++}]_o$. Recently, Hibberd and Jewell showed that sarcomere length controls Ca^{++} sensitivity of myofilaments,³⁹ and this length dependent sensitivity has been reported to account for the whole force-sarcomere length relation in rat heart,⁴⁰ such that Ca^{++} release at each sarcomere length is virtually constant.

In fact the observation that acidosis affects this relation at all sarcomere lengths can be explained as length independent competition of protons and Ca^{++} ions for binding to anionic sites of troponin, and a length independent depression of calcium release. Because of this competition, the Ca^{++} sensitivity of troponin decreases rapidly after the pH is lowered, and in order to develop a given tension a greater amount of Ca^{++} is required than under control conditions. This is consistent with a shift of the F-pCa relation to the right, and the effect of lowering the pH is therefore similar to that of lowering $[Ca^{++}]_o$.

Our results also show (fig 2b) that increasing $[Ca^{++}]_o$ during acidosis increases force and shifts the force-sarcomere length relation from convex towards the abscissa to convex towards the ordinate but fails to completely re-establish force. This observation can be accounted for if one of the steps of calcium loading or release or both is irreversibly depressed at low pH as well. Furthermore, high $[Ca^{++}]_o$ caused spontaneous activity in our preparations irrespective of the driving frequency, which affected force development at all sarcomere lengths. Force-velocity relations measured under different experimental conditions are shown in fig 4.

At low $[Ca^{++}]_o$ and during early acidosis both maximum developed tension and maximum sarcomere shortening velocity were reduced. There is general agreement that maximal velocity of sarcomere shortening reflects myofibrillar ATPase activity.^{41, 42}

and the latter has been shown to be depressed by acidosis^{38, 43} at intracellular pH below 6.6.⁸ This may explain the transient undershoot in v_o at low pH (see table). Subsequently, during the next 20 minutes, v_o returned to control values, whereas at low $[Ca^{++}]_o$ the relation was steadily depressed. The increase in maximum sarcomere shortening velocity may result from the increase in effective $[Ca^{++}]_i$ ²⁵ since it depends on $[Ca^{++}]_i$, as shown by ter Keurs and Wohlfart.²¹ Furthermore, it may result from recovery of the myofibrillar ATPase activity, when pH increases to a new and higher steady state level.^{29, 30, 32} The force-velocity relations that were found in this study were adequately described by rectangular hyperbolas — $(P+A)v = (P_o-P)b$ — both under normal conditions and during hypercapnic acidosis. It is likely, therefore, that the dynamics of actomyosin interactions during shortening and stretch do not alter fundamentally as a result of acidosis. A consequence of the drastic increase of force on stretch is that a chain of muscle elements of unequal force generating capacities, such as may result from geometrical factors or from differences in functional state, as during regional myocardial ischaemia, will be stable. Shortening of the strong elements in the chain then causes stretching of the weaker elements. The force balance can be attained at relatively small stretch velocity of the weaker one as a result of the small asymptotic value $v=-b$; ($b=1.00(0.45) \mu m \cdot s^{-1}$).²⁰

We thank Mr H M Kleyn for his excellent technical assistance, Fokker BV for providing force transducer's carbon rods, and Mrs A M A van Ditmarsch. Part of this work has been presented as a poster to the European Society for Clinical Investigation.⁴⁴ This work was supported by a grant from the Dutch Heart Foundation.

References

- 1 Cobbe SM, Poole-Wilson PA. The time of onset and severity of acidosis in myocardial ischemia. *J Mol Cell Cardiol* 1980;12:745-60.
- 2 Steenbergen C, Deleuw G, Rich T, Williamson JR. Effects of acidosis and ischemia on contractility and intracellular pH of rat heart. *Circ Res* 1977;41:849-58.
- 3 Klug F. Ueber den Einfluss gasartiger Körper auf die Funktion des Froschenherzens. *Arch Anat Par* 1879;435-78.
- 4 Gaskell WH. On the tonicity of the heart and the blood vessels. *J Physiol (Lond)* 1880;3:48-75.
- 5 Kohlhardt M, Wirtz K, Dudeck J. Ueber den Einfluss von metabolischer Alkalose und metabolischer Acidose auf die Kontraktilität des isolierten Herzens. *Pfluegers Arch* 1967;296:352-62.
- 6 Vaughan-Williams EM, Whyte JM. Chemosensitivity of cardiac muscle. *J Physiol (Lond)* 1967;189:119-37.
- 7 Nakamura Y, Schwartz A. Possible control of intracellular calcium metabolism by $[H^+]$: sarcoplasmic reticulum of skeletal and cardiac muscle. *Biochem Biophys Res Commun* 1970;41:830-6.

- 8 Fabiato A, Fabiato F. Effect of pH on the myofilaments and the sarcoplasmic reticulum of skinned cells for cardiac and skeletal muscle. *J Physiol (Lond)* 1978;278:233-55.
- 9 Safer B, Morad M, Williamson JR. Effects of $[H^+]$ on myocardial contractility. *Circulation* 1973;48(suppl IV):212.
- 10 Philipson KD, Bersohn MM, Nishimoto AY. Effect of pH on Na^+/Ca^{++} exchange in canine cardiac sarcolemmal vesicles. *Circ Res* 1982;50:287-93.
- 11 Katz AM, Hecht HH. The early "pump" failure of the ischemic heart. *Am J Med* 1969;47:497-502.
- 12 Tsien RW. Possible effects of hydrogen ions in ischemic myocardium. *Circulation* 1976;53(suppl 1):14-16.
- 13 Poole-Wilson PA, Langer GA. Effect of pH on ionic exchange and function in rat and rabbit myocardium. *Am J Physiol* 1975;229:570-81.
- 14 Kohlhardt M, Haap K, Figulla HR. Influence of low extracellular pH upon the Ca inward current and isometric contractile force in mammalian ventricular myocardium. *Pfluegers Arch* 1976;366:31-8.
- 15 Pannier JL, Leusen I. Contraction characteristics of papillary muscle during changes in acid-base composition of the bathing fluid. *Arch Int Physiol Bioch* 1968;76:624-34.
- 16 Cingolani HE, Mattiazzi AR, Blesa ES, Gonzalez NC. Contractility in isolated mammalian heart muscle after acid-base changes. *Circ Res* 1970;36:269-78.
- 17 Fry CH, Poole-Wilson PA. Effect of acid-base changes on excitation-contraction coupling in guinea-pig and rabbit cardiac ventricular muscle. *J Physiol (Lond)* 1981;313:141-60.
- 18 van Heuningen R, Rijnsburger WH, ter Keurs HEDJ. Sarcomere length control in striated muscle. *Am J Physiol* 1982;242:H411-H420.
- 19 ter Keurs HEDJ, Rijnsburger WH, van Heuningen R, Nagelsmit MJ. Tension development and sarcomere length in rat cardiac trabeculae. Evidence of length dependent activation. *Circ Res* 1980;46:703-14.
- 20 Daniels M, Noble MIM, ter Keurs HEDJ, Wohlfart B. Velocity of sarcomere shortening in rat cardiac muscle: relationship to force, sarcomere length, calcium and time. *J Physiol (Lond)* 1984;355:367-81.
- 21 ter Keurs HEDJ, Wohlfart B. Influence of calcium concentration on maximal velocity of sarcomere shortening in rat trabeculae. *J Physiol (Lond)* 1982;330:41P.
- 22 Hill AV. The heat of shortening and the dynamic constants of muscle. *Proc R Soc London* 1938;B126:136-95.
- 23 Katz AM. The ischemic heart. In: *Physiology of the heart*. New York: Raven Press, 1977: 419-433.
- 24 Kentish JC, Nayler WG. Ca^{++} -dependent tension generation in chemically skinned cardiac trabeculae: effect of pH. *J Physiol (Lond)* 1978;284:90P-91P.
- 25 Robertson SP, Johnson JD, Potter JD. The effect of pH on calcium binding to the Ca^{++} - Mg^{++} and the Ca^{++} specific sites of bovine cardiac TnC . *Circulation* 1973;48(suppl IV):212.
- 26 Allen DG, Kurihara S, Orchard CH. The effect of reducing extracellular carbon dioxide concentration on intracellular calcium transients in mammalian cardiac muscle. *J Physiol (Lond)* 1981;317:52P.
- 27 Mandel F, Galani-Kranias E, Grassi de Gende A, Sumida M, Schwartz A. The effect of pH on the transient state kinetics of Ca^{++} - Mg^{++} -ATPase of cardiac sarcoplasmic reticulum. *Circ Res* 1982;50:310-7.
- 28 Ellis D, MacLeod KT. The dependence of intracellular pH regulation on extracellular Na in sheep Purkinje fibres. *J Physiol (Lond)* 1983;336:69P-70P.
- 29 MacLeod KT. Intracellular pH regulation: interaction between Ca and pH regulation. *Proc Physiol Soc* 1984.
- 30 Vaughan-Jones RD. The contribution of various systems to the regulation of pH_i . *Proc Physiol Soc* 1984.
- 31 Thomas RC. Experimental displacement of intracellular pH and the mechanism of its subsequent recovery. *J Physiol (Lond)* 1984;354:3P-22P.
- 32 Saborowski F, Lang D, Albers C. Intracellular pH and buffer curves of cardiac muscle in rats as affected by temperature. *Resp Physiol* 1973;18:161-70.
- 33 Roos A, Boron WF. Intracellular pH . *Physiol Rev* 1981;61:297-403.
- 34 De Hemptinne A. Intracellular pH and surface pH in skeletal and cardiac muscle measured with a double-barrelled pH microelectrode. *Pfluegers Arch* 1980;386:121-6.
- 35 Fabiato A, Fabiato F. Calculator programs for computing the composition of the solutions containing multiple metals and ligands used for experiments in skinned muscle cells. *J Physiol (Paris)* 1979;75:463-505.
- 36 Fabiato A. Myoplasmic free calcium concentration reached during the twitch of an intact isolated cardiac cell and during calcium-induced release of calcium from the sarcoplasmic reticulum of a skinned cardiac cell from the adult rat or rabbit ventricle. *J Gen Physiol* 1981;78:457-97.
- 37 Fabiato A, Fabiato F. Effects of magnesium on contractile activation of skinned cardiac cells. *J Physiol* 1975;249:497-517.
- 38 Kentish JC, Nayler WG. The influence of pH on the Ca^{++} -regulated ATPase of cardiac and white skeletal myofibrils. *J Mol Cell Cardiol* 1979;11:611-7.
- 39 Hibberd MG, Jewell BR. Calcium- and length-dependent force production in rat ventricular muscle. *J Physiol (Lond)* 1982;329:119-37.
- 40 Kentish JC, ter Keurs HEDJ, Noble MIM, Ricciardi L, Schouten VJAS. Force, free calcium ion concentration and sarcomere length in rat cardiac trabeculae. *J Physiol (Lond)* 1983;345:24P.
- 41 Bárány M. ATPase activity of myosin correlated with speed of muscle shortening. *J Gen Physiol* 1967;50:197-216.
- 42 Hamrell BB, Low RB. The relationship of mechanical v_{max} to myosin ATPase activity in rabbit and marmot ventricular muscle. *Pfluegers Arch* 1978;377:119-24.
- 43 Blanchard EM, Solaro RJ. Inhibition of the activation and troponin calcium binding of dog cardiac myofibrils by acidic pH. *Circ Res* 1984;55:382-91.
- 44 Ricciardi L, Bucx JJJ, ter Keurs HEDJ. The effect of acidosis on sarcomere mechanics of rat heart. [Abstract] *Eur J Clin Invest* 1984;14:110.

CHAPTER 6

SARCOLEMMMA, SARCOPLASMIC RETICULUM, AND SARCOMERES AS LIMITING FACTORS IN FORCE PRODUCTION IN RAT HEART

Vincent JA Schouten, Jeroen JJ Buxx, Pieter P de Tombe, and Henk EDJ ter Keurs

Published in Circulation Research 1990; 67: 913-922

.

Sarcolemma, Sarcoplasmic Reticulum, and Sarcomeres As Limiting Factors in Force Production in Rat Heart

Vincent J.A. Schouten, Jeroen J.J. Bucx, Pieter P. de Tombe, and Henk E.D.J. ter Keurs

Inotropic interventions were compared with respect to their maximum effect on force of contraction in rat myocardium to identify limiting steps in calcium handling. Peak force, sarcomere length, and action potentials were measured in thin ventricular trabeculae. Relevant control conditions were stimulation frequency, 0.2 Hz; $[Ca^{2+}]_o$, 1 mM; $[K^+]_o$, 5 mM; $[Na^+]_o$, 150 mM. The inotropic interventions and results were as follows. 1) The interventions of high $[Ca^{2+}]_o$, low $[Na^+]_o$, high $[K^+]_o$, addition of tetraethylammonium chloride, or postextrasystolic potentiation resulted in approximately the same (within 5%) maximum force (F_{max}). Above the respective optimum doses, force declined and aftercontractions were often observed. Combinations of the different interventions never enhanced force to above F_{max} . This suggests that F_{max} is determined by a maximum level of Ca^{2+} in the sarcoplasmic reticulum, above which spontaneous release occurs. 2) Sr^{2+} (10 mM) caused an increase of force to $1.3 \times F_{max}$ and lengthening of contraction and action potentials. The force-sarcomere length relation was, then, similar to that in skinned fibers at maximum activation. Hence, $1.3 \times F_{max}$ reflects saturation of the sarcomeres. We postulate that a large influx of Sr^{2+} during the long action potential can circumvent the reticulum and activate the sarcomeres directly. When the reticulum was blocked with ryanodine, maximum force of tetanic contractions was about $1.1 \times F_{max}$. This result supports the above conclusions. 3) Isoproterenol increased force to a maximum that was 20% below F_{max} and shortened the contraction. This may be due to a decreased sensitivity of the sarcomeres to Ca^{2+} or to stimulation of the Ca^{2+} pump in the reticulum, that is, an increasing fraction of the released Ca^{2+} is sequestered before it can activate the sarcomeres. Thus, three factors that limit force production were identified, depending on the inotropic stimulus. (*Circulation Research* 1990;67:913-922)

Force of contraction in heart muscle can be increased by a number of drugs, ions, and stimulus patterns. Naturally, the ultimate maximum force is reached when the contractile filaments are saturated with Ca^{2+} and work at maximum capacity. So far, there is no evidence, however, that this condition occurs in normal, intact heart muscle. On the contrary, indications are that force of con-

traction in fully activated skinned heart muscle is about 30% greater than maximum force in fibers with intact sarcolemma.^{1,2} Hence, there may be a limiting factor that prevents full activation of the sarcomeres in intact heart muscle. Because the sarcoplasmic reticulum is the main source of activator Ca^{2+} , maximum force may be determined by the maximum capacity of the reticulum to store and release Ca^{2+} . It has been suggested that once Ca^{2+} in the reticulum exceeds a certain level, spontaneous release occurs,³⁻⁵ and this may curtail the maximum inotropic effect of an intervention.⁶

We observed earlier⁷ that force in intact trabeculae of rat heart at high $[Sr^{2+}]_o$ was 30% greater than at high $[Ca^{2+}]_o$. Thus, maximum force may be limited by a Ca^{2+} -dependent mechanism that is abolished or circumvented by Sr^{2+} . We tested this hypothesis by measuring the maximum effect of various interventions in intact trabeculae. We used laser diffraction to measure sarcomere length and microelectrodes to measure membrane potential, that is, methods that

From the Laboratory for Physiology (V.J.A.S.), Free University, Amsterdam, The Netherlands, and the Department of Medical Physiology (J.J.J.B., P.P.T., H.E.D.J.K.), University of Calgary, Calgary, Canada.

Partial results published in abstract form (*J Physiol* [Lond] 1986;381:96P).

Supported in part by a grant from the Alberta Heritage Foundation for Medical Research (AHFMR) and from the Heart and Stroke Foundation of Alberta. H.E.D.J.K. holds a Medical Scientist Award of the AHFMR. J.J.J.B. held an AHFMR Fellowship, and P.P.T. held an AHFMR Studentship.

Address for correspondence: V.J.A. Schouten, Laboratory for Physiology, Free University, Van der Boechorststraat 7, 1081 BT Amsterdam, The Netherlands.

Received November 16, 1989; accepted May 29, 1990.

give information about organelle activity while having no influence on their properties.

Materials and Methods

Details of the preparation and methods have been described earlier.^{8,9} In brief, long (2.5–4-mm) and thin (0.05–0.15-mm) free-running trabeculae were dissected from the right ventricle of rat heart and suspended in a 0.5-ml chamber between a force transducer (type AE801, Mikro-Elektronikk, Horten, Norway) and a length adjustment device. The muscle was stretched to a length at which passive force was about 2% of the active force at 2.5 mM $[Ca^{2+}]_o$ and stimulated at 1 Hz for 1 hour before the experiment was begun.

The composition of standard solution was (in mM): NaCl 120, KCl 5, $MgCl_2$ 1.2, $CaCl_2$ 1.0, NaH_2PO_4 2, Na_2SO_4 1.2, $NaHCO_3$ 27, and glucose 10. The solution was recirculated via a 0.5-l reservoir in which it was gassed with 95% O_2 and 5% CO_2 ; P_{O_2} was 590–650 mm Hg, P_{CO_2} was 39–45 mm Hg, and pH was 7.35–7.45. Flow through the muscle chamber was 10 ml/min, and temperature was $27 \pm 0.3^\circ C$. The calcium and strontium concentrations in the superfusion solution ($[Ca^{2+}]_o$ and $[Sr^{2+}]_o$) were varied by adding amounts of 1 M stock solutions of the chloride salts to standard or Ca^{2+} -free solution. Low $[Na^+]_o$ was obtained by substitution of 15–90 mM NaCl by 15–90 mM LiCl. In experiments with isoproterenol, a calibrated syringe and infuser pump were used to inject the drug into the Tyrode's solution just before the inlet of the muscle bath to prevent time-dependent effects of oxidation. The Tyrode's solution was not recirculated during the isoproterenol experiments.

Ryanodine-treated muscles were used to study tetanic contractions at high $[Ca^{2+}]_o$. To prevent precipitation, $NaHCO_3$ and NaH_2PO_4 were replaced with 20 mM NaCl and 10 mM HEPES. The pH was adjusted with NaOH. The solutions were equilibrated with 100% O_2 . Contractures were induced with Tyrode's solution with the following modifications: 60–120 mM NaCl was replaced by LiCl, $[KCl]_o$ was increased to 20 mM, and 10 mM caffeine was added.

Sarcomere length was measured with laser diffraction, as described earlier.⁸ Briefly, the parallel sarcomeres act as an optical grating, and the incident laser beam is split into a zero- and multiple higher-order bands. The spacing between the bands is a measure of sarcomere length. The first-order band was scanned twice per millisecond by a photodiode array. Sarcomere length was computed electronically from the scans. Calibration was performed with test gratings before each experiment.

Transmembrane potential was measured by means of flexible glass microelectrodes. The resistance of the electrodes (filled with 3 M KCl) was 60–100 M Ω , as measured in the muscle chamber.

Stimulus pulses of 3-msec duration and 20% above threshold strength were derived from a programmable pulse generator via a stimulus isolator and two platinum wire electrodes. The frequency of stimulation

was 0.2 Hz during all experiments; however, postextrasystolic potentiation was induced by interposing trains of 1–100 intervals of 0.25 second (see Figure 1).

Results

Influence of $[Ca^{2+}]_o$

To determine the peak force- $[Ca^{2+}]_o$ relation, the $[Ca^{2+}]_o$ was first reduced to 0.3 mM and subsequently increased in several steps, at intervals of 5 minutes, to a final concentration of 5–10 mM. The result was a sigmoid relation, and maximum force (F_{max}) occurred at about 3 mM. Above 3 mM, force declined (e.g., Figures 2, 4, and 8) and aftercontractions were observed. F_{max} determined at optimum $[Ca^{2+}]_o$ was used as a reference; that is, the maximum effects of all other interventions were compared with that value.

Postextrasystolic Potentiation

The optimum interval to induce postextrasystolic potentiation in rat myocardium is 0.25 second,⁷ and short trains of 0.25-second intervals in low $[Ca^{2+}]_o$ potentiated force severalfold until a maximum effect, which is indicated as "saturation" (Figure 1). The figure also shows that increasing the number of extrasystoles above the optimum caused a small decrease of peak force. The latter effect was associated with aftercontractions. The number of extrasystoles that caused saturation decreased with increasing $[Ca^{2+}]_o$ (Figure 1).

It should be noted that aftercontractions were well visible through the microscope but generally not in the record of force. This follows from the fact that the aftercontraction was a propagated wave. Thus, at a given moment only a small fraction of the muscle contracted; the rest was passively stretched. Hence, external force was negligible.^{4,5}

We tested whether saturation corresponded with a unique, maximum value of force or varied with $[Ca^{2+}]_o$ or steady-state force. The procedure shown in Figure 1 was used to determine maximum potentiation, and Figure 2 demonstrates that, except for a few points at very low steady-state force and $[Ca^{2+}]_o$, the maximally potentiated beats were within a few percent of F_{max} ; that is, independent of steady-state force and $[Ca^{2+}]_o$.

Low $[Na^+]_o$ and High $[K^+]_o$

Both low $[Na^+]_o$ and elevated $[K^+]_o$ (depolarization of the membrane) inhibit extrusion of Ca^{2+} via the Na^+/Ca^{2+} exchanger. This causes intracellular accumulation of Ca^{2+} and enhanced force.^{10,11} In addition, increased $[K^+]_o$ lengthens the action potential in heart muscle of rat (see Figure 4C).

In each preparation we first determined F_{max} by means of postextrasystolic potentiation and usually by varying $[Ca^{2+}]_o$. Reduction of $[Na^+]_o$ in the presence of 1 mM Ca^{2+} , led to enhanced force and shortening of the action potential, as has been shown earlier.⁹ The maximum inotropic effect was found at about 75 mM $[Na^+]_o$, and force was then $(1.04 \pm 0.04) \times F_{max}$ ($n=5$). Reduction of $[Na^+]_o$ below 75

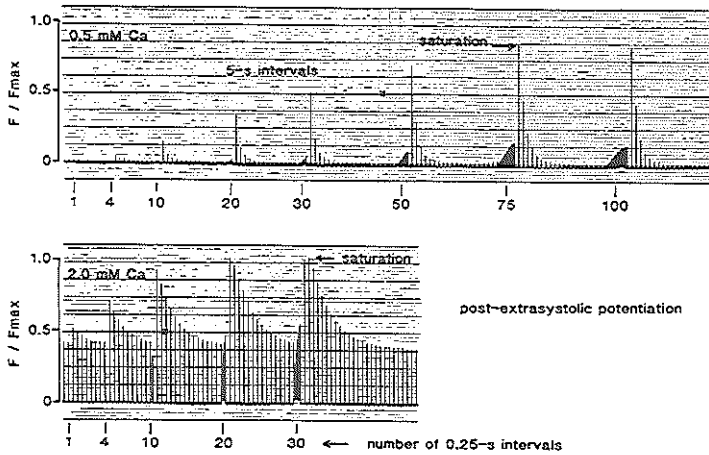


FIGURE 1. Maximum effect of interspersed extrasystoles. Upper panel: At 0.5 mM $[Ca^{2+}]_o$, maximum potentiation (indicated as saturation) was obtained with a train of 75 extrasystoles (0.25-second intervals). In this preparation peak force (F/F_{max}) was relatively low (diamonds in Figure 2); in other preparations a smaller number of extrasystoles was sufficient to induce saturation. Lower panel: At 2 mM $[Ca^{2+}]_o$, the maximum effect occurred after 20 extrasystoles. These two recordings were from the same preparation as represented by the diamonds in Figure 2. F_{max} maximum force at optimum $[Ca^{2+}]_o$.

mM caused aftercontractions and a decline in force (Figure 3).

The resting membrane potential became more positive after elevation of $[K^+]_o$, while the upstroke of the action potential became slower and action potential duration at 50% of the amplitude increased. To compensate for the decreased excitability at 15–20 mM $[K^+]_o$, the strength and duration of the stimulus had to be increased threefold. Force increased with $[K^+]_o$ to a maximum at about 15 mM and remained constant (Figure 4A) or decreased slightly at higher concentrations. Aftercontractions were not distinguishable in the recordings of force. Maximum peak force obtained with high $[K^+]_o$ was always equal to or slightly less than F_{max} obtained with postextrasystolic potentiation or optimum $[Ca^{2+}]_o$. The mean was $(0.95 \pm 0.05) \times F_{max}$ ($n=5$).

We tested whether the combination of high $[K^+]_o$ and high $[Ca^{2+}]_o$ or low $[Na^+]_o$ and high $[Ca^{2+}]_o$ could enhance force to above F_{max} . This was not the case, and when applied at optimum $[Ca^{2+}]_o$, elevation of $[K^+]_o$ (Figure 4B) or reduction of $[Na^+]_o$ caused aftercontractions and a decline in force. Elevation of $[K^+]_o$ always lengthened the action potential, also at optimum $[Ca^{2+}]_o$ (Figure 4C).

Influence of Tetraethylammonium

Tetraethylammonium (TEA) blocks the K^+ outward currents I_{K1} and I_{K2} ,^{12,13} which explains the marked lengthening of the action potential (Figures 5A and 5B). When added to standard solution (1 mM $[Ca^{2+}]_o$), TEA enhanced force to a maximum of $(0.96 \pm 0.07) \times F_{max}$ ($n=3$). The optimum concentration was 5–10 mM; at higher concentrations force declined and aftercontractions were observed. Action potential duration continued to increase with $[TEA]_o$. In the presence of 2.5 mM $[Ca^{2+}]_o$, when force was already close to F_{max} , TEA induced only a

small increase in force, or a decrease (Figure 5C). Action potential duration always increased with $[TEA]_o$ (Figures 5A and 5B).

Influence of Isoproterenol

Commonly observed effects of β -receptor agonists are enhanced force, shortened twitch duration, and lengthened action potential duration.^{14–16} We found the same effects in the rat trabeculae. In the experiments with this drug we first determined F_{max} by variation of $[Ca^{2+}]_o$ and postextrasystolic potentiation. Subsequently, an isoproterenol dose-response relation was measured in control solution. Above the threshold concentration of 10 nM, peak force began to increase and maximum force was found at about 1

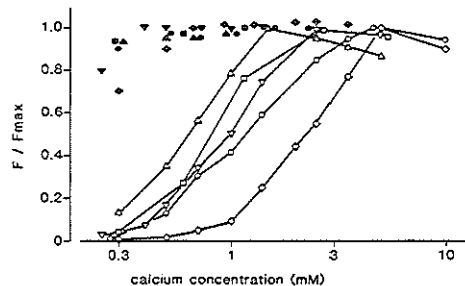


FIGURE 2. Dependence of normalized peak force (F/F_{max}) on $[Ca^{2+}]_o$ in five trabeculae. Open symbols represent steady-state force measured 3 minutes after each increment in concentration. At each concentration, maximum postextrasystolic potentiation (solid symbols) was determined with the protocol shown in Figure 1.

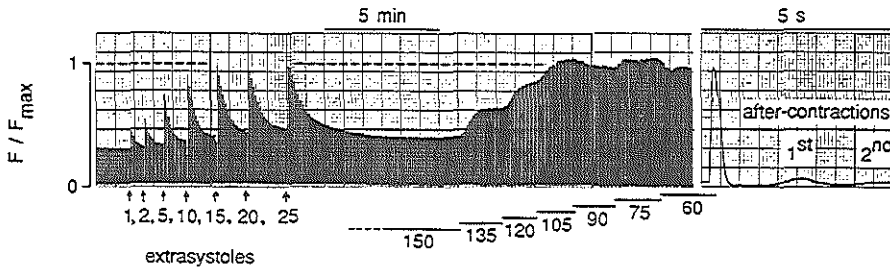


FIGURE 3. Maximum effect of low $[Na^+]_o$ (Li^+ substitution) on peak force (F/F_{max}) compared with maximum postextrasystolic potentiation. The recording at high paper speed shows that stimulated contractions at 60 mM $[Na^+]_o$ were followed by aftercontractions. F_{max} , maximum force at optimum $[Ca^{2+}]_o$.

μM . This maximum was consistently about 20% below F_{max} obtained with postextrasystolic potentiation or optimum $[Ca^{2+}]_o$ (eight preparations). In three preparations we measured maximum postextrasystolic potentiation at different concentrations of isoproterenol (for the method, see Figure 1). Although potentiation after a single extrasystole was enhanced by low concentrations of the drug, peak force of the maximally potentiated beats decreased (Figure 6). Above 0.5–1 μM isoproterenol force was constant, but action potential duration continued to increase, which indicates that the β -receptors were not yet saturated.

Influence of Ryanodine and Caffeine

Application of 5 μM ryanodine reduced steady-state force (at 1 mM $[Ca^{2+}]_o$, 0.2 Hz) to 5% and completely abolished postextrasystolic potentiation. These effects are consistent with the general assumption that this drug abolishes the sarcoplasmic reticulum as a functional Ca^{2+} store.^{17–19}

Rapid stimulation induced tetanic contractions that peaked within a few seconds and then decreased. The most effective frequency was 6–8 Hz, at which the amplitude of the tetanus was greater than that of single twitches (0.2 Hz) and increased with $[Ca^{2+}]_o$. When we switched from bicarbonate to

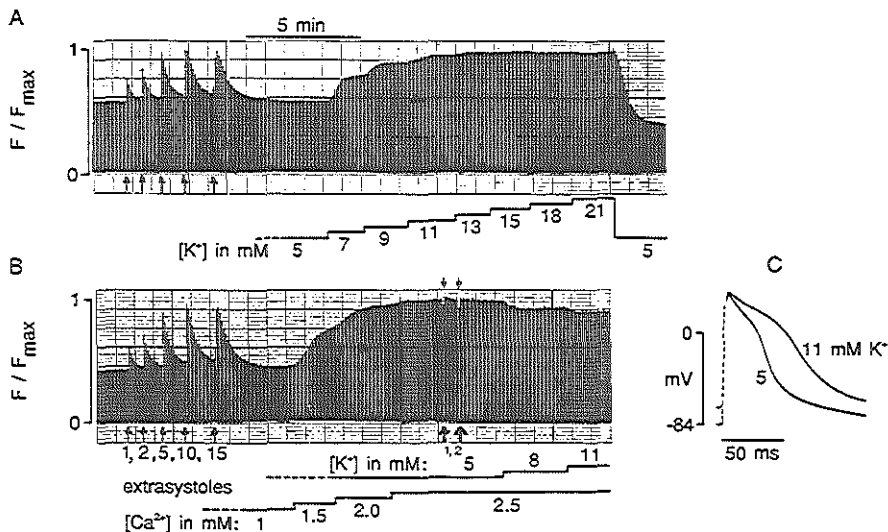


FIGURE 4. Panel A: Maximum effect of postextrasystolic potentiation and of high $[K^+]_o$ on force. Panel B: Maximum effect of postextrasystolic potentiation and of high $[Ca^{2+}]_o$ on force. Note that, in the presence of 2.5 mM $[Ca^{2+}]_o$, extrasystoles were followed by depressed contractions (arrows above the recording) and increased $[K^+]_o$ also depressed contraction. Panel C: Action potentials at 5 and 11 mM K^+ in the presence of 2.5 mM $[Ca^{2+}]_o$. Recordings in panels A, B, and C were from one preparation. F/F_{max} , peak force. F_{max} , maximum force at optimum $[Ca^{2+}]_o$.

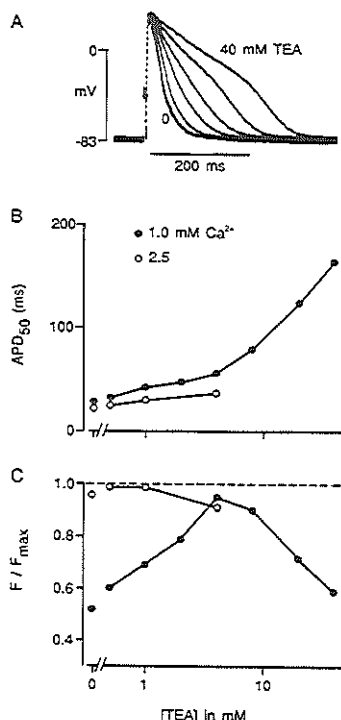


FIGURE 5. Effect of tetraethylammonium (TEA) on the action potential and contraction. Three minutes after each increment in $[TEA]_o$, an action potential was photographed (panel A), and action potential duration at 50% of the amplitude (APD_{50}) (panel B) and peak force (F/F_{max}) (panel C) were measured. The experiment was performed first at 1 mM $[Ca^{2+}]_o$ and subsequently at 2.5 mM $[Ca^{2+}]_o$ as indicated in panel B. All data in this figure were from one trabecula.

HEPES-buffered solution (1 mM $[Ca^{2+}]_o$ in both), a transient increase in force was observed that lasted about 15 minutes and was followed by a decrease in force to a lower level. An example of tetanic contractions after ryanodine treatment is shown in Figure 7. In four of five preparations, the maximum tetanic force at 8–15 mM Ca^{2+} was greater than F_{max} and the average was $(1.10 \pm 0.17) \times F_{max}$ ($n=5$). It should also be noted that diastolic force was $11 \pm 8\%$ of F_{max} in ryanodine-treated muscles at 8 mM Ca^{2+} , whereas diastolic force induced by the other interventions never exceeded 2%.

Caffeine (5–10 mM) reduced force to 50% and abolished postextrasystolic potentiation, which is consistent with the hypothesis that caffeine inhibits reticulum function.^{19–21} The action potential was lengthened by about 100%, probably as a result of intracellular cyclic AMP accumulation and cyclic AMP-induced enhancement of the inward Ca^{2+} cur-

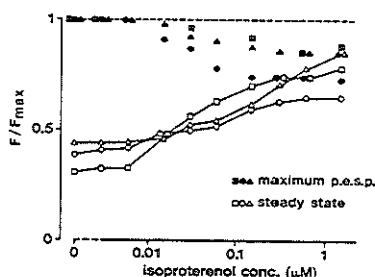


FIGURE 6. Effect of the β -agonist isoproterenol on force of contraction and on maximum postextrasystolic potentiation (p.e.s.p.) at $[Ca^{2+}]_o = 1$ mM. Steady-state peak force (F/F_{max}) and maximum potentiation were measured 3 minutes after each increment of $[isoproterenol]_o$. For the protocol to measure maximum potentiation, see Figure 4. Each pair of symbols represents one trabecula.

rent (I_{Ca}).²² During rapid stimulation, a tetanic contraction with variable amplitude developed in the presence of caffeine, and without electrical stimulation a large contracture developed when the muscle was superfused with a caffeine solution at a low $[Na^+]_o$ and high $[K^+]_o$. The amplitude of these contractures was rather variable, $(0.95 \pm 0.21) \times F_{max}$ ($n=5$).

Influence of Sr^{2+}

Strontium was of special interest because we found earlier⁷ that it could enhance peak force substantially above F_{max} . Because replacement of all extracellular Ca^{2+} by Sr^{2+} led to rapid deterioration of the muscle (irreversible depolarization and visible changes in cell structure), we tested the effect of Sr^{2+} in standard solution (1 mM $[Ca^{2+}]_o$). As shown in Figure 8 (open symbols), 1–5 mM $[Sr^{2+}]_o$ was less effective than Ca^{2+} to increase force, but at higher concentrations force reached a plateau that was 20–40% greater than F_{max} obtained with postextrasystolic potentiation or high $[Ca^{2+}]_o$ in the absence of Sr^{2+} .

Besides an increase of peak force, addition of Ca^{2+} to control solution also led to increase of contraction duration (+30% at 3 mM Ca^{2+}) and shortening of the action potential (–25% at 3 mM Ca^{2+}).⁷ When we added Sr^{2+} instead of Ca^{2+} , the prolongation of the contraction (+150%) was more pronounced, and the action potential was prolonged (+200%) (Figure 9A). As a consequence of this slow relaxation, rapid stimulation caused fusion and summation of contractions. At 10–19 mM $[Sr^{2+}]_o$, 4 Hz stimulation induced a tetanic contraction that never exceeded the amplitude of single twitches and was followed by a series of aftercontractions (Figure 9B). Such tetanic contractions did not develop at high $[Ca^{2+}]_o$ in the absence of Sr^{2+} .

Force–Sarcomere Length Relation

At control length of the muscle (2% passive force), sarcomere length was 2.2–2.3 μ m. During the contractions, however, sarcomere length in the central region

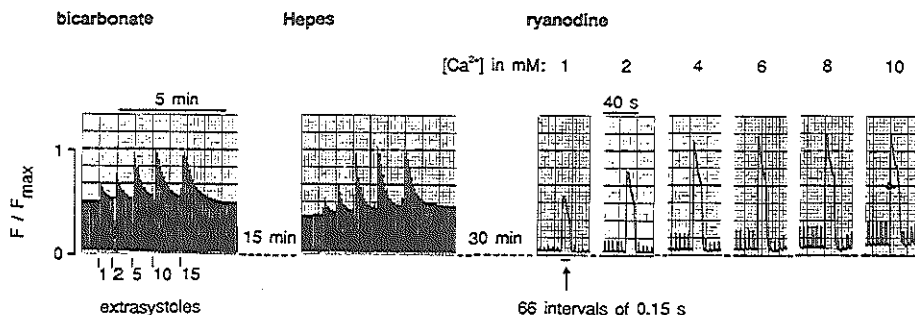


FIGURE 7. Tetanic contractions in a ryanodine-treated trabecula. Maximum postextrasystolic potentiation was recorded in standard solution with bicarbonate as the pH buffer (left panel) and subsequently after replacement of the bicarbonate with HEPES (middle panel). $[Ca^{2+}]_o$ was 1 mM in both solutions. The trabecula was exposed to 5 μ M ryanodine for 20 minutes, and after that tetanic contractions were induced with 6 Hz stimulation for 10 seconds at increasing $[Ca^{2+}]_o$ (right panels). F/F_{max} , peak force. F_{max} , maximum force at optimum $[Ca^{2+}]_o$.

shortened to about 1.9 μ m at the expense of stretch in the damaged ends, as reported earlier.⁸ Every 10th beat, muscle length was changed for one beat so that active sarcomere length at the moment of peak contraction varied from 1.6 to 2.2 μ m. In between the test beats the muscle was held at control length. At 0.8 mM $[Ca^{2+}]_o$, force increased in a linear fashion with sarcomere length (triangles in Figure 10). At 2.5 mM the relation was nonlinear (circles in Figure 10), and at 5 mM a similar curve was obtained, but force was smaller than at 2.5 mM at any sarcomere length (solid triangles in Figure 10), which is consistent with Figures 2 and 8. At 9–19 mM $[Sr^{2+}]_o$ (1 mM $[Ca^{2+}]_o$ present), however, peak force increased to values well above those measured at optimum $[Ca^{2+}]_o$, and as shown in Figure 10, the effect of Sr^{2+} was greatest at short sarcomere length. Thus, the force-sarcomere length curve at high $[Sr^{2+}]_o$ is remarkably similar to

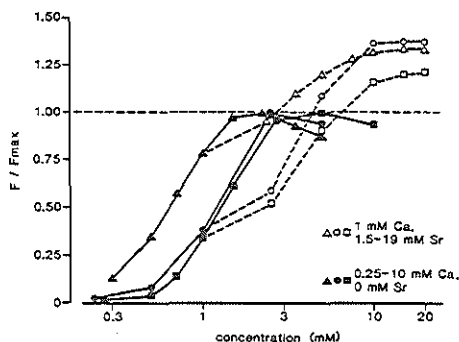


FIGURE 8. Dependence of steady-state peak force (F/F_{max}) on $[Ca^{2+}]_o$ (solid symbols) and $[Sr^{2+}]_o$ (in the presence of 1 mM $[Ca^{2+}]_o$; open symbols). Each pair of curves represents one preparation. F_{max} is the maximum force recorded at optimum $[Ca^{2+}]_o$, and data were normalized to that value.

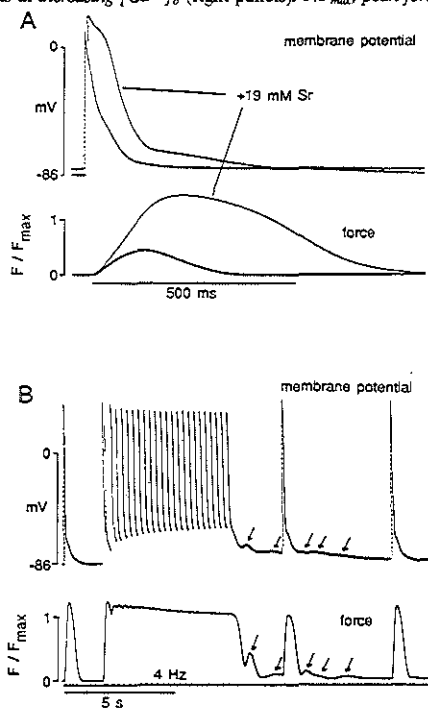


FIGURE 9. Panel A: Effect of 19 mM $[Sr^{2+}]_o$ (in the presence of 1 mM $[Ca^{2+}]_o$) on contraction and action potential. The unlabeled action potential and contraction were recorded at 1 mM $[Ca^{2+}]_o$. Panel B: In the presence of 1 mM $[Ca^{2+}]_o$ and 19 mM $[Sr^{2+}]_o$, rapid stimulation (4 Hz) caused a decrease in action potential amplitude and incomplete repolarization (top tracing) and a tetanic contraction (middle tracing). The bottom tracing shows the stimulus pulses. The arrows point at afterdepolarizations (top tracing) and aftercontractions (middle tracing). F/F_{max} , peak force. F_{max} , maximum force at optimum $[Ca^{2+}]_o$.

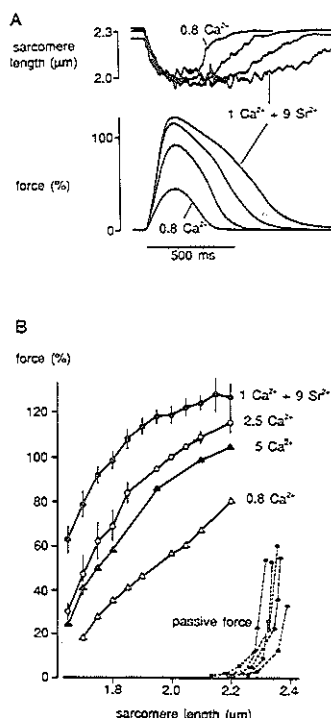


FIGURE 10. Panel A: Original recording of sarcomere length and force of contraction in the absence and presence of Sr^{2+} . Panel B: Force-sarcomere length relations at different Ca^{2+} concentrations and at $1 \text{ mM } [\text{Ca}^{2+}]_o + 9 \text{ mM } [\text{Sr}^{2+}]_o$. The values of force were averaged within $0.5 \mu\text{m}$ bins of sarcomere length per preparation. The symbols represent the mean values from five (minimum four) preparations, and vertical bars represent SEM (omitted in the 0.8 and $5 \text{ mM } [\text{Ca}^{2+}]_o$ curves). Force developed at $2.5 \text{ mM } [\text{Ca}^{2+}]_o$ and sarcomere length of $2.0 \mu\text{m}$ was taken as 100%. Note that data are given only for the range of sarcomere lengths at which passive force was negligible.

that reported for skinned myocytes¹ and skinned trabeculae² of rat heart.

Discussion

This study shows that high $[\text{Ca}^{2+}]_o$, low $[\text{Na}^+]_o$, K^+ depolarization, TEA, and postextrasystolic potentiation led to the same (within $\pm 5\%$) maximum force (F_{max}) in trabeculae of rat heart. This suggests a common limiting factor or saturation of a single mechanism. On the other hand, a value of $1.3 \times F_{\text{max}}$ was obtained with high $[\text{Sr}^{2+}]_o$, whereas force did not increase above $0.8 \times F_{\text{max}}$ after β -adrenoceptor stimulation. Hence, maximum force assumes different values depending on conditions, indicating the presence of several limiting factors.

It should be noted that at a sarcomere length above $2.2 \mu\text{m}$ and below $1.8 \mu\text{m}$, passive elastic forces occur, which contribute to the externally measured force. At slack length (about $1.9 \mu\text{m}$) the passive forces cancel each other.^{23,24} In our experiments, the sarcomere length at peak contraction was about $1.9 \mu\text{m}$, so that passive forces can be ignored and external force was equal to the active force generated by the sarcomeres.

Peak force of contraction is assumed to be proportional to the amount of activator Ca^{2+} available in the sarcoplasm. This amount is determined mainly by transport mechanisms in the sarcolemma (I_{Ca} , $\text{Na}^+/\text{Ca}^{2+}$ exchange) and in the sarcoplasmic reticulum (Ca^{2+} release channels, Ca^{2+} pump). On the time scale of a contraction, the role of the mitochondria and of the Ca^{2+} pump in the sarcolemma is probably minor.^{15,25-27} Thus, the limiting factors are expected to be located in the sarcolemma, the sarcoplasmic reticulum, or the contractile filaments.

Sarcolemma

The primary effects of increased $[\text{Ca}^{2+}]_o$, K^+ depolarization, TEA, and reduced $[\text{Na}^+]_o$ are at the level of the sarcolemma: High $[\text{Ca}^{2+}]_o$ enhances Ca^{2+} influx via I_{Ca} ^{18,28} and via the $\text{Na}^+/\text{Ca}^{2+}$ exchanger.^{10,11} The ensuing rise in intracellular Ca^{2+} , probably stored in the sarcoplasmic reticulum, explains the observed enhancement of peak force. Low $[\text{Na}^+]_o$ and K^+ depolarization inhibit Ca^{2+} extrusion via $\text{Na}^+/\text{Ca}^{2+}$ exchange.^{10,11} Low $[\text{Na}^+]_o$ may influence the intracellular pH via the Na^+/H^+ exchanger, but since $[\text{Na}^+]_o$ was reduced by only 10–60% and Li^+ was the substitute, the effect on pH is expected to be negligible.^{29,30}

Finally, TEA blocks the K^+ outward currents, I_{K} and $\text{I}_{\text{K}2}$ ^{12,13} that are prominent in rat heart and responsible for the short duration of the action potential. Therefore, TEA lengthened the action potential and presumably allowed for a longer-lasting, and hence a greater total, influx of Ca^{2+} , which explains the associated increase in peak force. It is remarkable that despite their different mode of action, all interventions at the level of the sarcolemma led to approximately the same (within $\pm 5\%$) maximum force (Figures 3–5). Furthermore, in the case of high $[\text{Ca}^{2+}]_o$ and low $[\text{Na}^+]_o$ the action potential was slightly shortened,^{7,9} whereas action potential duration continued to increase even when peak force declined with further addition of K^+ or TEA (Figures 4 and 5). Thus, it appears that the F_{max} was not related to action potential duration and was almost independent of the type of intervention on the $\text{Na}^+/\text{Ca}^{2+}$ exchanger (influx facilitation with high $[\text{Ca}^{2+}]_o$, inhibition of efflux with low $[\text{Na}^+]_o$). It is concluded that mechanisms in the sarcolemma (i.e., the action potential, I_{Ca} , and $\text{Na}^+/\text{Ca}^{2+}$ exchange) may be responsible for the $\pm 5\%$ variation in F_{max} . Apparently, the main limiting factor is in a later step in excitation-contraction coupling.

Sarcoplasmic Reticulum

Postextrasystolic potentiation. A simple method to test the capacity of the reticulum is postextrasystolic potentiation. The current explanation for this phenomenon is as follows^{15,21,22}: Recovery of the release mechanism in the reticulum is slow, and therefore, an extra stimulus after a very short interval elicits the release of only a small amount of Ca^{2+} , and the extrasystole is small. The influx of Ca^{2+} via I_{Ca} , however, is enhanced during the extrasystole.^{7,23} This combination of reduced release and enhanced influx causes accumulation of extra Ca^{2+} in the reticulum and potentiation of the next beat after a normal interval. Thus, maximum potentiation is probably a good indicator for the capacity of the reticulum to accumulate Ca^{2+} . The maximum force obtained with this method was remarkably similar to that obtained with optimum $[\text{Ca}^{2+}]_o$, $[\text{Na}^+]_o$, $[\text{K}^+]_o$, and $[\text{TEA}]_o$ (Figures 2–5). Hence, in all four cases the limiting factor was probably the capacity of the reticulum, or as proposed previously,^{4,6} spontaneous release occurs when the accumulated Ca^{2+} exceeds a certain level. Because replenishment of the releasable Ca^{2+} store takes time, the amplitude of stimulated contractions is reduced by the preceding spontaneous releases. In accordance with this hypothesis, aftercontractions (Figure 3) and a decline in force (Figures 2–5) occurred at supramaximal Ca^{2+} loading.

Influence of Sr^{2+} . Sr^{2+} can replace Ca^{2+} in at least two mechanisms. First, Sr^{2+} serves as a charge carrier for the current through the Ca^{2+} channels in the sarcolemma (I_{Ca}) but slows the inactivation of this current.^{18,28,34} This explains the prolonged action potential (Figure 9A). Second, Sr^{2+} is a potent activator of sarcomere contraction,^{35,36} with the same affinity for the contractile system as Ca^{2+} ,³⁷ which in combination with the prolonged action potential explains enhanced force. On the other hand, there is evidence that Sr^{2+} is not stored in the sarcoplasmic reticulum. First, when external Ca^{2+} was replaced by Sr^{2+} , peak force was delayed and relaxation was slowed (Figure 9A). Such slow contractions may occur under various conditions and indicate that part of the contraction is due to direct activation by Sr^{2+} (or Ca^{2+}) influx and not to release from the sarcoplasmic reticulum.^{25,27,38} Furthermore, ryanodine, which inhibits Ca^{2+} channels in the sarcoplasmic reticulum, greatly reduces contraction in the presence of Ca^{2+} but not when Ca^{2+} has been replaced by Sr^{2+} .^{18,39} Thus, there is reason to assume that Sr^{2+} is not transported by the sarcoplasmic reticulum and that, in the presence of 1 mM Ca^{2+} , activation of the sarcomeres occurs via two parallel paths: release of Ca^{2+} from the sarcoplasmic reticulum and influx of Sr^{2+} from the extracellular space. It should be noted that Sr^{2+} did not block Ca^{2+} transport by the sarcoplasmic reticulum, since the early component of contraction was not abolished, and rapid stimulation induced aftercontractions (Figure 9B).

We conclude that F_{max} is determined by the capacity of the sarcoplasmic reticulum, and force can exceed F_{max} (Figures 8 and 10) because Sr^{2+} circumvents this limiting factor.

Caffeine and ryanodine. These two drugs caused slowing of twitch relaxation and abolished postextrasystolic potentiation, indicating that the reticulum was effectively abolished as a functional Ca^{2+} store. Caffeine, however, has multiple effects, and recent reports suggest that it may affect the sensitivity of the sarcomeres to Ca^{2+} .^{19,21} The variable amplitude of contractures and tetanic contractions obtained with caffeine (see "Results") may be related to the complexity of the effects and precludes firm conclusions in the present context.

Ryanodine suppresses reticulum function in a much more selective way than caffeine does.^{18,19,40} Therefore, after ryanodine treatment, activation of the sarcomeres presumably depends entirely on Ca^{2+} influx from the extracellular space. The slow relaxation causes summation of contractions (tetanic contractions) at high frequencies of stimulation and $[\text{Ca}^{2+}]_o$, which is expected to lead to saturation of the sarcomeres.⁴⁰ Our results partly support this idea. In HEPES-buffered solution with 8–12 mM $[\text{Ca}^{2+}]_o$, maximum force of tetani was $(1.1 \pm 0.17) \times F_{\text{max}}$, that is, greater than the maximum effect of various other interventions (e.g., Figure 7) but some 20% lower than the maximum at high $[\text{Sr}^{2+}]_o$ in bicarbonate-buffered solution. Two types of complications may be mentioned. 1) The transition to HEPES-containing solution led to a transient increase in force, which was presumably due to a transient increase in pH, and the associated increase in the sensitivity of the sarcomeres to Ca^{2+} .⁴¹ Steady-state pH, was probably normal, however, and tests with $[\text{Ca}^{2+}]_o$ and postextrasystolic potentiation showed that F_{max} was unchanged (Figure 7). 2) Ryanodine-treated muscles always developed substantial diastolic force, which may have imposed an extra load on energy metabolism and caused accumulation of metabolites and acidosis. Furthermore, the continuous elevation of intracellular $[\text{Ca}^{2+}]$ probably inactivates I_{Ca} . This second group of complications is supported by the observations that the tetanic contraction reached a peak within a few seconds and then decreased, and in one preparation a steep increase in diastolic force at 12 mM $[\text{Ca}^{2+}]_o$ was accompanied by a decrease in the amplitude of the tetanic contraction. Nevertheless, the ryanodine results support our hypothesis that force can exceed F_{max} if the reticulum is abolished as a limiting factor.

Isoproterenol. Stimulation of β -adrenoceptors leads 1) to enhanced I_{Ca} ,²² which explains the lengthened action potential; 2) to faster sequestration of Ca^{2+} by the reticulum, which accounts for shortening of twitch duration^{16,42}; and 3) to a decrease in the sensitivity of the sarcomeres to Ca^{2+} .^{43,44} Enhanced Ca^{2+} uptake by the reticulum implies that a smaller fraction of the released Ca^{2+} is extruded from the cell via $\text{Na}^+/\text{Ca}^{2+}$ exchange because the two mechanisms

compete. Both the reduced loss of Ca^{2+} per beat and the increased influx via I_{Ca} explain the positive inotropic effect of isoproterenol.

We found that maximum force at the optimum $[\text{isoproterenol}]_0$ was 20% below the F_{max} obtained with optimum $[\text{Ca}^{2+}]_0$ and various other means. This was not simply due to saturation of the β -receptors because the action potential duration at 50% of the amplitude continued to increase with isoproterenol concentration. Rather, the drug introduced a new, lower maximum level of force, and at optimum $[\text{isoproterenol}]_0$ postextrasystolic potentiation (Figure 6) and elevation of $[\text{Ca}^{2+}]_0$ (not shown) failed to enhance force above $0.8 \times F_{\text{max}}$. This remarkable finding can be explained from rapid uptake of Ca^{2+} by the sarcoplasmic reticulum or reduced sensitivity of the sarcomeres to Ca^{2+} . The first explanation implies that the Ca^{2+} pump in the reticulum, when stimulated by isoproterenol, sequesters a fraction of the released Ca^{2+} before it reaches the sarcomeres. According to the second explanation, the same amount of Ca^{2+} will be less effective when the sensitivity of the sarcomeres is reduced. Therefore, if the maximum amount of releasable Ca^{2+} is constant, both mechanisms decrease the associated maximum force to below F_{max} .

Sarcomeres

The force produced at a given level of intracellular Ca^{2+} (and Sr^{2+}) is determined by the affinity of the sarcomeres to Ca^{2+} (and Sr^{2+}) and on the maximum effect of saturation. There is evidence for effects of β -adrenoceptor stimulation on sarcomere affinity, probably via cyclic AMP-dependent phosphorylation of the inhibitory component of troponin.^{43,44} This may have contributed to the decrease in maximum force at optimum $[\text{Ca}^{2+}]_0$ and postextrasystolic potentiation (Figure 6). Nevertheless, the enhanced relaxation of both force and intracellular Ca^{2+} transient suggests a prominent role of enhanced sequestration by the reticulum in the reduction of maximum force.

Caffeine may affect both properties of the sarcomeres: it increases the affinity but reduces maximum force at saturating levels of Ca^{2+} .^{19,21} These complications, in addition to the effects on reticulum function, may explain the variability of the caffeine results but render the interpretation difficult.

Ryanodine has no direct influence on the sarcomeres so that its primary effect mainly, or exclusively, concerns abolition of the reticulum as a limiting step in Ca^{2+} availability. Thus, maximum force in ryanodine-treated muscles may reflect Ca^{2+} saturation of unchanged sarcomeres. As argued above, the extreme rate of energy turnover during the tetanic contractions, however, may have caused intracellular acidosis and inorganic phosphate accumulation, which is known to depress force production.^{45,46} This might have influenced the results, although we used thin trabeculae in which diffusion of metabolites is normally adequate.⁴⁷ As a consequence, tetanic con-

tractions may lead to underestimation of force in maximally activated sarcomeres.

Force-sarcomere length relations. The force-sarcomere length relations in Figure 10 at different $[\text{Ca}^{2+}]_0$ s are similar to those reported by ter Keurs et al⁸ and Gordon and Pollack.²³ It has been proposed earlier that F_{max} in intact myocardium corresponds to some 70% saturation of the sarcomeres because greater force could be induced in skinned myocytes¹ and skinned trabeculae² of rat heart. According to percentages, the difference in maximum force between skinned and intact preparations increased at shorter sarcomere lengths, and Figure 10 shows the same: in the presence of Sr^{2+} , maximum force increased by 15% at 2.2 μm and by more than 100% at 1.6 μm . This obviates the possible criticism that the greater force in skinned preparations could be an artifact of the skinning procedure and supports Fabiato's¹ hypothesis that under "normal" conditions saturation of the sarcomeres does not occur in intact preparations. The exception is that abolition of the reticulum as a limiting factor apparently does allow for full activation of the sarcomeres, the ultimate limit of force production. It should be noted that saturation with Sr^{2+} caused 10% greater force in skinned fibers than did saturation with Ca^{2+} .³⁵ We conclude that maximum Ca^{2+} -activated force is between the values obtained with ryanodine and Sr^{2+} , that is, between 1.1 and 1.3 of F_{max} .

In conclusion, F_{max} obtained at optimum $[\text{Ca}^{2+}]_0$, $[\text{Na}^+]_0$, $[\text{K}^+]_0$, $[\text{TEA}]_0$, and postextrasystolic potentiation was shown to depend mainly on the capacity of the reticulum to store Ca^{2+} . Maximum activation of the sarcomeres was possible when the reticulum was abolished as a limiting factor with high $[\text{Sr}^{2+}]_0$ and ryanodine. The force-sarcomere length relation was then similar to that in skinned fibers at maximal Ca^{2+} activation. The isoproterenol results suggest that a reduced affinity of the sarcomeres to Ca^{2+} and rapid uptake of Ca^{2+} by the reticulum decreased the contractile response to the maximum amount of released Ca^{2+} .

References

1. Fabiato A: Myoplasmic free calcium concentration reached during the twitch of an intact isolated cardiac cell and during calcium-induced release of calcium from the sarcoplasmic reticulum of a skinned cardiac cell from the adult rat or rabbit ventricle. *J Gen Physiol* 1981;78:457-497
2. Kentish JC, ter Keurs HEDJ, Ricciardi L, Bucx JJJ, Noble MIM: Comparison between the sarcomere length-force relations of intact and skinned trabeculae from rat right ventricle: Influence of calcium concentrations on these relations. *Circ Res* 1986;58:755-768
3. Fabiato A, Fabiato F: Contraction induced by a calcium triggered release of calcium from the SR of skinned cardiac cells. *J Physiol (Lond)* 1975;249:469-495
4. Allen DG, Eisner DA, Pirolo JS, Smith GL: The relationship between intracellular calcium and contraction in calcium-overloaded ferret papillary muscles. *J Physiol (Lond)* 1985; 364:169-182
5. Mulder BJM, de Tombe PP, ter Keurs HEDJ: Spontaneous and propagated contractions in rat cardiac trabeculae. *J Gen Physiol* 1989;93:943-961

6. Kort AA, Lakatta EG: Spontaneous sarcoplasmic reticulum calcium release in rat and rabbit cardiac muscle: Relation to transient and rested-state twitch tension. *Circ Res* 1988; 63:969-979
7. Schouten VJA: The relationship between action potential duration and force of contraction in rat myocardium. *Eur Heart J* 1984;5:984-992
8. ter Keurs HEDJ, Rijnsburger WH, Van Heuningen R, Nagelsmit MJ: Tension development and sarcomere length in rat cardiac trabeculae. *Circ Res* 1980;46:703-714
9. Schouten VJA, ter Keurs HEDJ: The slow repolarization phase of the action potential in rat heart. *J Physiol (Lond)* 1985;360:13-25
10. Sheu S-S, Fozzard HA: Transmembrane Na^+ and Ca^{2+} electrochemical gradients in cardiac muscle and their relationship to force development. *J Gen Physiol* 1982;80:325-351
11. Chapman RA, Coray A, McGuigan JAS: Sodium/calcium exchange in mammalian ventricular muscle: A study with sodium-sensitive micro-electrodes. *J Physiol (Lond)* 1983; 343:253-276
12. Ito S, Surawicz B: Effect of tetraethylammonium on action potential in cardiac Purkinje fibers. *Am J Physiol* 1981; 241:H139-H144
13. Kass RS, Scheuer T, Malloy KJ: Block of outward current in cardiac Purkinje fibers by injection of quaternary ammonium ions. *J Gen Physiol* 1982;79:1041-1063
14. Morad M, Rollett EL: Relaxing effects of catecholamines on mammalian heart. *J Physiol (Lond)* 1972;224:537-558
15. Wohlfart B, Noble MIM: The cardiac excitation-contraction cycle. *Pharmacol Ther* 1982;16:1-43
16. Kurihara S, Konishi M: Effects of beta-adrenoceptor stimulation on intracellular Ca transients and tension in rat ventricular muscle. *Pflügers Arch* 1987;409:427-437
17. Sutko JL, Willerson JT: Ryanodine alteration of the contractile state of rat ventricular myocardium: Comparison with dog, cat, and rabbit ventricular tissues. *Circ Res* 1979;46:332-343
18. Mitchell MR, Powell T, Terrar DA, Twist VW: Electrical activity and contraction in cells isolated from rat and guinea pig ventricular muscle: A comparative study. *J Physiol (Lond)* 1987;391:527-544
19. Hilgemann DW, Roos KP, Brady AJ: Slowly relaxing caffeine responses in rat ventricle: Relationships of ryanodine and caffeine actions. *Am J Physiol* 1989;256:H1100-H1109
20. Nieman CJ, Eisner DA: Effects of caffeine, tetracaine, and ryanodine on calcium-dependent oscillations in sheep cardiac Purkinje fibers. *J Gen Physiol* 1985;86:877-889
21. Kitazawa T: Caffeine contracture in guinea pig ventricular muscle and the effect of extracellular sodium ions. *J Physiol (Lond)* 1988;402:703-729
22. Trautwein W, Cavalié A, Flockerzi V, Pelzer D: Modulation of calcium channel function by phosphorylation in guinea pig ventricular cells and phospholipid bilayer membranes. *Circ Res* 1987;61(suppl 1):I-17-I-23
23. Gordon AM, Pollack GH: Effects of calcium on the sarcomere length-tension relation in rat cardiac muscle: Implications for the Frank-Starling mechanism. *Circ Res* 1980;47:610-619
24. ter Keurs HEDJ, Rijnsburger WH, Van Heuningen R: Restoring forces and relaxation of rat cardiac muscle. *Eur Heart J* 1980;1(suppl A):67-80
25. Reiter M: Calcium mobilization and cardiac inotropic mechanisms. *Pharmacol Rev* 1988;40:189-217
26. Carafoli E: The homeostasis of calcium in heart cells. *J Mol Cell Cardiol* 1985;17:203-212
27. Morad M, Cleemann L: Role of Ca^{2+} channel in development of tension in heart muscle. *J Mol Cell Cardiol* 1987;19:527-553
28. Mitchell MR, Powell T, Terrar DA, Twist VW: Characteristics of the second inward current in cells isolated from rat ventricular muscle. *Proc R Soc Lond* 1983;B219:447-469
29. Ellis D, MacLeod KT: Sodium-dependent control of intracellular pH in Purkinje fibres of sheep heart. *J Physiol (Lond)* 1985;359:81-105
30. Chapman RA: Sodium/calcium exchange and intracellular calcium buffering in ferret myocardium: An ion-sensitive micro-electrode study. *J Physiol (Lond)* 1986;373:163-179
31. Yue DT, Burkhoff D, Franz MR, Hunter WC, Sagawa K: Postextrasystolic potentiation of the isolated left ventricle. *Circ Res* 1985;56:340-350
32. Schouten VJA, van Deen JK, de Tombe P, Verveen AA: Force-interval relationship in heart muscle of mammals: A calcium compartment model. *Biophys J* 1987;51:13-26
33. Tseng G-N: Calcium current restitution in mammalian ventricular myocytes is modulated by intracellular calcium. *Circ Res* 1988;63:468-482
34. Vereecke J, Carmeliet E: Sr action potentials in cardiac Purkinje fibres: I. Evidence for a regenerative increase in Sr conductance. *Pflügers Arch* 1971;332:60-72
35. Donaldson SKB, Best PM, Kerrick WGL: Characterization of the effects of Mg^{2+} on Ca^{2+} - and Sr^{2+} -activated tension generation of skinned rat cardiac fibers. *J Gen Physiol* 1978; 71:645-655
36. Yamamoto K: Sensitivity of actomyosin ATPase to calcium and strontium ions: Effect of hybrid troponins. *J Biochem* 1983;93:1061-1069
37. Babu A, Scordilis SP, Sonnenblick EH, Gulati J: The control of myocardial contraction with skeletal fast muscle troponin C. *J Biol Chem* 1987;262:5815-5822
38. King BW, Bose D: Mechanism of biphasic contractions in strontium treated ventricular muscle. *Circ Res* 1983;52:65-75
39. Kondo N: Can strontium replace calcium as an activator of internal calcium release in cardiac muscles? A study on a dual action of A23187. *J Mol Cell Cardiol* 1987;19:391-397
40. Marban E, Kusaka H, Yue DT, Weisfeldt ML, Wier WG: Maximal Ca^{2+} -activated force elicited by tetanization of ferret papillary muscle and whole heart: Mechanism and characteristics of steady contractile activation in intact myocardium. *Circ Res* 1986;59:262-269
41. Allen DG, Orchard CH: The effects of pH on intracellular calcium transients in mammalian cardiac muscle. *J Physiol (Lond)* 1983;335:555-567
42. Beekman RE, Van Hardeveld C, Simonides WS: On the mechanism of the reduction by thyroid hormone of β -adrenergic relaxation rate stimulation in rat heart. *Biochem J* 1989;259:229-236
43. Solaro RJ, Rapundalo ST, Garvey JL, Kranias EG: Mechanics of cardiac contraction and the phosphorylation of sarcotubular and myofibrillar proteins, in ter Keurs HEDJ, Tyberg JV (eds): *Mechanics of the Circulation*. Boston, Martinus Nijhoff Publishing, 1987, pp 135-152
44. Winegrad S: Regulation of cardiac contractile proteins: Correlations between physiology and biochemistry. *Circ Res* 1984; 55:565-574
45. Fabiato A, Fabiato F: Effects of pH on the myofibrillar and the sarcoplasmic reticulum of skinned cells from cardiac and skeletal muscles. *J Physiol (Lond)* 1978;276:233-255
46. Kentish JC: The effects of inorganic phosphate and creatine phosphate on force production in skinned muscles from rat ventricle. *J Physiol (Lond)* 1986;370:585-604
47. Schouten VJA, ter Keurs HEDJ: The force-frequency relationship in rat myocardium: The influence of muscle dimensions. *Pflügers Arch* 1986;407:14-17

KEY WORDS • sarcomere length • calcium • strontium • isoproterenol • ryanodine

CHAPTER 7

HIGH-ENERGY PHOSPHATE METABOLISM IN NORMOXIC AND HYPOXIC TRABECULAE AND NORMOXIC PAPILLARY MUSCLES FROM RAT HEART.

Jeroen JJ Buxx, Peter W Achterberg, A Selma Nieukoop, Tin Nguyen,
Vincent JA Schouten, Jan W de Jong, Henk EDJ ter Keurs

Preliminary results of this work have been published previously in the forms of abstracts:

Achterberg PW, Buxx JJJ, de Jong JW, ter Keurs HEDJ, Nieukoop AS, Schouten VJA. High-energy phosphate metabolism and force production in normoxic and ischemic rat cardiac trabeculae and papillary muscle. *J Physiol* 1985; 366: 85P

Achterberg PW, Buxx JJJ, AS Nieukoop, JW de Jong, ter Keurs HEDJ. High-performance liquid chromatography of high-energy phosphates in isolated normoxic and hypoxic cardiac trabeculae. *Int J Pur Pyr Res* 1990; 1: 25-29

HIGH-ENERGY PHOSPHATE METABOLISM IN NORMOXIC AND HYPOXIC TRABECULAE AND NORMOXIC PAPILLARY MUSCLES FROM RAT HEART.

Jeroen JJ Buxx, Peter W Achterberg, A Selma Nieukoop, Tin Nguyen, Vincent JA Schouten, Jan W de Jong, Henk EDJ ter Keurs

ABSTRACT

High-energy phosphate concentrations (HEP) in trabeculae (T) and papillary muscles (P) from rat heart were measured by means of high pressure liquid chromatography (HPLC) and related to performed work during normoxia (N) and hypoxia without flow (H). Force (F) was measured with a strain gauge, sarcomere length (SL) with laser diffraction techniques. Performed work was expressed as force-frequency product (FFP). In normoxic T, both CrP and ATP decreased with increasing FFP. Mean [PCr], [ATP] and [ADP] was 5.1, 3.2 and 0.6 mmol/l, or 32.6, 19.5 and 4.2 μ mol/g protein. Mean [HEP] of papillary muscles was lower than normoxic T when expressed in mmol/l and higher when expressed in μ mol/g protein. At 3.3 Hz, FFP was 2.2 and [ATP] was lower than in normoxic T at the same FFP. [AMP] in P increased with muscle diameter, independent of FFP.

Hypoxia of T was induced by interrupting flow of hypoxic, glucose-free medium; this resulted in stimulus rate dependent decrease of active F and increase of unstimulated F. Resting SL and sarcomere shortening decreased. At maximal unstimulated F, SL did not change upon release of the muscle. [PCr] and [ATP] were about 40% of control.

In conclusion [HEP] can be measured with HPLC techniques in isolated cardiac muscle and related to sarcomere mechanics. [HEP] decreased both in P and T with increasing work load, although in P at a lower FFP; this is consistent with inadequate oxygenation of the core of larger muscle preparations. H of T resulted in rate dependent decrease of twitch force and increased unstimulated F due to rigor, in presence of [PCr] and [ATP] that were 40 % of control levels.

INTRODUCTION

Isolated papillary muscles and trabeculae have been frequently used to study mechanical and electrophysiological properties of cardiac muscle^{1,22,25}. The results of such studies may ultimately be extrapolated to the heart in vivo. Energy-rich phosphates, like adenine nucleotides and creatine phosphate (PCr), are required for all cell functions during normoxia¹⁸. Likewise, recovery of myocardial performance following ischemia is closely related to high-energy phosphate content as has been shown in human heart³⁶, isolated dog heart³² and cultured heart cells¹¹.

It has been reported that contractility of heart muscle preparations decreases after isolation³⁹. This phenomenon is most outspoken when preparations are stimulated at higher rates. It may be related to restricted oxygen diffusion, leading to insufficient oxygen availability, which ultimately leads to impaired oxydative phosphorylation and decreased force of supposedly normoxic muscles^{7,13,26}. As a result of their larger dimensions papillary muscles are more likely to show this phenomenon, in contrast with trabeculae that would be expected to be well oxygenated even at higher stimulus rates.

The concentrations of ATP, ADP and PCr have been measured in papillary muscles, however these measurements were not always correlated with mechanical function^{23,28,29}.

The purpose of this study therefore was to analyse high-energy phosphate metabolism in normoxic papillary muscles and normoxic and hypoxic trabeculae at varied stimulus rates, and to relate this to mechanics of the same preparations.

Our results show that contractility of thin, superfused trabeculae is maintained upto a force frequency product of 4.5 at decreased PCr and ATP concentrations. In contrast, papillary muscles only

attained a force frequency product of 2.2 when ATP content was decreased, which is compatible with impaired oxygen availability in the latter preparations.

Moreover we show that trabeculae develop rigor tension following hypoxia without flow at levels of PCr and ATP, that are still 40% of control.

METHODS

Preparation of trabeculae and papillary muscles

Wistar rats of either sex (200-300 gram) were anesthetized with diethylether. The hearts were quickly removed and the aorta was retrogradely perfused according to the Langendorff technique with a Krebs-Henseleit solution (11 mM glucose, 1.5 mM Ca^{2+} , pH 7.35, 20 °C), which was oxygenated with a gasmixture of 95% O_2 and 5% CO_2 . The pO_2 in this solution was 550 mm Hg. Uniform, unbranched trabeculae and papillary muscles were dissected from the right ventricle. The sample dimensions were measured with the micrometer in the objective of the dissection microscope. The dimensions of the trabeculae were (mm): length 3.03 ± 1.13 mm, width 0.44 ± 0.27 , thickness 0.13 ± 0.05 mm ($n = 49$; mean \pm S.D.). Those of the papillary muscles, which were usually tapered, were (mm): length 3.97 ± 1.96 , width 0.83 ± 0.31 , thickness 0.57 ± 0.32 ($n = 19$). The volume of the samples was calculated from their dimensions.

After mounting in a muscle chamber (content 500 μl) the trabeculae were superfused with Krebs-Henseleit medium at constant temperature (30 °C) and flow (6 ml/min). Since the bottom and cover of the bath were made of glass, laser diffraction techniques could be used to measure sarcomere length (SL) (22). Force was measured with a silicon strain gauge (AME AE 801). Both force and SL were recorded on a chart recorder (Gould Brush 2800). The preparations were stimulated by platinum electrodes, that were embedded in the chamber walls (pulsewidth 5 msec, stimulus strength 10 volts).

Stimulus protocol

The trabeculae were stimulated at 1.0 Hz during 1 hour at constant muscle length in order to certify stable mechanical characteristics. Thereafter either normoxia was continued during another 60 minutes at a stimulus rate of 1.0, 2.0 or 3.3 Hz, or hypoxia was induced (see below) and stimulation continued (at 1.0, 2.0 or 3.3 Hz) until unstimulated force reached its maximum. At the end of the experiment the remnants of the right ventricular free wall and the tricuspid valve were quickly removed from the preparation. Subsequently, the preparation was sucked into a modified plastic Pasteur pipette equipped with a pre-washed glass wool plug. Within 2 - 4 seconds the muscle was transferred to liquid nitrogen and stored until further analysis.

The papillary muscles were mounted in an open muscle chamber, that was perfused at a flow of 12 ml/min either at 26.5 ± 0.3 or 30 ± 0.2 °C. The Krebs-Henseleit buffer for these muscles contained 2.5 or 1.5 mM Ca^{2+} . The preparations were stimulated at 1.0 Hz for 1 hour at constant muscle length. During the next hour the stimulus rate was either kept constant or changed to 0.1 or 3.3 Hz for the preparations at 26 °C or increased to 3.3 Hz for the muscles at 30 °C. At the end of the experiment the papillary muscles were treated as described for the trabeculae and stored in liquid nitrogen until further analysis.

Performed work expressed as force-frequency product

The relation between performed work and [HEP] was analyzed in normoxic trabeculae and papillary

muscles. Performed work was expressed as a force-frequency product as follows. Following the change in stimulus rate after the first hour, force attained a stable level within 5 minutes. Then, force was expressed as a percentage of control force at 1 Hz and multiplied by the frequency of stimulation to obtain the force-frequency product.

Hypoxia in trabeculae

Prior to an hypoxia experiment, the setup was covered with a hood, that was flushed with a gasmixture of 95% N₂ and 5% CO₂ in order to eliminate possible exchange of oxygen between the fluid in the muscle bath and ambient air. Hypoxia was induced by changing from control Krebs-Henseleit solution to a glucose-free medium, that was in equilibrium with 95% N₂ and 5% CO₂ (pO₂ 5 - 9 mm Hg). Subsequently flow was stopped within one minute after the switch.

Sample preparation for biochemical analysis

The frozen specimen was added to 500 µl of frozen 0.4 M perchloric acid in a precooled (liquid nitrogen) Teflon cup of a Mikro-dismembrator (Braun, Melsungen, BFR). A precooled Teflon marble was added and the acid mixture was shaken at 50 Hz for 60 seconds. Next the frozen homogenate was transferred to a centrifuge tube, that had been weighed before to allow exact determination of the weight of the sample. After thawing and centrifugation (Eppendorf 54148 microcentrifuge, 12,000 rpm, 2 min, 5 C), the supernatant fluid was neutralized (final pH 5 to 7, 0 C) with a mixture of 2 M KOH and 1 M K₂CO₃. KClO₄ was removed by centrifugation and the supernatant was used for HPLC determination of high-energy phosphates. Adenine nucleotide and PCr concentrations were expressed in mmol/l of muscle volume and µmol/g protein (see below).

Protein determination

The protein pellet, which remained after as much as possible of the acid supernatant of the centrifuged mixture was removed, was dissolved in 1 ml 0.3 M KOH solution (20 C, 60 min). After centrifugation, 100 µl of the supernatant fluid was used for protein determination (Biorad Protein Assay; Biorad, Munich, GFR)⁶. Bovine serum albumin (BSA, 100 µl; 5 µg) was treated like samples in order to determine protein recovery in the procedure. The procedure allowed detection of at least 2 µg protein per muscle sample. The volume of all preparations that were available for biochemical analysis, was calculated from their dimensions and ranged from 20 to 18000 nl (median 240 nl; n = 55). The amount of protein in the preparations varied between 2.6 and 2062.9 µg (median 32.7; n = 52). The relation between protein content and volume of all trabeculae and papillary muscles, where both parameters were available, was $P = 0.05 * V + 26.3$ ($r = 0.938$) where P represents protein in µg and V = volume in nl. The protein - volume relation of the trabeculae was $P = 0.11 * V + 14.1$ ($r = 0.72$). The difference of the regression coefficients of both relationships was not significant.

Determination of high-energy phosphates

ATP, ADP, AMP and PCr were determined by HPLC with slight modifications of the method of Harmsen et al.¹⁰. Samples (200 µl) were injected onto a Partisil-10-SAX ion-exchange column (Whatman, Maidstone, UK). The sample was eluted (flow: 2 ml/min) with a linear gradient of 100% 16 mM H₃PO₄ (adjusted to pH 2.85 with NH₄OH, Buffer A) to 100% 750 mM NH₄H₂PO₄ (pH 4.6, Buffer B) (30 min, Waters Model 660 solvent programmer, Waters Associates, Milford MA). After this gradient

the column was equilibrated (5 min) with 100% buffer B followed by a return gradient to 100 % buffer A (in 10 min), again followed by equilibration with 100% buffer A (15 min). Peaks were determined by UV light absorption (254 nm for ATP, ADP, AMP and 214 nm for PCr (Waters 440, 441 UV Monitors). Peak heights were compared with those of standards. Standards (high-energy phosphates plus BSA) were processed as muscles and recoveries were found to be ATP: $92 \pm 1\%$, ADP: $91 \pm 1\%$ and PCr: $92 \pm 5\%$ ($n = 26$; mean \pm S.E.M.). The minimum amounts of high-energy phosphates that could be detected were (in pmoles): ATP 20, ADP 15, PCr 20 and AMP 15. AMP could not be detected in normoxic trabeculae.

Chemicals

All chemicals were analytical grade. Water was purified with the Milli-Ro4/Milli-Q system (Millipore, Bedford, MA). Salts, acids and bases for buffers and media were from Merck (Darmstadt, GFR). Adenine nucleotides and creatine phosphate were obtained from Boehringer (Mannheim, GFR).

STATISTICS

Results are presented as means \pm standard error of the means, with n as the number of experiments, unless mentioned otherwise. When two means were compared, Student's unpaired t-test was used. Analysis of variance (two-way classification) followed by Bonferroni's method of correction for multiple comparison was used in all other cases. $P > 0.05$ was considered not significant (NS).

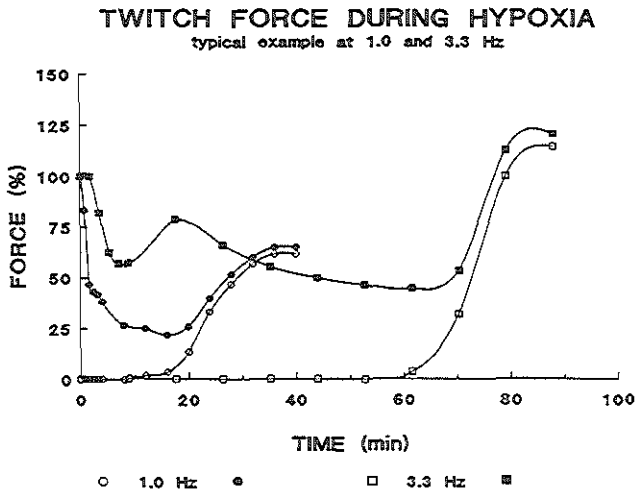


Figure 1: Contractile force and development of passive force in isolated ischemic trabeculae. Time course of total twitch force (closed symbols) and unstimulated force (open symbols) of two trabeculae, that were stimulated at 1 and 3.3 Hz during hypoxia without flow. Twitch force is expressed as a percentage of the twitch force prior to hypoxia.

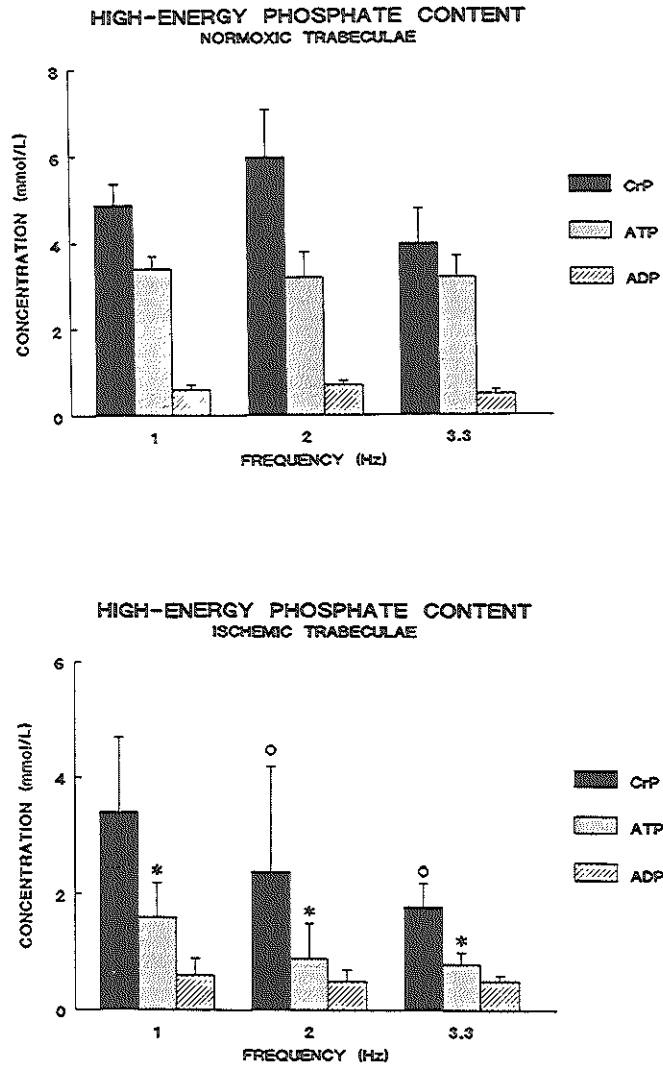


Figure 2: The top panel shows mean [PCr], [ATP] and [ADP], expressed as mmol/l muscle volume, in normoxic trabeculae that were stimulated during 60 minutes at 1 Hz and subsequently for another hour at 1, 2 or 3.3 Hz. The bottom panel shows mean [HEP] in hypoxic trabeculae at the moment when unstimulated force had reached its maximum. The figures under the bars indicate the frequency of stimulation. * denotes $p < 0.05$ versus normoxic trabeculae that were stimulated at the same frequency.

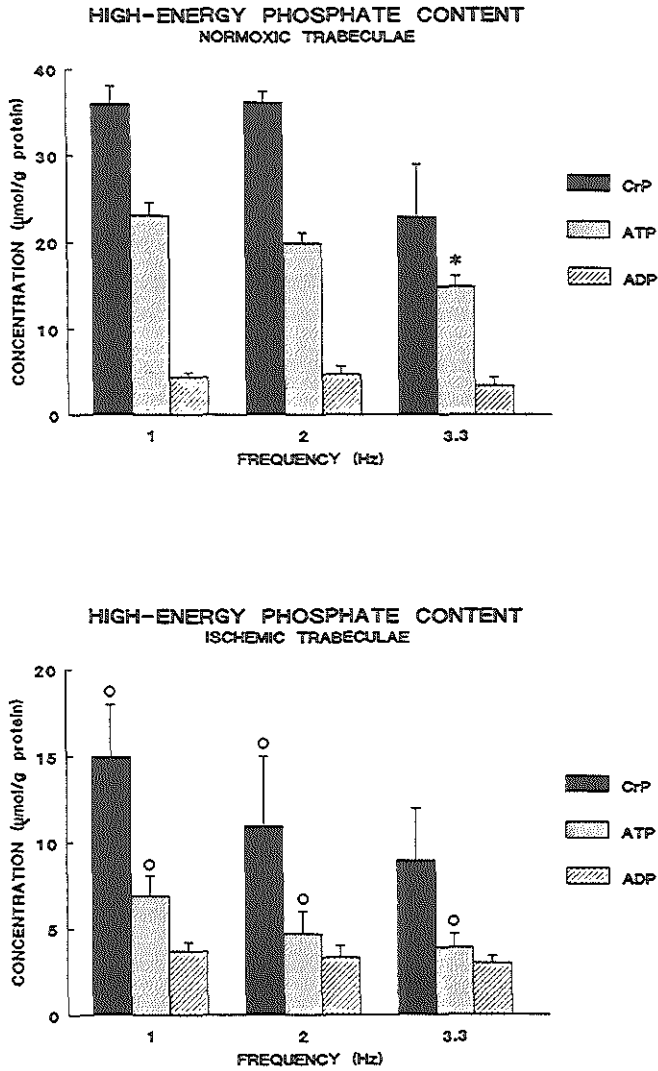


Figure 3: The top pannel shows mean [PCr], [ATP] and [ADP], expressed as $\mu\text{mol/g protein}$, in normoxic trabeculae that were stimulated during 60 minutes at 1 Hz and subsequently for another hour at 1, 2 or 3.3 Hz. The bottom pannel shows mean [HEP] in hypoxic trabeculae at the moment when unstimulated force had reached its maximum. The figures under the bars indicate the frequency of stimulation. * denotes $p < 0.05$ versus normoxic trabeculae that were stimulated at the same frequency.

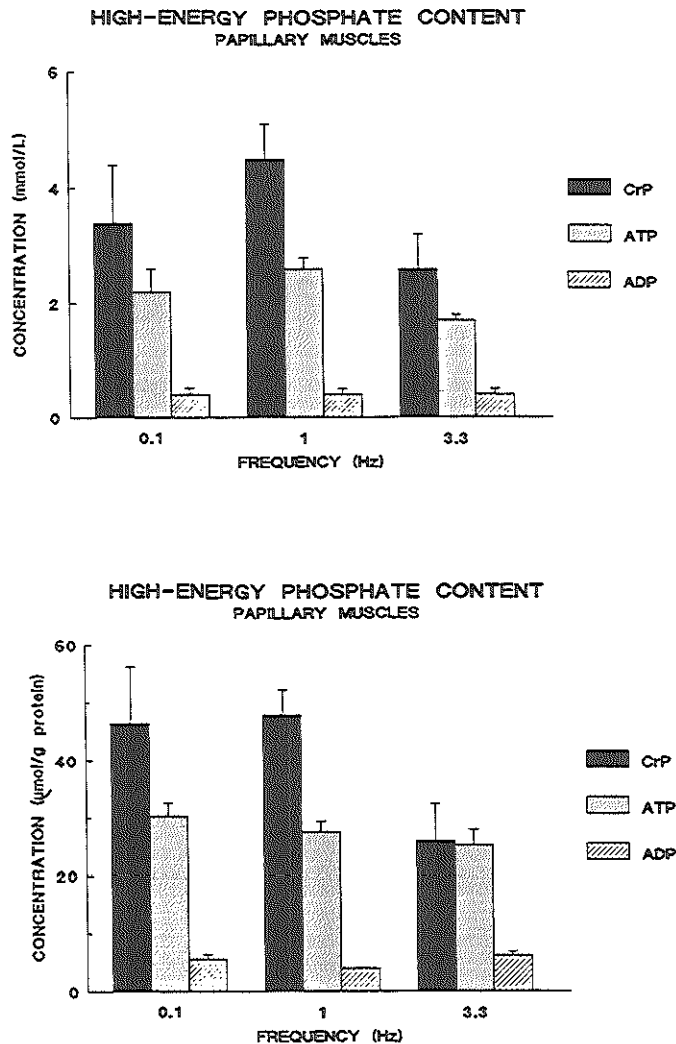


Figure 4: High energy phosphate concentrations in papillary muscles. [PCr], [ATP] and [ADP] are expressed in mmol/l muscle volume in the top panel, and in $\mu\text{mol/g}$ protein in the bottom part of the figure. The figures under the bars indicate the frequency of stimulation. Papillary muscles were stimulated at 1 Hz for 60 minutes prior to any intervention. Thereafter, stimulation was continued for the next 60 minutes at the indicated stimulus frequencies. Next the papillary muscles were rapidly frozen and analyzed for content of high-energy phosphates (HEP) by HPLC. For further details see text.

RESULTS

Normoxic trabeculae

The concentrations of PCr, ATP and ADP in muscles (stimulus rate 1, 2 or 3.3 Hz) are shown in figure 2 and 3 / table I and II, expressed in mmol/L and in $\mu\text{mol/g}$ protein, respectively. The mean [PCr], [ATP] and [ADP] were 5.1 ± 0.5 , 3.2 ± 0.3 and 0.6 ± 0.1 mmol/L ($n = 19$), and 32.6 ± 2.2 , 19.5 ± 1.0 and 4.2 ± 0.5 $\mu\text{mol/g}$ protein, respectively ($n = 18-19$). The mean ATP/ADP ratio for all normoxic trabeculae was 5.6 ± 0.44 ($n = 19$), independent of stimulus frequency. [PCr] and [ATP], expressed in $\mu\text{mol/g}$ protein, declined with increasing stimulus rate ($p < 0.04$ and $p < 0.001$, respectively), whereas [ADP] did not vary with stimulus rate. [HEP] (mmol/L) was independent of stimulus frequency.

Hypoxic trabeculae

Hypoxia followed by interruption of flow resulted in a rapid decline of active force and concomitant slow increase of unstimulated force. This pattern evolved more rapidly during continued perfusion with hypoxic glucose-free medium. Figure 1 shows the time course of active and unstimulated force of two representative trabeculae, that were stimulated at 1 and 3.3 Hz, respectively. Maximal resting tension was attained after 88 and 40 minutes of hypoxia respectively. The average time to maximal unstimulated force decreased with increasing frequency of stimulation; it was 56 ± 11 minutes, 46 ± 5 minutes and 40 ± 2 minutes at 1, 2 and 3.3 Hz respectively ($n = 5$; N.S.). During the increase of unstimulated force, resting sarcomere length and sarcomere shortening decreased. At maximal unstimulated force, no further shortening of the sarcomeres was observed after release of the muscle.

HEP content in trabeculae at maximal hypoxic unstimulated force is shown in figure 2 and 3 / table I and II, expressed in mmol/L and $\mu\text{mol/g}$ protein. [ATP], expressed in mmol/L, decreased significantly ($p < 0.05$) whereas [CrP] and [ADP] remained unchanged. [PCr] and [ATP], expressed in $\mu\text{mol/g}$ protein, decreased significantly during hypoxia ($p < 0.0001$ both), whereas [ADP] was comparable to normoxic muscles; [HEP] during hypoxia was independent of stimulus rate. The [ATP]/[ADP] ratio declined to 2.1 ± 0.4 ($n = 19$; $p < 0.001$), independent of stimulus frequency.

Papillary muscles

Mean [HEP] of papillary muscles is shown in figure 4 / table III and appeared independent of stimulus frequency (0.1, 1 or 3.3 Hz), irrespective of the expression of HEP (ie in mmol/L or $\mu\text{mol/g}$ protein). Only [ATP] at 1 and 3.3 Hz (expressed in mmol/L) differed significantly ($p < 0.01$). The ATP/ADP ratio in the muscles that were stimulated at 3.3 Hz was significantly lower than at 1.0 Hz; the difference between muscles that were stimulated at 3.3 Hz and at 0.1 Hz almost reached significance, respectively ($p = 0.09$).

The average [HEP] (expressed in mmol/L) was comparable in papillary muscles and trabeculae at the same stimulus rate except for [ATP] and [ADP] that were significantly higher at 3.3 Hz in papillary muscles compared to trabeculae ($p < 0.05$). [HEP] expressed in $\mu\text{mol/g}$ protein in papillary muscles and trabeculae at the same stimulus frequency were not significantly different, except for [ATP] that was higher in trabeculae than papillary muscles at 3.3 Hz ($p < 0.01$).

The average concentrations of PCr, ATP and ADP in papillary muscles that were stimulated at 3.3 Hz (Ca^{2+} 1.5, 30 C; 60 minutes) were 57.9, 24.9 and 9.4 $\mu\text{mol/g}$ protein or 6.3, 2.7 and 1.0 mmol/L respectively. These concentrations were not significantly different from the values in papillary muscles that were paced at 0.1 Hz (26 C, Ca^{2+} 2.5 mMol/L).

Comparison of performed work and [ATP] in normoxic trabeculae and papillary muscles

Following an increase of the stimulus rate of normoxic trabeculae from 1 Hz to 2.0 or 3.3 Hz, the force-frequency product increased from 1 to 2.4 ± 0.1 ($n = 7$) and 4.6 ± 0.4 ($n = 5$) respectively ($p < 0.0001$). The force-frequency product of normoxic papillary muscles increased from 1.0 at steady state conditions to 2.2 ± 0.1 at a stimulus frequency of 3.33 Hz ($n = 9$; $p < 0.0001$); the average FFP of the papillary muscles at 30 C was 4.3 ± 0.3 ($n = 5$) which was significantly higher than papillary muscles that were paced at 26 C and not different from FFP of trabeculae at 3.3 Hz ($p < 0.001$ and N.S., respectively).

The relationship between [HEP] and the force-frequency product for both groups of preparations is shown in figure 4. In both groups [ATP] tended to decrease at higher FFP. [ATP] in the normoxic trabeculae was independent of the FFP. In contrast, [ATP] of papillary muscles tended to decrease at force-frequency product of 2.2; the mean [ATP] then was 1.7 ± 0.1 mmol/l ($n = 9$) which was significantly lower than trabeculae (3.2 ± 0.6 mmol/l; $n = 7$). Likewise [CrP] and [ADP] decreased significantly; when expressed in mmol/l only the decrease of [ATP] reached significance.

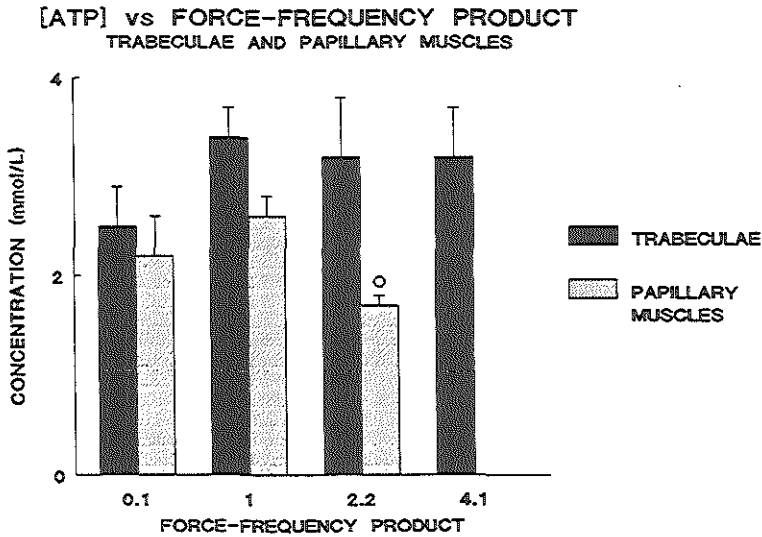


Figure 5: Relation between [ATP] and force frequency product. [ATP] expressed in mmol/l in normoxic trabeculae (closed bars) and papillary muscles (hatched bars) that were stimulated at varied frequencies. The numbers under the bars indicate the the force-frequency product (for explanation, see method section). The difference between [ATP] in trabeculae and papillary muscles with a force-frequency product of 2.2 was statistically significant ($p = 0.014$). Mean force-frequency product for the muscles stimulated at 0.1 Hz was 0.11 ± 0.01 ($n = 4$) and 2.2 ± 0.27 ($n = 5$) for the muscles stimulated at 3.3 Hz.

[AMP] vs Thickness of papillary muscles

The linear relation between [AMP] and papillary muscle thickness at force-frequency products of 2.2 ($n = 5$; pacing rate 3.3 Hz) and 0.11 ($n = 4$; pacing rate 0.1 Hz) is shown in figure 6 ($r = 0.69$). Despite the large variation in force-frequency products, all points seemed to fit the same linear relationship.

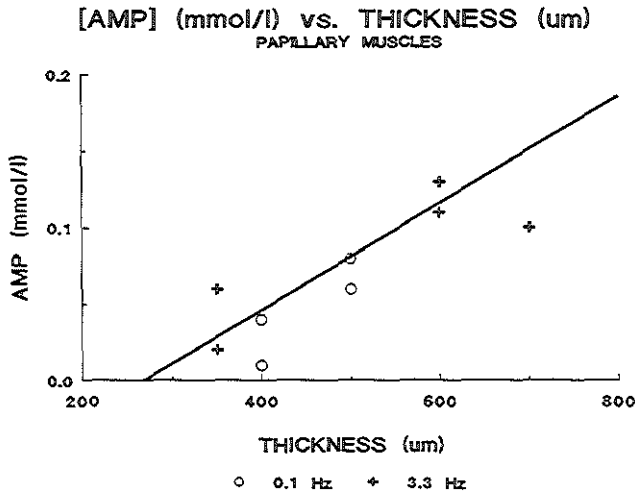


Figure 5: Relation between [AMP] and thickness of papillary muscle. [AMP] expressed in mmol/l muscle volume, in isolated papillary muscles that were stimulated (60 minutes) at 1 Hz and subsequently during 60 minutes at 0.1 Hz (circles; FFP 0.11) or 3.3 Hz (asterisk; FFP 2.2). The correlation coefficient for the regression line through all data point was 0.69 and the slopes for the regression lines through the data of muscles stimulated at different frequencies were not statistically different.

DISCUSSION

Trabeculae

Assuming a protein content of myocardial tissue between 15 and 17%^{14,27} one can recalculate data from literature and express [PCr], [ATP] and [ADP] in isolated rat heart in mmol/l and $\mu\text{mol/g}$ protein. Harmsen reported values of 4.6, 3.8 and 0.8 mmol/l, respectively¹⁷. Roberts measured [ATP] of 3.1 mmol/l in normoxic rat hearts whereas Zimmer reported [ATP] of 4.1 mmol/l^{31,28}. Dhalia reports PCr, ATP and ADP values of 6.7, 3.5 and 0.6 mmol/l⁸. Fossel measured PCr and ATP with NMR techniques and reported values of 5.1 and 4 mmol/l respectively¹². Piper reported [PCr] and [ATP] in isolated rat myocytes of 6 and 8.7 mmol/l²⁷. Morris reported [ATP] of 4.4 mmol/l in ferret heart²⁴. Our values of

[PCr], [ATP] and [ADP] in normoxic trabeculae are in the same range. Opie reported decreased [PCr] and [ATP] in Langendorff hearts when work load increased. We also observed significant changes in [ATP] and [PCr] trabeculae that were working at different force-frequency products²⁵. However apparently ATP production was sufficient to meet the consumption over a large range of force-frequency products and allowed stable mechanical force upto 2 Hz. Our data on the force-frequency relation in rat cardiac trabeculae are in agreement with the data reported by others³³.

Hypoxia of trabeculae

During hypoxia without flow, active force decreased gradually. Both the time when minimum force was reached and the time course of the changes in active force depended on the pacing frequency. In preparations stimulated at 1 Hz force decreased initially, followed by a temporary recovery, which was followed by a further decline. In some preparations we observed an increase in force immediately after the switch to glucose-free anoxic perfusate. This increase is consistent with transient intracellular alkalosis due to breakdown of PCr immediately after anoxia^{3,16}. The second transient recovery of force was less pronounced in presence of flow than without and decreased at higher stimulus rates. It is unlikely that this resulted from decrease of pH_i as a result of PCr breakdown since this occurs immediately following the switch to hypoxia. Alternatively, NMR studies have shown that free $[Ca^{2+}]_i$ is increased following 10 - 20 minutes of hypoxia; Allen and Orchard also reported that free diastolic $[Ca^{2+}]_i$ measured by luminescence of aequorin injected into superficial cells of papillary muscles, increased as a result of hypoxia⁴. The increased $[Ca^{2+}]_i$ may have resulted from accelerated Na^+/Ca^{2+} exchange as a result of decreased intracellular pH due to accumulation of lactate and phosphate ions³. Whether catecholamine release by the muscle or the onset of anaerobic glycolysis are related to it awaits further research².

Although Ca^{2+} overload may also be involved in the development of maximal unstimulated force, there are no data available on the dynamic properties of the muscles to support this hypothesis. Our observation that no further sarcomere shortening took place upon release of muscle at this stage may indicate possible rigor development but this awaits further validation.

It was striking that unstimulated force of trabeculae increased more rapidly when superfusion with oxygen-free medium was not interrupted (results not shown). This may be explained by a smaller decrease of pH_i, resulting in less inhibition of anaerobic glycolysis and actomyosin ATPases such that HEP stores were more rapidly depleted than during hypoxia without flow.

The procedure that was used to induce hypoxia without flow in rat cardiac trabeculae resulted in a decrease of [PCr] and [ATP] to 40 and 30% of control values. In contrast, [ADP] remained unchanged. These observations are in agreement with data from Humphrey et al, who observed that [ATP] of 22 mmol/g protein (3.7 mmol/l) in normoxic Langendorff perfused hearts decreased to 9.0 μ mol/g protein (1.5 mmol/l) following introduction of global ischemia or 3.9 μ mol/g protein (0.65 mmol/l) following perfusion with anoxic glucose-free medium²¹. The measurements were performed at maximal resting tension, which was reached after 6 minutes in case of anoxic perfusion and after 30 minutes in case of global ischemia. Other authors also measured [PCr] which decreased to much lower values than in our preparations. This could be related to differences in the models that were used and to the amount of work performed during the ischemia^{3,27}. Differences in species could also be an explanation for these discrepancies¹⁹.

One of the main drawbacks of the model we used is the difference between muscle bath / muscle content ratio (average ratio 100 : 1) and the real ratio of myocyte and interstitial volume (1 : 0.1). Yet the model provided a reproducible imitation of other conditions of ischemia like hypoxia, limited substrate availability and lack of metabolites washout.

Following ischemia we observed breakdown of high-energy phosphates and subsequent release of purines and oxypurines in the perfusion bath. Accumulation of metabolic products may have played a role in the rate of rise of resting tension in our model, since passive tension increased morerapidly when perfusion with hypoxic, glucose-free medium was not interrupted.

Papillary muscles

High-energy phosphates in papillary muscles (expressed in mmol/l) tended to be lower than in normoxic trabeculae; when expressed in $\mu\text{mol/g}$ protein, the values in papillary muscles seemed to exceed those of trabeculae. However, irrespective of the way high-energy phosphate concentration was expressed, [ATP] and [PCr] in our preparations, were comparable to values reported in literature. For instance, Dobson reported [PCr] and [ATP] in guinea-pig papillary muscles of 5.6 mmol/l and 4.7 mmol/l respectively ¹⁰. Lee measured high-energy phosphate concentration in cat papillary muscles and found [PCr] 5.9 mmol/l and [ATP] 2.9 mmol/l ²³. Pool reports [PCr] 9.9 mmol/l and [ATP] 6.6 mmol/l in cat papillary muscle at rest^{28,29}.

ATP content of papillary muscles, that were stimulated at high frequency, was lower than in preparations that were stimulated at low rate; under comparable conditions [ATP] of normoxic trabeculae either remained constant or showed only a slight decrease (see fig. 4). The decline was independent of the way high-energy phosphates concentration was expressed. The same applied to the ratio of [ATP] and [ADP]; at higher frequency of stimulation this parameter tended to decrease. The decrease of [ATP]/[ADP] with stimulus rate was greater in papillary muscles than in normoxic trabeculae.

These observations suggest that ATP production in papillary muscles was lower than ATP consumption. We further tested this hypothesis by measuring AMP concentration in papillary muscles. AMP concentration increased in proportion to muscle diameter. The detection limit of our HPLC system for AMP clearly allowed detection of this compound in normoxic papillary muscle preparations with diameters in excess of 250 μm . A clear correlation between work load and [AMP] was absent in our data, despite the fact that there was a difference in the force-frequency product of a factor of 20. The concentration of AMP seemed to increase with muscle diameters exceeding 250 μm .

Oxygen diffusion into tissues and especially papillary muscles has been the object of elaborate studies^{7,20,33}. Most of these investigations have related oxygen consumption and muscle diameter to mechanical parameters^{7,20}. The critical muscle diameter was smaller at higher rates of stimulation and higher bath temperatures²⁸. In the same study, adequate oxygenation was not demonstrated at a stimulus rate of 1 Hz at either 30 or 37 C, when muscle diameter exceeded 600 μm . Frezza and Bing reported an inverse linear relationship between normalized tension development and papillary muscle cross-sectional area over a range of 0.32 to 1.68 mm^2 , which is equivalent to diameters between 0.64 and 1.46 mm ¹³. This suggests that all muscles studied were larger than the critical diameter. In another study, the critical diameter was 0.74 mm at a stimulus rate of 0.8 Hz and a temperature of 25 C ³⁴.

Our data are in agreement with these observations and are consistent with the hypothesis that the core of papillary muscles with diameters exceeding 300 - 350 μm is not optimally oxygenated, which causes impairment of high-energy phosphate production.

We showed that papillary muscles were able to attain stable force at 30 C (stimulus frequency 3.3 Hz) whereas twitch force declined at 26 C. This may be explained by the fact that at 30 C the energy required for twitch force was reduced by 75% compared to 25 C since both twitch force and twitch duration are decreased by 50%. Apparently HEP production in these thick preparations was sufficient to assure stable mechanical performance at higher temperature whereas it was insufficient at lower temperature.

TABLE I

HIGH-ENERGY PHOSPHATE CONCENTRATION OF NORMOXIC AND HYPOXIC TRABECULAE

	stimulus frequency Hz	n	CrP	ATP (mean \pm s.e.m.) $\mu\text{mol/g}$ protein	ADP
Normoxia	1.0	7	36.0	23.1	4.4
			\pm	\pm	\pm
			2.0	1.5	0.2
	2.0	7	36.2	19.9	4.7
			\pm	\pm	\pm
			1.2	1.2	1.0
Hypoxia	3.3	6	23.0	14.9*	3.4
			\pm	\pm	\pm
			6.0	1.2	1.0
	1.0	7	15.0°	6.9°	3.7
			\pm	\pm	\pm
			3.0	1.2	0.5
Hypoxia	2.0	5-6	11.0°	4.7°	3.3
			\pm	\pm	\pm
			4.0	1.3	0.7
	3.3	3-4	9.0	3.9°	3.0
			\pm	\pm	\pm
			3.0	0.8	0.4

2-way ANOVA

P stimulus frequency	0.04	0.0001	0.53
P normoxia vs hypoxia	<0.0001	<0.0001	0.18
Interaction	0.41	0.14	0.80

The concentrations of high-energy phosphates are expressed in $\mu\text{mol/g}$ protein. For summary of experimental conditions see text. ° $p < 0.05$ vs comparable normoxic trabeculae;

* $p < 0.05$ vs comparable muscles stimulated at 1 Hz (One way ANOVA).

TABLE II

HIGH-ENERGY PHOSPHATE CONCENTRATION OF NORMOXIC AND HYPOXIC TRABECULAE

	stimulus frequency Hz	n	CrP (mean \pm s.e.m.) mmol/l muscle volume	ATP (mean \pm s.e.m.) mmol/l muscle volume	ADP (mean \pm s.e.m.) mmol/l muscle volume
Normoxia	1.07	7	4.9	3.4	0.6
			\pm	\pm	\pm
			0.5	0.3	0.1
	2.0	7	6.0	3.2	0.7
			\pm	\pm	\pm
			1.1	0.6	0.1
Hypoxia	3.3	5	4.0	3.2	0.5
			\pm	\pm	\pm
			0.8	0.5	0.1
	1.0	7	3.4	1.6*	0.6
			\pm	\pm	\pm
			1.3	0.6	0.3
Hypoxia	2.0	4-6	2.4°	0.9*	0.5
			\pm	\pm	\pm
			1.8	0.6	0.2
	3.3	4-6	1.8°	0.8*	0.5
			\pm	\pm	\pm
			0.4	0.2	0.1

2-way ANOVA

P stimulus frequency	0.48	0.47	0.78
P normoxia vs hypoxia	0.014	< 0.001	0.61
Interaction	0.61	0.84	0.65

The concentrations of high-energy phosphates are expressed in mmol/L muscle volume. For summary of experimental conditions see text.

* denotes $p < 0.05$ versus normoxic trabeculae that were stimulated at the same frequency. ° denotes $p < 0.1$ versus normoxic trabeculae that were paced at the same stimulus rate (one-way ANOVA).

TABLE III

HIGH-ENERGY PHOSPHATE CONCENTRATION OF PAPILLARY MUSCLES

	stimulus frequency Hz	n	CrP	ATP (mean \pm s.e.m.)	ADP
mmol/l muscle volume	0.1	5	3.4	2.2	0.4
			\pm	\pm	\pm
			1.0	0.4	0.1
	1.0	3	4.5	2.6	0.4
			\pm	\pm	\pm
			0.6	0.2	0.1
μ mol/g protein	3.3	9	2.6	1.7	0.4
			\pm	\pm	\pm
			0.6	0.1	0.1
	0.1	5	46.5	30.3	5.6
			\pm	\pm	\pm
			9.6	2.3	0.8
μ mol/g protein	1.0	3	47.9	27.5	4.0
			\pm	\pm	\pm
			4.4	1.9	0.1
	3.3	7	26.0	25.2	6.2
			\pm	\pm	\pm
			6.4	2.7	0.7

One-way ANOVA

P stimulus frequency (mmol/l)	0.28	0.10	0.88
----------------------------------	------	------	------

P stimulus frequency (μ mol/g protein)	0.042	0.165	0.37
--	-------	-------	------

Papillary muscles were stimulated at 1 Hz for 60 minutes prior to any intervention. Thereafter, stimulation was continued for the next 60 minutes at the indicated stimulus frequencies. Next the papillary muscles were rapidly frozen and analyzed for content of high-energy phosphates (HEP) by HPLC.

GENERAL CONCLUSION

Both superfused trabeculae and papillary muscles have the advantage over isolated perfused hearts that the dynamics of contraction can be studied in more detail. We used a modified H.P.L.C. technique to assess high-energy phosphate concentrations in one measurement. The technique was used to correlate mechanics by normoxic and hypoxic trabeculae and normoxic papillary muscles with content of high-energy phosphates. The data of normoxic trabeculae and papillary muscles were comparable to values found in literature. H.E.P. concentrations in the first were independent of work load. In contrast, H.E.P. content in papillary muscles tended to decrease with increasing work load. This is most likely accounted for by a combination of normal H.E.P. metabolism in the outer layers and lower H.E.P. content in the hypoxic inner core of these preparations. The observed positive correlation between tissue [AMP] and diameter of the muscles supports the hypothesis that oxygen availability in papillary muscles is limited.

Our model of hypoxia without flow in trabeculae resulted in a reproducible decrease of H.E.P. concentrations and concomitant increased unstimulated force, like in the intact heart. Changes in sarcomere mechanics suggested that the muscles developed diastolic rigor tension in spite of high residual H.E.P. concentrations. The latter conclusion awaits further validation in future experiments.

ACKNOWLEDGEMENTS

J.J.J. Buxx, P.W. Achterberg, and A. Selma Nieukoop were supported by grants (82.075 and 84.075) from the Dutch Heart Foundation. The stimulating support and contribution of Prof PG Hugenholtz and Dr. E Harmsen is gratefully acknowledged.

REFERENCES

1. Abbott BC, Mommaerts WFHM. A study of inotropic mechanisms in the papillary muscle preparation. *J Gen Physiol* 1959; 42: 533-551
2. Allen DG, Blinks JR. Calcium transients in aequorin-injected frog cardiac muscle. *Nature* 1978; 273: 509-513
3. Allen DG, Morris PG, Orchard CH, Pirolo JS. A nuclear magnetic resonance study of metabolism in the ferret heart during hypoxia and inhibition of glycolysis. *J Physiol* 1985; 361: 185-204
4. Allen DG, Orchard CH. Intracellular calcium concentrations during hypoxia and metabolic inhibition in mammalian ventricular muscle. *J Physiol* 1983; 339: 107-122
5. Bailey IA, Seymour A-ML, Radda GK. A ³¹P-NMR study of the effects of reflow on the ischaemic rat heart. *Biochem Biophys Acta* 1981; 637: 1-7
6. Bradford MM. A rapid and sensitive method for the quantitation of microgram quantities of protein utilizing the principle of protein-dye binding. *Anal Biochem* 1976; 72: 248-254
7. Cranefield PF, Greenspan K. The rate of oxygen uptake of quiescent cardiac muscle. *J Gen Physiol* 1960; 44: 235-249
8. De Jong JW, Harmsen E, De Tombe PP, Keyzer E. Nifedipine reduces adenine nucleotide breakdown in ischemic rat heart. *Eur J Pharmacol* 1982; 81: 89-96
9. Dhalla NS, Yates JC, Walz DA, McDonald VA, Olson RE. Correlation between changes in the

- endogenous energy stores and myocardial function due to hypoxia in the isolated perfused rat heart. *Canad J Physiol Pharmacol* 1972; 50: 333-345
10. Dobson JG, Schwab GE, Ross J, Mayer SE. Comparison of the biochemical composition of four preparations of contracting cardiac muscle. *Am J Physiol* 1974; 227: 1452-1457
11. Doorey AJ, Barry WH. The effects of inhibition of oxidative phosphorylation and glycolysis on contractility and high-energy phosphate content in cultured chick heart cells. *Circ Res* 1983; 53: 192-201
12. Fossel ET, Morgan HE, Ingwall JS. Measurement of changes in high energy phosphates in the cardiac cycle by using gated ^{31}P nuclear magnetic resonance. *Proc Natl Acad Sci* 1980; 77: 3654-3658
13. Frezza WA, Bing OHL. PO_2 -modulated performance of cardiac muscle. *Am J Physiol* 1976; 231: 1620-1624
14. Gevers W. Protein metabolism of the heart. *J Mol Cell Cardiol* 1984; 16: 3-32
15. Harmsen E, De Jong JW, Serruys PW. Hypoxanthine production by ischemic heart demonstrated by high pressure liquid chromatography of blood purine nucleosides and oxypurines. *Clin Chim Acta* 1981; 115: 73-84
16. Harmsen E, DeTombe PP, De Jong JW. Simultaneous determination of myocardial adenine nucleotides and creatine phosphate by high-performance liquid chromatography. *J Chromatogr* 1982; 230: 131-136
17. Harmsen E, De Tombe PP, De Jong JW, Achterberg PW. Enhanced ATP and GTP synthesis from hypoxanthine or inosine after myocardial ischemia. *Am J Physiol* 1984; 246: H37-H43
18. Hearse DJ. Oxygen deprivation and early myocardial contractile failure: A reassessment of the possible role of adenosine triphosphate. *Am J Cardiol* 1979; 44: 1115-1121
19. Hearse DJ, Humphrey SM, Feuvray D, de Leiris J. A biochemical and ultrastructural study of the species variation in myocardial cell damage. *J Mol Cell Cardiol* 1976; 8: 759-778
20. Hill AV. Diffusion of oxygen and lactic acid through tissues. *Proc R Soc London* 1928; Ser B 104: 39-96
21. Humphrey SM, Hollis DG, Seelye RN. Adenine pool catabolism in the ischemic, the calcium-depleted ischemic, and the substrate free anoxic isolated rat heart; relationship to contracture development. *J Mol Cell Cardiol* 1984; 16: 1127-1136
22. Krueger JW, Pollack GH. Myocardial sarcomere dynamics during isometric contraction. *J Physiol* 1975; 251: 627-643
23. Lee KS, Yu DH. Effects of epinephrines on metabolism and contraction of cat papillary muscle. *Am J Physiol* 1964; 206: 525-530
24. Morris GM, Allen DG, Orchard CL. High time resolution ^{31}P NMR studies of the perfused ferret heart. *Adv Myocard* 1984; 6: 27-38
25. Opie LH, Owen P, Mansford KRL. Metabolic adjustments to acute heart work: observations in the isolated perfused rat heart. *Cardiovasc Res* 1971; (suppl I): 87-95
26. Paradise NF, Schmitter JL, Surmitis JM. Criteria for adequate oxygenation of isometric kitten

papillary muscle. *Am J Physiol* 1981; 241: H348-H353

27. Piper HM, Schwartz P, Hutter JF, Spieckermann PG. Energy metabolism and enzyme release of cultured adult rat heart muscle cells during anoxia. *J Mol Cell Cardiol* 1984; 16: 995-1007
28. Pool PE, Chandler BM, Sonnenblick EH, Braunwald E. Integrity of energy stores in cat papillary muscle: Effect of changes in temperature and frequency of contraction on high energy phosphate stores. *Circ Res* 1968; 22: 213-219
29. Pool PE, Sonnenblick EH. The mechanochemistry of cardiac muscle. I. The isometric contraction. *J Gen Physiol* 1967; 50: 951-965
30. Reichel H. The effect of isolation on myocardial properties. *Basic Res Cardiol* 1976; 71: 1-16
31. Roberts JJ, Walker JB. Feeding a creatine analogue delays ATP depletion and onset of rigor in ischemic heart. *Am J Physiol* 1982; 243: H911-H916
32. Schaper J, Mulch J, Winkler B, Schaper W. Ultrastructural, functional, and biochemical criteria for estimation of reversibility of ischemic injury: A study on the effects of global ischemia on the isolated dog heart. *J Mol Cell Cardiol* 1979; 11: 521-541
33. Schouten VJA, ter Keurs HEDJ. The force - frequency relationship in rat myocardium: the influence of muscle dimensions. In: Schouten VJA. Excitation - contraction coupling in heart muscle. Thesis (1985)
34. Snow TR, Bressler PB. Oxygen sufficiency in working rabbit papillary muscle at 25°C. *J Mol Cell Cardiol* 1977; 9: 595-604
35. ter Keurs HEDJ, Rijnsburger WH, van Heuvingen R, Nagelsmit MJ. Tension development and sarcomere length in rat cardiac trabeculae. Evidence of length-dependent activation. *Circ Res* 1980; 46: 703-714
36. van der Vusse GJ, Coumans WA, van der Veen E, Drake AJ, Flameng W, Suy R. ATP, Creatine phosphate and glycogen content in human myocardial biopsies: markers for the efficacy of cardioprotection during aorto-coronary bypass surgery. *Vasc Surg* 1984; 18: 127-134
37. Zak R, Galhotra SS. Contractile and regulatory proteins. In: *Cardiac Metabolism*, edited by Drake-Holland AJ, and Noble MIM. (1983) John Wiley and Sons Ltd.
38. Zimmer H-G, Ibel H. Ribose accelerates the repletion of the ATP Pool during recovery from reversible ischemia of the rat myocardium. *J Mol Cell Cardiol* 1984; 16: 863-866

CHAPTER 8

HYPOXIC CONTRACTURE IN RAT CARDIAC TRABECULAE: ANALYSIS OF DYNAMIC SARCOMERE STIFFNESS

Jeroen JJ Bucx, Peter P de Tombe, HEDJ ter Keurs

Submitted to Circulation Research (1993)

Preliminary results of this work have been published previously in the forms of abstracts:

Bucx JJJ, Backx PHM, de Tombe PP, ter Keurs HEDJ. Rigor development in hypoxic rat cardiac trabeculae. *Circulation* 1986; 74: II-165.

Bucx JJJ, ter Keurs HEDJ. The transfer function of hypoxic cardiac muscle suggests rigor. *Biophys J* 1987; 51: 467a.

CHAPTER 8

HYPOXIC CONTRACTURE IN RAT CARDIAC TRABECULAE: ANALYSIS OF DYNAMIC SARCOMERE STIFFNESS

Jeroen JJ Buxx, Peter P de Tombe, HEDJ ter Keurs

ABSTRACT

Hypoxic contracture in myocardium has been attributed either to rigor cross-bridge formation or active cross-bridge cycling. The purpose of the present experiments was to quantify the relative contributions of these mechanisms to the increase of diastolic force during hypoxia in isolated rat cardiac trabeculae. Sarcomere length was measured by laser diffraction techniques and force by silicon strain gauge. The dynamic transfer function between sarcomere length and force (DTF) was characterized by measuring the response to small ($<1\%$) sinusoidal sarcomere length perturbations.

Hypoxia resulted in a rapid initial decline of active twitch force, followed by a transient recovery of twitch force between 10 and 30 minutes of hypoxia. Thereafter, active twitch force ultimately declined, concomitant with a rapid increase in diastolic force which reached a plateau at 39 ± 5 minutes of hypoxia. In one series of experiments, the DTF was analyzed between 0.1 and 100 Hz perturbations frequency in 1) normoxic relaxed muscles, 2) tetanized normoxic muscles, and 3) during the plateau of the hypoxic contracture. Whereas the DTF was markedly frequency dependent in tetanized muscles, it was frequency independent in normoxic relaxed muscles and during the plateau of the hypoxic contracture. In a second series of experiments, we measured the DTF at 1 and 100 Hz during the development of the hypoxic contracture. With this method, some active cross-bridge cycling could be detected, but only during the transient recovery phase.

These observations demonstrate that hypoxic contracture in myocardium is due predominantly to rigor cross-bridge formation rather than active cross-bridge cycling.

INTRODUCTION

It is well known that diastolic force increases during prolonged ischemia or hypoxia in myocardium¹⁻⁴. The mechanism that underlies the increase of unstimulated force however, is not well understood. The hypoxic contracture could be due to active cycling of cross-bridges, caused by increased cytosolic calcium concentration⁵⁻¹³. On the other hand, an alternative hypothesis has been put forward in which unstimulated force increases as the results of the formation of rigor cross-bridges due to decreased ATP concentration in the vicinity of the myofilaments¹⁴⁻¹⁸.

In support of the first hypothesis, studies with calcium sensitive indicators in the isolated perfused heart have shown an increase in diastolic calcium concentration and decreased rate of decline of systolic calcium concentration in the cytosol upon induction of ischemia or hypoxia^{5,7,11-13}. These, and similar results in isolated cardiac muscle during hypoxia^{8,10}, suggest that the effects of ischemia or hypoxia on diastolic characteristics of the heart may be caused by diminished calcium extrusion from the cardiac cytosol. Reduced calcium extrusion could result from diminished calcium ATP-ase activity in the sarcoplasmic reticulum and sarcolemma, or diminished calcium extrusion by the sarcolemma $\text{Na}^+/\text{Ca}^{2+}$ exchanger. The latter would be due to a reduction in the electrochemical sodium gradient that drives this exchanger¹⁹⁻²¹. The observation of recovery of ventricular end-diastolic pressure following a quick ventricular volume change early during hypoxia also supports the suggestion that the hypoxic contracture is, at least in part, due to active cross-bridge cycling²². On the other hand, it has consistently been

observed that ATP levels are substantially reduced during hypoxia¹⁴⁻¹⁸, which implicates rigor cross-bridge formation as cause of the hypoxic contracture. Consistent with this conclusion, Koretsune and Marban⁴ in a recent report showed that the onset of hypoxic contracture in perfused ferret hearts correlates more closely with the decrease in ATP levels than with the increase in intracellular calcium concentration. Both ATP and intracellular calcium concentration were measured simultaneously by NMR techniques in that study⁴.

A confounding factor in discriminating between the two hypothesis however, is the notion that the sensitivity of the myofilaments to calcium increases with decreasing ATP levels in the muscle^{18,23}, while acidosis during hypoxia is associated with a decreased sensitivity of the cardiac myofilaments to calcium ions²⁴. Absence of force recovery following a quick release in isolated hypoxic papillary muscles suggests that the contracture is caused by the development of rigor cross-bridges^{25,26}. Similarly, absence of tension dependent heat production by hypoxic papillary muscles is also consistent with the rigor cross-bridge hypothesis²⁷. Hence these studies indicate that mechanical or energetic parameters may be more suitable indicators than the measurement of intracellular concentrations of ATP or calcium ions to discriminate between the two hypothesis discussed above.

The purpose of the present study was to quantify the relative contribution of each of the two proposed mechanisms to the development of hypoxic contracture in isolated rat cardiac trabeculae. For this purpose, we employed the technique of transfer function analysis of dynamic sarcomere stiffness and phase angle. In short, this technique entails measurement of the force response of the muscle to length perturbations over a wide range of frequencies (about 0.1 to 100 Hz). Tonically activated skeletal^{28,29} and cardiac^{30,31} muscle display a characteristic stiffness and phase angle transfer function. That is, a predominant feature of the transfer function of tonically activated muscle is a 'dip' in the stiffness spectrum at about 1 Hz, concomitant with a marked phase angle shift at that frequency^{28,31}. This phenomenon is consistent with the active cycling of cross-bridges^{29,30}. Increase of stiffness due to the formation of rigor bonds (i.e. non-cycling cross-bridges) on the other hand, is expected to add a frequency independent component to the dynamic transfer function.

We have employed laser diffraction techniques in this study to measure sarcomere length in the central segment of isolated rat cardiac trabeculae. Adoption of the method is essential to the measurement of the dynamic transfer function at the level of the cardiac sarcomere. We have previously shown³²⁻³⁴ that isolated cardiac muscle preparations consist of assumedly normal sarcomeres in series with sarcomeres that contract only partially. The latter sarcomeres are located near the damaged, compliant ends of the isolated muscle. It is probable that these partially contracting sarcomeres contribute significantly to force responses invoked by the length changes that are applied to the entire muscle. Furthermore, we will present evidence in the present study that the mechanical properties of these damaged end regions of the muscle change profoundly upon induction of hypoxia. Hence, an accurate assessment of the dynamic transfer function of the muscle during the development of hypoxic contracture requires that the measurements are made at the level of the cardiac sarcomere.

Our results indicate that the hypoxic contracture in rat cardiac trabeculae can nearly completely be explained on the basis of formation of rigor bonds.

METHODS

Muscle preparation and experimental apparatus

Sprague-Dawley rats (200-300 grams) of either sex, age 12 - 20 weeks, were anaesthetized with ether. The heart was rapidly removed and transferred in cold saline to a dissecting chamber. Perfusion of the coronary arteries with a modified Krebs-Henseleit solution equilibrated with a 95% O₂ - 5% CO₂ gas mixture was started within 30 seconds. This solution was composed of (in mM): Na⁺ 150.0, K⁺ 5.0, Cl⁻ 127.5, Mg²⁺ 1.2, H₂PO₄⁻ 2.0, SO₄²⁻ 1.2, HCO₃⁻ 27.0, glucose 10.1, and Ca²⁺ 1.5, pH 7.3-7.4. Demineralized Millipore-filtered water and salts of analytical grade purity were used for all solutions. During the dissection procedure the Krebs-Henseleit solution (20 - 23 C) also contained 20 mM K⁺ in order to stop spontaneous beating of the heart.

Uniform, unbranched trabeculae (3 ± 1.1 mm in length; 0.4 ± 0.3 in width; 0.1 ± 0.05 mm in thickness; mean \pm S.D.; $n = 49$) were dissected from the right ventricle and transported to the experimental chamber. A piece of the tricuspid valve and a cube of the wall of the right ventricle remained attached to the trabeculae for mounting purposes. Force was measured with a silicon strain gauge covered with silicon adhesive (model AE 801, Akers Micro-Electronics, Horten, Norway) and extended with a lever of carbon fiber (Fokker Aviation Industries, The Netherlands). A stainless steel hook at the end of this lever was connected to the valvular end of the trabecula. The other end of the trabecula was mounted in a basket, specially designed to hold the cube of ventricular muscle. The basket was glued onto a carbon fiber motor arm, which was connected to the axis of a servo controlled motor (Model 300 Cambridge Technology, Cambridge, MA; 90% step response 1.25 msec; see reference²⁵). The sensitivity of the force transducer was 3 V/N, and the resonance frequency was at least 750 Hz. The preparations were observed through the glass bottom by means of an inverted microscope and by video-camera, connected to a TV monitor. Horizontal and vertical displacement of the muscle during the contraction were kept minimal by appropriate mounting.

The muscle bath was covered with a hood, flushed with a gas-mixture of 95% N₂ and 5% CO₂ during hypoxia, in order to prevent oxygenation of the bath fluid by ambient air. The rate of flow of the Krebs Henseleit solution through the muscle chamber (content 500 μ l) was 6 ml/min. The temperature in the bath, measured with a thermistor, was kept at 30 ± 0.1 C by a heat exchanger connected to a cryostat. Platinum wires, embedded in the chamber walls, were used to stimulate the muscle; the muscles were stimulated at 1 Hz and at 50% above the stimulus threshold. The latter was repeatedly determined during hypoxia and adjusted if necessary.

Measurement of sarcomere length

Sarcomere length in the center of the muscle was measured, by laser diffraction techniques, which have been described in detail previously³²⁻³⁵. In short, the muscle was illuminated with a laser beam (Spectra-Physics; wave length 632.8 nm), focused to a spot of 400 μ m. The zero order diffraction band was used to observe the preparation. One of the first order maxima was projected through the glass bottom of the muscle chamber on a photodiode array (model 256C, Reticon, Sunnyvale, CA). The array was scanned twice per millisecond. Following subtraction of superimposed light from the zero order band, the position of the median of the first order diffraction band was detected electronically and converted to a voltage proportional to sarcomere length. Prior to experiments the system was calibrated with standard glass gratings placed at the level of the muscle³²⁻³⁵. We have recently shown that potential artifacts associated with the use of the laser diffraction technique to measure sarcomere length are less

than 4%³². Sarcomere length, muscle and force were recorded on a chart recorder (model 2800 S, Gould, Cleveland, OH), data storage tape FM tape recorder (Gould), and storage oscilloscope connected to a hard copy unit (Tektronix models 5103, 613, 4631).

Experimental protocols

Following mounting, muscle length was adjusted such that passive force was 3-5 % of total twitch force. This muscle length corresponded to an average central sarcomere length of 2.2 μm (range 2.10 μm to 2.35 μm). The muscles were left to equilibrate for 60 minutes at that muscle length and 1 Hz stimulus rate.

In a first series of experiments, the full frequency dependence of the dynamic transfer function (i.e. 0.1 to 100 Hz) was analyzed in unstimulated muscles under normoxic conditions, and at the time at which the hypoxic contracture had reached a maximum (cf Figure 1 and below). In addition, the dynamic transfer function of maximally activated, normoxic muscles was analyzed. For this purpose, 10 mM caffeine was added to the Krebs-Henseleit solution, the calcium concentration was increased to 4 mM, and the muscles were tetanized by stimulation at 10 Hz (see Figure 4)^{36,37}. No more than 5 tetani were elicited in each preparation to avoid propagated aftercontractions and arrhythmias in the muscles, although all muscles showed some asynchronous sarcomere activity both during and shortly after tetani, and in between twitches. The interval between the tetani was 10-20 times longer than the duration of the tetanus (10-20 seconds) to allow metabolic recovery of the muscles; steady state twitch force decreased 0-15 % following the tetani ($n = 7$). Following assessment of the transfer function at rest and during the tetani, the muscles were again superfused with control Krebs-Henseleit solution and allowed to recover for 30 minutes. Next, hypoxia was induced by changing from control Krebs-Henseleit solution to glucose-free Krebs-Henseleit solution that was in equilibrium with 95% N_2 and 5% CO_2 ; the pO_2 in this solution was 5-9 mm Hg. The transfer function was analyzed again when the hypoxic contracture had reached a maximum level (cf Figure 1).

In a second series of experiments, sarcomere stiffness was assessed using 1.0 and 100.0 Hz 1% sarcomere length perturbations during the development of the hypoxic contracture at intervals of 5 minutes. During this analysis, which lasted for about 30 seconds, stimulation of the muscle was interrupted.

Analysis of dynamic transfer function of the trabeculae

Sine waves were derived from a function generator (model 3310A, Hewlett-Packard) at frequencies of 0.1, 0.2, 0.4, 0.8, 1.6, 3.2, 6.4, 12.5, 25, 50, and 100 Hz, and fed into the position command of the servo motor in order to induce muscle length changes. Care was taken to ensure that the amplitude of the muscle length changes were limited to about 1%. The dynamic transfer function of the sarcomeres, that is their stiffness-frequency and phase-frequency relationship, was analyzed off-line from the signals stored by FM tape recorder using a digital oscilloscope (model 2200, Dataprecision). In order to increase signal to noise ratio, several successive cycles of the sinusoidal force and sarcomere length signals were averaged using the digital oscilloscope (cf Figures 4 and 5). Next, the amplitude and phase of the sinusoidal sarcomere length perturbations and the corresponding force responses were measured directly from the digital oscilloscope. Stiffness was calculated as the ratio of the force amplitude and the sarcomere length amplitude, and normalized to the maximum stiffness measured at 100 Hz during the hypoxic contracture.

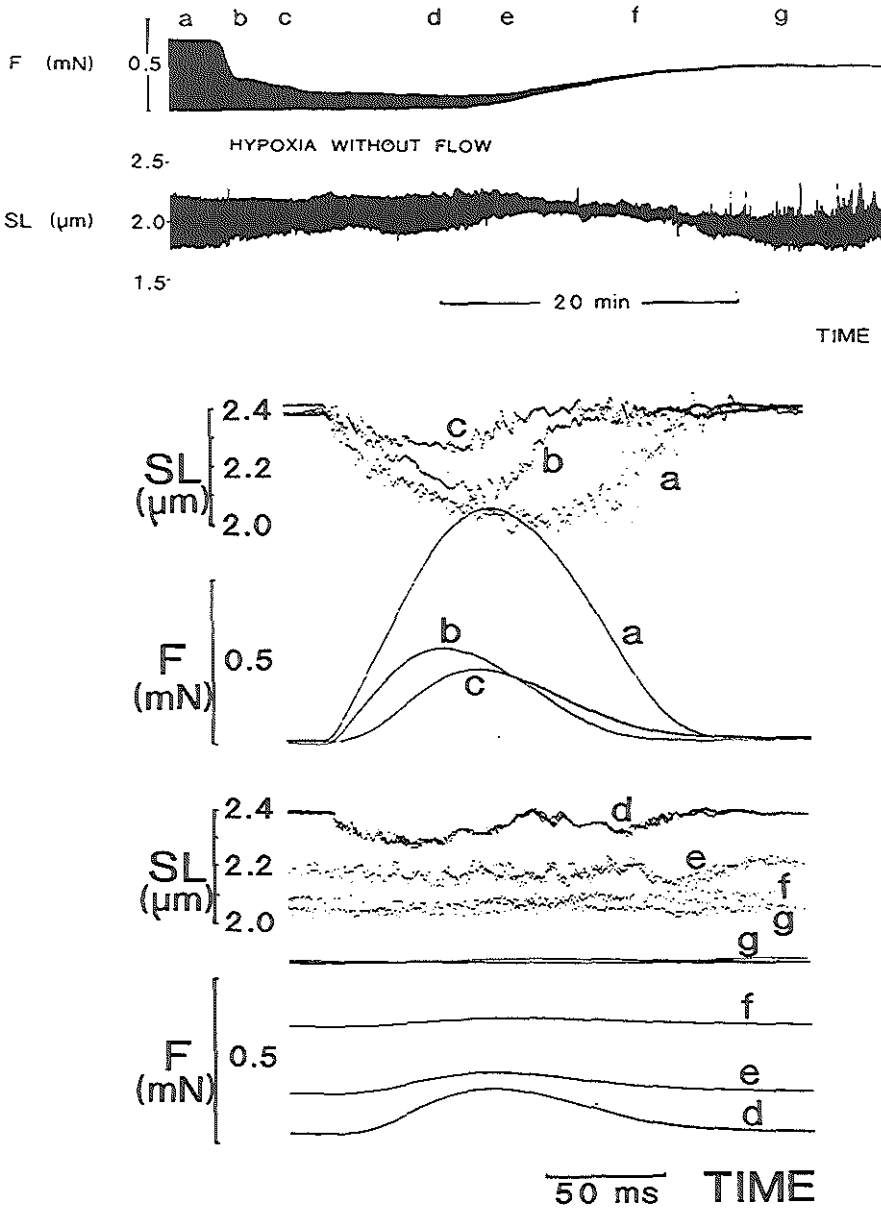


Figure 1. Effect of hypoxia on twitch force and sarcomere length.

The top panels show the changes in twitch force and sarcomere length induced by switching from control Krebs-Henseleit solution to glucose-free Krebs-Henseleit solution which was in equilibrium with 95% N_2 - 5% CO_2 , at the time indicated by the arrow. The bottom panels show recordings of force and sarcomere length at a higher time resolution. Note that the overall length of the muscle was kept constant during the entire protocol. Hence, systolic sarcomere shortening occurred at the expense of stretch of the damaged ends of the muscle (see text for details).

Statistical analysis

Results are presented as mean \pm S.E.M., with n as the number of experiments. When two means were compared, Student's unpaired t -test was used³⁸. Differences were considered significant if $P < 0.05$.

RESULTS

Force and sarcomere length during hypoxia

Figure 1 shows the changes of twitch force and sarcomere length in a representative trabecula in response to the induction of hypoxia. The inset to figure 1 shows twitch force and sarcomere length on a faster time base, recorded at various times after the induction of hypoxia as indicated in the figure. Figure 2 shows the average results of seven 7 trabeculae. Twitch force changed typically in a triphasic manner following onset of hypoxia. An acute decline of twitch force was followed by either a sudden decrease of the rate of decline or by a transient recovery. As figure 2 shows, this phase occurred, on average, between 10 and 30 minutes after the induction of hypoxia. Eventually a gradual total loss of active force occurred. The slower decline of twitch force or its transient recovery was accompanied by a rapid but small increase of unstimulated force as is most apparent from the average data shown in figure 2 (i.e. between 10 and 20 minutes). Figure 1 also shows that during this period, the relaxation phase of the twitch prolonged markedly. In addition, at the microscopic level, spontaneous sarcomere motion could be observed in the preparation during this phase. The final decline of twitch force was accompanied by a second faster mono-phasic increase of unstimulated force, which on average started about 25 minutes after the induction of hypoxia (cf figure 2). In all muscles, unstimulated force reached a plateau after the final decline of active twitch force. The time to maximum hypoxic contracture was somewhat variable, however (39 ± 5 minutes). Hence, this plateau in unstimulated force is obscured in the average data presented in figure 2. Diastolic sarcomere length in the center of the muscle decreased during the rapid increase of unstimulated force to reach a minimum at the time of maximal unstimulated force. The extent of systolic sarcomere shortening decreased during the rapid decline of twitch force early during hypoxia. This was followed either by a slower decline of the degree of shortening or a temporary increase of sarcomere shortening during the period of transient force recovery. Figure 3 shows that the width of the first order of the diffraction pattern increased during the development of the hypoxia contracture, while the intensity of the first order decreased. This observation suggests an increase in the non-uniformity of the striation spacing in the muscle.

Because muscle length was kept constant during these experiments, both changes in the mechanical properties of the sarcomeres in the center of the trabeculae and changes of the properties of the ends of the preparation, linking the sarcomeres with the measuring equipment (the series elastic element) contribute to the changes of active and passive sarcomere length during hypoxia. Figure 3 was obtained by plotting force against sarcomere shortening during the twitch, and illustrates that the sarcomeres in the central segment of the muscle contracted against a nonlinear elastic element; the properties of this element appeared to change during hypoxia, as was apparent from the increase in slope of the relationship between twitch force and sarcomere shortening and the apparent leftward shift of the relation late during hypoxia. We estimated the contribution of stiffness of the series elastic element from the ratio of fractional shortening of the active sarcomeres in the center of the preparation, at constant muscle length, versus externally developed force (normalized for control twitch force). The stiffness constant was subsequently estimated from the ratio of stiffness of the series elastic element and

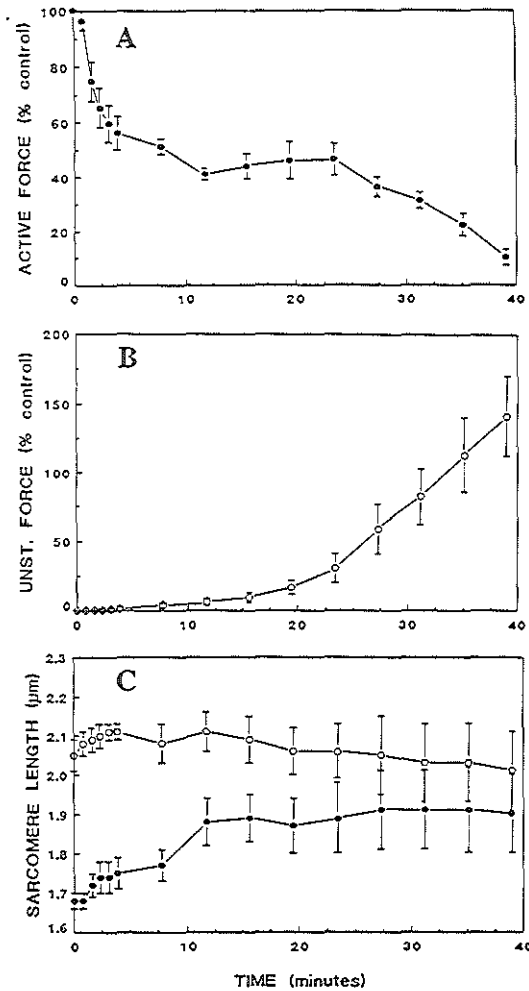


Figure 2. Average twitch force and sarcomere length.

Shows average response of seven trabeculae to the induction of hypoxia. Panel A: active developed twitch force. Panel B: Diastolic i.e. unstimulated force. Panel C: Systolic and diastolic length of the central sarcomeres of the muscle.

corresponding normalized active force. The stiffness constant of the series elastic element was 6.2 ± 0.7 at normoxia, while during late hypoxia the stiffness constant increased to 21.3 ± 3.8 ($p < 0.05$). This increase in stiffness must have caused an overestimate of the force generating capacity of the sarcomeres, because sarcomere length at the moment of peak twitch force increased during hypoxia, while the force sarcomere length relation of cardiac muscle has a positive slope³⁴. Furthermore, and of greater importance to the present study, this observation clearly demonstrates that measurement of central sarcomere length is a prerequisite for the accurate assessment of the dynamic transfer function of isolated cardiac muscle during hypoxia.

Dynamic transfer function

Hypoxia resulted consistently in an increase of unstimulated force. The observation that during the initial small rise of unstimulated force spontaneous sarcomere motion activity increased, suggests that calcium loading and calcium mediated ATP dependent cross-bridge cycling could have been responsible

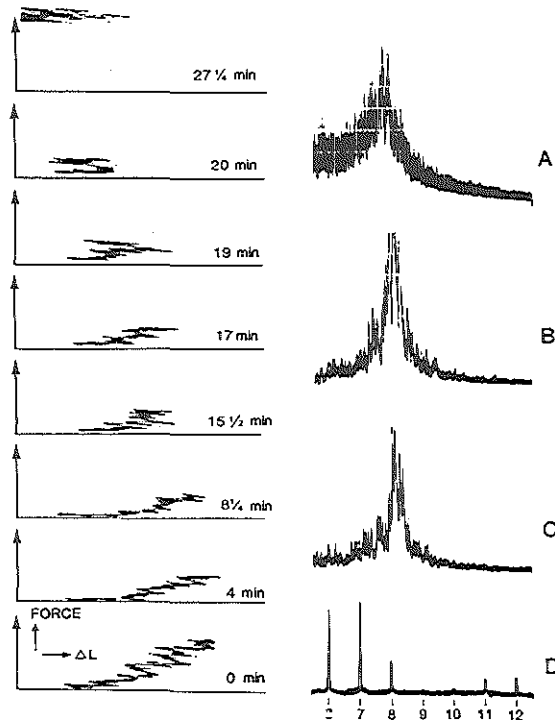


Figure 3. Stiffness of series elastic element during hypoxia.

Illustrates the change of stiffness of the series elastic element, i.e. damage end regions, of a representative trabecula during the development of hypoxic contracture. The left panel shows sarcomere length plotted on the X axes and force plotted on the Y axes during the twitches, just before hypoxia ($t = 0$ min) and at increasing times after the onset of hypoxia. Sarcomere shortening during the twitch is indicated as a rightward defection (starting sarcomere length $2.12 \mu\text{m}$ at $t = 0$ min; length of abscissa $0.5 \mu\text{m}$) reflecting equivalent stretch of the series elastic elements (i.e. damaged end compliance) by approximately 14%. Force (vertical arrow = 50 mN/mm^2) increases as a non-linear function of stretch of the series elastic element, while between 17 and 20 minutes after onset of hypoxia the force length relation of the series elastic element becomes complex as a result of non-uniform contraction during the relaxation phase (cf figure 1). The dotted lines indicate the force-length relation of the damaged end regions, recorded under control conditions (bottom left panel).

The right panels show the first order diffraction band recorded under control conditions, and after 5 and 30 minutes of hypoxia. The bottom right panel shows for comparison the sixth through twelfth diffraction lines of $17.22 \mu\text{m}$ calibration grating.

for the development of the hypoxic contracture. However, when the muscle was quickly released at the time of the plateau, force immediately fell to zero without recovery, and neither the whole muscle nor the central sarcomeres shortened appreciably after the quick release. This suggests that, at least at the time when the hypoxic contracture was fully developed, the muscle was in rigor.

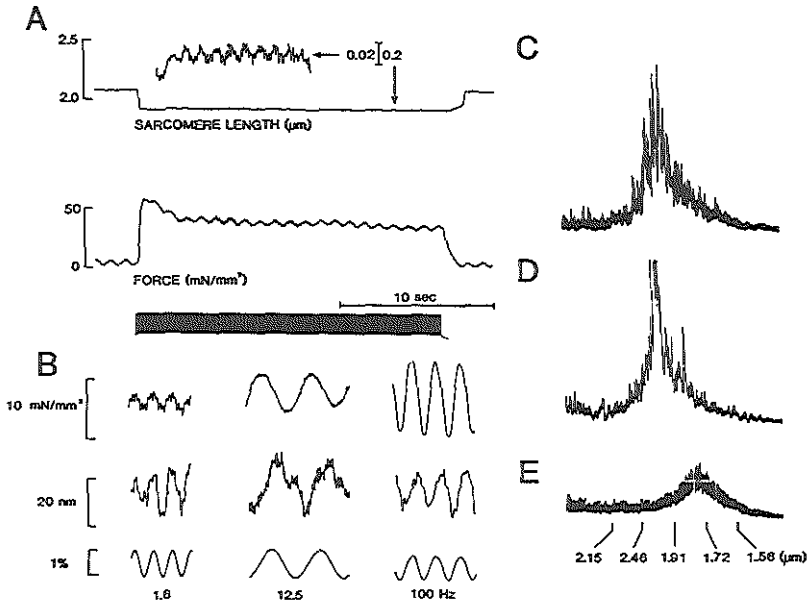


Figure 4 Dynamic stiffness during caffeine tetani

Shows the methods used to assess the dynamic transfer function during caffeine tetani. Trabeculae were tetanized by 10 Hz stimulation in the presence of 10 mM caffeine and 4 mM Ca^{2+} .

Panel A shows sarcomere length (top panel) and force development (middle panel) during a 20 seconds tetanus. The bottom panel shows the stimulus pulses. The inset in the top panel shows sarcomere length during the tetanus at a higher gain. During the tetanus, sarcomeres in the central segment of the muscle shortened initially by about 0.2 μm , whereafter sarcomere length remained constant. The length perturbations, 1 Hz, were applied both prior to and during the tetanus (note that the dynamic stiffness at this frequency is similar during tetanus compared to that at rest).

Panel B shows the response of force (top tracings) and sarcomere length (middle tracings) to the perturbations of muscle length (bottom panel) during the tetanus in a representative trabecula. Calibrations and frequencies as indicated. Note the increase in dynamic stiffness with increasing frequency of the length perturbations. Furthermore, note that the phase shift between sarcomere length and force progressively increases with increasing perturbation frequency.

Panel C shows the first order diffraction bands of a representative trabecula in control Krebs-Henseleit solution, while panels D and E show the first order diffraction band generated by the trabecula in the presence of 10 mM caffeine and 4 mM Ca^{2+} at rest and during tetanus, respectively. Sarcomere length calibrations as shown below panel E.

As we have discussed above, because the properties of the series elastic element are expected to contribute significantly to the transfer function of the muscle as a whole, and particularly because the properties of the series elastic element changed during hypoxia, we studied the transfer function of the

muscles at the level of the central sarcomeres. First the behavior of unstimulated trabeculae under normoxia conditions was studied, that is a condition in which cross-bridge activity is supposed to be minimal. This was compared with the transfer function during tetani in which maximal force was developed. These were induced by high frequency stimulation (10 Hz) in presence of 4 mM Ca^{2+} and 10 mM caffeine in the bathing solution and created a condition of maximal cross-bridge activity in the muscle (see figures 4 and 5; ^{38,37}).

The stiffness modulus of instimulated, relaxed normoxic muscles did not vary with the frequency of the sinusoidal length perturbations (see figure 5). The phase shift between the sarcomere length and force in passive normoxic muscles was small but significantly positive (about -10 degrees) and also independent of frequency. During the tetanus, the stiffness modulus at low frequencies (<0.1 Hz) was twice that of the relaxed muscle. It decreased between 0.1 and 0.8 Hz; above this "dip-frequency" the stiffness modulus increased mono-phasically, while up to 100 Hz no maximum was observed. In addition, the phase shift was negative (-10 to -15 degrees) at frequencies below 1.6 Hz and increased mono-phasically to +80 degrees at 100 Hz. This observation suggests viscous behavior at the higher perturbation frequencies, that is the rate of sarcomere length change dictates the force change (see figure 5).

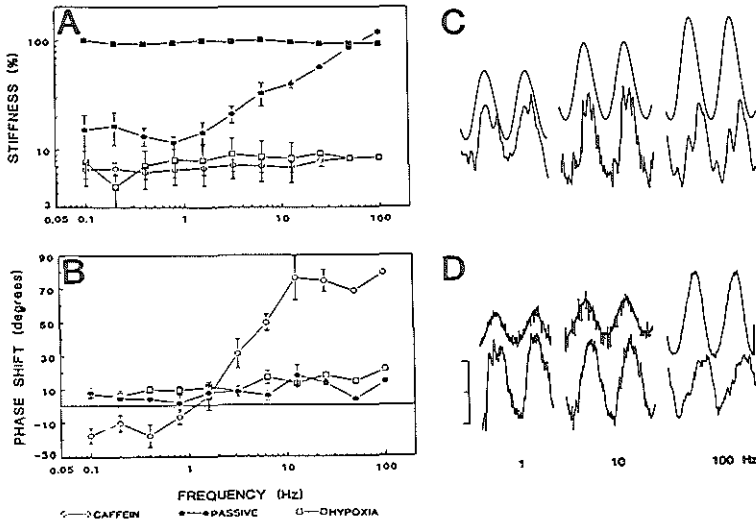


Figure 5 Average dynamic transfer functions.

Panel A shows the average transfer functions between the length of the central sarcomeres and force of five trabeculae during normoxia at rest (open circles) and during the tetanus (filled circles), and during the plateau of the hypoxic contracture (open triangles). The top panel shows the modulus, i.e. the dynamic stiffness, normalized to the maximum modulus during hypoxia. The bottom panel shows the average phase shift between sarcomere length and force.

Panel C and D show the force response (top tracings) and sarcomere length response (bottom tracings) to muscle length perturbations during the plateau of the hypoxia contracture and at rest during normoxia in a representative trabecula. Note that the dynamic stiffness and phase shift are independent of perturbation frequency in both panels, and the marked difference in dynamic stiffness during rest (panel D; modulus = 0.4 $\mu\text{N}/\text{nm}$ at 1 Hz) and during hypoxia (panel C; modulus = 11 $\mu\text{N}/\text{nm}$ at 1 Hz). The calibration bar represents 0.02 μm and 200 μN in panel C, and 0.02 μm and 20 μN in panel D, respectively.

The stiffness of the sarcomeres at the moment of maximal hypoxic contracture increased approximately 12 times compared to control conditions and was totally independent of the frequency of the sinusoidal sarcomere length perturbation (see figures 4 and 5). The phase - frequency relationship, at that time, was also frequency independent as in unstimulated normoxic muscles. As is illustrated in figure 3, the first order band of the diffraction pattern became broader and its intensity decreased during hypoxia, indicating increased sarcomere length dispersion. This resulted in reduced accuracy of the calculated median sarcomere length and increased noise on the calculated sarcomere length (see also figure 1). Hence, in order to compensate for this decrease in signal to noise ratio, force and sarcomere signals were averaged for reliable assessment of the transfer function (see METHODS). Because such analysis of stiffness was time consuming, and thus caused either systematic variation, during the rising phase of unstimulated force, or scatter of the measured transfer function, we limited these measurements to the stage at which the hypoxic contracture was fully developed (cf figure 1).

In order to observe rigor bridges formation during hypoxia, we evaluated the transfer function of a second series of trabeculae at 1 and 100 Hz perturbation frequency. The choice of these perturbations frequencies was prompted by the results from the first series of experiments (cf figures 4 and 5). That is, the ratio of the stiffness modulus at 1 and 100 Hz was maximal during the tetanus under normoxic conditions. Hence, these frequencies provide the maximum sensitivity for discriminating between active cycling of cross-bridges and passive rigor cross-bridges. Figure 6 shows that the stiffness constants at 1 and 100 Hz were similar during the development of the hypoxic contracture, suggesting formation of rigor cross-bridges.

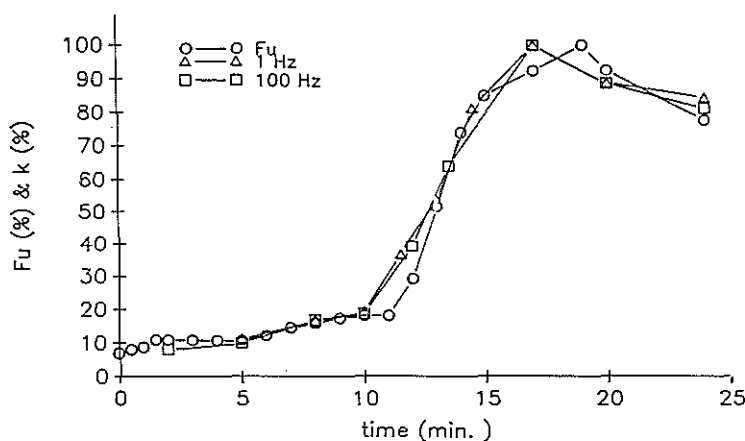


Figure 6 Stiffness at 1 and 100 Hz sinusoidal length perturbations during development of hypoxic contracture

This figure shows the development of unstimulated force (F_u , %) during metabolic inhibition. It is clear that F_u correlates strongly with the increase in stiffness (k , %) both at high frequency and at low frequency during sinusoidal length changes, suggesting that F_u at all time during metabolic inhibition is due to formation of rigor bridges.

DISCUSSION

Force and sarcomere length during hypoxia

Upon induction of hypoxia, twitch force declines in a triphasic manner. The delay between onset of hypoxia and complete loss of active twitch force and development of maximal unstimulated force was substantially longer in our study than in previous reports on the effect of hypoxia on isolated papillary muscles^{2,9,39}. The hypoxic solution that we used in the present study still contained some oxygen ($pO_2 = 5-9$ mm Hg), similar to the pO_2 that was used in the previous studies^{2,9,39}. This fact, combined with the short diffusion distance between the hypoxic solution and the core of the muscle may have been sufficient to maintain oxidative phosphorylation⁹, albeit at reduced level. The trabeculae that were used in the present study sustained stable twitch force development at a high stimulus rate for long periods. In fact, twitch force development decreases about 10% per hour in our trabeculae, independent of stimulus frequency (Bucx & ter Keurs, unpublished observations). The trabeculae used in this study had an average thickness of about 100 μm , which is crucial to their ability to sustain twitch force at high stimulus rates⁴⁰. Isolated cardiac papillary muscle preparations on the other hand, require much lower rates of stimulation for stable twitch force development⁴¹.

The first response to hypoxia was a rapid decline of active twitch force. It seems unlikely that proton accumulation contributed to this decline, since NMR studies have shown that the intracellular pH either slightly decreases or is unaffected shortly after onset of hypoxia^{14,42}. The negative inotropic effect may have been caused by accumulation of inorganic phosphate in the cytosol^{43,44}. This hypothesis is consistent with the observation that the force generated by skinned cardiac fibers is still 40% at an inorganic phosphate concentration of 30 mM, a level one would expect in the cytosol following rapid breakdown of all available creatine phosphate and ATP⁴³. In a recent report Koretsune and Marban⁴² also concluded that accumulation of inorganic phosphate in hypoxic, isolated perfused ferret heart was responsible for the decline in cardiac function during hypoxia. However, reduced delivery of activator calcium ions to the contractile proteins during hypoxia must also be considered as plausible cause of the contractile dysfunction early during hypoxia¹³.

A transient recovery of active force was observed between 10 and 30 minutes after the induction of hypoxia (cf Figure 2). This observation differs from the result of Allen's group⁴⁵ on isolated ferret papillary muscles, in that force recovered much later during our experiments (10-15 min.) than in that study (2 - 5 min), despite the higher stimulus rate in the present study (that is 1 Hz vs 0.33 Hz). Intracellular pH has been shown to increase transiently during the first minutes of hypoxia, probably as a result of phosphocreatine breakdown^{14,45}, which would explain the increase in twitch force that occurs almost immediately after onset of anoxia. It is not likely that this explanation also applies to the temporary recovery of force in these experiments, because we would expect that such alkalosis would occur earlier, rather than later because of the higher stimulus rate that we have used. On the other hand our use of higher stimulus rates may have obscured an increased of force, concurrent with the breakdown of phosphocreatine.

An alternative explanation for the observed late transient rise of force is that Ca^{2+} ions accumulate in the cytosol as several investigators have reported⁵⁻¹³. Accumulation of calcium ions in the cytosol, due to decrease of the extrusion rate of calcium by the sarcoplasmic reticulum and Na^+/Ca^{2+} exchange of the sarcolemma, would not only explain a temporary increase of the force of the twitch, but is also consistent with the increase of the duration of the relaxation phase of the twitch and increase of spontaneous

sarcomere activity during the transient increase of twitch force (as shown in figures 1 and 2). The increase of intracellular calcium ions would be expected to lead to spontaneous sarcomere fluctuations, because of spontaneous Ca^{2+} release by the sarcoplasmic reticulum⁴⁸. The transient increase in the stiffness during this phase is also consistent with active, diastolic, calcium activated cycling of cross-bridges during this phase (see below).

Dynamic transfer function analysis in caffeine tetani

The stiffness in relaxed muscle during normoxia was frequency independent, as one would expect from a simple spring with negligible viscosity. The viscosity of relaxed cardiac muscle is indeed small (less than 4% of twitch force at 50 $\mu\text{m/s}$ velocity of sarcomere length change⁴⁷), which predicts that the modulus of the transfer function at a frequency of 100 Hz would amount to 0.2 which is comparable to the measured value of 10%. The transfer function of the central sarcomeres during normoxic caffeine tetani was similar to that which has been reported for isolated papillary muscles^{30,31}. Those studies were performed either at the level of the entire muscle³⁰ or at the level of a central segment of the muscle, delineated with needles piercing the muscle³¹. During the tetanus, the sarcomeres were compliant at perturbation frequencies below 1 Hz, their stiffness was minimal at 0.8 Hz, and then rose ten fold at 100 Hz. Distinct from previous studies, however, is the observation that the difference between the minimal stiffness at 0.8 Hz and the stiffness at 0.2 Hz was hardly significant. Furthermore, the frequency at which minimal stiffness was found in this study was lower than previously reported for rabbit papillary muscle³¹ and for rat papillary muscle³⁰, even though the temperature in this study was about 5 C higher (30 C) and we used rat trabeculae which are capable of higher velocity of shortening than rabbit myocardium. The reasons for these differences are not clear. They may reside in the preparations used, or in the fact that we studied caffeine tetani, whereas previous studies have used barium or potassium contracture. Thirdly, it is possible that damaged regions in the muscle may be compliant in the frequency range of minimal stiffness. Further analysis of this difference is warranted because the frequency at which minimal stiffness is found has been suggested to reflect the cycling rate of cardiac cross-bridges during isometric contraction^{30,31}. Important to the purpose of the present study however, is that the ratio between the stiffness at high frequency (e.g. 100 Hz) and low frequency (i.e. 1 Hz) increased greatly during caffeine induced tetani. This showed that sensitive measurement of active cycling cross-bridge activity was possible in our trabeculae.

Dynamic transfer function analysis during hypoxia

As was pointed out in the introduction, active cycling of cross-bridges can occur both in the presence and absence of raised levels of cytosolic calcium^{18,23}, a notion which complicates discrimination between the two alternative hypothesis of hypoxic contracture, i.e. rigor cross-bridge or intracellular calcium overload. Therefore, in the present study dynamic transfer function analysis was employed to quantify the relative contribution of active cross-bridge cycling and rigor cross-bridge bonds to the development of hypoxic contracture in myocardium. For this purpose, the properties of unstimulated trabeculae during hypoxia were compared to those of relaxed and tetanized muscles during normoxia. Following the development of maximal hypoxic contracture, a rapid release of the muscle was not followed by recovery of force. Furthermore, no spontaneous sarcomere motion was observed during this phase. Similarly, the stiffness of hypoxic muscles during this phase of the hypoxic contracture was independent of the frequency of the sarcomere length perturbations, as in relaxed muscle, except that the stiffness was 12 to 20-fold higher (cf Figure 5). Figure 6 shows, that also during the development of the hypoxic contracture the increase in unstimulated force can almost completely be ascribed to the

formation of rigor cross-bridges. Hence, our mechanical measurements, made at the level of the sarcomeres, clearly demonstrate that the source of unstimulated force in hypoxic contracture in myocardium is caused by rigor cross-bridge formation, rather than active cycling of cross-bridges.

Why would rigor cross-bridges form during the development of hypoxic contracture in these trabeculae, while the ATP concentration is not likely to have decreased during this phase⁴². Two possibilities come to mind. First, the actual threshold concentration of ATP required for rigor cross-bridge bonds is a function of phosphocreatine⁴⁸ and ADP concentrations^{48,49}, and is facilitated by elevated levels of calcium ions in the cytosol²³. The second possibility is the existence of non-uniformity of ATP concentrations in the muscle, either at the intercellular or intracellular level.

At the intercellular level, this implies that ATP could decrease in some myocytes to levels that cause rigor in some cells, while it is still in the normal range in others. Experiments on the effects of anoxia in myocytes indeed have shown considerable non-uniformity among cells^{50,51}. The increase of the width and the decrease in the amplitude of the first order diffraction band during hypoxia (cf. Figure 3) reflect an increase in the non-uniformity of sarcomere length in the muscle, consistent with this hypothesis. Also, one would expect that the development of rigor in a subset of cells in the muscle would decrease external developed twitch force by the still contracting cells. This might have contributed to the observed coincidence of the increase in unstimulated force and the decline in active developed twitch force during the development of the hypoxic contracture (cf. Figures 1 and 2).

Finally, non-uniformity in ATP levels at the intracellular levels could also explain rigor cross-bridge formation in the presence of a relatively high overall level of ATP. During hypoxia, transportation of ATP from the mitochondria to the cytosol of the myocyte may be impaired, as was suggested by Gudbjarnason⁵². Recent evidence of differences in ATP content in various cellular organelles lends support to this hypothesis⁵³.

In summary, in the present study the dynamic transfer function between force and sarcomere length was studied during hypoxia in rat cardiac trabeculae. The dynamic stiffness at the time at which the hypoxic contracture was fully developed indicated the presence of rigor cross-bridges only. Similarly, the development of the hypoxic contracture could also be ascribed to the formation of rigor cross-bridges, although a small component of active cross-bridge cycling was transiently detected.

ACKNOWLEDGEMENTS

The skillful technical assistance of Mrs Tin Nguyen and A.S. Nieukoop is gratefully acknowledged. The secretarial contribution of Mrs C.W.J.M. Lutikhuis is appreciated.

REFERENCES

1. Tennant R, Wiggers CS. The effect of coronary occlusion on myocardial contraction. *Am J Physiol* 1935; 112: 351-361
2. Allen DG, Orchard CH. Myocardial contractile function during ischemia and hypoxia. *Circ Res* 1987; 60: 153-168
3. Leijendekker WJ, Gao WD, ter Keurs HEDJ. Unstimulated force during hypoxia of rat cardiac muscle: stiffness and calcium dependence. *Am J Physiol* 1990; 258: H861-H869
4. Koretsune Y, Marban E. Mechanism of ischemic contracture in ferret hearts: relative roles of intracellular calcium elevation and ATP depletion. *Am J Physiol* 1990; 258: H9-H16

5. Steenbergen C, Murphy E, Levy L, London RE. Elevation in free calcium concentration early in myocardial ischemia in perfused rat heart. *Circ Res* 1987; 60: 700-707
6. Allen DG, Orchard CH. Intracellular calcium concentration during hypoxia and metabolic inhibition in mammalian ventricular muscle. *J Physiol (Lond)* 1983; 339: 107-122
7. Lee H-C, Mohabir R, Smith N, Franz MR, Clusin WT. Effect of ischemia on calcium-dependent fluorescence transients in rabbit hearts containing indo. 1. Correlation with monophasic action potentials and contraction. *Circulation* 1988; 78: 1047-1059
8. Barry WH, Peeters GW, Rasmussen CAFJr, Cunningham MJ. The role of changes in $[Ca^{2+}]_i$ in energy deprivation contracture. *Circ Res* 1987; 61: 726-734
9. Nayler WG, Poole-Wilson PA, Williams A. Hypoxia and calcium. *J Mol Cell Cardiol* 1979; 11: 683-706
10. Smith GL, Allen DG. Effects of metabolic blockade on intracellular calcium concentration in isolated ferret ventricular muscle. *Circ Res* 1988; 62: 1223-1236
11. Steenbergen C, Murphy E, Watts JA, London RE. Correlation between cytosolic free calcium, contracture, ATP, and irreversible ischemic injury in perfused rat heart. *Circ Res* 1990; 66: 135-147
12. Marban E, Kirakaze M, Koretsune Y, Yuc DT, Chacko VP, Pike MM. Quantification of $[Ca^{2+}]_i$ in perfused hearts. Critical evaluation of the 5F-BAPTA and nuclear magnetic resonance method as applied to the study of ischemia and reperfusion. *Circ Res* 1990; 66: 1255-1267
13. Kihara Y, Grossman W, Morgan JP. Direct measurement of changes in intracellular calcium transients during hypoxia, ischemia, and reperfusion of the intact mammalian heart. *Circ Res* 1989; 65: 1029-1044
14. Allen DG, Morris PG, Orchard CH, Pirolo JS. A nuclear magnetic resonance study of metabolism in the ferret heart during hypoxia and inhibition of glycolysis. *J Physiol* 1985; 361: 185-204
15. Humphrey SM, Holliss DG, Seelye RN. Adenine pool catabolism in the ischemic, the calcium-depleted ischemic, and the substrate free anoxic isolated rat heart: Relationship to contracture development. *J Mol Cell Cardiol* 1984; 16: 1127-1136
16. Lowe JE, Jennings RB, Reimer KA. Cardiac rigor mortis in dogs. *J Mol Cell Cardiol* 1979; 11: 1017-1031
17. Lewis MJ, Grey AC, Henderson AH. Determinants of hypoxic contracture in isolated heart muscle preparations. *Cardiovasc Res* 1979; 13: 86-94
18. Nichols CG, Lederer WJ. The role of ATP in energy-deprivation contractures in unloaded rat ventricular myocytes. *Can J Physiol Pharmacol* 1989; 68: 183-194
19. Bridge JHB, Spitzer KW, Ershler PR. Relaxation of isolated ventricular cardiomyocytes by a voltage dependent process. *Science* 1988; 241: 823-825
20. Anderson SE, Murphy E, Steenbergen C, London RE, Cala PM. Na^+-H^+ exchange in myocardium: Effects of hypoxia and acidification on Na^+ and Ca^{2+} . *Am J Physiol Cell Physiol* 1990; 259: C940-C948
21. Poole-Wilson PA, Tones MA. Sodium exchange during hypoxia and on reoxygenation in the isolated rabbit heart. *J Mol Cell Cardiol* 1988; 20(Sup II): 15-22
22. Wexler LF, Weinberg ED, Ingwall JS, Apstein CS. Acute alternations in diastolic left ventricular chamber distensibility: Mechanistic differences between hypoxemia and ischemia in isolated perfused rabbit and rat hearts. *Circ Res* 1986; 59: 515-528
23. Bremel RD, Weber A. Cooperation within actin filaments in vertebrate skeletal muscle. *Nature* 1972; 238: 97-101
24. Hajjar RJ, Gwathmey JK. Direct evidence of change in myofilament responsiveness to Ca^{2+} during hypoxia and reoxygenation in myocardium. *Am J Physiol Heart Circ Physiol* 1990; 259: H748-H795
25. Lewis MJ, Housmans PR, Claes VA, Brutsaert DL, Henderson AH. Myocardial stiffness during

- hypoxic and reoxygenation contracture. *Cardiovasc Res* 1980; 14: 339-344
26. Holubarsch Ch. Force generation in experimental tetanus, KCl contracture, and oxygen and glucose deficiency contracture in mammalian myocardium. *Pflug Arch* 1983; 396: 277-284
 27. Holubarsch Ch, Alpert NR, Goulette R, Mulieri LA. Heat production during hypoxic contracture of rat myocardium. *Circ Res* 1982; 51: 777-786
 28. Kawai M, Brandt PW. A high resolution method for correlating biochemical reactions with physiological processes in activated skeletal muscles of rabbit, frog and crayfish. *J Mol Cell Cardiol* 1980; 1: 279-303
 29. Calancie B, Stein R. Measurement of the rate constants for the contractile cycle of intact mammalian muscle fibers. *Biospys J* 1987; 51: 149-159
 30. Rossmann GH, Hoh JFY, Kirman A, Kwan LJ. Influence of V_1 and V_3 isoenzymes on the mechanical behaviour of rat papillary muscle as studied by pseudo-random binary noise modulation length perturbations. *J Muscle Res Cell Motil* 1986; 7: 307-319
 31. Shibata T, Hunter WC, Yand A, Sagawa K. Dynamic stiffness measured in central segment of excised rabbit papillary muscles during barium contracture. *Circ Res* 1987; 60: 756-768
 32. de Tombe PP, ter Keurs HEDJ. Force and velocity of sarcomere shortening in trabeculae from rat heart: effects of temperature. *Circ Res* 1990; 66: 1239-1254
 33. Kentish JC, ter Keurs HEDJ, Ricciardi L, Bucx JJJ. Comparison between the sarcomere length-force relations of intact and skinned trabeculae from rat right ventricle. *Circ Res* 1986; 58: 755-768
 34. ter Keurs HEDJ, Rijnsburger WH, van Heuningen R, Nagelsmit MJ. Tension development and sarcomere length in rat cardiac trabeculae: Evidence of length-dependent activation. *Circ Res* 1980; 46: 703-714
 35. Daniels M, Noble MIM, ter Keurs HEDJ, Wolhfarth B. Velocity of sarcomere shortening in rat cardiac muscle: relationship to force, sarcomere length, calcium and time. *J Physiol* 1984; 355: 367-381
 36. Hyltgren PB, Hamrell BB. Increased active elastic stiffness in tetanized papillary muscles from hypertrophied rabbit hearts. *Basic Res Cardiol* 1986; 81: 508-516
 37. Forman R, Ford LE, Sonnenblick EH. Effect of muscle length on the force-velocity relationship in tetanized cardiac muscle. *Circ Res* 1972; 31: 195-206
 38. Snedecor GW, Cochran WG. Statistical methods, Ames, Iowa, Iowa State University Press, 1973.
 39. Cobbe SM, Poole-Wilson PA. Tissue acidosis in myocardial hypoxia. *J Mol Cell Cardiol* 1980; 12: 761-770
 40. Schouten VJA, ter Keurs HEDJ. The force-frequency relationship in rat myocardium. The influence of muscle dimensions. *Pflug Arch* 1986; 407: 14-17
 41. Paradise NF, Schmitter JL, Surmitis JM. Criteria for adequate oxygenation of isometric kitten papillary muscle. *Am J Physiol Heart Circ Physiol* 1981; 241: H348-H353
 42. Koretsune Y, Marban E. Relative roles of Ca^{2+} -dependent and Ca^{2+} -independent mechanisms in hypoxic contractile dysfunction [see comments]. *Circulation* 1990; 82: 528-535
 43. Kentish JC. The effects of inorganic phosphate and creatine phosphate on force production in skinned muscle from rat ventricle. *J Physiol* 1986; 370: 585-604
 44. Nosek TM, Leal-Cardoso JH, McLaughlin M, Godt RE. Inhibitory influence of phosphate and arsenate on contraction of skinned skeletal and cardiac muscle. *Am J Physiol Cell Physiol* 1990; 259: C933-C939
 45. Allen DG, Morris PG, Orchard CH. A transient alkalosis precedes acidosis during hypoxia in ferret heart. *J Physiol* 1983; 343: 58P-59P
 46. Fabiato A. Spontaneous versus triggered contractions of "calcium-tolerant" cardiac cells from the adult rat ventricle. *Basic Res Cardiol* 1985; 80(Suppl 2): 83-88

47. de Tombe PP. Determinants of velocity of sarcomere shortening in mammalian myocardium. PhD Thesis. University of Calgary, 1989.
48. Ventura-Clapier R, Mekhfi H, Vassort G. Role of creatine kinase in force development in chemically skinned rat cardiac muscle. *J Gen Physiol* 1987; 89: 815-837
49. Miller DJ, Smith GL. The contractile behaviour of EGTA and detergent-treated heart muscle. *J Muscle Res Cell Motil* 1985; 6: 541-568
50. Stern MD, Chien AM, Capogrossi MC, Pelto DJ, Lakatta EG. Direct observation of the "oxygen paradox" in single rat ventricular myocytes. *Circ Res* 1985; 56: 899-903
51. Haworth RA, Nicolaus A, Goknur AB, Berkoff HA. Synchronous depletion of ATP in isolated adult rat heart cells. *J. Mol Cell Cardiol* 1988; 20: 837-846
52. Gudbjarnason S, Mathes P, Ravens KG. Functional compartmentation of ATP and creatine phosphate in heart muscle. *J Mol Cell Cardiol* 1970; 1: 325-339
53. Geisbuhler T, Altschuld RA, Trewyn RW, Ansel AZ, Lamka K, Brierley GP. Adenine nucleotide metabolism and compartmentalization in isolated adult rat heart cells. *Circ Res* 1984; 54: 536-546

CHAPTER 9

SARCOMERE DYNAMICS AND RELAXATION CHARACTERISTICS OF RAT CARDIAC TRABECULAE DURING REPEATED HYPOXIA AND REOXYGENATION

Jeroen JJ Buxx, Peter P de Tombe, John V Tyberg and Henk EDJ ter Keurs

Preliminary results of this work have been published previously in the forms of abstracts:

Buxx JJJ, Sethi S, ter Keurs HEDJ. Sarcomere dynamics and relaxation during hypoxia and reoxygenation in Rat myocardium. *Circulation* 1987; 76: IV-57

CHAPTER 9

SARCOMERE DYNAMICS AND RELAXATION CHARACTERISTICS OF RAT CARDIAC TRABECULAE DURING REPEATED HYPOXIA AND REOXYGENATION

Jeroen JJ Buxx, Peter P de Tombe, John V Tyberg and Henk EDJ ter Keurs

ABSTRACT

In the heart, ischemia results in an upward shift of the end-diastolic pressure - volume relationship and impaired relaxation rate, which may be accounted for by Ca^{2+} overload and rigor bond formation, alone or in combination. Since these mechanisms are difficult to study in the intact heart, the effects of repeated hypoxia was analyzed in isolated rat cardiac trabeculae. Twitch force (F_a) was measured with a strain gauge, and sarcomere length (SL) by laser diffraction techniques. Twitch parameters TPT (time to peak tension), RT (time from 100% to 50% F_a), T_{90-80} (time from 90% to 80% F_a) and T_{80-40} (time from 60% to 40% F_a) was calculated from sampled twitches. RMS SL noise was quantified from mean SL obtained by a running average technique. $[\text{Ca}^{2+}]$ of normoxic medium (pH 7.4, pO_2 500 - 600 mm Hg) was adjusted to 80% of maximal twitch force, assessed by extrasystolic potentiation (resting SL = 2.1 μm ; 30 °C). Following baseline measurements, hypoxia (pH 7.4, pO_2 6 - 9 mm Hg, no glucose) was continued until twitch force had decreased by 50%, followed by reoxygenation until complete recovery; the procedure was repeated twice. At normoxia a unique relationship between relaxation parameters and twitch force was observed, independent of Ca^{2+} and SL; all twitch parameters, except T_{80-40} , decreased during hypoxia, followed by a recovery with overshoot during reoxygenation. Except for TPT, twitch parameters, relative to normoxia, initially increased during hypoxia, and further increased shortly after reoxygenation, followed by a gradual normalization. Diastolic RMS SL noise increased to 192% shortly after reoxygenation. Microscopic examination, then, showed localized SL shortening and propagated aftercontractions. The diastolic force - SL relation during repeated hypoxia was indistinguishable from normoxia; neither did sarcomere shortening pattern, reflecting compliance of the series elastic element, change during the experiment. The increased RMS SL noise following stepwise increased stimulus rate during hypoxia followed a comparable pattern.

Our results suggest that impaired relaxation during repeated hypoxia is accounted for by calcium overload without evidence for rigor bound formation or a shift of the diastolic force - SL relation.

INTRODUCTION

Ischemia depresses contractility of the myocardium and interferes with normal relaxation (Tennant and Wiggers, 1935). This may lead to dyskinetic wall motion, both during systole and early relaxation, as has been shown by contrast ventriculography in animal experiments and in patients with ischemic heart disease (Helfant, 1977). Likewise, ischemia may impede diastolic function of the left ventricle; it has been hypothesized that this may be accounted for changed active and passive elasticity of the left ventricle (Barry, 1974; Bourdillon, 1983; Grossman, 1990; Hess, 1983; Nakamura et al., 1986; Paulus, 1982; Serizawa, 1981; Tyberg, 1969).

Both systolic and diastolic dysfunction may become evident or aggravate at increased left ventricular work. Sometimes dyskinesia occurs without signs of ischemia, sometimes it is aggravated or provoked by spontaneous angina pectoris or elicited by atrial pacing (Pasternac, 1972; Sharma, 1980). Likewise diastolic dysfunction may be provoked or aggravated by atrial pacing in presence of a critical coronary artery stenosis (McLaurin, 1973; Paulus, 1985; Serizawa, 1980).

It has been shown that the initial effects of ischemia on relaxation rate and compliance of the ventricular wall may be, at least in part, related to Ca^{2+} overload as a result of disturbed calcium handling by the myocyte. Studies of drugs that affect transmembrane or sarcoplasmic reticulum calcium transport are in agreement with this hypothesis (Carter, 1986; Fabiato and Fabiato, 1978; Nakaya, 1985; Narita et al, 1982; Paulus, 1982; Wilde and Kleber, 1986). During protracted ischemia, the decreased compliance may be accounted for by rigor bond formation between actin and myosin filaments as a consequence of decreased intracellular ATP levels (Ventura-Clapier and Vassort, 1981; Holubarsch, 1982).

In the present study we tested the hypothesis that repeated hypoxia and reoxygenation triggers spontaneous repetitive Ca^{2+} release by the sarcoplasmic reticulum, leading to impaired relaxation.

In view of analysis problems, that are inherent to the use of intact hearts, we preferred to use linear preparations, i.e. isolated rat cardiac trabeculae, to study this phenomenon. Sarcomere length of the viable central part of the muscle was measured continually. Noise of the sarcomere length signal was quantified off-line and related to relaxation indices. Diastolic stiffness was evaluated by comparison of the passive force - sarcomere length relation during normoxia with repeated hypoxia. The sarcomere shortening pattern during normoxia was used to evaluate the stiffness of the series elastic element and subsequently compared with hypoxia and reoxygenation.

Since increased performed work during hypoxia is known to have a negative effect on relaxation properties, we analysed this phenomenon and its underlying mechanism by a stepwise increase of the stimulus rate during hypoxia.

Parts of this study have been presented previously.

MUSCLE PREPARATION

Sprague-Dawley rats, weighting 200 - 300 gr, were anaesthetized with ethylether. Following excision from the animal, the heart was perfused within 30 seconds according the Langendorff technique with a modified Krebs - Henseleit solution. The composition of the medium was (in mM): Na^+ 150, K^+ 5, Cl^- 127.5, Mg^{2+} 1.2, H_2PO_4^- 2, SO_4^{2-} 1.2, HCO_3^- 27, glucose 10.1, Ca^{2+} 1.5. Fifteen mM of KCl was added to stop spontaneous beating. Trabeculae ($n = 10$, average length 3.1 ± 0.3 mm, average width 226 ± 59 μm , average thickness 104 ± 36 μm), attached to both the tricuspid valve and the free wall of the right ventricle, were dissected. All muscles were ribbon shaped and uniform in thickness and width. A piece of the valve and a cube of the right ventricle were retained for mounting. Following dissection, the muscles were transferred to the bath (width 3 mm, height 4 mm, length 30 mm, content 360 μl) and attached to a motor arm and a force transducer and superfused with Krebs-Henseleit solution (temperature 29.8 ± 0.3 C, flow 8 - 16 ml/min).

During the experiments at normoxia, the superfusate was in equilibrium with a gas mixture of 95% O_2 and 5 % CO_2 (pH 7.4, pO_2 500 - 600 mm Hg). During hypoxia, the preparations were superfused with glucose-free medium that was in equilibrium with 95% N_2 and 5% CO_2 (pH 7.4, pO_2 6 - 9 mm Hg). The muscles were stimulated at 1 Hz by platinum electrodes that were placed in the wall of the muscle chamber. Twitch force (F) was measured with a silicon strain gauge covered with silicon adhesive (AME AE 801, Norton, Norway). The sensitivity of the transducer was 3 mV/mN; resonance frequency 3 KHz; drift less than 0.1 mN/hour. The developed stress was calculated from peak twitch force at a sarcomere length of 2.0 μm , and the cross-sectional area of the muscle; the average stress was 71 ± 30 mN/mm². The valvular end of the preparation was attached to a stainless steel hook of a carbon fiber motor arm (Fokker Aviation Industries, The Netherlands) connected to the axis of a motor that was controlled by a dual servo amplifier (Model 300 Cambridge Technology, Cambridge, Massachusetts, U.S.A.). The step response time of the motorarm was 1.5 msec (ter Keurs et al., 1980a; Kentish et al., 1986).

The sarcomere length in the preparation was measured by a laser diffraction technique, as has been reported previously (van Heuningen, 1980). In short, an incident laser beam, diameter 400 μm , was projected on the muscle. Subsequently, the generated diffraction pattern was projected via mirrors on a photodiode array (Reticon RL 512) that was scanned twice per millisecond. Median sarcomere length was calculated from the light intensity distribution on the array. Prior to the experiments, the circuitry was calibrated with gratings that were placed at the level of the muscle. The calibration error was smaller than 1%. The resolution of the measurement in cardiac trabeculae was limited by noise to 5 nm optimally and 20 nm nominally. Horizontal and vertical displacement during the contraction were avoided by appropriate mounting. The bottom and cover of the bath consisted of thin glass plates to enable undisturbed detection of the diffraction pattern.

During the experiments the preparations were observed with an inverted microscope (Zeiss, 14612) and T.V. camera (Panasonic TV camera, model WV-1500) and video monitor (Panasonic video monitor, model TR-930 UC). Force, muscle length, sarcomere length as well as bath temperature and stimulus trigger were recorded on an instrumentation recorder (Gould Instrumentation Recorder 6500) and 8 channel paper pen recorder (Gould 2800S). Selected force and sarcomere length signals were digitized (DT2801, Data Translation, Inc., Marlborough, Mass., U.S.A.) and stored on a Winchester hard disc of a personal computer (IBM PC/AT) for further analysis of twitch characteristics (sampling rate 900 Hz/channel).

EXPERIMENTAL PROTOCOL

After one hour of stabilization of the muscles, the relation between force and sarcomere length was determined as follows. First, muscle length was adjusted to a resting sarcomere length of 2.1 - 2.15 μm . Then, muscle length was changed again and kept constant during the subsequent four test beats. Force and sarcomere length were measured immediately before and at peak twitch force of the last test beat. Active force was calculated as peak twitch force minus resting force at the sarcomere length that was attained during the twitch; this assumes that the parallel elastic elements are in, or in parallel with the sarcomeres (ter Keurs et al., 1980a). Between each series of test beats, sarcomere length was maintained at 2.1 μm for 6 - 10 beats. The procedure was repeated for a range of sarcomere lengths at calcium concentrations, that were varied between 0.3 mM and 5.1 mM in steps of 0.3 mM.

Maximum twitch force (F_{max}) was assessed by extrasystolic potentiation at $[\text{Ca}^{2+}]_o$ exceeding 0.6 mM; the protocol consisted of administering a series of 3, 5, 7, 10, 15 or 20 stimuli at intervals of 300 msec. F_{max} was defined as maximum twitch force that was attained following the last potentiating beat (Schouten et al., 1990). Steady state force at $[\text{Ca}^{2+}]_o$ of 1.2 mM varied from 50 - 85% F_{max} in 7 preparations. Prior to hypoxia, peak twitch force of all muscles was equal to 80 - 85% of F_{max} following adjustment of the superfusate $[\text{Ca}^{2+}]_o$ to values between 2.1 and 5.1 mM.

The following parameters were calculated from the twitches at control conditions and during repeated hypoxia: unstimulated force (F_u) and SL (SL_u), peak twitch force (F_a) and sarcomere length at the same moment (SL_a), time to peak tension (TPT) i.e. the interval between stimulus and peak twitch force, relaxation time (RT) i.e. the time interval for F_a to decrease to half of its value (see Figure 1). The twitch relaxation was also expressed as T_{90-80} and T_{60-40} , representing the interval required for twitch force to decrease from 90% to 80% and from 60% to 40% of its maximum, respectively. Under control conditions, the relationship between these twitch parameters and sarcomere length was complex and depended on $[\text{Ca}^{2+}]_o$ in the medium. This contrasted with the relation with force, that was independent of sarcomere length and $[\text{Ca}^{2+}]_o$, and comparable though not identical for different muscles. Therefore for

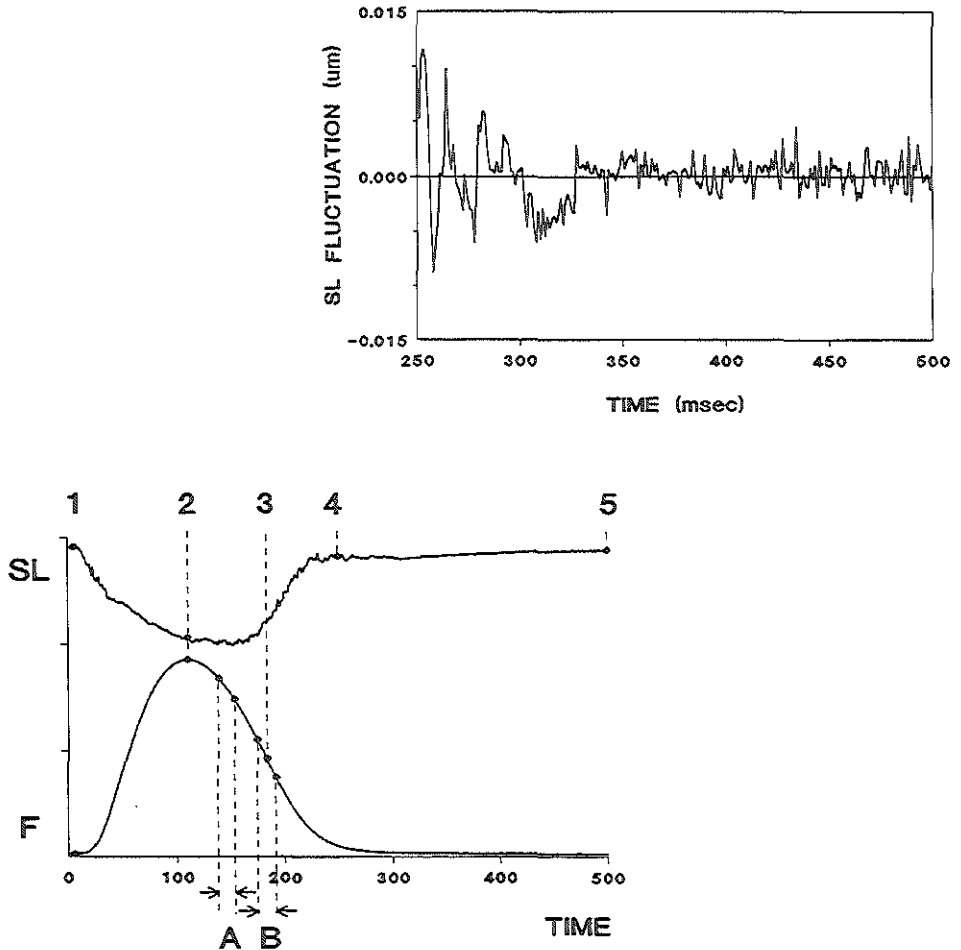
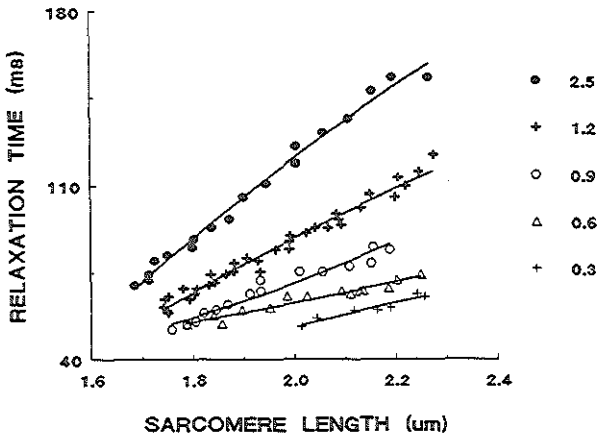


Figure 1: Sarcomere length and twitch force recordings

Sarcomere length (SL), top tracing, and twitch force (F), bottom tracing, are recorded simultaneously. Following stimulation, SL shortens from its resting value of $2.11 \mu\text{m}$ to $1.83 \mu\text{m}$ at peak twitch force (1.86 mN). Subsequently force declines to zero at 250 msec; initially SL is attained at its shortest length but then gradually lengthens again to control value. The twitch indices time to peak twitch (TPT) and relaxation time (RT), that were calculated from the sampled twitches, are also shown. TPT was defined as the interval between 1 and 2, RT between 2 and 3, respectively. T_{90-80} (A) and T_{60-40} (B) represent the time for twitch force to decrease from 90 to 80%, and 60 to 40 % of its peak, respectively. The presence of high frequency oscillations of the calculated sarcomere length signal was quantified by calculation of the root mean square (RMS) value of the sarcomere length noise. RMS SL noise was calculated during the intervals 90 - 250 msec, 250 - 500 msec (in the figure: 4 - 5) and 500 - 1000 msec. The inset shows the fluctuations of the SL around the mean SL, determined by the use of a running average of 70 datapoints. Stimulus rate 1 Hz. Sample frequency 900 Hz. Calibrations: total timescale 500 msec, sarcomere length $0.3 \mu\text{m}$, force 1 mN per division. $[\text{Ca}^{2+}]_0$ 5.1 mMol/L. Temperature 29.6°C . Stress 67 mN/mm^2 .

each muscle, the relationship between time to peak tension and the relaxation parameters, and steady state force (80% - 85% F_{max}), was fitted to the equation: Twitch parameter = $A * F_a + B + C * \exp(-D * F)$, where Twitch parameter was expressed in msec, F_a in mN, and the constants A, B, C and D in msec/mN, msec, msec and 1/mN, respectively. The constants were calculated by means of an iterative non-linear least-squares fitting program of the Marquardt type (Bevington, 1969). The relationships were used to relate the muscle parameters, that were measured during the hypoxia experiments, to their normoxic values; the calculated ratios were defined as RRT for relative relaxation rate, RTPT for relative time to peak tension, and Rt_{90-80} and Rt_{80-40} for the relative t_{90-80} and t_{80-40} , respectively.

RELAXATION TIME vs SARCOMERE LENGTH at varied Ca^{++} concentration



RELAXATION TIME vs FORCE

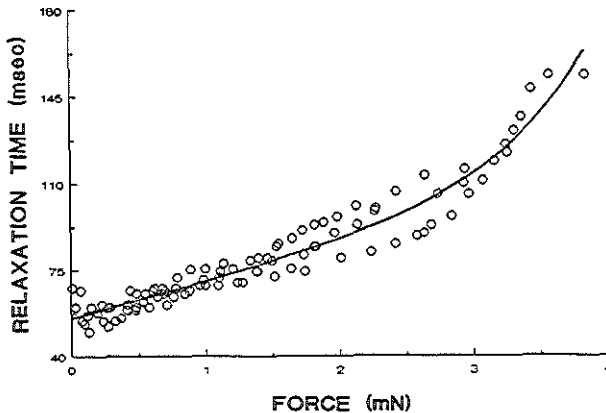


Figure 2A and 2B: Figure 2A (upper panel) shows the relation between relaxation time (msec) and sarcomere length (μm) at varied $[Ca^{2+}]$ of the perfusion medium (0.3 - 2.5 mmol/L). Figure 2B shows the dependence of relaxation time on force at $[Ca^{2+}] = 1.2$ mmol/l of the same muscle.

After assessment of control characteristics, superfusion was switched to hypoxic solution, followed by reoxygenation as soon as F_a decreased to 50% of control level. The intervention was repeated twice in all muscles, except one. Prior to repeated hypoxia, force had fully recovered and was stable again. During the experiments temperature, stimulus rate and resting sarcomere length were kept constant, since pilot studies had shown that the effect of hypoxia was influenced by these parameters.

F_a was determined at steady state normoxic conditions (N), and during hypoxia, at the moment of the transient plateau (A) and partial recovery of force (B) as well as immediately before reoxygenation (see figure 3). In addition, F_a was measured during reoxygenation following maximal recovery of force (C), at its transient undershoot that followed thereafter (D) and prior to the next hypoxic intervention. In individual muscles, F_a was not significantly different at comparable stages of the

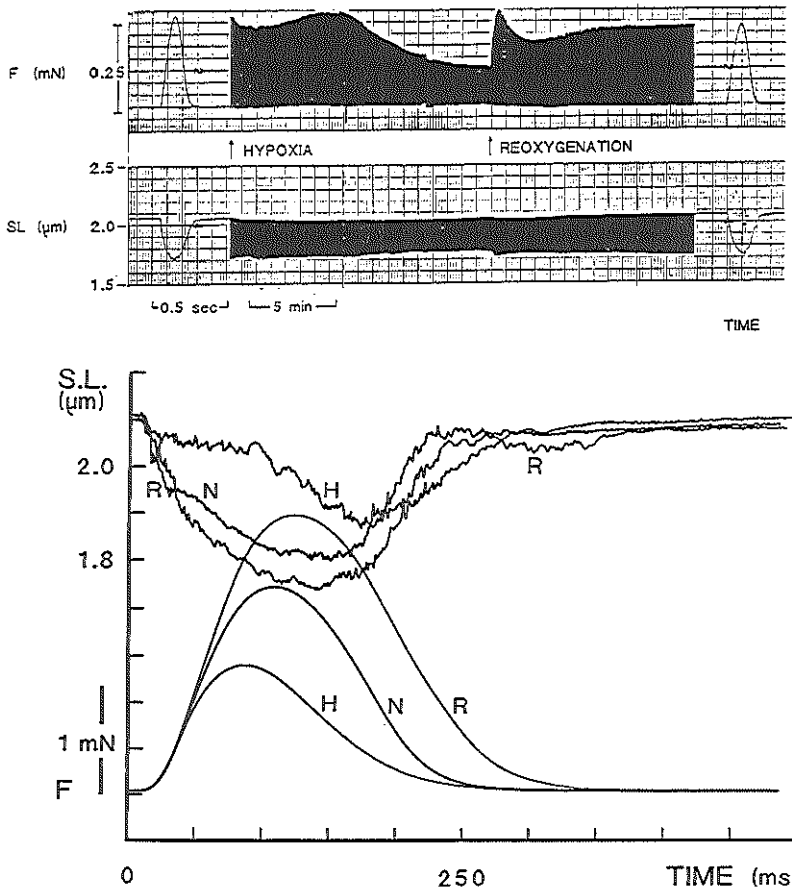


Figure 3 A and B: Figure 3A shows a typical example of the changes of peak twitch force (F) and sarcomere length (SL) that was recorded after the switch to hypoxia and subsequent reoxygenation. Figure 3B shows individual recordings of F and SL at normoxia (N), at the end of hypoxia (H) and shortly after reoxygenation (R) when F was maximal. Note the prolongation of twitch duration and a secondary shortening of SL following the initial SL shortening. For further explanation see text.

experiment (repeated measures analysis of variance (ANOVA), $p = \text{N.S.}$). Consequently, the means of consecutive interventions were calculated; paired Student T-tests were applied to assess the level of significance of the differences between the calculated means (see table I).

The same applied to the means of the absolute and relative TPT and relaxation parameters, that were determined at steady state conditions (N), at the end of hypoxia (H) and following reoxygenation (R) (see table III and IV). The timing of the latter measurements was determined by the moment when RT or RRT was maximal, respectively.

Sarcomere length was calculated prior to stimulation and at peak twitch force (SL_u and SL_{∞} , respectively). The diastolic passive force - SL_u relationship was assessed under normoxic conditions and compared with repeated hypoxia. The $[Ca^{2+}]$ in the medium differed by less than 0.3 mM/L under either condition.

The pattern of shortening of the sarcomeres in the viable center of our preparations is governed by the compliance of the series elastic element. Therefore, the sarcomere shortening pattern reflects the passive behaviour of this muscle component. It is conceivable that changes in the stiffness of the series elastic element may influence the relaxation indices; therefore the relation between instantaneous SL at increasing twitch force was analysed during separate twitches at normoxia, at the end of hypoxia and at maximal RRT; detection of possible shifts or changes in the slopes of these relationships was facilitated by superimposing consecutive records.

The spontaneous fluctuation of sarcomere length was determined as follows. The sarcomere length signal (900 data points) was filtered by calculating a running average of 70 datapoints. Subsequently the filtered signal was subtracted from the original signal; the standard deviation of the difference between both signals (RMS noise level) was calculated, representing fluctuations of the measured sarcomere length. Sarcomere length noise was not only quantified during the decline of twitch force (interval 100 - 250 msec; SLN_1), but also in between twitches (interval 250 - 500 msec (SLN_2), and 500 - 960 msec (SLN_3), respectively). The relationship between attained sarcomere length and noise of the sarcomere signal was evaluated under steady state conditions at $[Ca^{2+}]_o$ that was equal to hypoxia or 0.3 mM/L less. In addition, sarcomere length noise was quantified during repeated hypoxia.

The applicability of SLN_1 was limited for the following reasons. Typically, the switch from hypoxia to reoxygenation induced an increase of SLN_2 and SLN_3 without significant changes in SLN_1 (see below). This response of SLN_1 was explained by the use of a running average technique to obtain the mean sarcomere length tracing. As a result of the time delay between the processed and original signal, the calculated SL noise overestimated real SL fluctuations, notably when sarcomere length changed rapidly. Since SLN_1 was calculated at the moment when resting sarcomere length was not yet attained, we chose not to use it for the analysis of changes in sarcomere length fluctuations. SLN_2 was less hampered by this problem since the sarcomeres had resumed their resting length when this parameter was calculated. At high stimulus rates, when twitch duration was reduced and SLN_3 could not be calculated, SLN_2 was used as a measure of SL fluctuations.

STATISTICS

Repeated measures analysis of variance (repeated ANOVA) was employed to test for statistically significant differences within one twitch parameter at the same consecutive stages of hypoxia experiments. Since this analysis did not reveal significant differences, except for mean relaxation time, three consecutive measurements of all twitch parameters were averaged and compared by means of a paired Student's t-test, without Bonferroni correction. In the case of relaxation time, multiple paired Student's t-tests were applied with correction of the level of significance according to Bonferroni's inequality (Glantz, 1981). Likewise, repeated measures analysis of variance was used to detect differences

in sarcomere length noise during the hypoxia experiments with increased stimulus rate. Subsequently, the level of significance was determined by means of paired Students T-tests, with correction according to Bonferroni. A p -value < 0.05 was considered significant. All values are given as means \pm standard deviation, unless mentioned otherwise.

RESULTS

The relationship between twitch parameters and SL at varied $[Ca^{2+}]_o$ and F_a

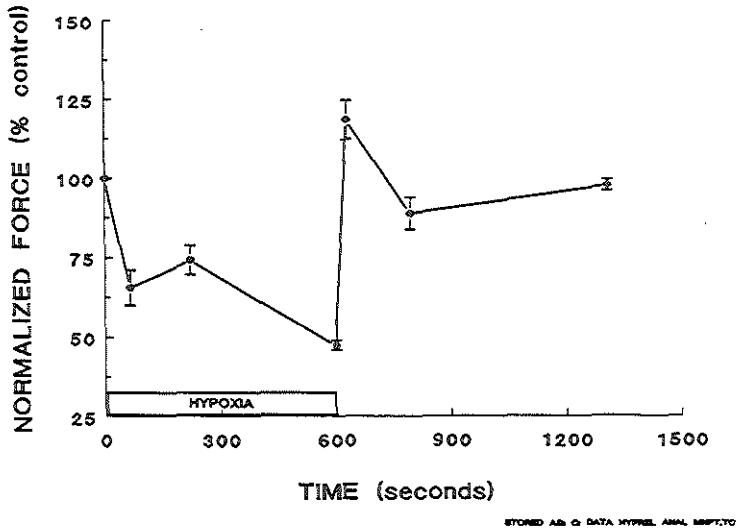
Figure 1 shows a typical recording of twitch force and sarcomere length during a twitch; the timing of the calculated twitch indices is indicated. The twitch parameters appeared to depend both on $[Ca^{2+}]_o$ and SL, as is illustrated in Figure 2A. This typical example shows that at low $[Ca^{2+}]_o$, RT increased with SL, either linearly or according to a relation that was curvilinear, convex to the abscissa. The relationship was curvilinear and convex to the ordinate at higher $[Ca^{2+}]_o$. In some muscles the relationship reached a plateau or decreased at SL beyond $2.0 \mu m$ at $[Ca^{2+}]_o$ where steady state force exceeded $80\% F_{max}$. Likewise, the relationships of SL and TPT, T_{90-90} and T_{90-40} , were dependent on $[Ca^{2+}]_o$. As in RT, the slopes of these relationships increased with $[Ca^{2+}]$ in the superfusate. In contrast, the relationships between TPT and the relaxation indices, and F_a were independent of $[Ca^{2+}]_o$ or SL and comparable for 6 muscles. The relation between TPT and force was convex toward the ordinate and reached a plateau at increasing F_a ; in some muscles TPT decreased slightly thereafter. The relationships between the other parameters and F_a were convex toward the abscissa and increased at higher F_a . A typical example of the relationship between RT and F_a is shown in figure 2B; the muscle preparation is the same as in figure 2A. The solid line that is drawn through the datapoints represents the fitted arbitrary function, as discussed before. In the other 5 muscles the calculated equations fitted equally well with mean correlation coefficients that varied between 0.91 and 0.97. The relationships were assessed for each preparation separately, since the values of the calculated parameters were only applicable to the respective muscles.

The relationship between twitch parameters and F_a was analysed in order to quantify the intrinsic effects of hypoxia. It enabled to differentiate changes in twitch characteristics due to decreased hypoxic twitch force, from variations that were caused by direct interference of hypoxia with excitation-contraction coupling and relaxation processes.

The effects of hypoxia and reoxygenation on force and sarcomere length parameters

Figure 3A shows a typical example of the changes of peak twitch force and sarcomere length that was recorded after the switch to hypoxia and subsequent reoxygenation. Figure 3B shows individual recordings of twitches at normoxia, at the end of hypoxia and shortly after reoxygenation. Repeated hypoxia of five muscles resulted in a reproducible, apparent exponential decline of F_a to a plateau at $65 \pm 22\%$ of control value, attained within 1 minute of hypoxia (A; F_a vs control twitch force: $p < 0.05$); occasionally the decay was preceded by a shortlasting initial increase. The decrease of F_a was followed by a transient increase to $74 \pm 18\%$ of control force at 4 minutes hypoxia (B; F_a vs control twitch force: $p < 0.05$), followed by a further exponential decrease of F_a . As soon as F_a had declined to 50% of control value, hypoxic glucose-free superfusate was replaced by normal, oxygenated medium. Subsequently force increased to $118 \pm 24\%$ of control F_a within 30 seconds (C; F_a vs control F_a : $p = N.S.$), in some muscles followed by a secondary transient undershoot to $89 \pm 20\%$ of control F_a at 3 minutes of reoxygenation (D; F_a vs control F_a : $p = N.S.$) (figure 4 and 5). Ultimately twitch force recovered to control value that was equal to steady state force. During the experiment the changes of

NORMALIZED FORCE vs TIME



MEAN SARCOMERE SHORTENING vs TIME

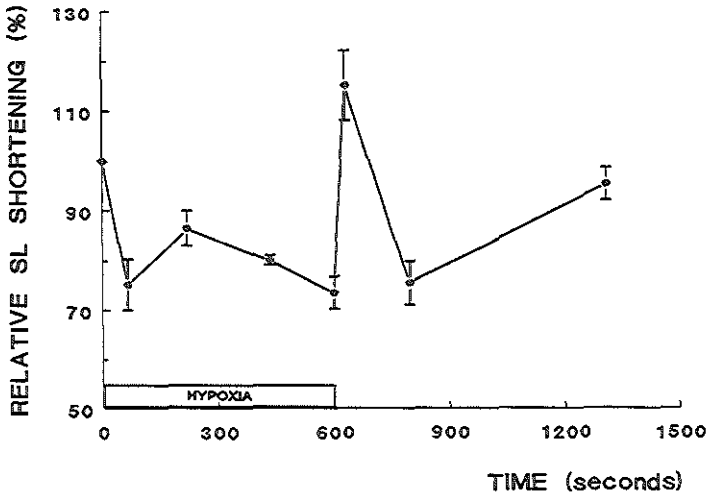


Figure 4 and 5: Mean normalized force (upper panel) and mean normalized sarcomere shortening (lower panel) of three consecutive interventions. Since repeated measures ANOVA showed that the difference between these parameters at successive stages of the interventions was not significant, the means of these parameters at comparable stages of the experiments was averaged and shown in figure 4 and 5. For further explanation see text.

measured sarcomere length closely followed the pattern of twitch force, though as the mirror image. Following consecutive hypoxic superfusions F_{\max} decreased by less than 5%. The average duration of the subsequent stages of the experiment in individual muscles were not significantly different (repeated measures analysis of variance, $p = \text{N.S.}$). This contrasted with the average time of force to decline to 50% of steady state value, which decreased significantly from 11 ± 3 minutes in the first hypoxic intervention to 6 ± 3 minutes during the third hypoxia (see Table I); the difference between the duration of the second and third intervention was not significant.

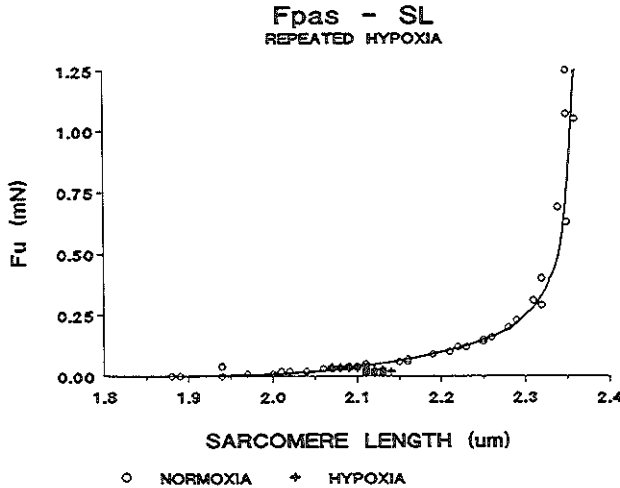


Figure 6: Passive force (F_u ; mN) plotted vs sarcomere length (SL; μm) in a typical trabecula. Note that F_u (+), assessed during hypoxia, closely follows the relation during normoxia.

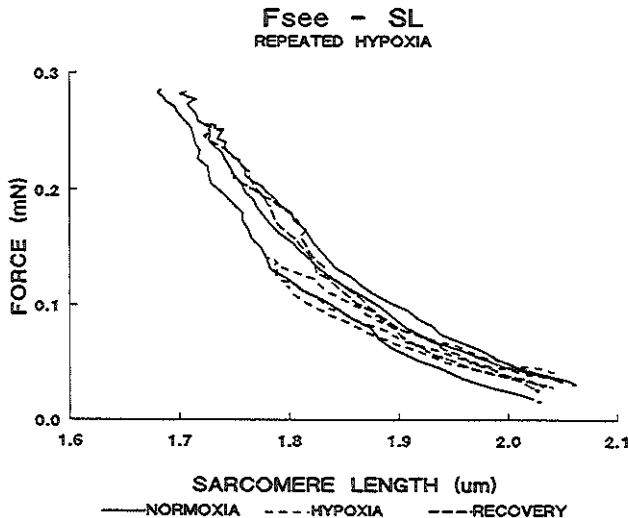


Figure 7: Active force (F , mN) plotted versus instantaneous sarcomere length (SL; μm), reflecting stiffness of the series elastic element. The relation was similar during normoxia, hypoxia and reoxygenation as is shown in this typical example of the relationship.

The relationship between F_0 and SL_0 was assessed in all muscles; the data obtained during hypoxia and reoxygenation superimposed the relation assessed at normoxic control conditions. A typical example of the absence of a shift or change in the slope of the relationship is presented in figure 6.

The relationships between instantaneous sarcomere length and increasing twitch force, were identical under either experimental condition, as is shown in figure 7. The only exception was one muscle, where sarcomeres in the center of the preparation were stretched during hypoxia and reoxygenation. Apparently, force generated by peripheral sarcomeres, exceeded twitch force generated by the central sarcomeres, resulting in a dyskinetic shortening pattern of the latter. Since it is impossible to conclude from this particular measurement whether the stiffness of the series elastic element changed, the results of this muscle were discarded.

Twitch characteristics

The mean time to peak tension (TPT) of control contractions in oxygenated Krebs-Henseleit solution was 110 ± 8 ms ($n = 5$) and decreased during superfusion with hypoxic glucose-free medium, after an occasional transient increase (2 muscles), monophasically to 83 ± 8 msec, just prior to reoxygenation (see Table II). Following reoxygenation TPT increased transiently to 116 ± 8 msec and subsequently returned to control value. In one muscle a second smaller transient increase of the time to peak tension preceded normalization. The response to repeated hypoxic exposure was similar; the interval to maximal TPT following reoxygenation increased from 25 ± 7 (first hypoxia) to 30 ± 5 sec during the third hypoxic intervention. However, the difference was not significant. The average time to maximal TPT of all interventions was 27 ± 8 sec ($n = 13$) (see Table II).

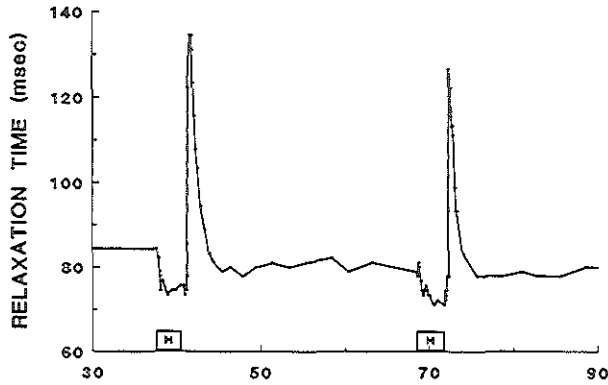
RTPT, i.e. TPT corrected for its dependence on F_{00} followed the same pattern; however, shortly after reoxygenation RTPT was not significantly different compared to normoxia (see Table III). The time to maximal RTPT of consecutive hypoxic superfusions increased from 26 ± 23 sec at the first hypoxic superfusion to 49 ± 43 sec at the third ($p = N.S.$). However, the differences were not statistically significant; the mean time to maximal RTPT was 37 ± 38.5 seconds ($n = 13$), equal to the time to maximal RRT (see below).

Relaxation characteristics

Following hypoxia, mean RT decreased from 76 ± 16 msec to 69 ± 11 msec ($n = 15$). Shortly after reoxygenation, mean RT increased to 102 ± 26 msec, followed by a monophasic decrease to steady state values (see Figure 8A). The trends were comparable for successive hypoxic interventions. Strikingly RT at reoxygenation decreased significantly when consecutive hypoxia experiments were compared; this explains why the differences with normoxic steady state and hypoxia were only significant in the first and second intervention and not in the third hypoxia (comparison H vs R and N vs R by paired T-test: $p < 0.05$ for first and second intervention, $p = N.S.$ for the third intervention).

The changes of relative RT (RRT) i.e. RT corrected for dependence on F^0 , during hypoxia and reoxygenation were reproducible from muscle to muscle (see figure 8B). Following an occasional small initial increase, mean RRT steadily increased from 102 ± 4 % at normoxia to 125 ± 19 % at the end of hypoxia. Reoxygenation resulted in a significant additional increase of mean relative RT to 135 ± 15 %; RRT never exceeded 160% (see table III). This was followed by an exponential decay to 118 ± 8 % and 102 ± 5 % at 105 ± 83 seconds and 12 minutes of reoxygenation, respectively. The first measurement was still significantly different from control values, in contrast with the latter value that was comparable to steady state levels ($p < 0.01$ and $p = N.S.$ vs control, respectively) (figure 9). Half maximal RRT and the time to attain this value were comparable during consecutive hypoxic interventions (repeated

RELAXATION TIME vs TIME



NORMALIZED RELAXATION TIME vs TIME

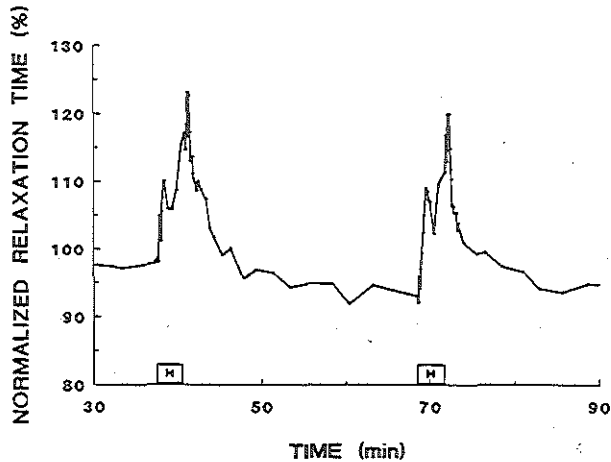


Figure 8A and 8B: Relaxation time (RT in msec, upper panel) and normalized relaxation time (RRT in %, lower panel) plotted versus time in a typical experiment (second and third hypoxic intervention). H means hypoxia.

measures analysis of variance, $p = \text{N.S.}$). In some muscles the recovery of RRT was preceded by a transient undershoot. The overshoot of RRT that resulted from reoxygenation was independent of the number of preceding hypoxic perfusions.

The mean time to maximal RRT increased from 26 seconds after the first hypoxia to 71 seconds following the third hypoxic intervention; however, the difference was not statistically significant. The mean time to maximal RRT was 37 ± 38.5 seconds ($n = 13$) (see tabel III). Tables II and III also summarize the changes of the relaxation parameters T_{90-80} and T_{60-40} and the calculated relative indices RT_{90-80} and RT_{60-40} at normoxia, immediately prior to reoxygenation and at the moment of maximal RT and RRT, respectively. The changes of the early relaxation, reflected by the mean T_{90-80} , were comparable to the changes of the average RT. The differences between the trends of the mean T_{90-80} ,

T_{60-40} , RT_{60-80} , and RT_{80-40} of successive hypoxic superfusions were not statistically significant.

Spontaneous sarcomere length oscillations during normoxia, hypoxia and reoxygenation.

Under normoxic conditions, mean SLN_3 varied between $1.3 - 2.0 \times E-3 \mu m$ at a range of SL_a of $1.6 - 2.2 \mu m$ (see table IV; figure 10). Analysis of variance did not show evidence for sarcomere length dependence of the sarcomere length fluctuations. The same applied to mean SLN_2 , that varied between $2.6-7.8 \times E-3 \mu m$ at the same SL_a range. Mean SLN_1 is summarized but will not be discussed for reasons that were mentioned before.

MEAN NORMALIZED RELAXATION TIME vs TIME

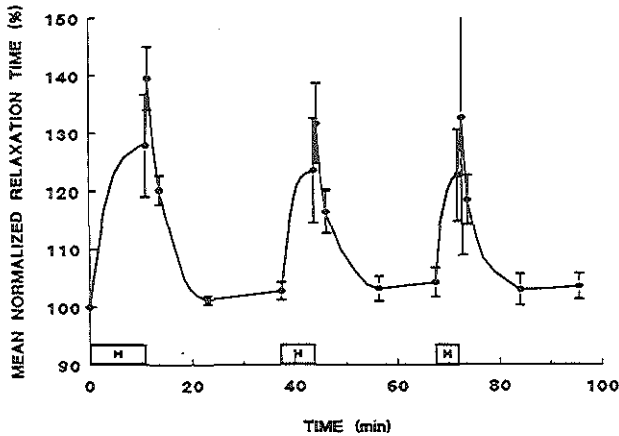


Figure 9: Mean normalized relaxation time (mean RRT in %) plotted versus time (min) of 3 consecutive hypoxic intervention. The line through the points is drawn by hand. H means hypoxia.

SARCOMERE LENGTH NOISE vs TIME
TWO CONSECUTIVE HYPOXIA EXPERIMENTS

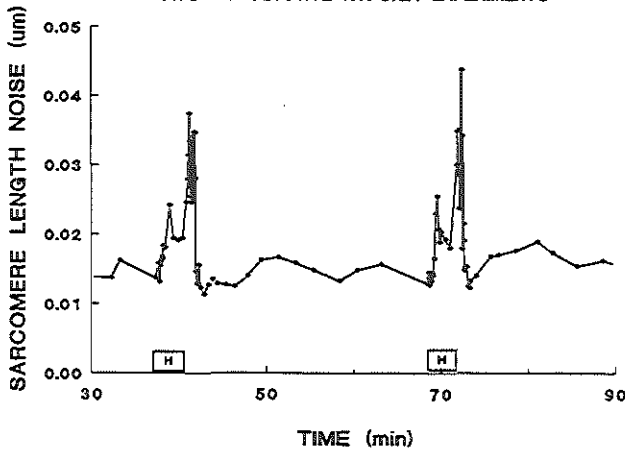


Figure 10: Sarcomere length noise (SLN_3 ; μm) plotted versus time of 2 consecutive hypoxic interventions in a typical experiment. H = hypoxia

Prior to hypoxia, mean SLN_3 was $1.4 \pm 0.3 \cdot E-3 \mu m$, and SLN_2 $5.8 \pm 3.2 \cdot E-3 \mu m$, comparable to sarcomere length fluctuations at steady state conditions (See tables IV and V). During hypoxia, mean SLN_3 showed a significant, gradual increase to $2.3 \pm 0.8 \cdot E-3 \mu m$, in contrast with SLN_2 that declined to $3.4 \pm 1.7 \cdot E-3 \mu m$. In some muscles, both parameters showed a transient, 3-fold increase at the beginning of hypoxia. Following reoxygenation, SLN_3 further increased to $2.7 \pm 0.9 \cdot E-3 \mu m$ and SLN_2 to $7.0 \pm 2.9 \cdot E-3 \mu m$ ($p = 0.12$ and $p < 0.05$, R vs H , respectively). At the same moment, localized and propagated aftercontractions were observed in the majority of the muscles. In the following 5 minutes of reoxygenation, SLN_2 and SLN_3 recovered to steady state levels. The differences between SLN_3 levels at comparable stages of consecutive interventions were not significant. The same applied to the repeated measurement of SLN_2 at the end of hypoxia and following reoxygenation; the level of normoxic SLN_2 on the other hand, decreased significantly during subsequent interventions. Time to maximal sarcomere noise increased from 26 ± 8 seconds in the first hypoxia to 71 ± 60 seconds in the third intervention. However, this increase was not significant, nor did these intervals deviate significantly from the time to maximal relative relaxation time (repeated measures ANOVA, $p = N.S.$).

The effect of changes in stimulus rate on sarcomere length noise during hypoxia

The effects of changes in performed work by increased stimulus rate during hypoxia, were studied in eight experiments. Following 90 seconds of hypoxia, stimulus rate was increased to 5 Hz. The resulting initial overshoot of twitch force was followed by a decline that was more accentuated than under normoxic conditions. After 2 minutes, diastolic tension gradually increased at constant resting SL. At the same moment, sarcomere length initially increased during the twitch, followed by a decrease during the relaxation phase. Immediately after stimulus rate was reduced to 1 Hz, localized spontaneous sarcomere contractions were visible microscopically, and resting tension further increased. After one minute of reoxygenation, aftercontractions gradually subsided in the next 3 minutes; in addition, sarcomere shortening and twitch force fully recovered and resting tension decreased to zero. Comparable results were obtained in three other preparations. Twitch force decreased significantly to 38% and recovered to 52%, immediately following high frequency stimulation. TPT than, decreased significantly from 88.5 to 57 msec. During the interventions, the other twitch parameters did not differ significantly from control values. SLN_2 tended to increase from $2.3 \cdot E-3 \mu m$ at normoxia to $2.5 \cdot E-3 \mu m$ during hypoxia; high frequency stimulation resulted in a further increase to $3.4 \cdot E-3 \mu m$. Both twitch force and sarcomere length noise completely normalized following switch to normoxic medium.

DISCUSSION

It is well known that ischemia affects contractility and relaxation of the myocardium. The pathophysiologic mechanisms involved are incompletely understood. Grossman et al. observed a left-upward shift of the pressure volume relationship during pacing induced ischemia. It was suggested that this could have been caused by impaired Ca^{2+} homeostasis in cases of shortlasting ischemia, and by rigor bond formation during protracted ischemia (Frist, 1977; Grossman, 1990; Serizawa, 1981). Although these observations have been confirmed by other researchers, there is controversy as to the mechanisms involved in the intact heart. Recently an alternative hypothesis was proposed by Kass et al.; they reported elevations in resting diastolic pressure-volume relations and apparent increased chamber stiffness during coronary occlusion in humans (Kass, 1990). It was concluded that was accounted for by altered right-ventricular or pericardial loading, without changes in intrinsic chamber stiffness and diastolic properties. Evidently analysis of results from intact hearts are difficult to interpret, owing to uncertainties about loading conditions, interaction between left and right ventricle and other factors. We therefore applied a

linear model to study changes in relaxation during repeated hypoxia.

In rat heart, the rate of relaxation depends on peak force development in contractions at constant muscle length, as is shown in this study. The same applies to relaxation rate of contractions at constant sarcomere length, as was demonstrated previously (Heuningen et al., 1982). This means that interventions that cause a variation of F_p are expected to affect the rate of relaxation as well. The mechanism for the relation between relaxation and F_p is not completely understood. However, it is consistent with the hypothesis by Bremel and Weber that cross bridge formation by stretch of the muscle, increases the affinity of the contractile apparatus for Ca^{2+} ions more than would be expected on the basis of the increase of the number of available cross bridges (Bremel and Weber, 1972). Consequently the off-rate constant for Ca^{2+} is decreased at long lengths and decreased at short sarcomere lengths. Ultimately this will lead to reduced tension at shorter lengths; following activation, Ca^{2+} will dissociate more rapidly from troponin C, resulting in shorter twitch duration and initially slow decline of the free Ca^{2+} transient (Allen and Kurihara, 1980). Our observation is also consistent with the observation by Kentish et al. that the affinity of the contractile filaments increases with stretch, leading to increased exposure of the actin filaments to cross bridges (Kentish et al., 1986). This behaviour cannot easily be explained on the basis of properties of the sarcoplasmic reticulum (SR) or sarcolemma because it is unlikely that the Ca^{2+} handling by these structures is governed by force development.

If one supports the hypothesis that the off-rate constant of Ca^{2+} is force dependent, and that the variable rate of relaxation is determined by this mechanism, it is necessary to quantify it in order to be able to distinguish it from possible direct effects of hypoxia on the relaxation process. Consequently, we first studied the relationship between twitch force on the one hand and the twitch parameters TPT, RT, T_{90-80} and T_{80-40} on the other.

It has been shown that the time to peak tension is related to the rate of decline of the Ca^{2+} transient following activation of the muscle (Allen and Kurihara, 1980). The rate of decay of $[\text{free Ca}^{2+}]_i$, in turn, is determined not only by the rate of binding of Ca^{2+} to troponin C, but also by the rate of sequestration of Ca^{2+} by the SR and the mitochondria and by the rate of Ca^{2+} extrusion from the cell by $\text{Na}^+/\text{Ca}^{2+}$ exchange. The interaction between these activation and inactivation processes is largely unknown (Allen and Kentish, 1985; Pasipoularides et al., 1985). We therefore applied an empirical equation, consisting of the sum of an exponential (e-power) and a line, as representation of these relationships and fitted it to the data. The calculated relationships were applied to differentiate changes of the twitch characteristics, that were accounted for by variations in twitch force, from the direct effects of hypoxia and reoxygenation on relaxation parameters. Our results suggest that each twitch parameter is well correlated with peak twitch force but not with $[\text{Ca}^{2+}]_i$ or sarcomere length at peak twitch force.

It was striking that the relationship between force and RT was convex to the abscissa for all preparations. This may be explained by stronger Ca^{2+} binding to troponin C at increased twitch force, based either on cooperativity of Ca^{2+} binding or on length-dependent increase of the sensitivity of troponin C for Ca^{2+} (Hibberd and Jewell, 1982; Allen and Kentish, 1985). Our observations are in agreement with the results of experiments on skinned fiber preparations that showed an increase of the Ca^{2+} affinity constant with sarcomere length and concomitant augmentation of twitch force (Kentish et al., 1986).

At normoxia, twitch force of individual muscles ($[\text{Ca}^{2+}]_i = 1.5 \text{ mM}$) varied considerably. This may be explained by inhomogeneity of sarcomere length at peak twitch force as a result of internal shortening of the sarcomeres in the center of the preparation at the expense of stretch of the cells in the compliant, non-viable ends of the preparation. Alternatively, spontaneous Ca^{2+} oscillations in the muscles may have induced sarcomere oscillations and hence inhomogeneous myofilament activation, leading to reduced peak twitch force. Notably rat heart is susceptible to spontaneous oscillatory release of Ca^{2+} , that may increase $[\text{Ca}^{2+}]_i$ by 4 to 40 μM , by virtue of its highly developed sarcoplasmic reticulum, in which it differs from

frog and ferret with relative paucity of this organel (Orchard et al., 1983).

In an attempt to compensate for differences in twitch force, $[Ca^{2+}]$ in the medium was adjusted to a steady state force of 80% F_{max} ; in addition, the muscles were stretched until passive force was equal to 5% of steady state force. At this $[Ca^{2+}]_o$, any further increase of intracellular $[Ca^{2+}]$, elicited by hypoxia or reoxygenation, would have been detected since it would lead to apparent, either localized or generalized, spontaneous sarcomere activation. $[Ca^{2+}]_o$ was not raised beyond values of 80% F_{max} since this may trigger spontaneous aftercontractions, even at normoxic conditions as has been reported previously (ter Keurs and Mulder, 1984; Kort and Lakatta, 1984). Since stimulus rate influences twitch duration, all preparations were paced at 1 Hz during the experiments, except when F_{max} was assessed (ter Keurs, 1983; Schouten, 1990).

During hypoxia, all absolute twitch parameters decreased, except for t_{90-40} . Apparently during hypoxia and subsequent reoxygenation, the latter parameter is more sensitive to the changes in twitch characteristics, notably of the secondary relaxation phase, than the other twitch parameters (see below). The data were further analysed by comparing the values of the individual twitch parameters, measured during hypoxia and reoxygenation, with their expected values derived from experiments under control conditions. By this approach it was shown that hypoxia increases the relative relaxation time (RRT) to 125 % of control value; reoxygenation resulted in a further increased to 135 %, that was followed by a monoexponential decay to control levels within 12 minutes. The discrepancy between our data and reports in the literature may be explained at least in part by the normalization of the data that was used in our experiments compared to others (Carter et al., 1986; Frist et al., 1978; Tyberg et al., 1969).

We assumed that t_{90-60} and t_{60-40} represented an initial and a secondary phase of the relaxation process. At normoxia, both parameters correlated equally well with changes in force. The parameters probably reflect phases in relaxation that are comparable to skeletal muscle; there, the initial relaxation to 70% of peak twitch force is slow, and followed by a secondary faster phase, that results from inhomogeneous sarcomere behaviour (Edman, 1980). In heart muscle, the transition from slow to fast relaxation is only as distinct as in skeletal muscle when contraction starts at long SL and little internal shortening of the muscle is allowed to take place. It is determined by the load that is carried by the muscle and the rate of decline of $[Ca^{2+}]$, that is governed by processes like Ca^{2+} sequestration by the SR and uptake in the mitochondria as well as Ca^{2+} extrusion from the cell by Na^+/Ca^{2+} exchange (Brutsaert, 1987).

Since the absolute values of the individual twitch parameters showed trends, that often were completely opposite to the trends of the relative twitch parameters, we will confine the remainder of the discussion to a critical evaluation of the latter indices. Our results show that RRT, RT_{90-60} and RT_{60-40} increased significantly during hypoxia, whereas relative TPT decreased; the trends in the twitch parameters were reproducible during three consecutive hypoxic interventions. The intrinsic prolongation of the twitch duration might be explained at least in part by increased intracellular proton production during anaerobic glycolysis (Allen et al., 1985; Gevers, 1977). During acidosis, H^+ and Ca^{2+} ions compete for binding to the Ca^{2+} -ATPase of the SR, thereby impeding relaxation rate (Levitsky and Benevolensky, 1986; Fabiato, 1985). Inhibition of the Na^+/K^+ ATPase and increased Na^+ entry through the Na^+/H^+ exchanger would provide alternative mechanisms that could lead to prolonged relaxation. Both pathways would lead to increased $[Ca^{2+}]_i$, either by inhibition of the Na^+/Ca^{2+} exchanger or by direct inflow of Ca^{2+} (Allen and Orchard, 1983; Nakaya, 1985). Increased off-rate of the Ca^{2+} - Troponin C complex by H^+ ions on the other hand would increase the relaxation rate. Since we observed that the relative relaxation time increases during acidosis (Bucx and ter Keurs, unpublished observations), we concluded that the inhibitory effects of H^+ ions on Ca^{2+} sequestration by the SR ATPase and on Ca^{2+} extrusion dominate the other effects. The decreased TPT could be compatible with competition of H^+ and Ca^{2+} ions for binding to troponin C or by decreased storage and subsequent release of Ca^{2+} by the SR. The

observation that the recirculating fraction of Ca^{2+} is decreased by acidosis (Bucx and ter Keurs, unpublished observations) is in agreement with the first observation, decreased twitch force with the latter. All observations are in agreement with the hypothesis that increased $[\text{Ca}^{2+}]_i$ triggers release of more Ca^{2+} by the sarcoplasmic reticulum. Regenerative release of Ca^{2+} by the sarcoplasmic reticulum has been mentioned in recent reports as underlying mechanism of the spontaneous increase of $[\text{free Ca}^{2+}]_i$ in myocardium during acidosis, irrespective of the presence of ouabain (Allen and Orchard, 1983; Orchard, 1986).

What mechanisms can be held responsible for the further increase of relative RT, that is observed during reoxygenation? As a result of reoxygenation, pH_i will normalize rapidly and oxydative phosphorylation will resume. However, initially the high-energy phosphate production is still limited, possibly also due to loss of the total adenine nucleotides pool. In addition, the ATP consumption by the sarcolemmal Na^+/K^+ ATPase, the sarcoplasmic reticulum Ca^{2+} ATPase and myofibrillar ATPase is still at maximum level. Even when SR ATPase is activated at this stage, its regulatory action on the cytosol Ca^{2+} concentration is abolished by activation of the $\text{Na}^+/\text{Ca}^{2+}$ and Na^+/H^+ exchangers, that tend to increase $[\text{Ca}^{2+}]_i$. Ultimately, the rate of normalization of the Na^+/K^+ ATPase activity determines the time required to restore normal ion composition of the cytosol, when sarcolemmal integrity is supposedly still well maintained (Allen and Orchard, 1987).

The observation that the sarcomere length fluctuations increased even further during reoxygenation, is in agreement with the hypothesis that cytosol Ca^{2+} is increased, as discussed before. Deitmer and Ellis have shown that the intracellular $[\text{Na}^+]_i$ becomes elevated, when the Na^+/K^+ ATPase is inhibited due to low or absent extracellular $[\text{K}^+]_o$. Strikingly, the time constant of the normalization of the $a_i\text{Na}^+$ that is observed when $[\text{K}^+]_o$ is brought back to normal levels, is identical to the half time required for RRT to attain steady state levels again (Deitmer and Ellis, 1980; Ellis, 1979). This mechanism therefore could at least in part explain the time course of the normalization of the twitch duration.

Recently the group of Lakatta has reported a method to quantify spontaneous light intensity fluctuations (SLIF) from backscattered laser light. It was shown that SLIF was virtually absent during 60 min of global ischemia of rat hearts but increased 3 fold following reoxygenation (Renlund et al., 1985). In our experiments, evidence for local Ca^{2+} overload was derived from direct measurement and calculation of sarcomere length fluctuations by laser diffraction techniques. Visual inspection during the experiment revealed that spontaneous sarcomere activity gradually increased during hypoxia and reached a maximum shortly after reoxygenation. At the same time, RMS values of SL noise were increased. In some muscles localized spontaneous sarcomere activity elicited propagated aftercontractions. In one muscle this even triggered an arrhythmia immediately following reoxygenation. The positive correlation between the sarcomere length noise and prolongation of the relaxation time suggested a direct or indirect link between these phenomena. We propose that the observations are compatible with the hypothesis that cytosol Ca^{2+} concentration was increased, either by impaired sequestration in the sarcoplasmic reticulum, leakage from the SR or by inhibition of the $\text{Na}^+/\text{Ca}^{2+}$ exchanger. Increased $[\text{Ca}^{2+}]_i$ may have caused regenerative Ca^{2+} release by the sarcoplasmic reticulum, leading to prolongation of the twitch by continued activation of the cross bridges. The same phenomenon has been observed in muscles that were treated with caffeine or strontium (ter Keurs et al., 1980; Bucx et al., 1986). The observation that anoxic perfusion or inhibition of oxydative phosphorylation by KCN is not accompanied by spontaneous sarcomere length fluctuations, is in agreement with the hypothesis that regenerative Ca^{2+} release by the sarcoplasmic reticulum may be responsible for these phenomena.

We observed that the time to increased sarcomere length noise of hypoxic muscles could be shortened by high frequency stimulation. We assume that this may be related to accelerated turnover of cellular ATP and CrP as a result of the increase of performed work. This, in combination with the

inhibition of synthesis of these compounds during hypoxia, may be responsible for the rapid depletion of these compounds. It is conceivable that the reduced content of intracellular ATP would subsequently lead to a combination of rigor cross bridge formation and Ca^{2+} overload (Grossman, et al.; Nayler et al., 1976; Ventura-Clapier and Vasort, 1981). However, as yet the contribution of either mechanism to the observed mechanical behaviour is not well established. The rate of normalization of the increased resting tension, that started prior to reoxygenation and further increased thereafter, is comparable to data reported by Grossman and Apstein in dog heart. They induced ischemia in dog hearts with artificial 90% stenoses of the left anterior descending and circumflex coronary arteries by pacing (Paulus et al., 1985; Serizawa et al., 1980). Pacing at 115 beats per minute during 10 - 15 beats, resulted in increased LVEDP, that recovered within 6 - 10 seconds after interruption of pacing. Strikingly the rate of recovery was identical to the rate of ATP production by the mitochondria (Jacobus et al., 1982), which is suggestive for a possible link between these two phenomena. A different explanation of possible rigor bond formation is based on observations by Miller and Smith, who reported that elevated ADP levels are able to induce rigor tension, even at ATP concentrations of 0.1 mM and over (Miller and Smith, 1985).

It is conceivable that the duration of the response to hypoxia is a function of the magnitude of the intracellular stores of glycogen that are available for anaerobic glycolysis. The observation that the time to 50% peak twitch force decreased from 11 minutes in the first intervention to 6 minutes in the third is in agreement with this assumption.

In summary, we presented evidence that hypoxia impairs relaxation. This impairment can only be fully appreciated when the measured relaxation parameters are compared with their expected values, as observed during normoxic twitches of comparable magnitude. On the basis of increased sarcomere length noise, coinciding with impaired relaxation, it is hypothesized that Ca^{2+} overload may be one of the underlying mechanisms of this phenomenon. The gradual increase of diastolic tension that is elicited by increased stimulus rate during hypoxia, can be equally well explained by Ca^{2+} overload, that quickly normalizes as soon as stimulus rate is reduced to steady state values.

ACKNOWLEDGEMENT

The skillful secretarial assistance by Mrs P. Janssen is gratefully acknowledged.

TABLE I

SUMMARY OF MEAN TWITCH FORCE AND SARCOMERE LENGTH MEASUREMENTS OF 5 MUSCLES DURING 3 CONSECUTIVE HYPOXIC INTERVENTIONS.

	N	H1	H2	H3	R1	R2	R3
%Fa	100.0	65.6°	74.3°	47.4°	118.4	88.7+	97.6
	0.0	21.6	17.7	6.0	23.6	19.8	6.8
SLu	2.12	2.10	2.11	2.15	2.18	2.13	2.13
	0.06	0.05	0.06	0.06	0.07	0.05	0.06
SL _a	1.84	1.89*	1.86 ^x	1.92°	1.88	1.92 ^x	1.86
	0.07	0.09	0.07	0.09	0.10	0.09	0.07
SLST	13.2	9.9 ^x	11.6 ^x	11.2°	14.2	9.7 ^x	
	3.2	4.1	2.3	2.4	2.1	4.0	
SLSH	100.0	75.2*	86.6	73.6°	115.2	75.6 ^x	
	0.0	21.4	14.6	13.2	28.9	18.2	
T	0	65	221		31	197	710
	0	22	114	§	7	59	163

§ HYPOXIA DURATION (min):

first intervention	11.0 ± 3.1
second intervention	6.6 ± 4.3
third intervention	6.1 ± 3.3

%F_a: active twitch force, relative to force prior to hypoxia (%); SL_u: unstimulated sarcomere length (μm); SL_a: active sarcomere length (μm); SLST: sarcomere length strain (%); SLSH: sarcomere length shortening, relative to shortening at the beginning of the experiment (%); T: time of the intervention that is mentioned one line below (seconds); N: normoxic control; H: hypoxia; R: reoxygenation. H1: initial stabilization of force shortly after the beginning of hypoxia; H2: partial recovery of force during hypoxia; H3: end of hypoxia; R1: initial recovery of force following reoxygenation; R2 partial relapse of force during reoxygenation; R3: prior to repeated hypoxia (for further explanation see text).

Note duration of T is mentioned in seconds, and hypoxia duration in minutes. All values are means ± s.d.; °: p < 0.10 vs N; * : p < 0.05 vs N; ° : p < 0.001 vs N; +: p < 0.10 vs R1.

TABLE II

SUMMARY OF MEAN ABSOLUTE TIME TO PEAK TENSION AND RELAXATION PARAMETERS OF 5 MUSCLES DURING 3 CONSECUTIVE HYPOXIC INTERVENTIONS.

	Normoxia	Hypoxia	Reoxygenation
TPT	109.3 7.9	83.2° 8.3	116.5* 7.9
RT	75.8 15.9	69.1 11.1	102.4 25.9
T ₉₀₋₈₀	14.1 3.6	12.0 2.5	19.3° 6.5
T ₆₀₋₄₀	17.4 3.6	20.8 1.8	23.1* 4.6

Table III summarizes the means of the twitch parameters TPT, RT, T₉₀₋₈₀, and T₆₀₋₄₀ of 5 muscles during 3 consecutive hypoxic interventions. Repeated measures analysis of variance of the results in individual muscles did not reveal significant differences within the measured parameters at comparable stages of the experiment. Therefore, only the means at normoxic conditions (N) immediately prior to hypoxia, at the end of hypoxia (H), and following 27 ± 8 seconds of reoxygenation, when RT was maximal, are shown in the table (for further explanation, see text). The data are given as means \pm s.d. with $n = 13 - 15$. The level of significance of the differences between the calculated means of each twitch parameter was tested by paired Student T-tests, as indicated in the table. Abbreviations: TPT: Time to peak tension (msec); RT: time for peak twitch force to decrease to 50% (msec); T₉₀₋₈₀: time for twitch force to decrease from 90 to 80% (msec); T₆₀₋₄₀: time for twitch force to decrease from 60 to 40% (msec); N: normoxia; H: hypoxia; R: reoxygenation; *: $p < 0.05$ vs N; °: $p < 0.01$ vs N; °: $p = 0.10$ vs N.

TABLE III

SUMMARY OF MEAN RELATIVE TIME TO PEAK TENSION AND MEAN RELATIVE RELAXATION PARAMETERS OF 5 MUSCLES DURING 3 CONSECUTIVE HYPOXIC INTERVENTIONS.

	Normoxia	Hypoxia	Reoxygenation
RTPT	100.4 2.0	84.4* 8.3	99.5* 11.6
RRT	102.4 4.2	124.8 19.2	135.0° 15.1
RT ₉₀₋₈₀	104.3 6.9	122.6 22.6	132.5* 18.3
RT ₆₀₋₄₀	103.2 7.4	159.3* 32.1	153.9° 32.5

Table III shows the means of the relative twitch parameters RTPT, RRT, RT₉₀₋₈₀ and RT₆₀₋₄₀ of 5 muscles during 3 consecutive hypoxic interventions. As in table III, the measurements of parameters at identical stages of the experiment did not differ significantly within individual muscles (repeated ANOVA, $p = \text{N.S.}$). Consequently, only the means at normoxic conditions (N) immediately prior to hypoxia, at the end of hypoxia (H), and at maximal RRT following 37 ± 38.5 seconds of reoxygenation (R), are shown in the table (for further explanation see text). The level of significance of the differences between the calculated means of each twitch parameter was tested by paired Student T-tests, as indicated in the table; the data are given as means \pm s.d. with $n = 13 - 15$. Abbreviations: RTPT: Relative time to peak tension (%); RRT: relative time for peak twitch force to decrease to 50% (%); RT₉₀₋₈₀: relative time for twitch force to decrease from 90 to 80% (%); RT₆₀₋₄₀: relative time for twitch force to decrease from 60 to 40% (%); N: normoxia; H: hypoxia; R: reoxygenation; *: $p < 0.05$ vs N; °: $p < 0.01$ vs N; °: $p = 0.06$ vs N; *: $p < 0.05$ vs H.

TABLE IV

SUMMARY OF MEAN SARCOMERE LENGTH FLUCTUATIONS AT STEADY STATE CONDITION AND VARIED ACTIVE SARCOMERE LENGTH (N = 5 - 6).

RANGE OF SL_a	$SLN_1 \cdot E-3$	$SLN_2 \cdot E-3$	$SLN_3 \cdot E-3$
1.6 - 1.7 μm	17.9	2.6	2.0
	7.1	0.9	0.4
1.7 - 1.8 μm	20.5	4.4	1.6
	4.5	2.2	0.2
1.8 - 1.9 μm	18.0	7.8	1.5
	3.6	3.1	0.2
1.9 - 2.0 μm	13.9	7.7	1.3
	3.1	2.9	0.3
2.0 - 2.1 μm	9.5	6.4	1.7
	2.2	2.0	0.7
2.1 - 2.2 μm	8.7	5.0	1.7
	1.9	1.4	0.5

SLN_1 : sarcomere length fluctuation, 100 - 250 msec following stimulation; SLN_2 : sarcomere length fluctuation, 250 - 500 msec following stimulation; SLN_3 : sarcomere length fluctuation, 500 - 960 msec following stimulation; SL_a : sarcomere length at peak twitch force.

Data (n = 6) are given as means \pm s.d.. Temperature 29.8 ± 0.2 °C. Mean $[Ca^{2+}]_o$ 2.2 ± 1.2 mMol/L. Stimulus rate 1 Hz.

TABLE V

SUMMARY OF SARCOMERE LENGTH FLUCTUATIONS AT NORMOXIA, HYPOXIA AND REOXYGENATION (N = 5 - 6).

	Normoxia	Hypoxia	Reoxygenation
SLN ₁ * E-3	14.0 6.2	10.1 3.2	11.4 3.7
SLN ₂ * E-3	5.8 3.2	3.4 1.7	7.0 ⁺ 2.9
SLN ₃ * E-3	1.4 0.3	2.3* 0.8	2.7° 0.9

SLN₁: sarcomere length fluctuation * E-3, 100 - 250 msec following stimulation (μm); SLN₂: sarcomere length fluctuation * E-3, 250 - 500 msec following stimulation (μm); SLN₃: sarcomere length fluctuation * E-3, 500 - 960 msec following stimulation (μm); N: normoxia; H: hypoxia; R: reoxygenation. * : $p < 0.05$ vs N; ° : $p = 0.12$ vs H; + : $p < 0.05$ vs H. The timing of H and R is comparable to the intervals mentioned in table III.

Data ($n = 15 - 18$) are given as means \pm s.d.. Temperature 29.8 ± 0.2 °C. Mean $[\text{Ca}^{2+}]_i$ 2.2 ± 1.2 mMol/L. Stimulus rate 1 Hz.

TABLE VI

CHANGES OF SARCOMERE LENGTH, TWITCH PARAMETERS AND SARCOMERE LENGTH NOISE INDUCED BY HIGH FREQUENCY STIMULATION DURING HYPOXIA.

	Normoxia	Hypoxia	High Frequency
SL _a	1.97 0.09	2.14 0.12	2.10 0.04
FORCE (%)	100.0 0.0	38.5* 20.6	52.1* 44.5
TPT	88.5 8.5	63.3 14.2	57.4* 14.6
RT	79.3 12.3	55.6 13.9	54.7 24.3
T ₉₀₋₈₀	14.5 2.7	10.0 2.1	9.8 4.2
T ₆₀₋₄₀	19.3 3.3	15.1 3.9	16.1 9.4
SLN ₁ * E-3	13.0 4.7	10.6 5.5	6.2* 4.1
SLN ₂ * E-3	2.3 1.9	2.5 1.7	3.4* 1.5
SLN ₃ * E-3	1.2 0.2	1.2 0.1	3.8 1.9

SL_a: sarcomere length at peak twitch force (μm); Force: peak twitch force, expressed as a percentage of control; TPT: time to peak tension (msec); RT: time for peak twitch force to decrease to 50% (msec); T₉₀₋₈₀: time for twitch force to decrease from 90 to 80% (msec); T₆₀₋₄₀: time for twitch force to decrease from 60 to 40% (msec); SLN₁: sarcomere length fluctuation * E-3, 100 - 250 msec following the stimulus (μm); SLN₂: sarcomere length fluctuation * E-3, 250 - 500 msec following the stimulus (μm); SLN₃: sarcomere length fluctuation * E-3, 500 - 960 msec following the stimulus (μm); *: $p < 0.05$ vs N.

All parameters were measured at control conditions (N), at hypoxia prior to pacing (H), and immediately following high frequency stimulation (HF) (for further explanation see text). Steady state stimulus rate was 3.3 Hz in 6 muscles and 1 Hz in 2 preparations. Maximal heart rate was 5 Hz in 7 muscles and 3.3 Hz in the remainder. The average duration of hypoxia prior to high frequency stimulation was 67 ± 44 seconds (15 - 150 seconds); the mean duration of high frequency stimulation was 68 ± 46 seconds (3 - 180 seconds). The data are given as means \pm s.d. with $n = 5 - 8$.

REFERENCES

1. Allen DG, Orchard CH. The effect of pH on intracellular calcium transients in mammalian cardiac muscle. *J Physiol* 1983; 335: 555-567
2. Allen DG, Orchard CH. The effect of hypoxia and metabolic inhibition on intracellular calcium in mammalian heart muscle. *J Physiol* 1983; 339: 107-122
3. Allen DG, Kentish J. The cellular basis of the length-tension relation in cardiac muscle. *J Mol Cell Cardiol* 1985; 17: 821-840
4. Allen DG, Kurihara S. Calcium transients in mammalian ventricular muscle. *Eur Heart J* 1980; 1 (supplement A): 5-15
5. Allen DG, Orchard CH. Contractile function in ischemia and hypoxia. *Circ Res* 1987; 60: 153-167
6. Allen DG, Morris PG, Orchard CH, Pirolo JS. A nuclear magnetic resonance study of metabolism in the ferret heart during hypoxia and inhibition of glycolysis. *J Physiol* 1985; 361: 185-204
7. Barry WH, Brooker JZ, Alderman EL, Harrison DC. Changes in diastolic stiffness and tone of the left ventricle during angina pectoris. *Circulation* 1974; 49: 255-263
8. Bevington PR. Data reduction and error analysis for the physical sciences. McGraw-Hill, New York, 1969: 204-246
9. Bourdillon PD, Lorell BH, Mirsky I, Paulus WJ, Wynne J, Grossman W. Increased regional myocardial stiffness of the left ventricle during pacing-induced angina in man. *Circulation* 1983; 67: 316-323
10. Bremel RD, Weber A. Cooperation within actin filament in vertebrate skeletal muscle. *Nature* 1972; 238: 97-101
11. Bricknell OL, Davies PS, Opie LH. A relationship between adenosine triphosphate, glycolysis and ischaemic contracture in the isolated rat heart. *J Mol Cell Cardiol* 1981; 13: 941-945
12. Brutsaert DL. Non-uniformity: a physiologic modulator of contraction and relaxation of the normal heart. *J Am Coll Cardiol* 1987; 9: 341-348
13. Bucx JJJ, de Tombe PP, Schouten VJA, ter Keurs HEDJ. Effect of Sr^{2+} on force and sarcomere length in heart muscle of rat. *J Physiol* 1986; 381: 96P
14. Bucx JJJ, Sethi S, ter Keurs HEDJ. Sarcomere dynamics and relaxation during hypoxia and reoxygenation in Rat myocardium. *Circulation* 1987; 76: IV-57
15. Carter JE, Palacios I, Frist WH, Rosenthal S, Newell JB, Powell WJ. Improvement in relaxation by nifedipine in hypoxic isometric cat papillary muscle. *Am J Physiol* 1986; 250 (Heart Circ Physiol 19): H208-212
16. Daniëls M, Noble MIM, ter Keurs HEDJ, Wohlfart B. Velocity of sarcomere shortening in rat cardiac muscle: relationship to force, sarcomere length, calcium and time. *J Physiol* 1984; 355: 367-381
17. Deitmer JW, Ellis D. Interactions between the regulation of the intracellular pH and sodium activity of sheep cardiac Purkinje fibres. *J Physiol* 1980; 304: 471-488
18. Edman KAP. The role of non-uniform sarcomere behaviour during relaxation of striated muscle. *Eur Heart J* 1980; 1 (Supplement A): 49-57
19. Ellis D. The effects of external cations and ouabain on the intracellular sodium activity of sheep heart. *J Physiol* 1979; 273: 211-240
20. Fabiato A. Use of aequorin for the appraisal of the hypothesis of the release of calcium from the sarcoplasmic reticulum induced by a change of pH in skinned cardiac cells. *Cell Calcium* 1985; 6: 95-108
21. Frist WH. Effect of hypoxia on myocardial relaxation in isometric cat papillary muscle. *J Clin Inv* 1978; 61: 1218-1224.

22. Gevers W. Generation of protons by metabolic processes in heart cells. *J Mol Cell Cardiol* 1977; 9: 867-874
23. Glantz S. Primer of biostatistics. McGraw-Hill Book Compagny. New York. 1981
24. Helfant RH, Bodenheimer MM, Banka VS. Asynergy in coronary heart disease; evolving clinical and pathophysiologic concepts. *Ann Intern Med* 1977; 87: 475-482
25. Hess OM, Osakada G, Lavelle JF, Gallagher KP, Kemper WS, Ross J. Diastolic myocardial wall stiffness and ventricular relaxation during partial and complete coronary occlusions in the conscious dog. *Circ Res* 1983; 52: 387-400
26. Heuningen R van, Rijnsburger WH, ter Keurs HEDJ. Sarcomere length control in striated muscle. *Am J Physiol* 1982; 242 (Heart Circ Physiol 11): H411-H420
27. Hibberd MG, Jewell BR. Length dependence of the sensitivity of the contractile system to calcium in rat ventricular muscle. *J Physiol* 1979; 290: 30P
28. Holubarsch Ch, Alpert NR, Goulette R, Mulieri LA. Heat production during hypoxic contracture of rat myocardium. *Circ Res* 1982; 51: 777-786
29. Jacobus WE, Poreas IH, Luca SK, Weisfeldt ML, Flaherty JT. Intracellular acidosis and contractility in the normal and ischemic heart as examined by $^{31}\text{-P}$ NMR. *J Mol Cell Cardiol* 1982; 14: 13-20
30. Kentish JC, ter Keurs HEDJ, Ricciardi L, Bux JJJ, Noble MM. Comparison between the sarcomere length-force relations in intact and skinned trabeculae from rat right ventricle. Influence of calcium concentrations on these relations. *Circ Res* 1986; 58: 755-768
31. Kort AA, Lakatta EG. Calcium-dependent mechanical oscillations occur spontaneously in unstimulated mammalian cardiac tissues. *Circ Res* 1984; 54: 396-404
32. Levitsky DO, Benevolensky DS. Effects of changing Ca^{2+} -to- H^{+} ratio on Ca^{2+} uptake by cardiac sarcoplasmic reticulum. *Am J Physiol* 1986; 250 (Heart Circ Physiol 19): H360-H365
33. McLaurin LP, Rolett EL, Grossman W. Impaired left ventricular relaxation during paced-induced ischemia. *Am J Cardiol* 1973; 32: 751-757
34. Miller DJ, Smith GL. The contractile behaviour of EGTA and detergent-treated heart muscle. *J Muscle Res Cell Motil* 1985; 6: 541-567
35. Nakamura Y, Wiegner AW, Bing OHL. Measurement of relaxation in isolated rat ventricular myocardium during hypoxia and reoxygenation. *Cardiovasc Res* 1986; 20: 690-697
36. Nakaya H, Kimura S, Kanno M. Intracellular K^{+} and Na^{+} activities under hypoxia, acidosis, and no glucose in dog hearts. *Am J Physiol* 1985; 249 (Heart Circ Physiol 18): H1078-H1085
37. Narita H, Nagao T, Sato M, Nakajima H, Kiyomoto A. Ischemia - reperfusion induced elevation of diastolic tension in the isolated guinea pig heart and the effects of calcium antagonists. *Jpn Heart J* 1983; 24:277-288
38. Nayler WG, Grau A, Slade AA. A protective effect of verapamil on hypoxic heart muscle. *Cardiovas Res* 1976; 10: 650-662
39. Orchard CH, Eisner DA, Allen DG. Oscillations of intracellular Ca^{2+} in mammalian cardiac muscle. *Nature* 1983; 304: 735-738
40. Orchard CH. Acidosis exacerbates oscillations of intracellular Ca^{2+} in isolated mammalian ventricular muscle. *J Physiol* 1986; 377: 112P
41. Paulus WJ, Serizawa T, Grossman W. Altered left ventricular diastolic properties during pacing-induced ischemia in dogs with coronary stenoses. *Circ Res* 1982; 50: 218-227
42. Paulus WJ, Grossman W, Serizawa T, Bourdillon PD, Pasipoularides A, Mirsky I. Different effects of two types of ischemia on myocardial systolic and diastolic function. *Am J Physiol* 1985; 248: H719-H728
43. Pasipoularides A, Palacios I, Frist W, Rosenthal S, Newell JB, Powell WJ. Contribution of activation-inactivation dynamics to the impairment of relaxation in hypoxic cat papillary muscle. *Am J*

- Physiol 1985; 248 (Regulatory Integrative Comp Physiol 17): R54-R62
44. Renlund DG, Weisman HF, Gerstenblith G, Weisfeldt ML, Stern MD, Lakatta EG. Exaggerated ATP-dependent Ca^{2+} cycling sensed by laser spectroscopy during reperfusion. *Circulation* 1985; 72: III-120
45. Schouten VJA, ter Keurs HEDJ. *Circ Res* 1990 (accepted)
46. Serizawa T, Vogel WM, Apstein CS, Grossman W. Comparison of acute alterations in left ventricular relaxation and diastolic chamber stiffness induced by hypoxia and ischemia; Role of myocardial oxygen supply-demand imbalance. *J Clin Invest* 1981; 68: 91-102
47. Serizawa T, Carabello BA, Grossman W. Effect of pacing-induced ischemia on left ventricular diastolic pressure-volume relations in dogs with coronary stenoses. *Circ Res* 1980; 46: 430-439
48. Sharma B, Hodges M, Asinger RW, Goodwin JF, Francis BS. Left ventricular function during spontaneous angina pectoris: Effect of sublingual nitroglycerin. *Am J Cardiol* 1980; 46: 34-41
49. Tennant R, Wiggers CS. The effect of coronary occlusion on myocardial contraction. *Am J Physiol* 1935; 112: 351-361
50. ter Keurs HEDJ, Rijnsburger WH, van Heuningen R. Restoring forces and relaxation of rat cardiac muscle. *Eur Heart J* 1980a; 1 (Supplement A): 67-80
51. ter Keurs HEDJ, Mulder BJM. Propagation of after-contractions in cardiac muscle of rat. *J Physiol* 1984; 353: 59P
52. ter Keurs HEDJ. Calcium and Contractility. In: AJ Drake-Holland and MIM Noble, eds. *Cardiac metabolism*. Chichester: John Wiley & Sons Ltd, 1983: 73-99.
53. ter Keurs HEDJ, Rijnsburger WH, van Heuningen R, Nagelsmit MJ. Tension development and sarcomere length in rat cardiac trabeculae; Evidence of length-dependent activation. *Circ Res* 1980b; 46: 703-714
54. Tyberg JV, Parmley WW, Sonnenblick EH. In-vitro studies of myocardial asynchrony and regional hypoxia. *Circ Res* 1969; 25: 569-579
55. Ventura-Clapier R, Vassort G. Rigor tension during metabolic and ionic rises in resting tension in rat heart. *J Mol Cell Cardiol* 1981; 13: 551-561
56. Wilde AAM, Kleber AG. The combined effects of hypoxia, high K^+ , and acidosis on the intracellular sodium activity and resting potential in guinea pig papillary muscle. *Circ Res* 1986; 58: 249-256

Ischemia depresses contractility and impairs relaxation of myocardial cells. In contrast with short lasting ischemia, from which the myocyte can easily recover ('stunning'), long lasting ischemia may change mechanical and biochemical function irreversibly.

A better understanding of the underlying pathophysiological mechanisms may ultimately improve treatment of patients that suffer from myocardial ischemia or infarction. The aim of the studies described in this thesis, was to assess the relation between biochemistry of energy-rich phosphates and sarcomere mechanics in heart muscle under conditions that mimic ischemia.

Although the pathogenesis of ischemia is incompletely understood it has been emphasized that absence of flow is an absolute prerequisite. Therefore the results of experimental models in which flow is maintained should be interpreted cautiously since they differ from models in which flow is interrupted. Our model confined the study of muscle mechanics to changes in sarcomere behaviour in the viable part of the preparation since the contribution of the damaged ends on both sides of the preparation and their role as series elastic elements was well controlled. Furthermore, the analysis and interpretation of the mechanical performance was greatly simplified due to the fact that our muscle preparations are linear.

Right ventricular trabeculae of the rat heart were used as a simple linear model. Muscle mechanics was studied during maximally 18 hours of stable force. The developed stress was comparable to the stress that exists in the wall of the intact left ventricle. Since the preparations were extremely thin, sarcomere length could be measured by means of laser diffraction techniques (ter Keurs et al., 1980). High pressure liquid chromatography (H.P.L.C.), a very sensitive biochemical analytical technique, was used to determine the content of high-energy phosphates in the same preparations (Harmsen et al., 1985).

We initially studied the mechanical performance of intact preparation during normoxia and defined the force - sarcomere length and force - velocity relationships (ter Keurs et al., 1986; Ricciardi et al., 1984). We showed that the relation between active force and sarcomere length is convex toward the ordinate at high $[Ca^{2+}]$ and convex toward the abscissa at low $[Ca^{2+}]$ of the perfusate. Even at higher $[Ca^{2+}]$ peak twitch force does not reach a plateau. This relation is similar in different species, including sheep, pig, dog, ferret, rat and guinea pig.

Subsequently the direct contribution of the myofilaments to force development was studied in the same muscles preparations following disruption of the cell membrane by chemical 'skinning'. This technique enabled direct activation of the myofilaments actin and myosin by varying the Ca^{2+} concentration in the buffered superfusate; subsequently the relation between Ca^{2+} , sarcomere length and force could be established.

We found that the relationship between force and sarcomere length in intact and skinned preparations was similar. The relation between pCa^{2+} and force development by the myofilaments could be described as a Michaelis-Menten relationship. Essentially our experiments were compatible with the notion that force generating properties of the myofilaments by direct stimulation of buffered Ca^{2+} solutions reflects the biochemical behaviour of myosin ATP-ase that is involved in the chemomechanical conversion of energy-rich phosphates to force. In addition, we presented evidence that the Ca^{2+} sensitivity of the contractile proteins is length-dependent (Kentish et al., 1986).

During the same set of experiments we observed that nifedipine, even at a concentration of 200 mM, has no effect on force development of the myofilaments. On the basis of this observation it was concluded that nifedipine neither directly inhibits the actomyosin ATP-ase nor interferes with the Ca^{2+} binding process.

Although the method is complicated and laborious, skinning techniques could serve as a useful

tool for studies of the interaction between any compound or drug and the contractile machinery, notably myosin ATP-ase.

Since acidosis is one of the important aspects of ischemia, we studied the effect of increased H^+ concentration in the superfusate on the force - sarcomere length and force - velocity relations (Ricciardi et al., 1986). An increase of $[H^+]_o$ caused a shift of the force - pCa^{2+} relationship to the right. This observation is in agreement with the hypothesis that the Ca^{2+} sensitivity of the myofilaments decreases as a result of competition of H^+ and Ca^{2+} ions for the same binding sites on troponin-C. However, the negative inotropic effect of H^+ ions can only partially be compensated for by increasing $[Ca^{2+}]$ in the perfusate. The effects of acidosis on cell metabolism and notably high-energy phosphate metabolism was not studied in our model. It is likely that the negative effect of protons on force generation - which indirectly limits high-energy phosphate consumption - outweighs the effect on energy metabolism. This assumption is supported by observations in skinned fibers where the effects of acidosis are qualitatively similar to our observations in the intact preparations, that is in presence of concentrations of energy-rich phosphates that are comparable to concentrations found in the intact heart. Moreover acidosis does not result in increased resting tension, which again suggests that the energy-rich phosphate concentration in the vicinity of the myofilaments is sufficient to prevent rigor bond formation. Lastly, since mechanical performance recovers completely following normalization of pH in the superfusate, the effects of acidosis are only temporary and do not give rise to irreversible damage to the contractile machinery.

It should be noted that the effects of hypercapnic acidosis may differ from metabolic acidosis as it occurs during ischemia. The advantage of the use of hypercapnic acidosis, however, is that in this model we were able to study the effects of the interaction between protons and the contractile process separate from other effects of ischemia on cell function.

In another series of experiments ischemia was mimicked by mounting comparable muscles in an experimental chamber with a content of only 360 μ L. Ischemia was induced by replacing oxygenated Krebs-Henseleit medium (pO_2 500 - 600 mm Hg) by glucose-free hypoxic superfusate (pO_2 6 - 9 mm Hg), followed by flow standstill. The subsequent decline of active force was reproducible and depended on the frequency of stimulation. Shortly after the beginning of ischemia / anoxia, the resting force of the muscles increased and reached a maximum after 40 - 55 minutes. At this stage, the muscles did not shorten upon release and the sarcomere length was constant. Furthermore, no spontaneous sarcomere motion was observed. This mechanical behaviour of the muscles strongly suggests rigor state, which is surprising in view of concentrations of CrP and ATP that were still 40% of control (Achterberg et al., 1985).

Since these observations are at variance with reports in literature this hypothesis was further tested in muscles at continuous hypoxic perfusion. In a normoxic muscle at rest cross-bridge activity is low; on the other hand the activity is very high during a tetanus that may be elicited by rapid pacing in presence of 4 mM Ca^{2+} and 10 mM caffeine (ter Keurs et al., 198 ****). The mechanical behaviour of the preparation can be assessed under both conditions by analysing the transfer function; the technique involves imposing sinusoidal muscle length changes and measuring the concomitant force fluctuations. This technique was applied to study mechanical behaviour of normoxic muscles at rest and during a tetanus. In addition the same muscles were analysed at maximal diastolic tension, following continued hypoxic superfusion. The transfer function of normoxic muscles at rest and muscles at maximal diastolic tension was comparable except that stiffness of the latter had increased by a factor of 15 compared to the former. Our observations therefore are in agreement with the hypothesis that rigor develops during hypoxic superfusion (Buck and ter Keurs, 1992). Preliminary analyses of the transfer function of hypoxic muscles during the development of increased diastolic tension indicated that the initial increase of resting

tension is caused by a combination of Ca^{2+} overload and lack of high-energy phosphates in the vicinity of the myofilaments, which is in agreement with observations by others (Steenbergen et al., 1990).

The effect of early reoxygenation on mechanical function was evaluated with emphasis on changes in relaxation. It is well known that twitch force decreases during hypoxia. Moreover, relaxation time varies with twitch force. Therefore, we first assessed the relationship between force and relaxation time at normoxia, in order to be able to assess the relative changes in relaxation time that were observed during hypoxia. Following hypoxia by glucose-free hypoxic medium (pO_2 6 - 9 mm Hg), the preparations were reoxygenated as soon as active force had decreased by 50%. In contrast with data in the literature we observed that relaxation is impaired during hypoxia with further deterioration during reoxygenation. At the same moment spontaneous sarcomere activity in the preparations increases considerably, notably during reoxygenation. These observations suggest spontaneous Ca^{2+} leakage from the sarcoplasmic reticulum with subsequent Ca^{2+} induced Ca^{2+} release as underlying mechanism. The demonstration of increased sarcomere length noise, expressed as RMS values, both during hypoxia and reoxygenation, is interpreted as expression of the increased spontaneous localized sarcomere shortening which also is in agreement with the hypothesis discussed above.

The observation that muscle mechanics of ischemic myocardium is comparable with rigor in spite of concentrations of high-energy phosphate compounds that are still 40% of control values is striking and warrants further study.

The hypothesis that relaxation in hypoxic and reoxygenated myocardium is impaired on the basis of spontaneous Ca^{2+} release by the sarcoplasmic reticulum, is in agreement with our observations. The favourable effects of Ca^{2+} antagonists may be explained, at least partially, on their interference with Ca^{2+} entry during the slow phase of the action potential. However, since $\text{Na}^+/\text{Ca}^{2+}$ exchange plays a more important role in the regulation of $[\text{Ca}^{2+}]_i$, the exact mode of action of Ca^{2+} entry blockers should be studied in more detail.

In more recent experiments we were able to compensate for the negative inotropic effect of H^+ ions by the addition of Sr^{2+} to the perfusate; this ion may either replace Ca^{2+} ions that are sequestered in the sarcoplasmic reticulum without triggering spontaneous release by this organel or directly activate the myofilaments. It would be worthwhile to apply this technique for studies that are intended to verify normal force development by the myofilaments, obviating the necessity of direct stimulation as in the time consuming and laborious technique of chemical 'skinning'. Using this approach the effects of ischemia on different cell processes like function of the cell membrane (action potential measurements), SR (mechanical restitution) and contractile machinery can be studied separately (ter Keurs, 1992).

IMPLICATIONS OF THE CURRENT STUDIES FOR CLINICAL TREATMENT OF ACUTE ISCHEMIA

Survival of ischemic myocytes is mainly determined by preservation of energy rich phosphates. In order to favour this, myocardial oxygen consumption (MVO_2) should be limited during ischemia. Amongst others, this may be accomplished by administration of beta-blocking agents. The mechanisms underlying the efficacy of the administration of beta-blocking agents during and shortly after a myocardial infarction are incompletely understood. It is likely that the protective effects of these agents is related to the negative inotropic and chronotropic properties of these drugs (Gerber and Hies, 1985). Furthermore adrenergic stimulation is also known to activate α -receptor sites. Since α activation is associated with malignant reperfusion arrhythmias, that may be elicited by increased intracellular Ca^{2+} ,

concomitant administration of α -blockers has been advocated in order to prevent this deleterious effect (Sharma and Corr, 1983). For a more extensive discussion of the rationale of a number of currently applied clinical measures and early management of patients with myocardial infarction, including the use of thrombolytic agents, the reader is referred to excellent reviews that recently have been published (ACCA/AHA Task Force, 1990; Weaver and Kennedy, 1992; Yusuf, 1990).

Likewise, the role of the coronary vasculature during myocardial ischemia and infarction is incompletely understood. As discussed before, phosphorus magnetic resonance spectroscopy has demonstrated that after 30 seconds of total global ischemia by aortic flow occlusion, the levels of inorganic phosphate and phosphocreatine levels are virtually unchanged. Likewise, the concentration of ATP and intracellular pH are comparable to levels in normoxic perfused hearts at this stage. Still, isovolumic left ventricular pressure is reduced by more than 50% at that time. The time course of the decrease of pressure development is slower and follows the concomitant changes in inorganic phosphate and pH, more closely after global coronary embolization by means of microspheres (diameter 15 μm). Based on these observations Koretsune et al. concluded that vascular collapse modulates the contractile performance of (ischemic) myocardium by mechanism(s) that as yet is (are) incompletely understood. These authors hypothesized that unsplitting of the myocytes would change sarcomere length to less favourable end-diastolic length, resulting in a fall in force development according to the Frank-Starling curve (Koretsune et al., 1991). Alternatively, they suggested that distended coronaries (erectile effect) could act as struts, potentiating the strength of myocardial contraction, independent of sarcomere length changes (Kitakaze and Marban, 1989).

Alternatively, Schouten et al. (1991) recently showed a paradoxical enhancement of contractility in postischemic rat hearts with depressed function. They suggested that this could be an expression of Ca^{2+} overload, resulting in local injury, followed by regional and ultimately general contractures. This would prevent regional increase of contractility as a result of Ca^{2+} accumulation to be expressed as increased twitch force. Schouten also showed the effect of intravascular pressure per se on force development. They suggested stress induced increase in Na^+ loading, followed by an increase in $[\text{Ca}^{2+}]_i$ via inhibition of $\text{Na}^+/\text{Ca}^{2+}$ exchange (Schouten et al., 1992).

It may be clear from these opposing explanations that further investigation of the role of the coronary vasculature in the process of ischemia is warranted. The suggestion that the coronary vasculature might be involved in the decrease of force development supports the clinical strategy that thrombolysis should be applied as soon as possible in order to restore flow in thrombosed coronary arteries. This might be one of the explanations of the favourable effects of thrombolytic agents, even when administered 12 - 24 hours after the onset of the coronary occlusion (Topol et al., 1992; Wilcox et al., 1992). It is possible that not only a phased development of myocardial infarction is prevented or interrupted, but also that the erectile vasculature is restored which may enhance contractility (Schouten et al., 1992).

Consecutive short episodes of ischemia lead to reduced contractility of the myocardium and may trigger arrhythmias. The persistence of high intracellular calcium levels, resulting in triggered activity and subsequent decreased force development by the myocardium, as well as depletion of the pool of high-energy phosphates can either alone or in combination be responsible for this phenomenon, that in the literature is referred to as 'stunned myocardium' (Geft, 1982). Several interventions, such as administration of Ca^{2+} channel antagonists, ACE inhibitors, and free radical scavengers have shown to be able to shorten the recovery time (Smiseth, 1983) or to prevent stunning to occur (Heusch, 1992; Nayler et al., 1980; Opie, 1992).

FAVOURABLE CLINICAL INTERVENTIONS INTENDED TO LIMIT MYOCARDIAL DAMAGE DURING ISCHEMIA

Reduction of $[Na^+]_i$

As discussed before, developed tension is proportional to $[Na^+]_i$ which directly affects Na^+/Ca^{2+} exchange and thereby $[Ca^{2+}]_i$. $[Na^+]_i$ is determined by several mechanisms (Ellis, 1977). Influx is governed by a) voltage dependent sodium channels such as the fast Na^+ channel that opens during phase 0 of the action potential, and b) Na^+ ion exchangers, like the Na^+/H^+ and the Na^+/Ca^{2+} exchanger. Efflux of sodium is determined by the Na^+/K^+ pump, exchanging 2 K^+ ions in exchange for extrusion of 3 Na^+ ions, at the expense of one molecule of ATP. The direction of operation of these exchangers is determined by the gradient of each ion, the stoichiometry and the membrane potential.

At first sight the idea to restrict influx of Na^+ ions during phase 0 of the action potential seems appealing, since in this way intracellular Ca^{2+} concentration could be reduced. It is possible to inhibit fast Na^+ channels selectively by administration of tetrodotoxin (TTX) or saxitoxin, that bind to the outer orifice of the Na^+ channel (Ritchie and Rogart, 1977). Inhibitors that bind to the inner surface of the cell membrane include amiodarone, lidocaine and procaine. However, prevention or inhibition of the duration and/or height of the action potential would ultimately reduce the slow Ca^{2+} inflow during the plateau phase which would reduce twitch force development by ischemic myofilaments even further or even lead to complete blockade of excitation-contraction coupling with obvious deleterious effects.

Decrease of Ca^{2+} influx (Ca^{2+} channel blockade) during phase 2 of the action potential

The prototypes of the slow Ca^{2+} current inhibitors include the dihydropyridine nifedipine, the phenylalkylamine verapamil and the benzothiazepine diltiazem. Verapamil and diltiazem pass the cell membrane and exert their inhibitory effects on the inside of the sarcolemma in contrast to nifedipine that binds on the outside. Their favourable short term effects are believed to result from inhibition of the slow inward Ca^{2+} flux. This induces coronary vasodilation which subsequently increases the rate of oxygen supply and removal of metabolites. In addition, the well known cardiac effects i.e. the negative chronotropic and inotropic effects, are associated with decreased oxygen utilization. This is expected to result in a reduction of the number and the severity of ischemic episodes. The observed favourable effects of Ca^{2+} blocking agents may also result from their vasodilating properties that allow the heart to work at an energetically more advantageous pressure volume trajectory (Suga, 1990). Finally, long term treatment with Ca^{2+} blocking agents has been shown to result in regression of atherosclerotic sequelae, preservation of endothelial integrity and reduction of incidence of arrhythmias (Weinstein and Heier, 1989).

Alternatively, Ca^{2+} influx during the action potential may be inhibited by administration of Mg^{2+} ions which may be one of the underlying mechanisms for the advantageous effects that have been attributed to this ion (Lansman et al, 1986; Shechter et al., 1990).

Recently, phosphodiesterase inhibitors, like amrinone and milrinone, as well as β -adrenoceptor agonists have been introduced and applied in patients with terminal pump failure. These drugs are administered in this category of patients in an attempt to increase contractility, though at the expense of increased oxygen consumption by the heart. Their supposedly favourable action is based on the assumed increase of the number of sarcolemmal L-type Ca^{2+} channels that open during the action potential, an effect that is mediated by elevation of c-AMP (Hönerjäger, 1989). In addition, this type of drugs raises the probability that Ca^{2+} ions will cross the activated channels (Tsien et al., 1986). Overall Ca^{2+} influx will be facilitated. Likewise intracellular Ca^{2+} concentration may be elevated by administration of digitalis

or ouabaine, that inhibit the $\text{Na}^+\text{-K}^+$ ATPase of the sarcolemma. It is obvious that administration of these drugs may lead to Ca^{2+} overload that may be associated with increased diastolic tension; in addition, dyssynchronous Ca^{2+} release by the SR may be triggered, leading to impairment of tension development (Cunningham et al., 1989). In view of the previous arguments, it is not recommended to apply these drugs in the setting of myocardial ischemia or infarction, notably because of their inherent propensity to increase myocardial oxygen consumption.

Modify Ca^{2+} release by the SR and Ca^{2+} sensitivity of the myofilaments

Administration of phosphodiesterase inhibitors results in elevated levels of c-AMP. As a result troponin I, a subunit of the troponin-tropomyosin complex, is phosphorylated. This in turn leads to decreased affinity of Troponin C for Ca^{2+} . Furthermore, increased levels of c-AMP cause phosphorylation of phospholamban in the SR, which causes increased uptake rate of Ca^{2+} ions by the SR. Together this leads to increased rate of force relaxation (Katz, 1983). Obviously this will prevent development of contracture under conditions of Ca^{2+} overload. However, since contractile force of ischemic myocardium is already severely impaired, administration of these drugs is not preferable.

Uptake and release of Ca^{2+} by the SR may be modified by Mg^{2+} . This ion promotes calcium uptake by the SR, whereas subsequent Ca^{2+} induced Ca^{2+} release is counteracted (Fabiato and Fabiato, 1975). Maybe the favourable effect that has been observed following the administration of Mg^{2+} to patients with acute myocardial infarction, may be based upon this mechanism (Shechter et al., 1990).

Ryanodine also interferes with Ca^{2+} handling by the SR. It causes a dose dependent leakage of Ca^{2+} from the sarcoplasmic reticulum; in addition it inhibits the Ca^{2+} release channels in the SR. Consequently, even nanomolar concentrations of ryanodine are able to elicit triggered propagated contractions, giving rise to depression of twitch force and delay of twitch relaxation (Daniels, 1991).

Promotion of Ca^{2+} extrusion from the cell

Ca^{2+} extrusion may be promoted in presence of increased levels of c-AMP, resulting from β -adrenergic stimulation. c-AMP is known to activate the sarcolemmal Ca^{2+} ATP-ase, that is responsible for Ca^{2+} extrusion from the cell; this effect however is small compared to facilitation of Ca^{2+} uptake and release by the SR, as well as increased Ca^{2+} influx during the action potential (Lamers et al., 1981).

Correct or prevent metabolic derangements during myocardial ischemia or infarction

Recently evidence has been presented in favor of administration of angiotensin-converting enzyme (ACE) inhibitors to patients with acute myocardial infarction. The apparent favourable effects are due to inhibition of the renin angiotensin system and associated with alterations of the activity of the sympathetic nervous system, myocardial perfusion and possible antiarrhythmic effects during myocardial infarction (Ertl, 1988). Their favourable effects in postinfarct heart failure may be explained by partial normalization of myocardial contractility and Ca^{2+} handling (Litwin and Morgan, 1992). In a subset of patients, ACE inhibitor therapy may reduce the risk of ventricular dilatation, increase exercise tolerance and reduce mortality following the acute events (Consensus, 1987).

Treatment with high-energy phosphates or precursors (inosine) appears to improve outcome following transient ischemia (Smiseth, 1983; Hearse et al., 1981). More recently, it has been shown that myoflazine, a potent nucleoside transport inhibitor, is able to maintain the nucleoside pool and notably adenosine at a high level; its effect is probably due to inhibition of the passage of nucleosides through the sarcolemma (Belle et al., 1986). As expected conservation of the energy pool leads to a faster and

more complete recovery following reoxygenation (Ronca-Testoni et al., 1985)

Prevention of myocardial damage

During ischemia, high-energy phosphate content of myocardium may be preserved by rapid induction of diastolic arrest prior to the ischemic event. This may be accomplished by administration of cardioplegic solutions, that contain high concentrations of potassium (> 15 mmol/L) (Melrose et al., 1955). Postischemic recovery can be further improved by hypothermia, that affords protection that is distinct from and additive to the effect of potassium arrest (Hearse et al., 1980). Usually calcium antagonists are also applied, since these drugs are known to inhibit slow Ca^{2+} inflow and thereby, at least partially, prevent the calcium overload that plays a pivotal role in the onset of irreversible injury. However, it should be stressed that the rationale for this approach is based on the simplification that most of the Ca^{2+} ions enters the myocyte during the slow phase of the action potential. As discussed before Ca^{2+} homeostasis is largely accounted for by the $\text{Na}^+/\text{Ca}^{2+}$ exchanger and other exchange mechanisms. At present, no selective blockers or accelerators of the $\text{Na}^+/\text{Ca}^{2+}$ exchanger are available.

In the mitochondria, reduction of oxygen to H_2O is associated with production of oxygen free radicals and H_2O_2 , metabolites that are capable of extensive tissue destruction. In normoxic biological tissues, these intermediates are neutralized in a sequence of reactions that is catalyzed by superoxide dismutase (S.O.D.), catalase and glutathione peroxidase (Hess and Manson, 1984; Kukreja and Hess, 1992). During experimental and clinical ischemia and reoxygenation these compensatory mechanisms are defective, however. Thus, the concentration of oxygen free radicals may then increase and extensive damage could result. Formation of oxygen free radicals may be inhibited by nonsteroidal anti-inflammatory agents; the hydroxyl radical scavengers dimethylsulfoxide (D.M.S.O.), mannitol or glucose are able to neutralize residual oxygen radicals (Hess and Manson, 1984). Butylated hydroxytoluene (BHT), an antioxidant, also has been shown to exert protective effects due to its neutralizing properties.

CLINICAL IMPLICATIONS AND FUTURE DIRECTIONS

With the introduction of interventional procedures for the treatment of acute ischemic syndromes, the clinical entities myocardial stunning and hibernation have gained more attention. It has been suggested that myocardial stunning encompasses prolonged contractile dysfunction after ischemic injury that is followed by gradual normalization. Hibernation, on the other hand, refers to chronically depressed myocardial function as a result of chronic low bloodflow; in the latter condition contractile function will promptly normalize upon relief of ischemia. It has been suggested that the depression of contractility -- either on the short or on the long term -- in patients following coronary revascularization procedures may be explained by either one of these phenomena. Alternatively, the same mechanisms may be involved in the temporary depression of regional or global contractile function in patients with acute myocardial infarction, even when coronary blood flow is restored following administration of thrombolytic agents. It is conceivable that the same pathophysiological mechanisms underly cardiac remodelling that is observed following extensive myocardial infarction or heart failure and the chronic low flow syndrome that may ultimately result in chronic ischemic cardiomyopathy. Future clinical research should be aimed at providing the clinical cardiologist with investigational tools, to discriminate between contractile dysfunction on the basis of hibernation or stunning or reduction of pump function as a result of irreversible loss of myocardial cells (Braunwald, 1990).

Recently evidence was presented that the cell membrane of the myocyte contains ATP sensitive K^+ channels (Noma, 1983). Activation of these K^+ channels when the ATP concentration is low would

effectively 'clamp' the membrane potential to the Nernst potential for potassium (± -90 mV) and thus prevent generation of action potentials. A number of drugs, including nicorandil, cromakalim, pinacidil and minoxidil appeared to be able to modulate the properties of these K^+ channels (Coetzee, 1992). At first sight administration of these drugs in the setting of ischemia seems appealing since they might contribute to restoration of potassium regulation, correct potassium efflux and prevent the arrhythmias that are frequently observed. However, one should be aware that hyperpolarization of the myocyte by ATP sensitive K^+ channels may prevent contraction, resulting in reduction of energy consumption related to excitation-contraction coupling and actomyosin induced contraction of the heart, which may be crucial for survival of the energy deprived myocyte. Therefore, prior to introduction of these drugs for treatment of acute ischemic syndromes, their possible favourable effects should be better defined in clinical studies, in particular in relation to infarct size.

Finally, the controversy about the moment at which irreversible damage to myocardial cells occurs still continues. The most important hypotheses explaining initial depression and ultimate loss of contractile function by the myocyte include inhibition of the actomyosin ATP-ase and / or decreased Ca^{2+} sensitivity of the myofilaments. The possibility of early morphologic changes of the myofilaments themselves has been suggested but not confirmed (Hajjar and Gwathmey, 1990). It is likely that the mechanisms discussed in this thesis are, in part, responsible for the temporary depression of contractile function that may follow after acute or chronic ischemia. Obviously, further clinical studies are warranted in order to better define the exact relation between cellular contractile dysfunction and pump function of the heart as a whole.

REFERENCES

1. ACC/AHA Task Force. Guidelines for the early management of patients with acute myocardial infarction. *JACC* 1990; 15: 249-292
2. Achterberg PW, Buxx JJJ, de Jong JW, Nieukoop AS, Schouten VJA, ter Keurs HEDJ. High-energy phosphate metabolism and force production in normoxic and ischaemic rat cardiac trabeculae and papillary muscle. *J Physiol* 1985; 366: 73P
3. Belle H van, Wijnants J, Xhonneux R, Flameng W. Changes in creatine phosphate, inorganic phosphate, and the purine pattern in dog hearts with time of coronary artery occlusion and effect thereon of miflazine, a nucleoside transport inhibitor. *Cardiovasc Res* 1986; 20: 658-664
4. Braunwald E. The stunned myocardium: Newer insights into mechanisms and clinical applications. *J Thorac Cardiovasc Surg* 1990; 100: 310-320
5. Buxx JJJ, ter Keurs HEDJ. Sarcomere dynamics in rat cardiac trabeculae during hypoxia with and without superfusion (to be submitted)
6. Coetzee WA. ATP-sensitive potassium channels and myocardial ischemia: Why do they open? *Cardiovasc Drugs Ther* 1992; 6: 201-208
7. Consensus Trial Study Group. Effects of enalapril on mortality in severe congestive heart failure. *N Engl J Med* 1987; 316(23): 1429-1439
8. Cunningham MJ, Apstein CS, Weinberg EO, Lorell BH. Deleterious effect of ouabain on myocardial function during hypoxia. *Am J Physiol* 1989; 256 (Heart Circ Physiol 25): H681-H687
9. Daniels MCG. Mechanism of triggered arrhythmias in damaged myocardium. Academic Thesis. Utrecht, 1991
10. Ellis D. The effects of external cations and ouabain on the intracellular sodium activity of sheep heart Purkinje fibres. *J Physiol (London)* 1977; 273: 211-240
11. Ertl G. Angiotensin converting enzyme inhibitors and ischaemic heart disease. *Eur Heart J* 1988; 9: 716-727
12. Fabiato A, Fabiato F. Effects of magnesium on contractile activation of skinned cardiac cells. *J Physiol* 1975; 249: 497-517
13. Geft IL, Fishbein MC, Ninomiya K, Hashida J, Chauv E, Yano J, Yrit J, Genov T, Shell W, Ganz W. Intermittent brief periods of ischemia have a cumulative effect and may cause myocardial necrosis. *Circulation* 1982; 66: 1150-1153

14. Gerber JC, Hies AS. Beta-adrenergic blocking drugs. *Annu Rev Med* 1985; 36: 145-164
15. Hajjar RJ, Gwathmey JK. Direct evidence of changes in myofilament responsiveness to Ca^{2+} during hypoxia and reoxygenation in myocardium. *Am J Physiol* 1990; 259: H784-H795
16. Harmsen E, de Tombe PP, de Jong JW, Achterberg PW. Enhanced ATP and GTP synthesis from hypoxanthine or inosine after myocardial ischemia. *Am J Physiol* 1985; 246 (Heart Circ Physiol 15): H37-H43
17. Hearse DJ, Braimbridge MV, Jynge P. Protection of the ischemic myocardium: cardioplegia. New York: Raven Press, 1981
18. Hearse DJ, Stewart DA, Braimbridge MV. The additive protective effects of hypothermia and chemical cardioplegia during ischemic cardiac arrest in the rat. *J Thorac Cardiovasc Surg* 1980; 79: 39-43
19. Hess ML, Manson NH. Molecular oxygen: friend and foe; the role of the oxygen free radical system in the calcium paradox, the oxygen paradox and ischemia/reperfusion injury. *J Mol Cell Cardiol* 1984; 16: 969-985
20. Heusch G. Myocardial stunning: a role for calcium antagonists during ischemia? *Cardiovasc Res* 1992; 26: 14-19
21. Hönerjager P. Pharmacology of positive inotropic phosphodiesterase III inhibitors. *Eur Heart J* 1989; 10(Suppl C): 25-31
22. Katz AM. Regulation of myocardial function in the normal and diseased heart: modification by inotropic drugs. *Eur Heart J* 1983; 3(suppl D): 11-18
23. Kentish JC, ter Keurs HEDJ, Ricciardi L, Bux JJJ, Noble MIM. Comparison between the sarcomere length-force relations in intact and skinned trabeculae from rat right ventricle. Influence of calcium concentrations on these relations. *Circ Res* 1986; 58: 755-768
24. Kitakaze M, Marban E. Cellular mechanism of the modulation of contractile function by coronary perfusion pressure in ferret hearts. *J Physiol (London)* 1989; 414: 455-472
25. Koretsune Y, Corretti MC, Kusuoka H, Marban E. Mechanism of early ischemic contractile failure; inexcitability, metabolite accumulation, or vascular collapse? *Circ Res* 1991; 68: 255-262
26. Kukreja RC, Hess ML. The oxygen free radical system: from equations through membrane-protein interactions to cardiovascular injury and protection. *Cardiovasc Res* 1992; 26: 641-655
27. Lamers JMJ, Stinis HT, de Jonge HR. On the role of cyclic AMP and calcium-calmodulin-dependent phosphorylation in the control of calcium-magnesium-ATPase of cardiac sarcolemma. *FEBS Lett* 1981; 127: 139-143
28. Lansman JB, Hess P, Tsien RW. Blockade of current through single calcium channels by cadmium, magnesium, and calcium; voltage and concentration dependence of calcium entry into the pore. *J Gen Physiol* 1986; 88: 321-347
29. Litwin SE, Morgan JP. Captopril enhances intracellular calcium handling and β -adrenergic responsiveness of myocardium from rats with postinfarction failure. *Circ Res* 1992; 71: 797-807
30. Melrose DG, Dreyer B, Bentall HH, Baker JBE. Elective cardiac arrest: preliminary communication. *Lancet* 1955; 2: 21-22
31. Nayler WG, Ferrari R, Williams A. Protective effect of pretreatment with verapamil, nifedipine and propranolol on mitochondrial function in the ischemic and reperfused myocardium. *Am J Cardiol* 1980; 46: 242-248
32. Noma A. ATP-regulated K^{+} channels in cardiac muscle. *Nature* 1983; 305: 147-148
33. Opie L. Myocardial stunning: a role for calcium antagonists during reperfusion? *Cardiovasc Res* 1992; 26:20-24
34. Ricciardi L, Bux JJJ, ter Keurs HEDJ. Effects of acidosis on force-sarcomere length and force-velocity relations of rat cardiac muscle. *Cardiovasc Res* 1986; 20: 117-123
35. Ritchie JM, Rogart RB. The binding of saxitoxin and tetrodotoxin to excitable tissue. *Rev Physiol Biochem Pharmacol* 1977; 79: 1-50
36. Ronca-Testoni S, Galbani P, Ronca G. Effect of creatine phosphate administration on the rat heart adenylate pool. *J Mol Cell Cardiol* 1985; 17: 1185-1188
37. Schouten VJA, Allaart CP, Westerhof N. Effect of perfusion pressure on force of contraction in thin papillary muscles and trabeculae from rat heart. *J Physiol* 1992; 451:585-604
38. Schouten VJA, Los GJ, Kuypers PD, Brinkman CJ, Huysmans HA. Paradox of enhanced contractility in postischemic rat hearts with depressed function. *Am J Physiol* 1991; 260: H89-99
39. Sharma AD, Corr PB. Adrenergic factors in arrhythmogenesis in the ischemic and reperfused

- myocardium. *Eur Heart J* 1983; 4 (Supplement D); 79-90
40. Shechter M, Hod H, Marks N, et al. Beneficial effects of magnesium sulfate in acute myocardial infarction. *Am J Cardiol* 1990; 66: 271-274
41. Smiseth OA. Inosine infusion in dogs with acute ischaemic left ventricular failure: favourable effects on myocardial performance and metabolism. *Cardiovasc Res* 1983; 17: 192-199
42. Steenbergen C, Murphy E, Watts JA. Correlation between cytosolic free calcium, contracture, ATP, and irreversible ischemic injury in perfused rat heart. *Circ Res* 1990; 66: 135-146
43. Suga H. Ventricular energetics. *Phys Rev* 1990; 70: 247-277
44. ter Keurs HEDJ. Post-extrasystolic potentiation and its decay. In: *The interval-force relationship of the heart*. Edited by MIM Noble and WA Seed. Cambridge University Press 1992, pg 259-276
45. ter Keurs HEDJ, Rijnsburger WH, van Heuvelingen R, Nagelsmit MJ. Tension development and sarcomere length in rat cardiac trabeculae; evidence of length-dependent activation. *Circ Res* 1980; 46: 703-714
46. ter Keurs HEDJ, Ricciardi L, Bucx JJJ, Grant DA, Lofgren DN. The force-sarcomere length relations in mammalian myocardium. *Eur J Clin Invest* 1986; 16: A4
47. Topol EJ, Califf RM, Vandormael M, et al. A randomized trial of late reperfusion therapy for acute myocardial infarction. *Circ* 1992; 85: 2090-2099
48. Tsien, RW, Bean HP, Hess P, Lansman JB, Nilius B, Nowicky MC. Mechanisms of calcium channel modulation by β -adrenergic agents and dihydropyridine calcium agonists. *J Mol Cell Cardiol* 1986; 18: 691-710
49. Weaver WD, Kennedy JW. Myocardial infarction - thrombolytic therapy in the prehospital setting. In: *Thrombosis in cardiovascular disorders*. Edited by V Fuster and G Verstraete. 1992, pg 275-287
50. Weinstein DB, Heider JG. Antiatherogenic properties of calcium antagonists; state of the art. *Am J Med* 1989; 86 (suppl 4A): 27-32
51. Yusuf S, Sleight P, Held P, McMahon S. Routine medical management of acute myocardial infarction. Lessons from overviews of recent randomized controlled trials. *Circulation* 1990; 82(suppl II): II117-II134

CHAPTER 11 SUMMARY

Ischemia depresses contractility and impairs relaxation of myocardial cells. Myocytes may recover from short lasting ischemia. Long lasting ischemia may result in irreversible mechanical and biochemical damage.

A better understanding of the underlying patho-physiological mechanisms may ultimately improve treatment of patients that suffer from myocardial ischemia or infarction. The aim of this thesis therefore was to assess the relation between biochemistry of energy-rich phosphates and sarcomere mechanics in heart muscle during normoxia and under conditions that mimic ischemia.

In Chapter 2 the literature of ischemia is reviewed with emphasis on the main functions of the myocardium at the level of the cell i.e. energy metabolism, excitation - contraction coupling, Ca^{2+} homeostasis and the contraction - relaxation cycle. The effects of normoxia, ischemia and reoxygenation on each of these myocyte functions are discussed separately.

Chapter 3 gives an overview of the methodology that has been applied for the studies that are included in this thesis. The mechanical performance of intact trabeculae from the right ventricle of rat heart is described in Chapter 4. By means of laser diffraction techniques the mechanical performance, expressed as force - sarcomere length and force - velocity relationships, was studied at normoxia. The calculated stresses were comparable to the stresses that exist in the wall of the intact left ventricle. Subsequently the contribution of the myofilaments to force generation was evaluated by direct activation following disruption of the cell membranes by chemical 'skinning'. The force - sarcomere length relationships in intact and skinned preparations appeared strikingly similar; the observations were compatible with length-dependent changes of the sensitivity of the contractile proteins for Ca^{2+} ions.

The effect of acidosis, one of the important features of ischemia, on the force - sarcomere length and force - velocity relations is described in Chapter 5. Increased $[\text{H}^+]$ in the superfusate appeared to shift the force - pCa^{2+} relationship to the right. This observation was in agreement with the hypothesis that the Ca^{2+} sensitivity of the myofilaments decreased as a result of competition of H^+ and Ca^{2+} ions for the same binding sites on troponin-C. This negative inotropic effect of acidosis could only partially be compensated for by increased $[\text{Ca}^{2+}]$ in the perfusate.

In Chapter 6 the limiting steps in calcium handling were studied by varying twitch force with respect to maximal twitch force, either by high $[\text{Ca}^{2+}]_o$, low $[\text{Na}^+]_o$, high $[\text{K}^+]_o$, addition of tetraethylammonium chloride or postextrasystolic potentiation, alone or in combination. Beyond the optimum dose, force declined and aftercontractions were observed, suggesting that the amount of Ca^{2+} released by the sarcoplasmic reticulum exceeded the optimum required to attain maximum twitch force. Strontium (Sr^{2+}) resulted in twitch force that exceeded maximal twitch force by 30%. Since the force - sarcomere length relation, then, was similar to that in skinned fibers, we assumed that the myofilaments were fully saturated both by Ca^{2+} and Sr^{2+} ions. In agreement with this hypothesis we observed that that addition of ryanodine, a blocker of the SR, and isoproterenol, an activator of SR Ca^{2+} ATPase and c-AMP dependent inhibitor of Ca^{2+} binding by the myofilaments, resulted in twitch force that exceeded its maximum by only 10%. It was therefore concluded that maximal activation of the sarcomeres and their affinity to Ca^{2+} as well as the rate of uptake of Ca^{2+} by the SR, all determine the contractile response of the myofilaments to Ca^{2+} .

Chapter 8 summarizes observations in comparable muscles that were mounted in a small bath

(content 360 μ L). Ischemia / anoxia was mimicked by replacing oxygenated Krebs-Henseleit medium (pO_2 500 - 600 mm Hg) by glucose-free hypoxic superfusate (pO_2 6 - 9 mm Hg), followed by flow standstill. The subsequent decrease of active force was reproducible and frequency dependent. Shortly after the beginning of hypoxia with flow standstill, the resting force of the muscles increased and reached a maximum after 40 - 55 minutes. Then muscles did not shorten upon release and the sarcomere length was constant; spontaneous sarcomere motion, that increased initially, had ceased completely. This mechanical behaviour of the muscles strongly suggested a rigor state. Subsequently the concentrations of CrP and ATP were measured in the same muscles with HPLC techniques. As described in [Chapter 7](#), the high-energy phosphate content was still 40% of control value which was a striking in view of the mechanical performance of the preparations. Therefore we further tested the 'rigor' hypothesis in comparable muscles during continued hypoxic perfusion ([Chapter 8](#)). The mechanical behaviour of the preparation was studied by transfer function analysis. For this purpose muscle length was changed sinusoidally at varied frequencies and the resulting force fluctuations were measured. First the muscles were studied during normoxia at rest and during a tetanus; then the analysis was repeated following development of maximal diastolic tension by continued hypoxic superfusion. The transfer functions of normoxic muscles at rest and muscles at maximal hypoxic resting tension were qualitatively similar though the latter were 15 times stiffer than the first. This observation was in agreement with the hypothesis that rigor had developed as a result of hypoxic superfusion.

The effects of repeated hypoxia and reoxygenation on relaxation is described in [Chapter 9](#). Since force influences relaxation, this relationship was analysed first at normoxia. Subsequently the relationship was used to evaluate the changes in relaxation that resulted from hypoxia by glucose-free medium (pO_2 6 - 9 mm Hg). The muscles were reoxygenated when active force had decreased to 50% of control; diastolic tension never increased. Relaxation was not only impaired during hypoxia but also and even more during reoxygenation, which is at variance with the literature. During the intervention localized spontaneous sarcomere activation increased considerably, notably during reoxygenation; the concomitant increase of sarcomere length noise during hypoxia and reoxygenation was in agreement with this. These observations led us to propose that hypoxia interfered with relaxation by triggering spontaneous regenerative Ca^{2+} induced Ca^{2+} release by the sarcoplasmic reticulum. The underlying mechanism may be either Ca^{2+} leakage from the SR or impaired uptake of Ca^{2+} in the SR.

In [chapter 10](#) the results are summarized and put into perspective of experimental data presented by other investigators. Some suggestions for further research are given, based on the observations that have been presented in this thesis.

HOOFDSTUK 12 SAMENVATTING

Ischemie leidt tot afname van de pompkracht en vertraagde relaxatie van myocard cellen. Myocyten blijken in staat om te herstellen van de gevolgen van kortdurende ischemie. Langdurige ischemie kan echter resulteren in onherstelbare mechanische en biochemische schade. Door een beter inzicht in de onderliggende pathofysiologische mechanismen zal de behandeling van patiënten met klachten ten gevolge van angina pectoris of een hartinfarct uiteindelijk verbeterd kunnen worden. Dit proefschrift beoogt de relatie tussen enerzijds de energie huishouding en anderzijds het mechanische gedrag van de kleinste krachtleverende elementen in de hartspier, de sarcomeren, te beschrijven. De experimenten werden zowel onder normale omstandigheden (aanwezigheid van zuurstof, flow) als onder experimentele omstandigheden die lijken op ischemie (zuurstof tekort, acidose, stroomstilstand) uitgevoerd.

In Hoofdstuk 2 wordt de literatuur over de gevolgen van ischemie voor verschillende basale functies van de hartspier cel samengevat. Achtereenvolgens worden de energie huishouding, excitatie - contractie koppeling, Ca^{2+} huishouding en de contractie - relaxatie cyclus besproken. De huidige inzichten ten aanzien van de gevolgen van normoxie, ischemie en reoxygenatie op deze fundamentele functies worden samengevat.

Hoofdstuk 3 beschrijft de methoden die gebruikt zijn tijdens de studies die in dit proefschrift zijn opgenomen. Het mechanische gedrag van trabekels uit de rechter ventrikel van het rattehart wordt in Hoofdstuk 4 beschreven. Met behulp van laser diffractie techniek werd het mechanische gedrag van deze preparaten tijdens normoxie bestudeerd en uitgedrukt in de vorm van kracht - sarcomeer lengte en kracht - snelheids relaties. De berekende wandspanning bleek vergelijkbaar te zijn met de wandspanning in de linker ventrikel van het intacte hart. Vervolgens werden de preparaten chemisch 'geskinned', een chemisch procedé waarbij de celmembraan wordt opgelost. Gelijktijdig wordt het preparaat omspoeld met een oplossing, die een vergelijkbare samenstelling heeft als de cytosol van de hartspiercel. Door de samenstelling van deze vloeistof vervolgens te veranderen kunnen de hartspier eiwitten geactiveerd worden. Hierdoor is het mogelijk om de bijdrage van deze myofilamenten aan het kracht leverende vermogen van de preparaten afzonderlijk te bestuderen. De kracht - sarcomeer lengte relaties in intacte en geskinnede preparaten bleken opvallende gelijkenis te vertonen. Deze waarneming bleek in overeenstemming te zijn met lengte-afhankelijke veranderingen van de gevoeligheid van de myofilamenten voor Ca^{2+} ionen.

In Hoofdstuk 5 is het effect van verzuring (acidose), een van de belangrijkste kenmerken van ischemie, op de kracht - sarcomeer lengte en kracht - sarcomeer snelheids relaties beschreven. Een afname van de pH (= toename acidose) in de perfusie vloeistof blijkt gepaard te gaan met een rechtsverschuiving van de kracht - pCa^{2+} relatie. Deze waarneming is in overeenstemming met de hypothese dat de gevoeligheid van de myofilamenten voor Ca^{2+} ionen afneemt ten gevolge van competitie van H^+ en Ca^{2+} ionen om dezelfde bindingsplaatsen op troponin-C. Dit zogenaamde negatief inotrope effect van acidose kan slechts gedeeltelijk ongedaan worden gemaakt door de Ca^{2+} concentratie in het perfusaat te verhogen.

In Hoofdstuk 6 worden de bepalende stappen in de Ca^{2+} huishouding bestudeerd door de contractie kracht te variëren. Hiertoe werd in het perfusie medium de $[\text{Ca}^{2+}]$ en $[\text{K}^+]$ verhoogd, de $[\text{Na}^+]$ verlaagd of tetraethylammonium chloride toegevoegd of postextrasystolische potentiatie toegepast, zowel afzonderlijk als in combinatie. Wanneer de optimale dosis werd overschreden, bleek de kracht te dalen en ontstonden nacontracties, hetgeen suggereerde dat de hoeveelheid Ca^{2+} die door het sarcoplasmatisch

reticulum werd uitgestort het optimum had overschreden dat vereist was om maximale kracht te kunnen leveren. Toevoeging van strontium (Sr^{2+}) leidde tot een toename van de contractiekracht tot 30% boven het maximum. Omdat de kracht - sarcomeer lengte relatie in Sr^{2+} geactiveerde spieren treffende gelijkenis vertoonde met de resultaten bij geskinnede preparaten werd aangenomen dat de myofilamenten op dat moment dus maximaal gesatureerd waren met Ca^{2+} en Sr^{2+} ionen. Dit effect kon gedeeltelijk ongedaan worden gemaakt door ryanodine, een blocker van het sarcoplasmatisch reticulum, of isoproterenol aan het perfusaat toe te voegen; de contractiekracht bleek dan nog slechts 10% boven het maximale niveau toe te nemen. Op grond van deze gegevens werd geconcludeerd dat het kracht leverend vermogen van de myofilamenten niet alleen afhankelijk is van maximale activatie en van de gevoeligheid voor Ca^{2+} maar ook van de snelheid waarmee Ca^{2+} in het sarcoplasmatisch reticulum wordt opgenomen.

In Hoofdstuk 8 wordt verslag gedaan van de waarnemingen bij trabekels die in een perfusie bad van slechts 360 μL werden gemonteerd. Hierin werd ischemie / anoxie nagebootst door de normaliter met zuurstof verzadigde Krebs-Henseleit perfusie vloeistof te vervangen door glucose-vrij, hypoxisch medium (pO_2 6 - 9 mm Hg), waarna de vloeistofstroom werd stilgezet. De afname van de contractie kracht bleek reproduceerbaar te zijn en afhankelijk van de stimulatie frequentie. Kort na het begin van de interventie nam de rust spanning van de preparaten toe en bereikte een maximum na 40-55 minuten. De spieren bleken niet meer te kunnen verkorten en de sarcomeer lengte bleef konstant. De aanvankelijke toename van spontane gelocaliseerde sarcomeer activiteit bleek dan ook vrijwel verdwenen. Dit mechanische gedrag deed sterk denken aan rigor.

Zoals beschreven in Hoofdstuk 7 werden in dezelfde spieren de concentraties van de energierijke fosfaatverbindingen creatinefosfaat (CrP) en adenosine trifosfaat (ATP) door middel van hoge druk vloeistofchromatografie (H.P.L.C.) gemeten. De concentraties van genoemde stoffen bleek slechts 60% afgenomen te zijn, hetgeen opvallend was in het licht van het waargenomen mechanische gedrag.

De 'rigor' hypothese werd daarom verder onderzocht tijdens experimenten waarbij met een hypoxisch medium werden geperfundeed. Zoals beschreven in Hoofdstuk 8 werd het mechanische gedrag van de preparaten aan de hand van de overdrachts functie geanalyseerd. Hierbij werd bij verschillende frequenties de spierlengte van een preparaat volgens een sinus functie met niet meer dan 1 % gevarieerd; de hierdoor geïnduceerde krachtsverandering werd geregistreerd. Beide signalen werden met elkaar vergeleken waarbij zowel de verschuiving van de fasehoek als de variatie in kracht werden gekwantificeerd. De overdrachtsfunctie werd bestudeerd onder normale proefomstandigheden en tijdens een tetanus van de spier d.w.z. maximale activatie door hoge stimulatie frequentie in aanwezigheid van cafeïne. De analyse werd herhaald nadat de spierspanning maximaal was geworden ten gevolge van continue hypoxie. Uit de analyse van de overdrachtsfunctie bleek dat de spier ten gevolge van hypoxie 15 maal stijver was geworden ten opzichte van een normale spier. Er werden geen aanwijzingen gevonden voor contractuur d.w.z. toegenomen spierspanning ten gevolge van toegenomen intracellulaire Ca^{2+} concentratie. Er werd dan ook geconcludeerd dat zich ten gevolge van de langdurige hypoxie rigor had ontwikkeld.

De effecten van herhaalde hypoxie en reoxygenatie werden bestudeerd in een aantal experimenten die in Hoofdstuk 9 zijn opgenomen. Aangezien de relaxatie tijd blijkt te variëren met de contractie kracht, werd deze relatie eerst onder normale omstandigheden geanalyseerd. Aan de hand hiervan werden veranderingen in de relaxatie tijdens perfusie met glucose-vrij, zuurstofarm (pO_2 6 - 9 mm Hg) medium beoordeeld. De spieren werden gereoxygeneed zodra de actieve contractiekracht tot 50% was

gedaald. Onder deze experimentele omstandigheden werd geen toename van de rustspanning waargenomen. De relaxatie bleek vertraagd tijdens hypoxie en verslechterde verder tijdens de eerste fase van reoxygenatie waarna volledige normalisatie optrad. Deze bevindingen wijken duidelijk af van gegevens uit de literatuur. Tijdens de interventie werden aanwijzingen gevonden voor gelocaliseerde, spontane intracellulaire sarcomeer verkorting, met name tijdens de reoxygenatie. De gelijktijdige toename van de ruis in het berekende sarcomeer lengte signaal bleek hiermee in overeenstemming. Daarom werd geconcludeerd dat de vertraagde relaxatie die tijdens hypoxie wordt waargenomen een gevolg is van spontane regeneratieve uitstorting van Ca^{2+} ionen door het sarcoplasmatisch reticulum. Dit zou enerzijds een gevolg kunnen zijn van lekkage van Ca^{2+} uit het sarcoplasmatisch reticulum, anderzijds van gestoorde opname van Ca^{2+} in dit celorganel.

In Hoofdstuk 10 worden de bevindingen samengevat en gerelateerd aan experimentele bevindingen door andere onderzoekers. Ten slotte wordt de mogelijke betekenis van het voorliggende onderzoek voor de dagelijkse praktijk besproken en worden suggesties gedaan voor verder onderzoek.

CURRICULUM VITAE

Jeroen J.J. Bucx, geboren op 27.2.54 te Amersfoort

- | | |
|-------------|---|
| 1966 - 1972 | Gymnasium B, Aloysius College, Den Haag |
| 1972 - 1979 | Medische opleiding, Rijksuniversiteit Leiden |
| 1979 - 1981 | Assistent in opleiding, Afdeling Cardiologie, Gemeenteziekenhuis Leyenburg, Den Haag
(Opleider Dr. C.M. Sparling) |
| 1981 - 1983 | Assistent in opleiding, Afdeling Interne Geneeskunde, Ziekenhuis St. Joannes de Deo, Haarlem (Opleider J.A. de Fockert) |
| 1983 - 1985 | Wetenschappelijk medewerker, Afdeling Experimentele Cardiologie, Rijksuniversiteit Leiden (Supervisor Dr. H.E.D.J. ter Keurs) |
| 1985 - 1986 | Research Fellow, Department of Medicine and Medical Physiology, University of Calgary, Calgary, Alberta, Canada (Supervisor Dr. H.E.D.J. ter Keurs) |
| 1985 - 1986 | Resident V, Department of Medicine, Foothills Hospital, University of Calgary, Calgary, Alberta, Canada (Head of the Department Dr. E. Smith) |
| 1987 - 1990 | Assistent in opleiding, Afdeling Cardiologie, Thoraxcenter, Academisch Ziekenhuis Dijkzigt, Rotterdam (Opleiders Prof. P.G. Hugenholtz en Prof. Dr. J.R.T.C. Roelandt) |
| Sinds 1990 | Geregistreerd als cardioloog, Junior stafid, Afdeling Cardiologie, Thoraxcenter, Academisch Ziekenhuis Dijkzigt, Rotterdam (Hoofd Prof. Dr. J.R.T.C. Roelandt)
Rotterdam |
| Sinds 1990 | Werkzaam als cardioloog, Afdeling Cardiologie, Streekziekenhuis Midden Twente, Hengelo (Ov) |